Strategic decision-making on low-carbon technology and network capacity investments using game theory

Merlinda Andoni

Supervisor: Dr. Valentin Robu

Co-supervisor: Dr. Wolf-Gerrit Früh

Institute of Sensors, Signals and Systems
School of Engineering and Physical Sciences
Heriot-Watt University

This dissertation is submitted for the degree of
Doctor of Philosophy

March 2020

Abstract

In recent years, renewable energy technologies have been increasingly adopted and seen as key to humanity's efforts to reduce greenhouse gases emissions and combat climate change. Yet, a side effect is that renewables have reached high penetration rates in many areas, leading to undesired curtailment, especially if existing grid infrastructure is insufficient and renewable energy generated cannot be exported at areas of high energy demand. The issue of curtailment is compelling at remote areas, where renewable resources are abundant, such as in windy islands. Not only renewable production is wasted, but often curtailment comes with high costs for renewable energy developers and energy end-users. In fact, procedures on how generators access the grid and how curtailment is applied, are key factors that affect the decisions of investors about generation and grid capacity installed.

Part of this thesis studies the properties of widely used curtailment rules, applied in several countries including the UK, and their effect on strategic interactions between self-interested and profit-maximising low-carbon technology investors. The work develops a game-theoretic framework to study the effects of curtailment on the profitability of existing renewable projects and future developments. More specifically, work presented in this thesis determines the upper bounds of tolerable curtailment at a given location that allows for profitable investments. Moreover, the work studies the effect of various curtailment strategies on the capacity factor of renewable generators and the effects of renewable resource spatial correlation on the resulting curtailment. In fact, power network operators face a significant knowledge gap about how to implement curtailment rules that achieve desired operational objectives, but at the same time minimise disruption and economic losses for renewable generators. In this context, this thesis shows that fairness and equal sharing of imposed curtailment among generators is important to achieve maximisation of the renewable generation capacity installed at a certain area. A new rule is proposed that minimises disruption and the number of curtailment events a generator needs to respond to, while achieving fair allocation of curtailment between generators of unequal ratings.

While curtailment can be reduced by smart grid techniques, a long term solution is increasing the network capacity. Grid reinforcements, however, are expensive and costs weight to all energy consumers. For this reason, debate in the energy community has focused on ways to attract private investment in grid reinforcement. A key knowledge gap faced by regulators is how to incentivise such projects, that could prove beneficial, especially in cases where several distributed generators can use the same power line to access the main grid, against the payment of a transmission fee. This thesis develops methods from empirical and algorithmic game theory to provide solutions to this problem.

Specifically, a two-location model is considered, where excess renewable generation and demand are not co-located, and where a private renewable investor constructs a power line, providing also access to other generators, against a charge for transmission. In other words, the privately developed line is shared among all generators, a principle known as 'common access' line rules. This formulation may be studied as a Stackelberg game between transmission and local generation capacity investors. Decisions on optimal (and interdependent) renewable capacities built by investors, affect the resulting curtailment and profitability of projects and can be determined in the equilibrium of the game.

A first approach to study the behaviour of investors at the game equilibrium, assumed a simple model, based on average values of renewable production and demand over a larger time horizon. This assumption allowed for an initial examination of the Stackelberg game equilibrium, by achieving an analytical, closed-form solution of the equilibrium and the investigation of its properties for a wide range of cost parameters.

Next, a refined model is developed, able to capture the stochastic nature of renewable production and variability of energy demand. A theoretical analysis of the game is presented along with an estimation of the equilibrium by utilisation of empirical game-theoretic techniques and production/demand data from a real network upgrade project in the UK. The proposed method is general, and can be applied to similar case studies, where there is excess of renewable generation capacity, and where sufficient data is available.

In practice, however, available data may be erroneous or experience significant gaps. To deal with data issues, a method for generating time series data is developed, based on Gibbs sampling. This attains an iterative simulation analysis with different time series data as an input (Markov Chain Monte Carlo), thus achieving the exploration of the solution space for multiple future scenarios and leading to a reduction of the uncertainty with regards to the investment decisions taken.

Energy storage can reduce curtailment or defer network upgrades. Hence, the last part of this thesis proposes a model consisted of a line investor, local generators and a third independent storage player, who can absorb renewable production, that would otherwise have been curtailed. The model estimates optimal transmission, generation and storage capacities for various financial parameters. The value of storage is determined by comparing the energy system operation with and without energy storage. All models proposed in this thesis, are validated and applied to a practical setting of a grid reinforcement project, in the UK, and a large dataset of real wind speed measurements and demand.

In summary, the research work studies the interplay among self-interested and independent low-carbon investors, at areas of excess renewable capacity with network constraints and high curtailment. The work proposes a mechanism for setting transmission charges that ensures that the transmission line gets built, but investors from the local community, can also benefit from investing in renewable energy and energy storage. Overall, the results of this work show how game-theoretic techniques can help energy system stakeholders to bridge the knowledge gap about setting optimal curtailment rules and determining appropriate transmission charges for privately developed network infrastructure.

I would like to dedicate this thesis to the memory of my loving grandmother Vasilika

Acknowledgements

First and foremost, I would like to thank my PhD supervisor Dr. Valentin Robu for the faith and trust he has shown in me. Without his expert guidance, academic support and unfailing patience, this thesis would not have been completed. I would also like to thank my PhD advisor Dr. Wolf-Gerrit Früh, who co-supervised this thesis, for his encouragement, in-depth analysis and technical discussions of excellent academic support that enabled me to complete this thesis and publications associated with it, and Prof. David Flynn for his guidance and support throughout the duration of my PhD studies.

Second, I would like to thank my PhD thesis examiners Prof. Liana Cipcigan and Dr. Jonathan Swingler for their useful feedback and academic support that significantly improved the contents of this thesis.

I am extremely grateful to the Institute of Sensors, Signals and Systems for their financial support throughout my PhD studies, including support for training and travel support for conference attendance. I would also like to thank the Engineering and Physical Sciences Research Council (EPSRC) for their supplemental support and for allowing me to contribute towards the research objectives of the UK's National Centre of Energy Systems Integration (CESI) [EP/P001173/1]. Obtaining results for several parts of my research work would not have been possible without the use of the Cirrus UK National Tier-2 HPC Service at EPCC (http://www.cirrus.ac.uk), which is funded by the University of Edinburgh and EPSRC [EP/P020267/1].

I am grateful to my colleagues and friends in the Smart Systems Group for all the useful discussions and encouragement since the early stages of my PhD studies, especially Ioannis Antonopoulos, Wenshuo Tang, Dr. Benoit Couraud, Sonam Norbu and Dr. Peter McCallum. Special thanks to my friend Georgia Anastasiadi for the joint experiences shared and support throughout my PhD studies.

Finally, a special word of thanks to my family, my parents Dhiogjen and Zhuljeta, my sister Mirela and my better half Nikos for their unconditional love and support, while trying to fulfil my dreams.

Research Thesis Submission

Name*:*	MERLINDA ANDONI		
School:	EPS/ISSS		
Version: *(i.e. First, Resubmission, Final)*	FINAL	Degree Sought:	PhD

Declaration

In accordance with the appropriate regulations I hereby submit my thesis and I declare that:

1. The thesis embodies the results of my own work and has been composed by myself
2. Where appropriate, I have made acknowledgement of the work of others
3. The thesis is the correct version for submission and is the same version as any electronic versions submitted*.
4. My thesis for the award referred to, deposited in the Heriot-Watt University Library, should be made available for loan or photocopying and be available via the Institutional Repository, subject to such conditions as the Librarian may require
5. I understand that as a student of the University I am required to abide by the Regulations of the University and to conform to its discipline.
6. I confirm that the thesis has been verified against plagiarism via an approved plagiarism detection application e.g. Turnitin.

ONLY for submissions including published works

7. Where the thesis contains published outputs under Regulation 6 (9.1.2) or Regulation 43 (9) these are accompanied by a critical review which accurately describes my contribution to the research and, for multi-author outputs, a signed declaration indicating the contribution of each author (complete)
8. Inclusion of published outputs under Regulation 6 (9.1.2) or Regulation 43 (9) shall not constitute plagiarism.

* *Please note that it is the responsibility of the candidate to ensure that the correct version of the thesis is submitted.*

Signature of Candidate*:*		Date:	

Submission

Submitted By *(name in capitals):*	
Signature of Individual Submitting:	
Date Submitted:	

For Completion in the Student Service Centre (SSC)

Limited Access	Requested	Yes		No		Approved	Yes		No	
*E-thesis Submitted (**mandatory for final theses)***										
Received in the SSC by *(name in capitals):*						Date:				

Inclusion of Published Works

Declaration

This thesis contains one or more multi-author published works. In accordance with Regulation 6 (9.1.2) I hereby declare that the contributions of each author to these publications is as follows:

Citation details	**Andoni, M**., Robu, V., Früh, W. G., & Flynn, D. (2017). Game-theoretic modeling of curtailment rules and network investments with distributed generation. *Applied Energy*, 201, 174-187.
Merlinda Andoni	Review of relevant research, model and algorithm development, analysis of results, writing up of publication, general management of paper submission
All other authors	Supervision on work, Feedback/comments on publication, Proofreading
Signature:	
Date:	

Citation details	**Andoni, M**., Robu, V., Flynn, D., Abram S., Geach D., Jenkins D., et al. (2019), Blockchain technology in the energy sector: A systematic review of challenges and opportunities. *Renewable and Sustainable Energy Reviews*, 100, 143-174.
Merlinda Andoni	Information collection, review of relevant research, classification of relevant works, writing up of publication
All other authors	Feedback/comments on publication, Proofreading
Signature:	
Date:	

Citation details	**Andoni, M.**, Robu, V., Flynn, D. & Früh, W. G. (2018, October). Gibbs sampling for game-theoretic modeling of private network upgrades with distributed generation. In *PES Innovative Smart Grid Technologies Conference Europe (ISGT-Europe), 2018 IEEE* (pp. 1-6). IEEE.
Merlinda Andoni	Review of relevant research, model and algorithm development, analysis of results, writing up of publication, general management of paper submission
All other authors	Supervision on work, Feedback/comments on publication, Proofreading
Signature:	
Date:	

Citation details	**Andoni, M.**, Robu, V., & Früh, W. G. (2016, October). Game-theoretic modeling of curtailment rules and their effect on transmission line investments. In *PES Innovative Smart Grid Technologies Conference Europe (ISGT-Europe), 2016 IEEE* (pp. 1-6). IEEE.
Merlinda Andoni	Review of relevant research, model and algorithm development, analysis of results, writing up of publication, general management of paper submission
All other authors	Supervision on work, Feedback/comments on publication, Proofreading
Signature:	
Date:	

Citation details	**Andoni, M.**, Tang, W., Robu, V., & Flynn, D. (2017). Data analysis of battery storage systems. *CIRED-Open Access Proceedings Journal*, 2017 (1), 96-99.
Merlinda Andoni	Literature review on energy storage/batteries for energy applications, Writing up of abstract, introduction, general management of paper submission
All other authors	Model development, result analysis

Signature:	
Date:	

Citation details	**Andoni, M**., & Robu, V. (2016, May). Using Stackelberg games to model electric power grid investments in renewable energy settings. In *International Conference on Autonomous Agents and Multiagent Systems* (pp. 127-146). Springer.
Merlinda Andoni	Review of relevant research, model and algorithm development, analysis of results, writing up of publication, general management of paper submission
Valentin Robu	Supervision on work, Feedback/comments on publication, Proofreading
Signature:	
Date:	

Citation details	**Andoni, M.**, & Robu, V. (2016, May). Game-theoretic Modeling of Transmission Line Reinforcements with Distributed Generation. In *Proceedings of the 2016 International Conference on Autonomous Agents & Multiagent Systems* (pp. 1291-1292). International Foundation for Autonomous Agents and Multiagent Systems.
Merlinda Andoni	Review of relevant research, model and algorithm development, analysis of results, writing up of publication, general management of paper submission
Valentin Robu	Supervision on work, Feedback/comments on publication, Proofreading
Signature:	
Date:	

Citation details	**Andoni, M.**, Robu, V., & Flynn, D. (2017). Blockchains: Crypto-control your own energy supply. Nature, 548 (7666), 158.
Merlinda Andoni	Writing up of publication
All other authors	Writing up of publication
Signature:	
Date:	

Table of contents

List of tables

List of figures

Notations

Roman Symbols

$\mathbb{E}()$	Expected value of $()$ variable under consideration
A	Location of large demand (mainland)
B	Location of favourable renewable resources
a	Beta distribution parameter
B	Beta function
b	Beta distribution parameter
BR_i	Best response of i player
c	Wind speed Weibull distribution scale parameter
c_r	Parameter related to Pearson's coefficient r
c_S	Cost of storage per unit of energy storage capacity installed
C_T	Total cost of transmission line T for period of study
c_T	Cost of transmission per unit of transmission line capacity installed
c_{G_i}	Cost of generation per unit of expected generation of i generator
$CR_{i,t}$	Curtailment rate of i generator at time t
CR_i	Curtailment rate of i generator for period of study
D	Power demand at Location A (remote demand)
d	Power demand at Location B (local demand)
DOD	Depth of discharge of energy storage system
DOD_{max}	Maximum depth of discharge of energy storage system
DOD_{min}	Minimum depth of discharge of energy storage system
$E_{C_i,t}$	Expected energy curtailed from i generator at time t

E_{C_i}	Expected energy curtailed from i generator for period of study
E_C	Aggregate expected energy curtailed from generators for period of study
E_{D_i}	Energy demand served by i generator
E_{d_i}	Local demand served by i generator
$E_{D_{oth}}$	Remote demand served by the main grid or other sources
$E_{d_{oth}}$	Local demand served by the main grid or other sources
E_D	Aggregate energy demand served by generators
$E_{G_i,t}$	Expected energy produced by i generator at time t without curtailment
E_{G_i}	Expected energy produced by i generator for period of study without curtailment
E_G	Aggregate expected energy produced by generators for period of study without curtailment
$E_{S,t}$	Energy stored in storage device at time t
E_{S_D}	Remote demand served by storage
E_{S_d}	Local demand served by storage
$E_{S_{ini}}$	Energy transferred from i generator to storage
$from\_store$	New storage state if discharging without capacity constraints
I_T	Capital cost (initial investment) of transmission line T for period of study
I_{G_i}	Capital cost (initial investment) of i generator
k	Wind speed Weibull distribution shape parameter
M_T	Operation & maintenance cost of transmission line T for period of study
M_{G_i}	Operation & maintenance cost of i generator
N	Number of realisations for Gibbs sampling
n	Number of generators/Sampling size
p_G	Generation tariff price
P_L	Generic demand profile
p_T	Transmission fee
P_{C_i}	Power curtailed by i generator

$P_{ch,t}$	Charging power of energy storage system at t
$P_{ch_{max}}$	Maximum power charged in energy storage system
P_C	Aggregate power of generators curtailed
P_{D_i}	Power demand at mainland location served by i generator
P_{d_i}	Power demand at generation location served by i generator
$P_{D_{oth}}$	Remote demand served by other sources
$P_{d_{oth}}$	Local demand served by other sources
$P_{dch,t}$	Discharging power of energy storage system at t
$P_{dch_{max}}$	Maximum power discharged from energy storage system
P_D	Aggregate power demand at mainland location served by generators
P_d	Aggregate power demand at generation location served by generators
P_{G_i}	Power generated by i generator without curtailment
P_G	Aggregate power of generators without curtailment
$P_{L_{h,s}}$	Power demand distribution per hour and season
P_{N_i}	Rated power of i generator
$P_{N_{max}}$	Maximum rated capacity in search space
P_{pu}	Per unit power of wind generator
P_{S_D}	Power demand at mainland location served by storage
P_{S_d}	Power demand at generation location served by storage
$P_{S_{in_i}}$	Power from i generator to storage
$P_{S_{in}}$	Power from generators to storage
r	Pearson's correlation coefficient
r_t	Power charged or discharged from storage device
RD	Residual demand
S	Storage energy capacity
S_0	Initial storage state considered for simulation
s_{dch}	Self-discharge rate of energy storage system

S_{max}	Maximum storage capacity considered in search space
SOC	State of charge of energy storage system
SOC_{max}	Maximum state of charge of energy storage system
SOC_{min}	Minimum state of charge of energy storage system
T	Capacity of transmission line
t	Time interval or sample
t_{burn}	Burn-in period for Gibbs sampling
T_{max}	Maximum transmission capacity considered in search space
to_store	New storage state if charging without capacity constraints
u_a	Wind speed at anemometer height
u_i	Cross-correlated wind speed data series of i generator
$u_{rand,i}$	Random sample of wind speed data of i generator
u_{Ref}	Reference wind speed data series
w	Wind speed extrapolated at hub height
x_i	Stochastic variable for normalised power produced by i generator
x_{G_i}	Normalised power generation data series of i player
z_a	Anemometer height
z_h	Wind turbine hub height
z_o	Surface roughness of environment where wind speed measurements were taken

Greek Symbols

α	Sigmoid function parameter
$\bar{\chi}$	Mean of the sampling distribution of the sample mean
β	Sigmoid function parameter
χ	Hypothetical variable
δt	Duration between two consecutive time intervals
δ	Increment rated capacity in search space

η	Efficiency of energy storage system
η_{ch}	Efficiency of energy storage system during charging
η_{dch}	Efficiency of energy storage system during discharging
η_{rt}	Round-trip efficiency of energy storage system
Γ	Gamma function
γ	Ratio of local to remote demand
κ	Observations from available historic data
μ_{χ}	Mean value of distribution derived from historic data
Π_i	Profit function of *i* player
$\sigma_{\bar{\chi}}$	Standard deviation of the sampling distribution of the sample mean or standard error of mean
τ_T	Threshold for profitable transmission investment
τ_{G_i}	Threshold for profitable generation capacity investment of *i* generator
τ_G	Threshold for profitable aggregate generation capacity investment

Subscripts

i	Quantity refers to *i* generator
max	Maximum value of variable under consideration
min	Minimum value of variable under consideration
t	Quantity refers to *t* time interval or data sample

Abbreviations

AI	Artificial Intelligence
ANM	Active Network Management
ASIC	Application Specific Integrated Circuit
BDA	Big Data Analytics
BESS	Battery Energy Storage System
CAES	Compressed Air Energy Storage
CAISO	California Independent System Operator

CES	Community Energy Storage
CF	Capacity Factor
CfD	Contracts for Difference
CHP	Combined Heat and Power
CR	Curtailment Rate
DECC	Department of Energy and Climate Change
DER	Distributed Energy Resources
DG	Distributed Generator
DLR	Dynamic Line Rating
DLT	Distributed Ledger Technologies
DNO	Distribution Network Operator
DSM	Demand Side Management
DSO	Distribution System Operator
EPRI	Electric Power Research Institute
ESS	Energy Storage System
EU	European Union
EV	Electric Vehicle
EVI	Electric Vehicle Initiative
FiT	Feed-in-tariff
FPP	Flexible Plug and Play
FRR	Fractional Round Robin
GDPR	General Data Protection Regulation
HVAC	High Voltage Alternating Current
HVDC	High-Voltage Direct Link
ICT	Information & Communication Technologies
ICT	Information and Communication Technology
IEEE	Institute of Electrical and Electronics Engineers

IoT	Internet of Things
IPCC	Intergovernmental Panel on Climate Change
IRENA	International Renewable Energy Agency
LCOE	Levelised Cost of Energy
LCOS	Levelised Cost of Storage
LIFO	Last In First Out
LV	Low-Voltage
MC	Markov Chain
MCMC	Markov Chain Monte Carlo
ME	Maximum Error
MIDAS	Met Office Integrated Data Archive System
ML	Machine Learning
MPEC	Mathematical Programs with Equilibrium Constraints
MV	Medium-Voltage
NASA	National Aeronautics and Space Administration
NINES	Northern Isles New Energy Solution
OFGEM	Office of Gas and Electricity Markets
P2G	Power-to-Gas
P2P	Peer-to-Peer
PBFT	Practical Byzantine Fault Tolerance
PHES	Pumped Hydro Energy Storage
PoA	Principles of Access
PoAu	Proof of Authority
PoS	Proof of Stake
PoW	Proof of Work
PV	Photovoltaic
RES	Renewable Energy Sources

ROC	Renewable Obligation Certificate
RUL	Remaining Useful Lifetime
RVM	Relevance Vector Machine
SKM	Sinclair Knight Merz
SSE	Scottish Southern Energy
TSO	Transmission System Operator
UK	United Kingdom
UoS	Use of System
US	United States
V2G	Vehicle-to-Grid
VPP	Virtual Power Plant
WCI	Width of the 95% Confidence Interval

List of publications

5 first-author and 1 co-author of scientific publications in peer-reviewed journals, 5 articles published in conference proceedings, 2 co-author of white papers for IEEE Smart Grid Society.

Original scientific peer-reviewed articles

1. **Andoni, M.**, Robu, V., Flynn, D., Abram S., Geach D., Jenkins D., et al. (2019). Blockchain technology in the energy sector: A systematic review of challenges and opportunities. *Renewable and Sustainable Energy Reviews*, 100, 143-174.

2. **Andoni, M.**, Tang, W., Robu, V., & Flynn, D. (2017). Data analysis of battery storage systems. *CIRED-Open Access Proceedings Journal 2017*, 1, 96-99.

3. **Andoni, M.**, Robu, V., Fruh, W. G., & Flynn, D. (2017). Game-theoretic modeling of curtailment rules and network investments with distributed generation. *Applied Energy*, 201, 174-187.

4. **Andoni M.**, Robu V. (2016) Using Stackelberg Games to Model Electric Power Grid Investments in Renewable Energy Settings. In: Osman N., Sierra C. (eds) Autonomous Agents and Multiagent Systems. AAMAS 2016. Lecture Notes in Computer Science, 10002, Springer, Cham

5. **Andoni, M.**, Robu, V., & Flynn, D. (2017). Blockchains: Crypto-control your own energy supply. *Nature*, 548 (7666), 158.

6. McCallum, P., Jenkins, D. P., Peacock, A. D., Patidar, S., **Andoni, M.**, Flynn, D., & Robu, V. (2019), A multi-sectoral approach to modelling community energy demand of the built environment, *Energy Policy*, 132, 865-875.

Articles in conference proceedings

1. **Andoni, M.**, Robu, V., Flynn, D. & Fruh, W. G. (2018, October). Gibbs sampling for game-theoretic modeling of private network upgrades with distributed generation. In PES Innovative Smart Grid Technologies Conference Europe (ISGT-Europe), 2018 IEEE (pp. 1-6). IEEE.

2. McCallum, P., Patidar, S., Jenkins, D., Peacock, A., Robu, V., **Andoni, M.**, & Flynn, D. (2018, May). The Use of Demand Modelling for Community Energy Analysis. In Circuits and Systems (ISCAS), 2018 IEEE International Symposium on(pp. 1-5). IEEE.

3. Tang, W., **Andoni, M.**, Robu, V., & Flynn, D. (2018, May). Accurately Forecasting the Health of Energy System Assets. In Circuits and Systems (ISCAS), 2018 IEEE International Symposium on (pp. 1-5). IEEE.

4. **Andoni, M.**, Robu, V., & Fruh, W. G. (2016, October). Game-theoretic modeling of curtailment rules and their effect on transmission line investments. In PES Innovative Smart Grid Technologies Conference Europe (ISGT-Europe), 2016 IEEE (pp. 1-6). IEEE.

5. **Andoni, M.**, & Robu, V. (2016, May). Game-theoretic Modeling of Transmission Line Reinforcements with Distributed Generation. In Proceedings of the 2016 International Conference on Autonomous Agents & Multiagent Systems (pp. 1291-1292). International Foundation for Autonomous Agents and Multiagent Systems.

Publications directed at societies of expertise

1. Lee, W-J., **Andoni, M.**, Bani-Ahmed, S., Flynn, D., Hartmann, B., Majd, A., Rostami, M., et al. (2018). Battery storage White paper # 1. IEEE Smart Grid [Online] http://resourcecenter.smartgrid.ieee.org/sg/product/publications/SGWP0005

2. Pullum, L. L., Jindal, A., Roopaei, M., Diggewadi, A., **Andoni, M.**, Zobaa, A., et al. (2018). Big Data Analytics in the Smart Grid: Big Data Analytics, Machine Learning and Artificial Intelligence in the Smart Grid: Introduction, Benefits, Challenges and Issues. IEEE Smart Grid [Online] http://resourcecenter.smartgrid.ieee.org/sg/product/publications/SGWP0003

.

Chapter 1

Introduction

This thesis uses game-theoretic modelling to study the effects of curtailment and line access rules to generation, transmission and energy storage capacity investments. Procedures on how renewable generators obtain grid access and how curtailment is applied, are key factors that determine, to a significant extent, strategic decisions on capacity investments. *Grid access* is used in this thesis as a broad term that describes grid connection terms, priority of dispatch and constraint management. *Curtailment* refers to restrictions in renewable power output due to oversupply or network constraints. The first part of this work focuses on the study of flexible and interruptible connections offered to distributed generators by power system operators and distribution companies. More specifically, this thesis studies the effect of curtailment rules and practices on the profitability of renewable generation projects. This thesis also studies important features and characteristics of curtailment rules, such as fairness, and their effect on existing and future volumes of renewable energy generation capacity, which are installed and connected in electricity grids.

The second part of this thesis focuses on the effect of curtailment and line access rules to transmission capacity investments of private and distributed ownership. This work is particularly relevant to settings where one private investor develops the required infrastructure to access the grid and multiple low-carbon technology projects (such as wind generation and energy storage) can use this infrastructure, against the payment of a transmission fee. A game-theoretic and multi-agent systems framework (Stackelberg and Cournot game formulations) is developed to model different types of investors as self-interested and profit-maximising entities that act autonomously in order to achieve their own local objective. Agent actions are interdependent on other agents (or opponents) activities. Theoretical results are generated in conjunction with practical applications of the developed models to relevant case studies. Methods developed achieved an estimation of optimal decisions with regards to generation, transmission and energy storage capacity installed by different players. The solution concepts developed in this work are relevant to empirical and algorithmic game theory. In summary, this work shows how game-theoretic formulations may assist energy system stakeholders to bridge the knowledge gap of setting optimal curtailment rules and determining appropriate transmission charges for private network infrastructure.

1.1 Research motivation

The following sections of Chapter 1 introduce the background area of the topic, along with the aims, objectives and main contributions of the research work presented in this thesis.

1.1.1 Energy landscape

Since the industrial revolution, the global economy has heavily relied on fossil fuels in almost all economy sectors including manufacturing, transportation, heating, synthetic materials and power generation. One of such fuels is petroleum. However, limited global oil reserves, managed and controlled from a small number of countries that are often located in conflict zones or politically unstable areas, has repeatedly led to extreme price volatility and threatened our energy security. In addition, the use of fossil fuels such as coal and oil have put great strains to the environment we live, ranging from air quality and pollution to extensive carbon emissions, considered by myriad scientists throughout the world, as the main cause for global warming [136].

Climate change and increasing global temperatures have emerged as an urgent issue threatening the longevity and prosperity of mankind, highlighting the importance to what is widely known as the sustainability and decarbonisation agenda. The Paris Agreement charts a new course of international effort to combat climate change with 195 countries agreeing to keep average global temperature rise well below 2^oC above pre-industrial levels [73]. A recent Intergovernmental Panel on Climate Change (IPCC) special report revealed potentially devastating impacts to ecosystems, biodiversity, livelihoods, health, food security, water supply and economic growth if drastic measures are not taken, and suggested that efforts should intensify in achieving a temperature rise of no more than 1.5^oC [114].

In the power sector, renewable energy sources (RES) have formed an integral part of the solution to tackling global climate change. Renewable generation has been highly promoted and incentivised within the European Union (EU). The key EU-wide objectives set for 2030 [74] include at least 40% reduction in EU greenhouse gas emissions with reference to the 1990 levels, a target of 32% share of renewable energy to energy consumption and 32.5% improvement of energy efficiency. Policy initiatives at a national and global level, such as tax exemptions or financial incentives, in accordance to technological advances, have permitted large volumes of RES be connected to electricity grids. According to a recent International Renewable Energy Agency (IRENA) report [113], renewable energy capacity reached 2.18 TW worldwide in 2017. In 2017, renewable power capacity (excluding hydro) reached 1,081 GW worldwide, including 402 GW of solar photovoltaic (PV) and 539 GW of wind power capacity, out of which 98 GW of solar PV and 52 GW wind power generation capacity was newly added capacity in 2017 alone. The total investment in the renewables sector reached an estimate of $279.8 billion [206].

The UK alone has agreed to reach net-zero carbon emissions by 2050 [43]. In 2017, 29.3% of the UK gross electricity consumption was generated by RES, mainly from

onshore and offshore wind farms and PV solar plants, accounting for 31.7%, 17.2% and 31.5% of the total installed RES capacity, respectively [57].

High levels of RES technologies adoption have been supported in many countries by novel incentive provision and new energy market models. These include green energy frameworks and policies, financial incentives and technical/regulatory structures, such as green energy certificates and feed-in-tariff (FiT) prices. The FiT support mechanism targeted small to medium renewable generation and guaranteed a fixed price for the electricity produced. Green energy certificates called Renewable Obligation Certificates (ROCs) [182] constituted the main supporting incentive mechanism for large renewable generators until 2017, in the UK. Electricity suppliers were obliged to source a proportion of their electricity supply from renewable energy sources and therefore, were required to obtain a level of ROCs each year, as determined by the Department of Energy and Climate Change (DECC) [52]. ROCs were issued by the UK's independent system regulator, the Office of Gas and Electricity Markets (OFGEM), per MWh of renewable electricity produced and their actual value differed by type of technology, in order to promote the development of new and more expensive technologies. ROCs were replaced by Contracts for Difference (CfD) in 2017 [53]. CfD is a price support mechanism, which pays eligible generators with a premium price in addition to the wholesale market electricity price, so that the agreed 'strike' price is reached. If wholesale electricity prices rise higher than the guaranteed price, generators are required to pay back the difference between the wholesale market electricity price and the strike price. The CfD scheme aimed to mitigate renewable investment long-term exposure to volatile electricity prices. For smaller scale renewable generation, such as residential RES developments, the most important mechanism was FiT prices i.e. a long-term guaranteed price for the energy produced [180]. Such incentives have gradually led to increased RES connections in both transmission and distribution networks, however cost reduction and large RES adoption have led to some of these incentives being reduced or removed. The levelised cost of energy (LCOE) for such technologies, such as onshore wind or large scale PV, is currently competitive with conventional generation, such as gas and nuclear [56]. However, integration costs of RES generation need also to be taken into account.

RES are variable, difficult to predict and depend on weather conditions, hence raise new challenges in the management and operation of electricity systems. More *flexibility measures* are required to ensure safe operation and stability [33, 103]. Different types of generators are required to compensate for the variability and potential loss of renewable supply, sources that so far have been predominantly fossil fuel-based, such as gas generators. However, such generators are less and less utilised and pushed out of the merit order, as more RES generators are deployed, leading to the reduction of the grid's inertial response and increased risks on power system's stability. The merit order refers to the positioning of generation assets according to their respective price or marginal cost and power output in ascending order. Traditionally, the merit order forms the energy supply curve, which combined with the demand curve results in the estimation of market clearing prices. Marginal costs for RES generators can be near zero, pushing conventional

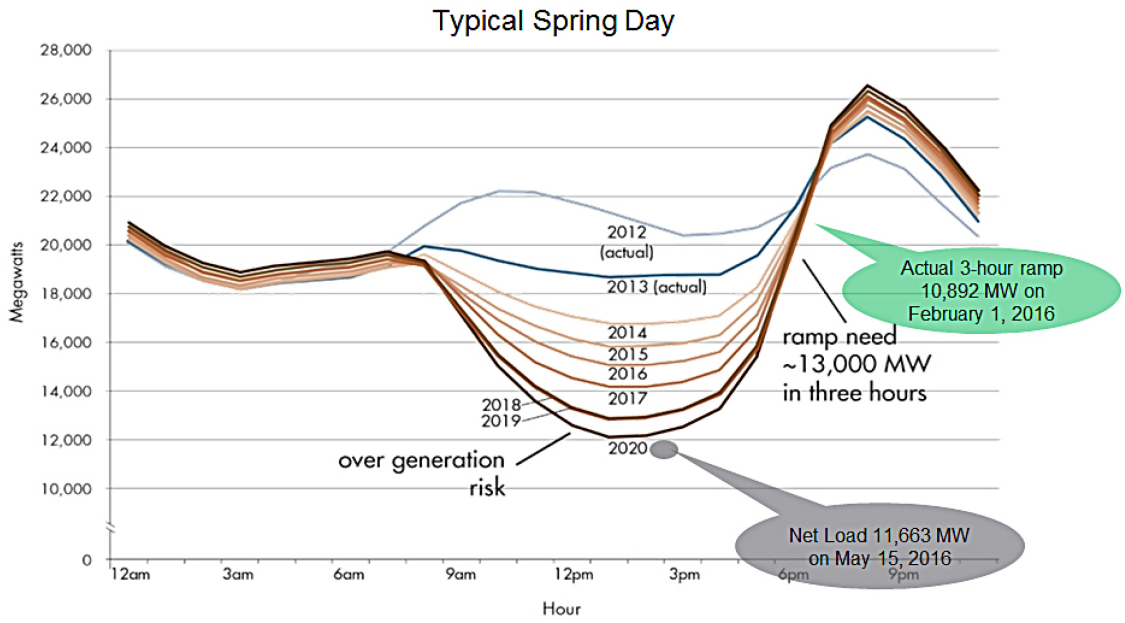

Fig. 1.1 The fundamental change in the shape of the net load of the Californian system, also known as the 'duck curve', caused by large volumes of solar generation [37]

generation further up in the curve and leading to short-term prices collapsing, at times even reaching negative values, when it is expensive to shut-down conventional power plants. In addition, RES generators cannot be dispatched, unlike conventional generators, and are more challenging to control [203]. In fact, large volumes of RES, such as embedded microgenerators, are often invisible to network/system operators and pose a significant challenge to the overall system control.

A prominent and well-known example that illustrates the new challenges system operators are facing with the increased adoption of variable renewable energy comes from the Californian grid. The California Independent System Operator (CAISO) published in 2013 the net load of the Californian system, as seen from the system's operator standpoint. The net load curve shown in Fig. 1.1 represents a fundamental change in the shape of electricity demand and became widely known as the *'duck curve'*. The curve is the difference between forecast load and expected electricity production from variable generation resources and represents the system electric load that needs to be met by conventional generation when solar generation is adopted at large scales [37]. As shown in Fig. 1.1, the system operator is faced with an increased risk of oversupply in the morning hours as the sun rises and conventional generation is replaced by solar generation. In the late afternoon hours, when solar production ends, the system operator needs to dispatch generating assets that can cope with the steep ramping-up curve, which can be at times equal to up to a third of the system's peak load in a period of just a few hours. These challenging requirements need to be met by flexibility services.

Moreover, distributed generators (DGs) connected in distributed networks are gradually transforming power systems into bidirectional energy flow networks, crucially challenging the way they were designed and managed. For instance, from the initial conception of the power system, protective equipment, frequency and voltage control were designed

assuming unidirectional energy flows that emanate from large generation plants to load demand centres. Reverse power flows needs to be carefully managed, desirably in an automated way, under minimal human intervention.

Adding to the transformational change caused by distributed energy resources (DERs) and renewables, energy systems are on the brink of entering the *digital era* as shown by the massive deployment of smart meters in numerous countries [275]. In the UK alone, 53 million electricity and gas smart meters are planned to be installed by 2020, one for every home and small business [179]. This goes hand in hand with the proliferation of intelligent devices being deployed in electricity networks that have opened new opportunities for value delivered by big data analytics (BDA) or promising technologies like artificial intelligence (AI) and machine learning (ML).

In recent years, significant progress has been made in terms of volumes of renewable energy assets installation in electricity grids, however additional efforts are required to achieve ambitious carbon emissions targets. Energy policy makers and researchers are turning their attention to *whole energy systems integration* and emissions reductions in the sector of transport and heating. Modern renewable energy accounted for only 10.6% of the total final energy consumption in 2016, with 79.5% still relying on fossil fuels use [206]. In fact, the majority of energy is consumed for heating/cooling (48%) and transport (32%), rather than for electricity use (20%) at a global level [206]. Domestic transport alone accounted for 25% of UK carbon emissions [45]. Energy storage, electrification of heat and electric vehicles (EVs) are key target areas for future energy systems.

Electric motors, having higher efficiencies, are expected to substitute internal combustion machines [63], however this will lead to increased electricity demand. In the following years, the number of EVs is expected to rise drastically. The Electric Vehicle Initiative (EVI) and the International Energy agency (IEA) are calling for deployment of EVs reaching at least 30% of new vehicles sold by 2030 [111]. Other factors leading to this potential rise in electricity demand are increasing global population and electrification and industrialisation of developing countries.

EVs consist of large loads, which can put strains on the local transformers and low voltage infrastructure. Moreover, load from EVs typically correlates and coincides with the peak demand, as most EVs are expected to be charged in the afternoon hours, when people return from work. Hence, EV charging schedule has to be carefully designed, and decentralised control mechanisms need to be deployed [268]. AI techniques can contribute to predicting the charging needs for each EV, depending on the travel needs of each consumer and estimating with great accuracy the aggregate demand to the local network. The role of ML is vital for achieving accurate predictions of energy demand. While EVs pose significant challenges, if managed properly, they can also bring about opportunities for better management of electricity grids. EVs can potentially be used for Demand Side Management (DSM), as their batteries can be discharged according to the system operator discretion [233]. This concept is also known as vehicle-to-grid (V2G) operation.

Demand side management is expected to play a key role in future energy systems that will achieve efficient operation of the load or demand side. Traditionally, the supply side is adjusted to the demand, by setting suitable power outputs of the generating units, which ensure increased reliability and safe operation within the network's operational limits. However, as RES power output is variable and difficult to predict, it would be highly beneficial to manage the demand and match it to the generation side.

Demand side management can be used to defer, shift or switch off load consumers at the discretion of the system operator, not limited to times of peak demand or network constrains, but also to other periods of time, which can optimise the system's operation. Some of the benefits of DSM [223] include 'peak shaving' or 'flattening' the demand. Usually, peak demand is served by carbon-intensive and expensive power plants, therefore demand response techniques could lead to lower electricity prices for end-consumers. It could be also beneficiary for system operators as it could lead to efficient grid operation and better recovery from power system faults, usually caused by generator failures or power line tripping.

DSM can be implemented with two main techniques: automatic control of the consumers' systems and appliances or price signalling, which can both be deployed in a smart grid environment. Several types of electricity tariffs other than standard types have been discussed in the literature, including Time-of-Use meters, Critical Peak Pricing or Real Time Pricing, which reflect the real cost of power generation. These tariffs can be used to reduce the peak demand. However, they can also shift the demand and create new peaks, at times when these are not expected. For this reason, sophisticated techniques, which account for the system's state, are required to predict both supply and demand. This is rather a complex problem, as it requires data from several devices or buildings, weather patterns, human preferences and activities. Such optimisation algorithms can be developed through machine learning [22].

Moreover, demand response needs to be deployed in a larger scale at grid level, meaning that multiple demand resources need to be aggregated so they can have a larger impact. Examples of commercial schemes in the UK include Flexitricity[1] and Upside Energy[2], which have mainly focused on aggregating demand resources from large office buildings. In general, office or industrial demand is easier to predict and has a larger impact than domestic demand response, which is considered more challenging. Several studies have proposed the aggregation of smaller energy assets such as heat pumps and refrigeration units acting as thermal storage [149, 171]. In these settings, successful delivery of demand response services is more complex and needs to account for emergency cases, related to social activities or extreme weather.

Another key pillar of future energy systems are energy storage systems (ESS). Energy storage devices and batteries are expected to play a key role in the operation and management of the electricity grids [192]. Promising use cases for ESS include assisting with RES

[1] https://www.flexitricity.com/en-gb/
[2] http://upsideenergy.co.uk/

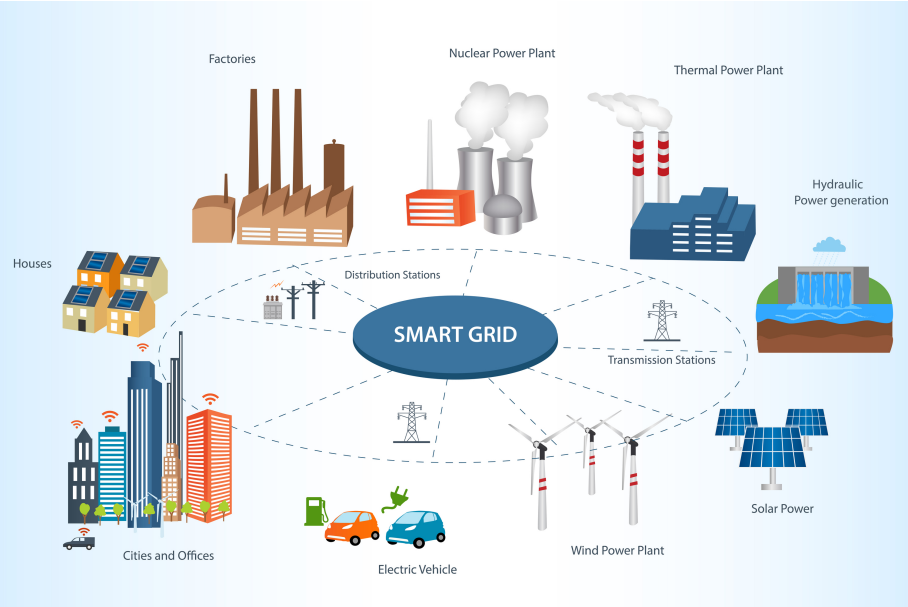

Fig. 1.2 A visualisation of future energy systems and the 'smart grid' according to the Institute of Electrical and Electronics Engineers (IEEE) [108]

integration and applications for grid upgrade deferral, energy arbitrage, ancillary services, regulation, frequency response, voltage support and black start services [4, 140].

The transformation of energy systems will most certainly require large sums of investment. To moderate requirements for funding, smart management and control need to be adopted, tasks that are increasingly challenging as energy systems are growing to become more active, decentralised, complex and 'multi-agent', with an increasing number of actors and possible actions. Advanced communication and data exchanges between different parts of the power network are to an increasing extent required, making central management and operation more and more challenging.

This transformation has led to a new vision for energy systems commonly described as the *smart grid*. According to the United States Department of Energy, the vision of future electricity grids can be defined as [247]: *'A fully automated power delivery network that monitors and controls every customer and node, ensuring a two-way flow of electricity and information between the power plant and the appliance, and all points in between. Its distributed intelligence, coupled with broadband communications and automated control systems, enables real-time market transactions and seamless interfaces among people, buildings, industrial plants, generation facilities, and the electric network.'*

The research fields affected by this transition are not limited to the power systems sector but expand to communication, information technologies, automation, security, economics, social and political sciences, *artificial intelligence (AI)* and *game theory* [202]. The latter are most relevant to the scope of this thesis. The following section elaborates on the value that game-theoretic approaches can bring to delivering the vision of optimised, low-carbon and smart energy systems.

In the context of deregulated electricity markets, game-theoretic models are increasingly required to explain strategic behaviour of multiple agents that might have conflicting

interests. Agents typically act in ways that maximise their own individual utility. Tools from microeconomics or coalitional game theory can be useful to aggregate many RES generators and demand response agents or to design appropriate incentivisation mechanisms. Equilibria need to be determined under settings of incomplete information, with uncertainty and dynamic environments. Relevant works that showcase the value game-theoretic modelling can bring to power systems are discussed in depth in Chapter 2.

On the other hand, AI techniques can develop algorithms and mechanisms for more efficient operation of networks and the power system [200]. As future power grids require smart interfaces and intelligent automation, we need to develop tools for prediction of generation and consumption from data collected by smart metering and sensing infrastructure that enable optimal management of electricity grids. These algorithms can be computationally challenging and should have the capability to provide optimisation solutions that are suitable for real-time operation. This can be extremely challenging as it requires the management of multiple generation units of different technology types including variable RES units, load curtailment, demand side management and energy storage devices, in a constantly changing environment with varying demand, volatile prices and increased uncertainty.

A key challenge studied in this thesis is the issue of renewable curtailment that has come up as a consequence of high RES development, insufficient grid infrastructure and a mismatch of local demand to supply. The background topic on curtailment and congestion management is introduced in the following section.

1.1.2 Renewable curtailment

In areas where renewable generators have achieved high penetration rates, technical limitations on the operation of energy systems, have led to *curtailment* of renewable production i.e. the restriction of RES production in safe operational limits for the energy system. Curtailment can happen at a system level (high voltage) or at a distribution level when local constraints may be more important (medium or low-voltage levels). According to Joos and Staffell (2018) variable renewable energy capacity, comprised of wind and solar developments, and RES penetration saw a four-fold increase in Britain between 2010 and 2016 [116]. Curtailment is typically imposed when the system is at risk and is most prominent at areas of favourable renewable resources, which may be remote regions located away from energy demand centres and where renewable projects meet least planning resistance. For instance, such areas can be windy islands where there is excess RES supply compared to the required local demand. Well-known examples of such areas in the UK include the Shetland and Orkney archipelagos and the Kintyre peninsula in the Western coast of Scotland. Realistic figures based on the latter case are used for a practical application of the theoretical models developed and presented in this thesis. Furthermore, curtailment can reach critical levels in areas where the existing network infrastructure is insufficient and therefore energy generated by renewable generators cannot be transferred where required. In these areas, the network places heavy dependence on curtailment at the

present time. The Orkney Islands (in north-western Scotland) are a classic example that have experienced curtailment levels that are among the highest in the UK [126]. This has significant social implications as many RES projects in Orkney are community-owned and suffer from large curtailment, thus potentially harming RES acceptance among consumers. The implications of curtailment extend to inefficient energy management and renewable utilisation, potential economic losses for RES generators, wasted energy and increased integration costs.

Curtailment not only means that clean energy produced by RES is wasted, but often curtailment comes with high costs for renewable energy developers and energy system end-users. Several works have studied the effects that RES intermittency has on electricity costs, known also as integration costs [99]. Integration costs represent balancing costs and constraint management costs. For example, in many countries, including the UK, when generators operate at areas with network constraints, they are usually compensated for reduced profits when imposed to curtailment, leading to increasing energy costs, which are essentially allocated to all energy system consumers. In the UK, RES curtailment costs rose from £5.9m to £81.9m between 2012 and 2016 and from 45 to $1,123$ GWh of curtailed energy. Onshore wind located in Scotland bore the major consequences, as up to 32% of onshore wind farms' annual output was curtailed over a period of 5 years. In Germany, a country where RES capacity has vastly increased in the recent years, wind curtailment increased 27-fold between 2010-2016 with a cost that reached €478m in 2015 (4,722 GWh) [116].

The issue of curtailment compensation has gained negative publicity in media channels with reports that threaten social acceptance and public perception on RES technologies. As more RES capacity continues to be installed, this practice cannot be sustainable and cost-effective, therefore smart solutions are required for further RES integration. Hence, system operators are gradually adopting new strategies with regards to curtailment, such as Dynamic Line Rating (DLR) and Active Network Management (ANM), typically deployed at distribution networks. DLR uses rating technology and instrumentation to monitor the thermal state of the lines in real time and may improve the estimated capacity between 30% to 100% [60, 165]. On the other hand, ANM is the automatic control of the power system by means of control devices and measurements that allow for real time operation and optimal power flows. DLR and ANM can be combined to provide greater benefits in terms of curtailment reduction [6].

From the DNO perspective, both techniques imply controlling generators' power outputs, hence innovative commercial agreements between generators and the system operator are required. More frequently, generators are offered interruptible, *'non-firm'* connections to the grid, along with a set of rules about the order they are dispatched or curtailed, as opposed to traditional 'firm' connections, which might require grid reinforcement and in which case any curtailment imposed by the grid operator is then offset by financial compensation. Non-firm connections are a solution preferred in many occasions to avoid high costs associated with grid reinforcement or enduring a long wait before permits are granted and grid infrastructure is finally built [49]. These terms and conditions are known

as *'Principles of Access' (PoA)* and are a key focus of this work. PoAs determine and specify how curtailment is allocated among generators in practical settings. Similar schemes have been supported by the UK Government through funding mechanisms encouraging DNOs to facilitate renewable connections [181].

In fact, procedures specifying how renewable generators get network access and how curtailment is applied are key factors affecting the decision-making process about investments for renewable generation and transmission capacity installed. The curtailment level and policy applied by the system operator can be crucial for the decision-making of renewable investors on whether to invest in new renewable generation capacity [20]. In this context, DNOs face a significant knowledge gap about how to implement curtailment rules that achieve desired operational objectives, but at the same time minimise disruption and economic losses for renewable generators. The study of curtailment rules, how curtailment should be shared among generators and how this impacts strategic behaviours of renewable investors, including their effect on the viability of RES projects, form the core research of this thesis. A detailed review of the relevant literature on curtailment rules is presented in Chapter 2.

System and network operators may also deal with curtailment issues by utilisation of market-based instruments. One prominent example is the 'six-hour rule' applied to subsidised RES generators in Germany. Oversupply of RES generation and inability of certain large conventional generators to curtail their power output, often leads to negative prices in wholesale electricity markets, including day-ahead markets. In the case of negative day-ahead prices, any subsidy payments to RES generators cease for the duration of at least six hours, hence providing a price signal for incentivising RES generators to undertake more curtailment.

Such techniques can help dealing with the issue of curtailment, however, a long term solution is investment in new grid capacity and network upgrades, that are preferably supported by private investment, so that renewable projects can bear part of the costs required for their integration. Grid reinforcement costs are recouped by network charges shared among all users of transmission and distribution systems, which raises issues of fair allocation. The energy community is increasingly engaging in discussions with policy makers regarding a restructuring of the ways network charges are allocated, in order to achieve a more efficient market operation [183]. The issues related to network upgrades are introduced in the following section.

Other solutions to mitigate curtailment come from the use of energy storage, demand side management and adoption of electric vehicles (EVs) that can be used to store excess RES generation and reduce technical constraints by absorbing RES variable outputs. Finally, another solution mentioned in the recent literature is the development of local energy markets in constrained areas of the grid that aim to alter consumer behaviours in order to better match demand to locally produced RES supply and minimise curtailment. The practical implementation of local energy markets is being supported by the advent of novel technologies such as *distributed ledger* or *blockchain* technologies [10]. A recent example is the 'Cornwall Local Energy Market', a £19m project developed by Centrica,

that aims to create a virtual marketplace and trading platform for energy and flexibility services to the grid and the wholesale energy market [40]. Another example is the £28.5m ReFLEX Orkney project, which aims to use smart grid techniques and local energy markets for better management of energy use, grid constraints and alignment of demand to locally produced renewable supply [185].

Use of energy storage and blockchain technologies are discussed in detail in the succeeding sections. At first, however, attention is drawn to the background area of network upgrades and grid reinforcements, discussed in detail in the following section.

1.1.3 Network upgrade investment

In most countries, the power grid was constructed many years ago taking a central and top-down approach, with power being generated in large central units, typically coal-based in the UK, and then transmitted and distributed to the consumers through power lines. Maintaining safe operation of this ageing power grid infrastructure requires vast amounts of (public) investment. Investing in new grid assets, such as the installation of transmission/distribution lines and substations, and grid reinforcement can be expensive with costs burdening grid network users and subsequently all energy consumers. It is estimated that in the EU alone, the transition towards a more sustainable and secure energy system would require an investment of €200 billion per year for generation, network and energy efficiency development [64]. A report published by the Rocky Mountain Institute estimated that $2 trillion in electricity network upgrades will be required by 2030 in the US [32]. Significant network upgrade projects are being deployed to accommodate more RES generation, such as the project of 'Western link', a high-voltage direct link (HVDC) that aims to unlock a transmission capacity of 2.25 GW, from production sites in Scotland to demand centres in England and Wales [226]. Similar developments are under way in the US in order to accommodate increasing wind generation capacity [117].

In many countries, public funding has been used by transmission system or local distribution network operators (TSO/DNOs) to reinforce such power lines. This is, however, expensive and increasingly harder to justify (since only a few companies benefit from what is essentially a public investment), and often leads to considerable delays in capacity being installed. From a public policy standpoint, it would be highly desirable to incentivise private investors to undertake part of the required grid infrastructure investment. As a result, recent discussions in the energy community have focused on ways to attract private investment in network upgrade projects, so that part of the costs required for renewable integration is recovered by private funding. System operators have started a debate on finding new ways to incentivise privately built lines [118], paid by the renewable generation companies [132], possibly partially supported by TSOs/DNOs. In fact, there is a key knowledge gap faced by network operators and regulators about how to best incentivise privately owned network upgrades.

This raises the crucial issue of the line access rules to be applied to the new transmission lines, as well as the interplay between the line access and the curtailment mechanism.

Deregulated electricity markets and RES integration in principle enable private investors participation in network investments. This market behaviour can be desirable from a public policy standpoint but it raises the question for system operators of defining the framework within which these private lines are incentivised, built and accessed by competing generators. Currently, DG investors bear a part of the costs required for their integration. In general the connection costs may vary, but usually include the full cost for the grid capacity installed for own use and a proportion of the costs for shared capacity with other customers, in the case of a network upgrade [7]. The remaining costs are recovered by the system charges borne by all grid users, representing approximately 18% of the average electricity bill of a typical UK household [258]. This has led to engagement in public debate for the Office of Gas and Electricity Markets (OFGEM), the UK's independent system regulators, on the reform of network charges that would achieve more efficient and fair allocation [183].

A special case that represented a key starting point for the models developed in this thesis is the value that privately developed grid capacity could provide in settings where several generators can use the same transmission/distribution line against the payment of a transmission fee. Current practices may lead to inefficient solutions in real-world settings. Consider, for instance, the problem of reinforcing transmission/distribution lines in outlying regions of Scotland, such as in the Kintyre peninsula, an area that has attracted major RES investment and is used for the practical demonstration of the game-theoretic tools developed in this work. The scheme providing grid access to the RES generators in this area followed a 'single access' principle, i.e. private lines for sole-use that were sufficient to accommodate only the RES capacity of each project. This practice resulted in the unintended effect of no less than three distribution lines being connected or under construction in the same area. While the marginal cost of building a larger capacity line is cited as a possible explanation, a less obvious, but potentially key reason is that each producer had no incentive to build a larger capacity line which permitted access to rival competitors. It is thus clear that current solutions are far from being optimal in terms of network use and economic efficiency.

While lines with completely private access (so called 'single merchant access') lines are possible, it would be beneficial if new power lines are built (partially) by private investors, keeping the access to this infrastructure public. An approach would be that power lines are built under a *'common access'* principle, where a private renewable investor may be granted a license to build a power line, under the obligation to also grant access to third parties, such as smaller local generators or energy storage devices. The line investor is able to recuperate line installation costs by charging other investors a transmission fee per unit of energy transported, the level of which is subject to a cap set by the regulator.

The interplay between curtailment rules and principles of access applied to power lines, raises potentially complex issues, especially as the line investor, regulator and local RES investors may have different underlying goals [222]. This thesis developed methods from empirical and algorithmic game theory that study these interactions and emergent complex behaviour. In this work, investors, also called *players* or *agents* in the context of this

work, are modelled as self-interested entities that aim to maximise their individual utility function or their profits. The work shows that a complex *Stackelberg game* can occur between the transmission capacity and other low-carbon generation and storage investors, in which the decision to build a transmission line depends on the equilibrium strategy of local investors to invest in additional capacity. The methods developed in this thesis may help network operators and system regulators to optimally determine the transmission charges that enable private infrastructure be installed, and thus achieving the development of more efficient and resilient networks.

In this thesis, a two-location problem is considered, where excess renewable energy generation and demand are not co-located. Next, the work studies the combined effect that curtailment schemes and line access rules have on the decision to invest in new transmission lines and renewable generation capacity built in an area.

The models developed in this thesis and their theoretical results were demonstrated and applied to a practical application, based on a grid reinforcement project between Hunterston and Crossaig, in the remote Kintyre peninsula in Western Scotland. This remote region is a good example of a location with high wind generation potential, where it became clear that private line investment would be needed to export the renewable energy generated.

The main analytical results of this thesis suggest that, in such cases, it is possible for system regulators and network operators, to encourage private line investors - possibly to build larger capacity lines under a 'common access' rule, as long as transmission charges, in the equilibrium of the game, are set in such ways that allow sufficient profits for investors.

Relevant literature to this vein of work is discussed in greater detail in Chapter 2. Next, the research aims and objectives are presented along with a summary of the main contributions of the work undertaken for the completion of this thesis.

1.2 Research objectives and contributions

The previous section introduced the broader topic area and problem statement of the research work presented in this thesis. Here, the reader can find a thorough discussion on the specific research objectives and the novelty of the research work undertaken in the context of this thesis.

The broader objective of this thesis is *to explore how game-theoretic and artificial intelligence techniques can address challenges caused by excess renewable generation at areas of the grid with network constraints and significant volumes of curtailment.* The specific goals contributing towards the main broader objective can be summarised into the following:

- This thesis aims to provide **an in-depth review of the topic of renewable curtailment**. The review aims to present a detailed analysis, description and comparison of curtailment rules and practices applied by network operators for curtailment allocation in ANM schemes. Secondly, this thesis aims to review the literature on

the utilisation of game-theoretic and economic models that are suitable for analysing market behaviour and strategic decision-making of investors in settings where renewable curtailment plays a significant role.

- In addition, this thesis aims to demonstrate how the economic performance of distributed generators (DGs) is influenced by different curtailment strategies, and what the long-term **effects of curtailment rules to existing and future renewable generation** capacity investments are.

- Next, this thesis aims to investigate the **impact of curtailment and line access rules to network upgrade expansion** investments that can be supported by private funding. In this vein, this work aims to develop suitable modelling techniques that capture the strategic decision-making of self-interested agents and low-carbon energy investors, such as renewable and energy storage investors.

- Finally, the thesis aims **to demonstrate the application of the developed theoretical models in practical settings**. To achieve this, theoretical results of the models under consideration will be applied in practical examples inspired by real-world applications and based on realistic assumptions from UK-based case studies with utilisation of large datasets of renewable resources and electricity demand. The latter aims to showcase the value of the models in practical settings with the ambition that this work can easily be replicated and applied to other cases and locations where potential renewable generation and demand are not co-located and where curtailment plays a significant role.

With these objectives in mind, this thesis developed several models and outputs, the findings of which can be related to fields of smart energy systems, energy economics, game theory, artificial intelligence and multi-agent systems. The main contributions and outputs of the work are summarised in the following summary statements:

- First, this thesis provided a principled study on different curtailment strategies and their underlying properties. The effects of curtailment rules on the RES capacity installed at a particular location are studied and formalised. The results show that the capacity installed and profitability of different generators can differ widely under different curtailment models. More specifically, this thesis focused on the analysis and study of three widely used curtailment rules and showed, in simulation, the effects these rules can have on the capacity factor (CF) of wind generators. This work also studied the effect of *spatial wind speed correlation* to the resulting curtailment and lost generator revenues. In fact, power network operators face a significant knowledge gap about how to implement curtailment rules that achieve desired operational objectives, but at the same time minimise disruption and economic losses for renewable generators. In this context, this thesis showed that fairness and equal sharing of imposed curtailment among generators is important to achieve maximisation of the renewable generation capacity installed at a certain area. A

competitive analysis approach, modelled as a Cournot game, is used to determine the feasible level of RES capacity that can be built at a single location with network constraints, including the determination of an upper bound of tolerable curtailment. Given the importance of the fairness property, this work proposed a new round-robin rule that minimises renewable generation disruption and number of curtailment events a generator needs to respond, while achieving fair allocation of curtailment between generators of unequal ratings.

- Secondly, a market model was developed for optimal decision making with regards to investments on generation capacity and upgrades or installation of new grid infrastructure at regions that are already experiencing significant volumes of curtailment. This model is analysed in the case of myopic agents, who take decisions without a foresight to the future, and in the case of strategic agents, where players have the ability to forecast their opponents behaviour and take this into account when making their own decisions.

- While other works have studied transmission constraints and congestion (these works are reviewed systematically in Chapter 2), to the best of our knowledge, this work is one of the first to study the effect of commercial agreements and curtailment rules in settings of private grid reinforcement. This work provides a novel formulation in modelling private investment in network expansion required for further integration of renewable generation. The problem under consideration included a two-location setting of a demand and a RES generation site. A private investor, shortly called the 'line investor' builds renewable generation capacity and constructs a power line, but also provides access to other RES generators, shortly called 'local generators', against a charge for transmission. In other words, the privately developed transmission line is shared among all renewable generators and follows a 'common access' principle. This leads to a Stackelberg game between the line and low-carbon generation investors. The decisions on optimal (and interdependent) renewable capacities built by investors, affect the resulting curtailment and profitability of projects and were determined in the equilibrium of the Stackelberg game. Stackelberg equilibria are classified as solutions to sequential hierarchical problems where a dominant player (here the line investor) has the market power to impose their strategies to smaller players (local generators) and influence the price equilibrium. A feasible range of the transmission fee is identified allowing both transmission and generation capacity investments to be profitable. Hence, this work developed a game-theoretic model that enables energy system stakeholders to bridge the knowledge gap of incentivising privately developed grid infrastructure, especially in settings where multiple generators can share access through the same transmission line, and determining suitable transmission charges.

- As a first approach, a simple model based on average values of renewable production and demand was studied. The line investor is the leader of the Stackelberg game,

as he is the first mover and builds the transmission line. The decision variables of investors were assumed to be the renewable generation capacities that players need to install in order to maximise their profit. The decisions on optimal (and interdependent) generation capacities, crucially affect the resulting curtailment and profitability of projects and can be determined in the equilibrium of the Stackelberg game. An average approach, based on expected values of generation and demand, allowed for the determination of an analytical solution to the problem and an initial examination of the Stackelberg game equilibrium properties over a wide range of cost parameters.

- Next, a detailed theoretical model was developed, able to capture the stochastic nature of renewable production and variability of energy demand. A theoretical analysis of the game was presented along with an algorithmic estimation of the equilibrium by utilisation of empirical game theory and real production/demand data from a real network upgrade project in Britain. As opposed to other works in the literature, which assume that the variables under optimisation are represented by simple mathematical functions that allow for an analytical solution of the game equilibrium, in this work, the game equilibrium is found numerically, hence bypassing the need for complex mathematical formulation. Moreover, the emerging strategic game is informed by complex energy system control schemes that lead to a more realistic analysis. The proposed method for equilibrium estimation is general and can be applied to similar case studies, where there is excess of renewable generation capacity and where sufficient data is available.

- In practice, however, available data may be erroneous and may experience significant gaps. To deal with this issue, a method for generating time series data was developed based on Gibbs sampling. A Gibbs sampler was used to to generate observations from historic resource and demand data in order to simulate multiple future scenarios. This allowed for multiple iterations of the simulation analysis with different time series data, on the principles of Markov Chain Monte Carlo (MCMC) analysis, that allowed the exploration of the solution space for multiple future scenarios, leading to a reduction of uncertainties when considering future renewable generation capacity decisions.

- Energy storage represents a promising solution that could reduce curtailment or delay/defer network upgrades. Hence, a new, three-player model was proposed consisting of a line investor, local generators and a third independent storage player, who can purchase energy from renewable generators that would otherwise have been curtailed. The model can estimate optimal capacity decisions on transmission, generation and storage capacity decisions, based on a Stackelberg-Cournot game analysis. An analysis on the operation of the energy system with and without introducing energy storage was performed for comparative purposes.

- Finally, the game-theoretic formulations proposed in this thesis were applied to a practical setting of a grid reinforcement project from the UK and a large dataset of wind speed measurements and demand. Examples of the models applied in practice were based on realistic figures from a network upgrade project in the UK. The financial parameters used for this analysis were released by OFGEM and Scottish Southern Energy (SSE), the local DNO, as part of a public consultation exercise [235]. Practical analysis included the utilisation of public datasets on real wind speed measurements and demand data that span over several years. Throughout the thesis, data is used to develop empirical game-theoretic models and algorithms that enable the search and identification of the game equilibrium. Finally, it is worth noting that, while the numerical application is specific to the UK case, the analysis and equilibrium results are general, and the underlying problem of renewable generation and demand not being co-located occurs in many other places around the globe, facing similar challenges.

In summary, the research work presented in this thesis studied the interplay among self-interested and independent low-carbon technology investors at areas of excess renewable capacity with network constraints and high curtailment rates. The work proposed a mechanism for setting transmission charges that ensures both that the transmission line gets built, but investors from the local community can also benefit from investing in renewable energy and energy storage. Overall, the results of this work show how game-theoretic techniques can help network operators to bridge the knowledge gap about setting optimal curtailment rules and determining appropriate transmission charges for private network infrastructure. The following section presents the outline of the thesis report.

1.3 Thesis outline

Chapter1 presents an introduction and the research motivation to the topic of this thesis. In particular, Chapter 1 presents the energy landscape of current and future energy systems, since the proliferation of renewable generation and deregulation of the energy markets. In this light, game-theoretic modelling and multi-agent techniques are required to model behaviours of independent players or agents that own and manage their own generation assets. The background research highlights the emerging issue of increasing volumes of renewable curtailment at several locations. Chapter 1 introduces curtailment rules and elaborates on the need for private network upgrade investments, two key topics that form the core research area of this work. Research aims and objectives are presented in detail along with a summary of the novelty and main contributions of this research work.

Chapter 2 of this thesis presents relevant literature reviews on the topics of ANM, curtailment strategies, grid infrastructure investment, game-theoretic modelling applied in energy systems and blockchain technologies that could enable local energy markets with direct consumer trading that could reduce curtailment by more better matching of locally produced renewable energy to demand.

Chapter 3 presents the work undertaken in this thesis to study the impact of curtailment mechanisms in the economic performance of generators and on the aggregate generation capacity investment at a particular location. Three curtailment mechanisms, widely used in projects across the UK, were used for the analysis. A new round-robin rule was proposed that ensures equal share of curtailment among generators of unequal rated capacity. Chapter 3 studies desired curtailment rules properties such as fair allocation of curtailment and proved that curtailment strategies that achieve equal sharing of curtailment can actually maximise the generation capacity installed at a single location.

Chapter 4 presents a two-node network expansion model of a line investor and local RES generators. The latter is analysed for two representative curtailment schemes and two agent scenarios, one where the market participants act as 'myopic' agents and the other as 'strategic' players. The model developed is analysed as a Stackelberg leader-follower game with the line investor having the 'first mover advantage' and local generators acting after observing the leader's actions. A closed-form, analytical solution of the game equilibrium is presented starting from average case assumptions. Moreover, Chapter 4 introduces the Kintyre-Hunterston grid reinforcement project, which is used for experimental validation of the models developed in the thesis.

Chapter 5 of this thesis formulates a Stackelberg game model that captures stochasticity of wind generation and variability of demand. A theoretical formulation of the problem is presented along with an empirical algorithmic approach for game equilibrium estimation. The approach followed utilises large datasets of wind speed and demand data that span across 17 years.

Chapter 6 of this thesis uses Gibbs sampling and MCMC techniques to draw correlated samples from the generation and demand distributions of available data, in order to perform repetitive runs of the simulation analysis. The process is crucial for time series data generation and for reducing uncertainties regarding decisions taken by investors on optimal generation capacities to be installed.

Chapter 7 studies the added value of introducing energy storage to the game-theoretic model. A three-player game is introduced in Chapter 7 of a line investor, local generators and a third independent storage player, who is able to absorb part of the renewable production that would otherwise have been curtailed. A comparison of the energy system before and after introducing energy storage is also shown in this chapter.

Finally, the thesis is concluded in Chapter 8, where key findings of the work are summarised. Directions on future work are also discussed in this final chapter of the thesis.

Additional information on the methodology and data used in this thesis are shown in the Appendix.

Chapter 2

Background and related work

Chapter 2 elaborates on the most significant research works relevant to the scope of this thesis, as found in the literature survey. Specifically, Chapter 2 presents the topics of renewable generation curtailment, smart grid solutions that aim to reduce curtailment, smart interruptible commercial arrangements and practices on curtailment rules. Moreover, this chapter presents works on network expansion and grid reinforcement, and on the application of game theory and agent-based modelling applied to energy systems. A review on enabling technologies for curtailment and congestion management is also presented in this chapter including energy storage and blockchain technology.

The first topic presented is generation curtailment applied by network operators when there is an oversupply of renewable generation or when renewable production causes technical violations that may put safe operation of power systems at risk.

2.1 Renewable generation curtailment

Generation curtailment is the total or partial reduction of the power production of a renewable or distributed generator, due to oversupply or network constraints. Large volumes of curtailment mean that an important part of potential renewable production is actually wasted or rejected, as it cannot be absorbed by the power grid.

Predominantly, renewable generators, such as wind turbines or photovoltaic (PV) generators have variable power outputs that primarily depend on time-variant weather conditions. Therefore, renewable production is typically difficult to control and predict. As a result, RES generators raise several challenges to the safe operation and management of power networks. The challenges relate to limited network capacity, increased difficulty in voltage and frequency control management, power quality and reliability issues. The adoption of renewable generation also poses challenges related to the security of supply, system balancing and backup reserve. These challenges can be briefly summarised and are more widely known as *network constraints*. Network constraints refer to the thermal, fault or voltage level violations that might occur during the operation of a RES generator and might jeopardise the safe operation of the power network, and may refer to different voltage levels. For example, curtailment might happen at a system level when constraints

refer to the high-voltage transmission network or at a distribution level i.e. at medium or low-voltage levels.

In more detail, system operators have limited control over the renewable production and in general RES generators cannot be dispatched as other conventional generation assets. This affects the operation and maintenance of electricity networks, markets and thermal generators operation [48]. For example, conventional generators can be displaced by the use of renewable energy, as the power supplied to consumers is significantly reduced, especially in times when primary renewable resources are highly available, such as in periods of high wind. Therefore, the load factor of conventional plants can be seriously affected and reduced, leading to economical implications. Conventional power plants with high marginal costs, such as gas-fired power stations, are mostly affected and displaced by renewable generators.

Moreover, thermal generators are often used as backup generation to compensate for variable RES production or sudden loss of renewable generation. Backup generation is required to provide acceptable security of supply and power system reliability levels. However, as a result, thermal generators are required to start up and shut down more frequently and provide more flexible operation. This leads to higher fuel consumption and increased operation and maintenance costs and CO_2 emissions. Brouwer et al. [33] showed how the efficiency of conventional generators is reduced by the deployment of renewable energy. Specifically, thermal generators are affected by a 4% reduction in their efficiency in the case when wind turbines represent an average of only 16% of firm generation. Flexible operation of thermal and gas-fired power station depends on the technology type. For example, combined cycle gas turbines are more flexible than coal or nuclear power plants and thus more suitable for cooperation with renewable generators [199]. However, flexible operation leads to increased running costs, increased downtime for maintenance and reduced power plant lifetime. These implications might lead to loss of conventional generation, if power plants investors are discouraged to build new power plants or extent the lifetime of the existing ones, leading to unacceptable reliability levels.

RES intermittency and variability increases the requirements for short-term reserves. An early study by Gross et al. [91] estimated the balancing costs of matching demand to supply for the UK electricity system to £2-3/MWh generated, while the costs for maintaining reliability and meeting peak demand were estimated to £3-5/MWh. According to the same study [91], the cost of intermittency and the final contribution to the electricity price was estimated to £10-15/MWh. The study however did not look above 20% of renewable adoption into the UK's generation mix. A more recent study by the same authors revealed that costs can vary significantly across studies depending on the RES penetration considered, hence costs are difficult to estimate. According to a study by the UK Energy Research Centre [98], for RES penetration of up to 30%, short-term system balancing reserve costs reported did not exceed £5/MWh and costs for maintaining reliability were between £4-7/MWh. For 50% RES penetration however, the costs reported were £15-45/MWh and £15/MWh, respectively. According to the same report [98] the transmission and network costs were estimated between £5-20/MWh, for up to 30%

penetration level for the UK energy system. Moreover, [98] reviewed research works that studied the relation of curtailment to RES penetration levels. Studies from the UK and EU suggest that curtailment levels are very low (i.e. below 5%) for low RES penetration and can remain low until over 50% RES penetration. However, other US studies suggest that curtailment can reach very high levels (in many cases surpassing 40%) even at moderate RES penetration levels (around 25-30%). A potential cause for such reported differences may be attributed to the different design characteristics and geographical distances between the US and European grids.

A recent study by Joos and Staffell (2018) focused on the estimation of short-term integration costs for RES generation in countries with high RES development and penetration, like Germany and the UK. In the UK, curtailment costs rose from £5.9m to £81.9m between 2012 and 2016, according to the study. Curtailed energy for the same period rose from 45 to $1,123$ GWh. The largest part of curtailment was allotted to onshore wind development located in Scotland reaching up to 32% of wind annual output curtailed over the 5-year period. Similarly, in Germany wind curtailment increased 27-fold between 2010-2016 with a cost that reached €478m in 2015 (4,722 GWh) [116]. A study by Luo et al. (2016) on wind curtailment in China showed a 10-20% curtailment on wind generation that reached the quantity of 7.2 TWh in 2013 and put great strains in the profitability of the projects themselves [147].

Such issues are even more imminent at remote or weak parts of the grid, such as islands or remote areas far from industrial/population centres, where RES integration is more challenging. Such remote areas can be completely autonomous or connected to the main grid with constrained capacity transmission lines. Inertial response, fast balancing, frequency or voltage control can be challenging in isolated systems, such as islands or systems with large wind integration [103]. The effects of network constraints in remote areas of the grid are widely discussed in [128] and [188].

According to Brouwer et al. (2014) [33], there are two main reasons for generation curtailment, namely the saturated grid capacity or insufficient transmission ability along with renewable generation oversupply. The dominant reason is currently network constraints, while oversupply is responsible for a small percentage, only in areas where large-scale development of renewable generators has already taken place, however this might significantly change in the future as more renewable generation is deployed. Several geographic locations in the UK fall into the latter category, such as the Orkney islands in the north of Scotland. In Orkney, RES generation supplies over 130% of the island electricity demand. However, at times, local demand in Orkney can be low compared to the renewable supply, such as for example during the winter night hours when the wind is strong. Moreover, Orkney is connected to the main grid with a transmission line of saturated capacity. These two factors have led to large volumes of curtailment that surpass 50% of the available RES power for several wind projects in the area. Apart from financial implications, large curtailment in the area has also social implications, as many RES projects are owned by residents from the local community. In addition, according to a recent study, Orkney

consists the area with the largest percentage of fuel poverty in the UK with over 63% of local households living in fuel poverty [184].

Aside technical issues with regards to the operation of power systems, new renewable projects are often rejected or delayed due to saturated grid capacity, costly and time-consuming network upgrade projects. To mitigate such issues and accelerate further deployment of renewable technologies, system operators are increasingly deploying flexibility measures. Measures depend on the causes for curtailment (system-wide or distribution level) and include smarter active network management (ANM) schemes, smart grid techniques, adopting real-time thermal rating of power lines or exploring novel commercial agreements and curtailment strategies. Such solutions are reviewed in the following sections.

2.2 Flexibility measures

As shown in Section 2.1, fluctuations of power system supply due to increasing volumes of RES generation and new peaks in the electricity demand caused by new type of loads, such as heat pumps and EVs, are eventually leading to lower utilisation of power system assets. The decreased utilisation of generation and network assets will eventually lead to increased system costs, as larger capacity requirements are needed to maintain the same level of system reliability [219]. According to Kubik et al. [133], more flexibility is required by conventional generators in order to accommodate larger penetration levels of renewable energy. According to a UK study the net benefit of flexibility services deployed in the UK energy system are estimated in the range of £1.4-2.4 bn/year in 2030 [219]. In addition, other technology solutions may be deployed to mitigate negative effects on system prices including strategies summarised in Figure 2.1. These strategies include energy storage, demand response, building interconnectors and additional grid capacity and application of generation curtailment schemes. Another potential solution is the geographical dispersion of RES generators that might lead to decreased availability uncertainty and can mitigate part of the intermittency effects and costs.

As suggested in Figure 2.1, operational flexibility techniques are relatively low-cost solutions. One such example is adopting smart curtailment strategies, typically deployed within ANM schemes, that can potentially make better use of the available grid capacity, especially at congested parts of the network. Curtailment strategies are the focus of this thesis and are presented in the following sections along with several examples of ANM schemes that operate in the UK. Other solutions, such as investing in energy storage assets or network upgrades are promising and are reviewed in the following sections. Despite recent reduction in storage costs, such as price reduction of Lithium-ion batteries, large scale energy storage solutions still come with high costs, except from pumped hydro storage, which has limited applicability due to geographical limitations. Reinforcing existing power lines or building new grid infrastructure presents a long-term solution, however may have prohibitively high costs and time-consuming procedures. In the following section, operational practices are discussed such as the deployment of ANM schemes.

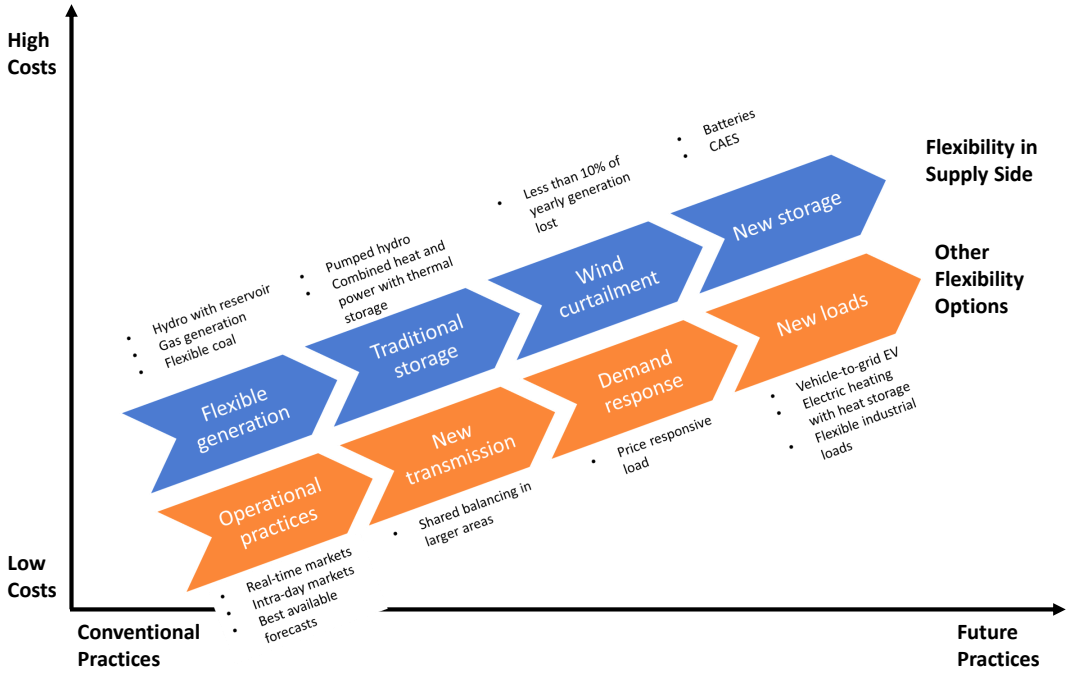

Fig. 2.1 Strategies to obtain power system flexibility adapted from [107]

2.3 Active Network Management Schemes

Integration of renewable energy resources can be increased if Active Network Management (ANM) techniques are implemented. In the UK, ANM is used to increase renewable energy penetration, as an alternative and less expensive approach to network upgrades or reinforcement. In fact, ANM can be used to optimise efficient use of grid resources, before any reinforcement or new network infrastructure is put in place.

A definition of an ANM can be found in a paper published by Liew et al. (2002) [143], where ANM describes *'a network where real-time management of voltage, power flows and even fault levels is achieved through a control system either on site or through a communication system between the network operator and the control devices'*. To achieve this, ANM relies on flexibility, monitoring, control, adaptability and automatic features applied in the network that may not be restricted only to dealing with faults, but include enhanced operation and optimisation of the power system [224]. A general review on ANM schemes operating in the distribution networks, along with techniques of control, monitoring and protection can be found in [272]. A list of several early research and commercial projects implemented in the UK can be found in [151].

ANM strategies can be applied to areas with network constraints, where grid reinforcement cost are high, where there is a significant variation in demand, and where there is diversification of different types of generators [224]. Mitigation of barriers to further deployment of distributed generation has been, in fact, one of the main drivers for ANM development in UK. From the generators' perspective, participation in a ANM scheme can provide a preferable economical solution [49], especially if the alternative of network upgrade is extremely expensive.

Smarter techniques for network constraint management can be part of an ANM strategy. An example of such smart techniques being part of the ANM strategy can be generation curtailment. The Transmission System Operator (TSO) or the Distribution Network Operator (DNO) can control the generators output according to the system needs, in order to ensure safe operation, power system stability and optimal power flows, with respect to the system's thermal limits and technical regulations. The DNO can not only switch on and off the grid the generators, but can also utilise control techniques to set a desired output, for instance by setting a power output set point to a wind generator. Curtailment strategies are analysed in greater detail in the upcoming sections of this chapter.

An additional smart grid technique used by network operators is Dynamic Line Rating (DLR). DLR uses rating technology and instrumentation to monitor the thermal state of the lines in real time and may improve the estimated capacity between 30% to 100%, according to several studies [60, 165].

The following sections focus on the most important ANM schemes deployed in the UK, including 'Orkney Smart Grid' (see Fig. 2.2) and 'Northern Isles New Energy Solution (NINES)', operated by Scottish Southern Energy (SSE) and 'Flexible Plug and Play', operated by UK Power Networks. SSE and UK Power Networks are DNOs operating in the UK electricity system.

2.3.1 Orkney Smart Grid

Orkney consists of a number of islands located just 6 miles away from the north coast of Scotland. The islands are one of the best UK areas for renewable deployment, with favourable renewable resources for wind, wave and tidal generation. Currently, RES generation supplies 130% of the islands' electricity consumption. The location represents an area of high interest for further RES investment. However, the area also suffers from large levels of renewable curtailment. The issue is exacerbated as renewable generators need to share the limited grid capacity available, with resulting curtailment being highly dependent on the cross-correlation and patterns of different renewable resources [24].

Orkney's electrical network consists of a generation mix of gas, wind, wave and tidal. 44.55 MW of wind power generators are currently connected to the grid [209], 2.75 MW of tidal and 2.8 MW of wave power generators [208]. The demand varies from 6 MW summer minimum to 31 MW winter peak demand, respectively. The power grid is connected to the mainland grid through 2×20 MW submarine cables of 33 kV. Moreover, there is a reactive power compensation system consisting of ± 8 *MVAr* D-VAR and 2×7 MVAR, 33 kV switched shunt capacitors. Due to increased volumes of RES deployed in the islands and great variability of local electricity demand, large volumes of renewable generation are curtailed.

To deal with the issues of curtailment, Scottish and Southern Energy (SSE) developed an ANM project called *'Orkney Smart Grid'* [224]. 'Orkney Smart Grid' (see Figure 2.2 for a detailed project map) has been operational since 2012. Generators are separated in distinct zones, according to the network topology, thermal limits and actual network constraints.

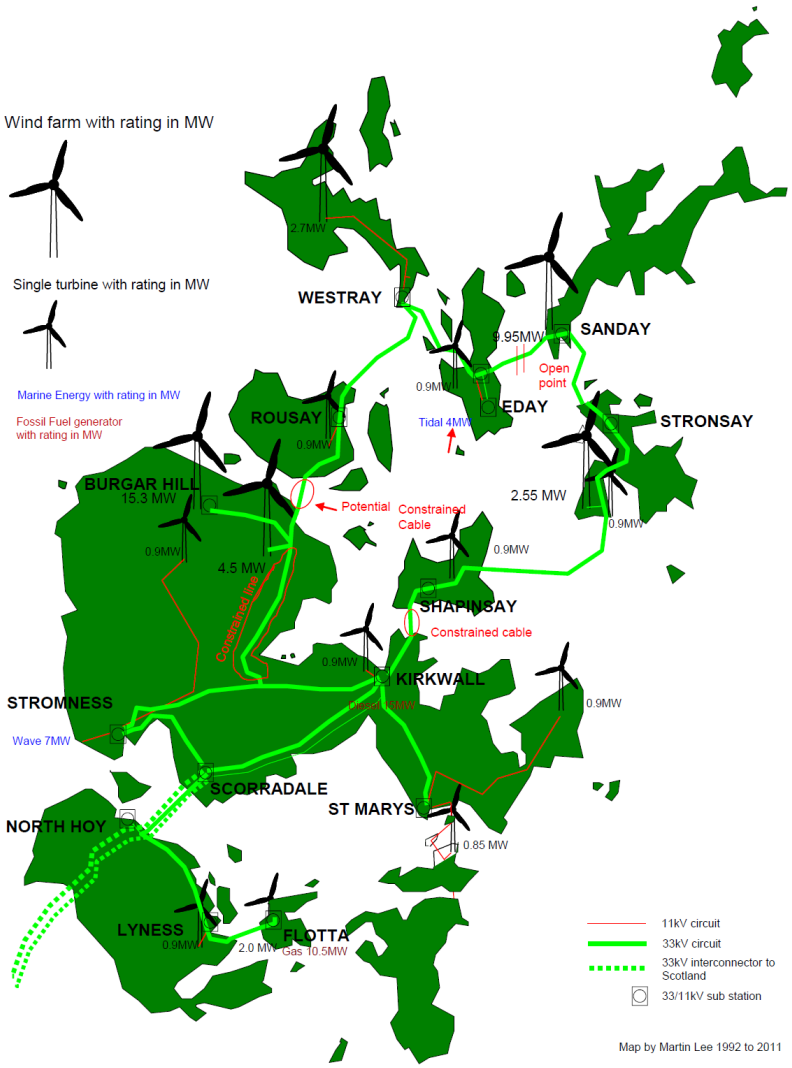

Fig. 2.2 Power network (33kV) at the Orkney islands in the UK [224]

Demand and renewable generation may vary significantly on a minute-to-minute basis, hence the ANM scheme was introduced, which has the capability of controlling the power flow within a time period of a few seconds. Each generator is connected to a local ANM controller, which receives a power output set point from the ANM scheme central controller. Sensing devices in different parts of the network and a reliable communication system are required to estimate and manage the network constraints.

The installation cost of the ANM scheme was estimated at £500 K, and was significantly lower than the cost of a network upgrade solution estimated at £30m. According to official figures, the ANM scheme allowed 20 MW additional renewable capacity to be connected to the existing electricity grid.

2.3.2 Northern Isles New Energy Solution - NINES

'Northern Isles New Energy Solution' (NINES) is an ANM scheme located in the Shetland islands and is operated by SSE, one of the UK distribution network operators [225]. The

Shetlands form a complex of islands 130 miles to the north of the British mainland. The islands are interconnected with each other, but have no have grid connection to the main British network system. As a result, the electric system is islanded and relies entirely on locally supplied generation.

Electric demand varies from a summer minimum of 11 *MW* to a winter peak demand of 48 MW, mostly coming from the largest town of Lerwick. At winter time, there is a large demand for residential and space heating, since the islands have no access to gas resources. The demand for heating is currently met by electricity or oil generators.

The Shetlands are classified as one of most favourable sites in Europe for wind generation. A privately owned wind farm of 3.68 MW nominal capacity, Burradale Wind Farm, and several smaller community wind projects are currently installed. There is high interest in investing in renewable energy, both wind and marine, especially as Burradale Wind Farm has one of the greatest capacity factors in European renewable projects, that surpasses 50%. However, additional capacity is currently not possible due to limited network capacity and ageing grid infrastructure. Further RES generation capacity would lead to imbalances between local demand and supply. Electricity supply comes mainly from diesel power stations. However, Lerwick power station is currently approaching its end of operational lifetime and is mostly operated as a backup for wind generators, causing very low efficiency rates.

The NINES project is led by Scottish Hydro Electric Power Distribution and aims at introducing innovative smart grid technologies and thermal energy storage with the aim to preserve and enhance the reliability and security of supply of the islands' complex. A long-term objective of the project is also the reduction of the system costs. Lerwick power station will be equipped with a battery energy system that allows larger flexibility to deal with the variability of local demand and renewable production. Demand side management techniques will also be deployed. System assets and critical parameters will be monitored and controlled through a communication system and advanced metering infrastructure. Sensing and metering equipment form the core of the ANM scheme, which is able to manage power flows in real time, by utilisation of real-time measurements in the network and automated control [236].

2.3.3 Flexible Plug and Play - FPP

'*Flexible Plug and Play' (FPP)* is a project developed by UK Power Networks, located in the south-eastern part of England [86]. The project aimed to exploit innovative technologies and new commercial arrangements to facilitate and accelerate the connection of RES generators or DGs, at congested areas of the distribution network. The overall implementation cost of the project reached £9.7*m* and the beneficiaries included an excess of 50 MW of distributed generators. FPP deployed an ANM scheme, which identified all critical constraints in the network exploring radio frequency mesh technology [86].

FPP and other ANM projects presented above used novel commercial arrangements and curtailment strategies to allocate the available grid capacity. From the DNO's perspective,

smart grid techniques imply controlling DG power outputs, hence innovative commercial agreements between generators and the system operator are required. Similar schemes have been supported by the UK Government through funding mechanisms encouraging DNOs to facilitate renewable connections [181] and are presented, in greater detail, in the following section.

2.4 Commercial agreements and curtailment strategies

Depending on the size of a renewable development, RES generators are connected to the transmission or distribution network. When connected to the transmission network, i.e. at a system level, generators are centrally dispatched and aim to achieve a unity power factor. Generator connections are legally described in commercial arrangements, in accordance to the relevant Grid Codes and regulatory framework. In order to accommodate RES generators in distribution networks, novel commercial agreements are being considered and increasingly proposed by network operators. A traditional practice in several countries, including the UK, is that when generators cannot fully access the network, such as in the case of network constraints, they receive financial compensation. Similar practices affect adversely electricity prices, meaning that the ultimate cost of curtailment is essentially borne by all end-consumers.

One way to reduce such negative impact and accelerate RES connections, is granting *non-firm connections* or *smart interruptible contractual arrangements* to renewable generators. In this occasion, RES generators agree to be curtailed at the discretion of the system or network operator, as opposed to firm standard connections. Broadly speaking, distributed generators can be offered different types of connection to distribution networks at the discretion of the DNO, which generally fall into two broad categories, standard firm connections or alternative, non-firm connections. Alternative connections represent all cases when a distributed generator agrees to reduce their capacity during times of network constraints. Examples of non-firm connections are [262]:

- **Export limiting** connection: Power output is restricted to a maximum agreed exported power at the point of connection.
- **Timed** connection: A constraint of power output is imposed on specific times of day (typically off-peak day time hours) or seasons (typically during the spring or summer), when demand is low.
- **Soft Intertrip** connection: Power output is constrained when a safe limit of the network operation is breached.
- **ANM** connection: Power output is restricted and orchestrated through the deployment of an ANM scheme.

This work focuses on non-firm ANM connections. The rules for imposed curtailment and order of dispatch are specified and dictated in the contractual agreement between the

generator and the system operator and are widely known as *Principles of Access (PoA)*. Such commercial arrangements give the right to the power system operator not only to switch on and off the power generators, but to control their real-time power output, by specifying power output set points to generating units. This implies that RES generators require additional control capabilities at a plant level. For older technology wind turbines that rely on stall control for limiting the rotor power, curtailment may only be achieved by shutting down completely one or more wind turbines of the wind farm. For pitch-controlled wind turbines or models that permit more advanced power electronics control, curtailment can be achieved by modifying the wind turbine's control system, in order to accept a power output set point, as defined by the system operator.

The terms and conditions of the applied curtailment scheme include the rules of connection of a distributed generator to the power grid along with the order or frequency of the imposed curtailment. Some early examples of wind curtailment practices on an international level, mainly relevant to network management at the transmission level, can be found in a study by Rogers et al. (2010) [213]. Apart from the level of curtailment itself, the curtailment strategy and PoA selected by the system operator, can have severe implications for the generators, the DNO and end-consumers, and may have economic implications for current and future generation capacity investments.

Several curtailment schemes or PoAs have been recommended by researchers, each providing distinct advantages and disadvantages. A general description of the most prevalent curtailment strategies found in the literature can be found in [49] and is summarised in the following:

- **LIFO:** Last-in-first-out strategy curtails first the generator that was last granted the right to connect in the ANM scheme. Clearly, LIFO provides a market advantage to the generators that were connected earlier in time. This scheme is currently used by SSE in the 'Orkney Smart grid' and 'NINES' projects.

- **Rota:** The generators are curtailed on a rotational basis or at a predetermined rota, as specified by the system operator. An early example of the Rota rule applied in a real-world context can be found in a project by Xcel Energy in the United States [216].

- **Shared Percentage or Pro Rata:** The curtailment is shared equally between all non-firm generators. Each generator is curtailed equally at a percentage that corresponds to the rated capacity of the power plant or the actual power output at the time of the network constraint. This strategy was used by UK Power Networks in the FPP scheme. UK Power Networks assessed at a theoretical level, different commercial arrangements to allocate curtailment. LIFO and Pro Rata were both considered, with the company finally proceeding with a proportional to the actual power output curtailment scheme [20].

- **Market-based:** This method requires the establishment of a curtailment market. The generators bid to get connected or to access the network capacity. Alternatively, generators may offer bids to accept curtailment.
- **Technical Best:** This method curtails first the generators which contribute the most in the network constraint. Alternatively, the generators with the most suitable technical characteristics for curtailment at a time period of a network constraint are curtailed first. The practical application of this strategy depends on the network configuration and type of constrains.
- **Greatest Carbon Benefit:** Curtailment priorities are linked with carbon emissions of the generators. More specifically, with this scheme, the generator with the largest CO_2/MWh emissions is curtailed first.
- **Generator Size:** The largest generator contributing to the fault is curtailed first. By generator size, either the rated capacity or the actual power output at the time of constraint can be considered.
- **Most Convenient:** The generator most likely to better respond to the network constraint is curtailed first. This scheme relies on historic responses of generators and practical knowledge of the system operator.

The determination of the most suitable strategy needs to account for technical, commercial and regulatory implications of each approach. Consequently, several assessment criteria can be used to evaluate the proposed strategies. The criteria as stated in several research works [23, 49, 62, 124] can be summarised in the following:

1. Fairness and transparency
2. Simplicity and practicability
3. Provision of efficient network operation
4. Assurance of safe, secure and reliable power system operation
5. Minimal impact on existing connection agreements
6. Sustainability and robustness to ensure future application
7. Compliance with regulations, codes and standards
8. Incentives of investment and support from stakeholders
9. Facilitation of low carbon technologies

An extensive review of different rules can also be found in more recent papers by Anaya and Pollit (2015) [7] and Kane and Ault (2015) [126]. Currie et al. (2011) [49] suggest that LIFO and market-based strategies outperform other approaches, when it comes

to the assessment criteria. Pro Rata offers transparency and equitability and can be used in combination with other strategies. Greatest Carbon Benefit favours renewable generation, as opposed to conventional or thermal-based generation. Therefore, on the one hand, it is not fair for all types of generators, but on the other hand it might contribute to EU policy about carbon emissions. In addition, the curtailment strategies were assessed in terms of their suitability with regards to a time framework. LIFO and Pro Rata were found easy to implement for a short-term basis, LIFO, Pro Rata and Market-based for the medium-term and LIFO, Pro Rata, Market Based and Greatest Carbon benefit were found suitable for a long-term basis due to their requirement for more complex and structural transformations. The PoA options chosen by DNOs follow different approaches and each rule has both advantages and disadvantages in achieving desired objectives, such as cost-effectiveness, economic efficiency and social optimality [6].

Kane et al. (2013) [125] presented a review of PoAs focusing on ANM schemes operating in distribution networks with wind generation. Four PoAs were compared, LIFO, Pro Rata, Market-based and Technical Best. The authors presented numerical results that compare different strategies based on figures from Orkney's electricity system. Potential discouragement for future deployment of renewable generation capacity installed was particularly stated in this paper. For example, if the Pro Rata approach is used, the capacity factor of generators was estimated to decrease as more capacity is installed, leading to larger uncertainty on the viability of future investments in the long term.

In a subsequent work, Kane et al (2015) [126] presented a quantitative analysis of curtailment strategies and their impact on the capacity factor (CF) of wind generators. CF is a widely used parameter in electrical engineering, equal to the ratio of the actual energy generated by a certain resource over the maximum energy it could generate, if operating under nominal conditions. Note that the CF of a typical wind turbine (even if output is never curtailed) depends on wind conditions at the site's location with typical values around 30%. Three arrangements requiring minimal changes in a regulatory level were considered: LIFO, Pro Rata and Rota. As shown, the minimum CF can increase significantly with the Pro Rata and Rota arrangements, as opposed to when compared to a LIFO approach. LIFO arrangements favour early connections and can potentially discourage future generation capacity expansion and investments.

In a study for UK Power Networks, LIFO was considered potentially inefficient since it does not promote optimal network use, especially in comparison to Pro Rata. Locations with favourable renewable resources are most likely to attract a larger pool of investors, therefore it would be reasonable to optimise the potential and energy outputs of these locations. Any PoA in favour of additional total generation capacity, can be beneficial from a social optimality perspective. Estopier et al (2013) [68] proved that while the volume of curtailment, or in other words the sum of curtailed energy at a certain location can be similar for different PoA, the most important factor affecting the decision-making of a future investor, was the capacity factor of the last generator to be connected at the ANM scheme, thus Pro Rata would in principle allow more future generation capacity than a LIFO arrangement.

Principle of Access/Curtailment order	Advantages	Disadvantages
LIFO: Last generator	Simple configuration No impact on existing connections Easily computable capacity factor Consistent and transparent	Not equitable Not favourable to RES generators Inefficient use of distribution network Generation capacity disincentivisation
Rota: Rotationally	Smaller capacity factor reduction with increased units	Greater impact for small-sized generators
Pro Rata: According to rated capacity or power output	Equitable Compliant with existing rules and standards Enhances competitiveness	Unknown long term impacts on capacity factor Increased curtailment for additional units Possible need cap generation connected
Market Based: Bidding for grid access or curtailment	Sustainable and future proof No impact on existing connections Enhances competitiveness	Necessity of market development More suitable for transmission than distribution networks
Greatest Carbon Benefit: Larger CO2 emissions generator	Easy technical implementation	Commercial implications Not easy to determine carbon footprint Needs regulatory changes
Generator Size: Larger generator	Quick removal of constraint	Possible discouragement of large generators
Technical Best: Most technically suitable	DNO Encouragement for grid reinforcement	Location dependable
Most convenient: Most likely to respond	Simple method	Discrimination on operator preference, size and location Not fair, not transparent

Table 2.1 A summary of the main features of common curtailment strategies according to relevant literature: [49] provided an assessment of different PoAs for interruptible contracts with respect to different criteria and stakeholders, [23] identified a range of different criteria for assessing the most suitable PoA for ANMs, [62] focused on technical challenges caused by increased wind penetration and [124] provided a comprehensive review on PoAs quality assessment for ANM settings

In a technical report by Baringa and UK Power Networks [20], an extensive and detailed comparison of different curtailment strategies was presented along with a comparative study regarding the criteria of network efficiency, certainty, simplicity, fairness and learning. Moreover, this study estimated to which extent an ANM is sufficient to allow more network capacity before a grid reinforcement or new grid infrastructure is actually required. Initially, a minimum capacity factor needs to be specified at a certain location, which allows the investment to be viable. Then, a maximum curtailment is calculated. When the level of curtailment exceeds this threshold, grid reinforcement is required. Throughout the project lifetime, the costs of curtailment are due to increase, while the cost of infrastructure decreases. The time period when these two curves meet is suitable for grid reinforcement. This method is therefore used to defer or delay any grid expansion. A further comparison between traditional connections with network upgrade to smart interruptible connections was performed by Anaya and Pollitt (2015) [7] in the form of a cost-benefit analysis.

The most important features of the proposed PoAs are summarised and presented in Table 2.1.

Novel commercial arrangements include also techniques to couple demand with distributed generation to achieve managed and controlled power export capability at specific points in the grid. Most notably, SP Energy Networks trialled such concepts in the south east region of Scotland through the 'Accelerated Renewable Connections' (ARC) project [88]. The project tested several architectures for energy systems in distribution networks comprising both of generation and demand:

- **Physical private wire** systems: Connection between generation and demand site is achieved through privately owned grid assets, moreover the generation/demand scheme is connected to the DNO-owned network through a single connection point.
- **Virtual private wire** systems: Connection between generators and flexible demand (one large demand site or multiple smaller flexible demands) is achieved through the DNO-owned network and operation of scheme needs to be managed behind a point of constraint.
- **Demand aggregators**: Multiple flexible demand here is represented by an aggregator acting as a single point of contact for the ANM scheme.
- **Local markets**: Both generation and demand sites participate in local markets to modify their energy profiles and avoid congestion.

Smart and interruptible connections can accelerate distributed generator connections, however a long-term solution would be to invest in new grid capacity investments. The following section focuses on relevant works found in the literature on network expansion with specific focus on works that apply game-theoretic modelling and AI techniques.

2.5 Network upgrade investments

Grid infrastructure development can provide an alternative to ANM in the mitigation of network congestion and energy curtailment. Nowadays, power network upgrade is mainly driven by increasing demand, energy market competition, requirement for security of supply and renewable energy integration.

Network expansion provides curtailment reduction, while enhancing competition in the deregulated electricity market. The generators can benefit from increasing their efficiency [221], leading consequently to cost reduction and lower electricity prices. Interconnection of geographically dispersed areas of the network allows remote sources integration and reduces uncertainty in forecasting of generation and demand, hence resulting in greater security of supply. The probabilities of unserved load or generation breakdown decrease with interconnection, leading to a significant improvement in the reliability of the system. In addition, potential future uncertainties can add further value to network capacity expansion investments [160]. Such uncertainties relate to fuel prices, carbon prices, costs for transmission, capital costs for RES generation, changes in markets, changes in regulatory frameworks and potential demand growth [102]. On top of strictly financial or technical benefits, Chamorro et al. (2012) claimed that grid expansion adds a strategic, environmental and social value, which is difficult to be counted in monetary value [42].

Increasing network capacity is performed in two ways, by reinforcement of existing grid infrastructure or by building up new distribution/transmission lines. The cost of increasing network capacity can often be prohibitive. According to Saguan et al. (2014), transmission investment is based on imperfect regulatory frameworks and forms a significant part of the renewable energy cost in the EU [218]. Grid expansion investment is characterised by high capital costs with Operation and Maintenance (O&M) cost depending on the power line technology and location. For instance, sub-sea cables present higher capital and O&M costs than overhead power lines.

Grid expansion is traditionally planned at a 5-15 years time horizon and performed by network operators, such as the TSO or DNO. However, the increasing development of RES generation have introduced private or merchant investors to grid infrastructure deployment, who may charge congestion rents. Individual objectives and interests of line investors, therefore, depend on their actual type and can be conflicting [222]. Network operators, the operation of which is typically controlled by an independent regulator, aim to maximise social welfare, while private investors aim to maximise their profits [157].

In this work, game-theoretic modelling is used to study the strategic decision-making of private investors deploying transmission capacity investments. The interaction of different market players along with externalities of technical, economical or regulatory factors dictate the system behaviour or an economic market equilibrium. Several mathematical principles can be used in modelling the electricity market, such as microeconomic models [47] or game theory [41]. Game theory represents a field that can explain complex strategic

behaviours that emerge by the interplay of different players. Relevant works related to this vein are discussed in detail in the following section.

2.6 Game-theoretic modelling and optimisation in network upgrades

Load forecasting techniques and generation capacity planning are utilised to design reinforcement or new power lines, which minimise financial and environmental costs, while ensuring safe and reliable operation. The decisions are typically supported by simulation analyses and load-flow models. Traditionally utilities have relied on intuitive approaches for the decision making, rather than using optimisation techniques [102]. According to Hobbs (1995), game-theoretic models were scarcely used by utilities since they add complexity and use simplistic assumptions [102]. On the other hand, research has focused in game-theoretic models, as a tool to demonstrate and simulate the effects of market regulation or decision-making. An overview of game-theoretic modelling is presented in [215] including Stackelberg game and Cournot game formulations, who form the core research of this thesis.

Stackelberg game equilibria are classified as solutions to bi-level problems where a dominant player has the market power to impose his strategies to smaller players and influence the price equilibrium. A Stackelberg game is a noncooperative game, originally played in two levels of hierarchy. The game consists of a leader or first-mover player, who dominates the market, and one or multiple followers, and it is also known as leader-follower competition. The players are rational and act to serve best their own interest, usually represented by a goal to maximise a certain utility, quantity or objective function. The leader decides its strategy by anticipating a certain response from the follower with ultimate target to maximise its own utility or profit. On the other hand, the follower observes the leader's strategy and decides to act according to its best response, or best strategy, which maximises the followers utility, given the strategy of the leader. The solution of this strategy game is known by the name *Stackelberg game equilibrium* [252].

In a Stackelberg game, the follower has to observe the leader's strategy and act as expected, while in a Cournot game, no player has a market advantage, meaning that players do not know their opponent's strategy and act simultaneously. At a Cournot game, the player anticipates to influence the market (typically represented by the supply-demand curve) through the inverse demand curve [47].

Stackelberg game formulations are frequently used in the security domain to model attacker-defender problems [191] or in other domains, such as efficient test designing [142]. In the energy systems domain, Stackelberg games have been used in several works for modelling transmission upgrades. These works considered economic analysis with social welfare [221], locational marginal pricing [228] or highlight the uncertainties introduced by the adoption of RES technologies [249]. Other works in the renewable energy domain used Stackelberg game analysis to study energy trading among microgrids [17, 139]. Lee

et al. (2015) developed a game-theoretic model of strategic players that is modelled as a multileader-multifollower Stackelberg game that converged to a unique equilibrium solution, which maximises the pay-off of the participating microgrids [139]. Other works in the same vein, aimed to minimise power line losses [217] or generation and transmission costs [154]. Asimakopoulou et al. (2013) used leader-follower strategies for analysing hierarchical decision making in competitive situations with multiple microgrids [17]. Zhu et al. (2017) suggested a crowdfunding scheme for the development of EV charging infrastructure, modelled as a three-level Stackelberg game between the utility company, the charging infrastructure operator and crowdfunders [276]. A Nash-Stackelberg game between two leaders and two followers is proposed in [146] for an energy system with users that can engage in demand response. A multileader-multifollower game is established in [261] to model multiple trading between distributed generators and consumers. DGs declare their prices in the market and consumers determine the energy quantity consumed according to supply prices. The majority of the aforementioned works assumes well-defined cost functions and follows an analytical approach for the analysis of the game. The work developed in this thesis follows a different approach that determines equilibrium results by virtue of simulation analysis and real large-scale dataset analysis, and considers energy flows, as dictated by control management schemes of the energy systems under consideration.

Game-theoretic approaches can add value, especially in the context of deregulated electricity markets. Once state-owned and monopolistic, markets are transforming to being competitive [121]. Traditional cost minimising techniques are being substituted by market models of self-interested private firms, which aim to maximise their profit while also competing with other rival firms. Introduction of competition in power networks remains challenging due to the nature and cost of the power network itself. However, as market transition affects generation planning, consequently grid expansion investment is also affected. Game-theoretic tools can be used by private investors to forecast future prices, decide market strategies and capacity investments. Regulators can use these models to assess players' strategies, infrastructure investment and estimate strategic behaviours and their effect on electricity prices and market efficiency. A detailed review on strategic interactions in oligopolistic markets is presented in [51], including Cournot game and Stackelberg equilibria used in this work. Moreover, several authors state that game-theoretic models, non-cooperative and cooperative, can be used to assess market behaviour of energy players, in a more realistic way [121]. This work aims to explore the feasibility and value of game-theoretic tools in the energy systems context and in particular relevance to grid capacity investment.

Van der Weijde et al. (2012) developed a two-stage bi-level optimisation model to evaluate network expansion and grid reinforcement, in the UK. At the first stage, a line investor decides on the transmission investment. Subsequently, the market response from energy producers is observed, which accounts for risks at a technological, economical or regulatory level. At the second stage the transmission investment is optimised according to the anticipated market response. Decisions taken in the second-stage are subject to first-

stage decisions. The model developed in [249] considers uncertainty and leads to lower cost decisions than the ones taken under deterministic methods. Baringo and Conejo (2012) claimed that stochastic mathematical programs with equilibrium constraints (MPEC) are suitable for analysing wind generation and transmission investments [21]. Moreover, the authors stated that small subsidies can potentially boost wind power investment. Chamorro et al. (2012) developed a multivariate stochastic model and optimisation techniques that can be used from utility companies or private investors to evaluate potential benefits of network upgrades. The model developed captured uncertainties in the supply and demand side [42].

The relation of grid investment to generation capacity is examined by Maurovich-Horvat et al. (2015) in [157] through a bi-level model in which the line investor decides the transmission capacity in the first level, followed by the investment decisions of the producers at a second level. The model developed is stochastic and able to capture the wind variability. Cournot equilibria and perfect competition market design are both examined in the paper. The work used Mathematical Programming with Equilibrium Constraints (MPEC) to solve power flows, but curtailment strategies were not considered in the work.

Other authors have formulated more complex models that are harder to solve, where decisions are taken in three levels. At the first level, the TSO decides the network upgrade investment with the objective to maximise social welfare. At a second level, self-interested producers decide on their generation capacity, while market clearing is achieved at the third level [221, 222]. Grid expansion at a national level was studied by Huppmann et al. in [104], as a three-stage hierarchical Nash game.

Many works have focused on network expansion planning techniques that incorporate multi-objective optimisation, such as in [81, 234] with special focus on distribution network expansion. Arabali et al. (2014) [15] considered complex optimisation criteria that combined consideration of investment and congestion costs, and the system's reliability. Akbari et al. [3] provided a stochastic short-term transmission planning model based in Monte Carlo simulations, while Zeng et al. (2016) [270] considered a multi-level optimisation approach for active distribution system planning with renewable energy harvesting, taking into consideration grid reinforcement and operational constraints. In [80, 122], the authors studied distributed generation expansion planning with game theory and probabilistic modelling with strategic interactions, respectively. Other works considered an integrated model for both generation and transmission capacity [21, 95]. Motamedi et al. (2010) [169] studied how generation capacity decisions may impact on transmission planning. They used agent-based modelling to study energy producers' behaviour with respect to transmission investment decisions.

Traditionally, grid infrastructure investment is assessed by evaluation of the social impact. Sauma and Oren (2006) recommended equilibrium models for the assessment of the economic impact, taking into account competitive interactions between producers in oligopolistic electricity markets that might emerge. Subsequent decisions on generation capacity investments are highly influenced by transmission capacity projects and congestion management protocols or curtailment mechanisms [221]. Game theory techniques for

distribution network tariffs determination were discussed in [186] with the objective of maximising social welfare.

Several works have discussed private investment in the field of grid infrastructure. Contreras et al. (2009) [115] introduced an incentive scheme based on the Shapley value to encourage private transmission investment. Maurovich-Horvat et al. (2015) [157] compared two alternate market structures for grid upgrades (either by system operators, such as the TSO, or private investors) and showed that they can lead to different optimal results. The authors found that social welfare is maximised under the TSO, since the private investor has a self-interest of withholding capacity to increase congestion rents. Moreover, this implies that the generation capacity is lower in the private investor case than in the TSO case. Perrault and Boutilier (2014) used cooperative game theory and coalition formation to coordinate privately developed grid infrastructure investments with the aim to reduce inefficiencies and transmission losses. Their findings point out there is a risk of decreasing efficiency due to transmission losses, if grid infrastructure investment is not controlled by the regulator or DNO, but performed by private investors [193]. The main focus of their work was the group formation and its results in configurations of multiple-location settings, not the effects of line access and curtailment rules, which form the scope of this thesis.

Moreover, in the above works, curtailment strategies and line access rules were not considered, albeit several works considered transmission congestion management protocols. An early study by Fang and David (1999) analysed transmission congestion management techniques for independent system operators in electricity markets [77]. Singh et al. (1998) analysed transmission costs in congested areas of the grid and in two model scenarios, a pool model based on nodal pricing and a bilateral model based on a game-theoretic analysis [230]. Other works consider transmission planning or expansion at congested areas of the power network. Joskow and Tirole (2000) analysed a two-node network market behaviour for settings of players with different market power and allocation of transmission rights [119]. The work analysed market behaviour and equilibrium prices in congested areas of the network. The work presented in this thesis estimates optimal transmission, generation and storage capacity investment decisions, as opposed to price decisions, at network areas where curtailment is large. Gu et al. (2017) developed a methodology for designing dynamic tariffs, imposed to generators participating in demand response schemes, that considered network costs, computed as a trade-off between congestion and investment costs [92].

The following section discusses research works that apply game-theoretic modelling in other key areas of energy systems or the power sector.

2.7 Game-theoretic applications in energy systems

In recent years several researchers have begun to show the benefits of game-theoretic, multi-agent modelling and artificial intelligence (AI) techniques applied to power markets, including for studies of distributed or intermittent RES integration. One such prominent

example in the multi-agent and AI community is the Power Trading Agent Competition, also known as PowerTac [129]. PowerTac aims to explore and simulate strategic behaviour of trading agents in real-time electricity trading markets. Game-theoretic models have been utilised across a wide spectrum related to energy systems and markets, such as the application of demand-side management [131, 141, 150, 267], virtual power plants (VPPs) [210, 211, 231, 251] and cost-sharing in electricity purchasing [194].

In the demand response domain, Kota et al. (2012) suggested the formation of consumer coalitions for demand side management using multi-agent mechanisms [131]. Li et al. (2015) used a supply function bidding method to distribute demand response according to the power system's needs in competitive and oligopolistic markets [141]. The method developed, took into account the supply uncertainties coming from the increasing number of renewable generators. Allocation of demand side management requirements to multiple consumers at minimum consumer utility loss was investigated in [267]. Ma et al. (2016) proposed a mechanism design policy that rewarded reliability in demand response schemes [150]. The work focused on uniform-price mechanisms and formulations of Bertrand and Cournot market competition. The article showed that the proposed methodology achieved best results with regards to social optimality for a competitive market structure. Castillo-Cagigal et al. (2018) developed an agent-based coordination algorithm for demand side management in electricity grids with distributed energy resources [38].

Both cooperative [271] and non-cooperative [238] game-theoretic models were used for the purpose of market clearing of deregulated electricity markets or to model operation of microgrids [198]. Wu et al. (2016) [264] discussed coalition formation and profit allocation of RES generators within a distributed energy network with controllable demand. Min et al. (2013) [168] followed an approach based on the Nash equilibrium concept to model generators' strategies.

Cooperative game theory was utilised in [211], where several distributed generators join coalitions in order to obtain similar characteristics to conventional generators, similarly to the operation of VPPs, such as enhanced predictability that facilitated the system supply schedule. Coalitional game theory was used for efficient tariff design in [212]. Robu et al. (2014) developed an efficient model of buyer groups using prediction-of-use electricity tariffs. The model managed to increase the predictability of consumer aggregate consumptions, and simultaneously encouraged consumers to abide to their predicted consumption patterns.

Pricing and cost-sharing of electricity group buyers in smart grids were investigated in [194]. Tools from cooperative game theory, such as the fairness metric of the Shapley value [214] were utilised to achieve fair cost-sharing and facilitate coordination.

Finally, these models can also be used in designing novel funding schemes for renewable projects. For example, Zheng et al. (2015) developed a novel sequential game-theoretic model for RES investment through crowdfunding [273]. The market participants involved an electricity supplier, the RES project owner and the crowdfunders. It was concluded that this innovative scheme can increase renewable energy penetration levels and reduce electricity costs. Investment in transmission/distribution assets however was not in the

scope of the work. In an similar fashion, Zhu et al. (2017) suggested a crowdfunding scheme for the development of EV charging infrastructure [276].

The following sections are dedicated to discussion of enabling technologies that could mitigate renewable energy curtailment and achieve better integration of renewables. A promising solution in this context is energy storage.

2.8 Energy storage

Multiple sources identify Energy Storage Systems (ESS) as a key factor and integral part of the agenda for low-carbon transition and sustainable future energy systems [100]. According to the US Sandia National Laboratories, up to date over 187 GW of energy storage capacity has been deployed at a global level [220]. The largest contribution is by far Pumped Hydro Energy Storage (PHES) accounting for over 96% of the total global storage capacity installed. However, it is increasingly being reported that electrochemical storage deployments have also risen in recent years and have reached approximately 3.3 GW of installed capacity worldwide. Only in the US, by the end of 2017 approximately 708 MW of large-scale batteries were connected to electricity grids [67]. A timely analysis on the development of energy storage in the US predicted that annual energy storage deployments will surpass 4.5 GW by 2024 and will reach a market value of $4.8 billion [263]. The potential for energy storage, according to a study by McKinsey could exceed 1 TW in the next 20 years [50]. In the UK, planning applications for energy storage projects exceeded 6.8 GW in 2018, an unprecedented rise from only 2 MW contracted in 2012 [207]. According to the same source, more than 4.8 GW of battery energy storage has planning consent and will be added to 3.3 GW of storage capacity already installed.

EES are diverse and each technology type has varying technical characteristics. EES can store energy across different geographical and time scales. Arguably, the most important technical characteristics of energy storage are the power capacity, energy capacity and the rate at which energy and power can be stored in the system and extracted from [140]. Other technical features may be equally important depending on the use case and application intended for storage, such as its useful lifetime, round-trip efficiency, response speed, ramping rate, weight-to-energy ratio, availability of materials, scalability, safety and reliability. Evaluation and apprehension of different technical characteristics and their implications are key factors in the identification of most suitable technology types and their potential applications. Moreover, ESS applications need to be beneficial and profitable, hence the actual cost of storage represents a key factor determining ESS investment decisions.

Well-known energy storage technology types for grid applications are Pumped Hydro Energy Storage (PHES) and Compressed Air Energy Storage (CAES). Both technologies are large scale and suitable for seasonal storage of energy. PHES represents the largest category in storage capacity worldwide and is a mature technology that has been around for over a century. Typically, PHES is used for load balancing. When energy demand is low, energy surplus is used to pump water uphill into a higher elevation reservoir, while

at times of peak demand, water is released and used to generate power through hydro turbines. With PHES, energy is stored in the form of potential energy. PHES schemes can be cost-effective, especially when natural reservoirs and elevation differences can be exploited. However, there are geographical limitations on suitable locations for PHES deployment and concerns about the environmental impact of such projects. CAES follows a similar operating principle by storing low-price electricity or RES generation surplus in caverns in the form of compressed air. CAES projects are limited however, with only three projects currently being operational [220]. Similarly to PHES, cost-efficiency can only be achieved in favourable geographical locations. For example, a study by Locatelli et al. (2015) found that unsubsidised PHES and CAES are not cost-effective in the UK [144]. A different approach is Power to Gas (P2G) i.e. storing energy in the form of hydrogen or methane. P2G is a promising solution especially in countries with already established gas networks, like the UK, but the technology is still at a demonstration level. A detailed recent review on large-scale storage and technology types can be found in [28].

Other systems store energy in the form of electrochemical storage, such as in Battery Energy Storage Systems (BESS), like Lead-acid, Lithium-ion and flow (redox) batteries. BESS are widely considered as a potential solution for further improvement on RES integration, power system reliability and grid flexibility. Electrochemical storage represents a category of storage with great diversity. Lead-acid batteries are one of the most mature battery technologies, however they have a poor performance with respect to their expected lifetime leading to large life-cycle costs. Lithium-ion batteries outperform lead-acid batteries with respect to their expected cycle life. Moreover, Lithium-ion batteries have high energy density, fast response capability, high round-trip efficiency, low self-discharge rate and high weight-to-energy ratio. The latter is one of the main reasons for adoption of Lithium-ion batteries for electric mobility applications, which has led to significant cost reduction in the recent years in the range of $200 per /kWh of capacity installed. Numerous sources predict further reductions of the cost in the following years. A survey by Bloomberg, for instance, predicted an average Lithium-ion battery pack to cost around $94/kWh by 2024 and $62/kWh by 2030 [31]. However, additional cost reduction is required for further adoption of energy storage in power and energy applications, especially for reaching full decarbonisation. A recent study [277] found that energy storage costs need to reduce to $20/ kWh to be competitive and enable energy systems that rely 100% on renewable generation. A promising technology for grid storage applications, still at demonstration phase, is flow batteries, such as vanadium redox flow batteries. Flow batteries have good life cycle performance, which does not depend on the depth of discharge. Moreover, energy and power in flow batteries are decoupled [140]. On the other hand, they require more complex and sophisticated control mechanisms for operation and currently experience high costs. A detailed review on energy storage and batteries can be found in [79].

In recent years, there has been a growth in interest of battery technologies for grid operation. Historically, high costs have limited the extensive use of battery storage devices for such applications, however different factors such as financial incentives, technology

advances and economy of scale expected by the growth of electric vehicles (EVs), are anticipated to be game-changing. Battery energy systems are a key pillar of smart grid applications. Compared to other storage solutions, battery devices provide several advantages such as high efficiency, fast response time, ability to scale and have no geographical limitations. The potential for batteries and energy storage systems expands in multiple use cases and applications and the value added to energy systems has ever been increasing in line with increasing adoption of variable and intermittent RES generation [120].

Promising use cases and applications highlight the importance of storage for integration of renewable generators in current and future energy systems [55]. ESS can mitigate some of the challenges faced due to the stochastic nature of renewable generation, such as to prevent voltage violations, match demand to supply and provide ancillary services that enhance power quality and reliability. ESS can provide load support in cases of power system contingencies or sudden increase of the energy demanded, playing the role of reserve power plants. Moreover, battery storage can reduce transmission and distribution losses [176]. Utilisation of storage devices can lead to network upgrade deferral, enhanced utilisation of distribution assets and lower power supply costs [96]. Energy storage applications vary from power quality applications, grid services, regulation, frequency response, voltage control [161], black start service provision and can also be sued for investment deferral or voltage excursion support at distribution level. An ever increasing challenge that network operators face are voltage excursions caused in residential distribution feeders that can cause thermal wear of grid assets especially in sunny/windy periods with insufficient local demand. For instance, the generation from PV arrays is at its highest point at noon, when household consumption is low. Usually, the peak residential demand is observed in the early evening, leading to a mismatch between generation and demand that can lead to voltage excursions and undesirable reverse power flows [256]. Fluctuating power output from PV generators can be mitigated by small storage capacity placed locally. In fact, the installation of distributed energy storage in the low-voltage (LV) part of the network may be cost-effective, especially when PV penetration is high, operation is close to the technical rating limits or in the case of unbalanced loads [25]. Additionally, batteries can be placed to support heavily loaded distribution feeders, by reducing the peak demand of the distribution transformer and thus improving the useful lifetime of distribution network assets [205]. Battery storage can be placed in several grid locations at feeders or substations, at medium-voltage (MV) [106] or LV level [25].

Battery storage systems can also mitigate transmission congestion. Several research works have considered battery storage systems in transmission expansion planning [1, 36]. Placing a storage system at congested areas of the grid can extend the lifetime of transmission assets that operate close to their operational limits and enhance their remaining useful lifetime. Transmission congestion relief can be achieved with ESS at a much lower investment cost than investing in additional transmission capacity [140].

In addition, energy storage systems and batteries can be utilised to minimise undesired curtailment. Vargas et al. (2014) combined wind power projects with energy storage systems to achieve mitigation of curtailment in transmission congestion management

systems and dispatching decisions [250]. By adopting a similar operating principle as an energy arbitrage application, curtailment can be reduced. Energy arbitrage aims to charge storage devices when prices are low (typically this occurs when demand is low or RES generation is abundant) and export back to the grid when prices are high (typically at peak energy demand times). Similarly, batteries can be used to store RES energy surplus that would otherwise be curtailed. Crucially, the economic viability of such endeavours depends on the cost of storage, but also on the ability to generate sufficient revenue, such as the price of energy obtained when energy is exported to the grid. This application is of particular interest for this study and an analysis of the topic is presented in Chapter 7.

Detailed reviews on battery and energy storage systems and their applications can be found in [78, 148]. Key applications for BESS and their positioning with regards to system ratings and time scale are shown in Fig. 2.3, according to a study performed by the Electric Power Research Institute (EPRI). The classification highlights not only the importance of the size of storage capacity, but also the response time a storage system can deliver its rated power. The latter may vary from a few seconds for supercapacitors or superconducting magnetic energy storage to several hours, weeks or months for PHES and CAES.

Comparison across different types of technology is difficult as storage systems may differ significantly in their technical characteristics and operational conditions. A common approach to deal with these difficulties has been to compare storage profitability for particular applications. Different technologies are compared in the literature by utilising a parameter called Levelised Cost of Storage (LCOS) or life cycle cost i.e. the discounted cost of electricity per unit of discharged electricity. LCOS represents the real cost of storage per energy discharged or delivered by the energy system throughout its lifetime. Zakeri et al. (2015) presented a review on electrical energy storage systems and their comparison on life cycle costs [269]. Other comparative studies on energy storage costs can be found in [112, 138].

Cost of storage including LCOS depend highly on the expected lifetime and battery degradation mechanisms. BEES experience reduced capacity with operation, due to 'cell ageing' and irreversible chemical reactions taking place during charging/discharging. Complex factors affect the Remaining Useful Lifetime (RUL) of batteries such as the depth of discharge and the ambient temperature during operation. Prediction of RUL of batteries is possible by Physics of Failure models and increasingly by utilisation of data analytics and machine learning techniques. Unlike model-based approach, data-driven approach does not rely on the physical modelling of cell degradation. It uses historical data and battery metrics (such as current, voltage, battery and ambient temperature) to derive a non-parametric model and develop trends that can predict future asset behaviour [14]. Research works use machine learning methods for asset health management of batteries, can be found in [44, 177, 229]. In [14, 241] the RUL of Lithium-ion batteries was predicted by using a machine learning technique, based on relevance vector machine (RVM). The data used for the analysis was open-source, life cycle test data from the National Aeronautics and Space Administration (NASA) battery repository. Results showed the proposed algorithm is able

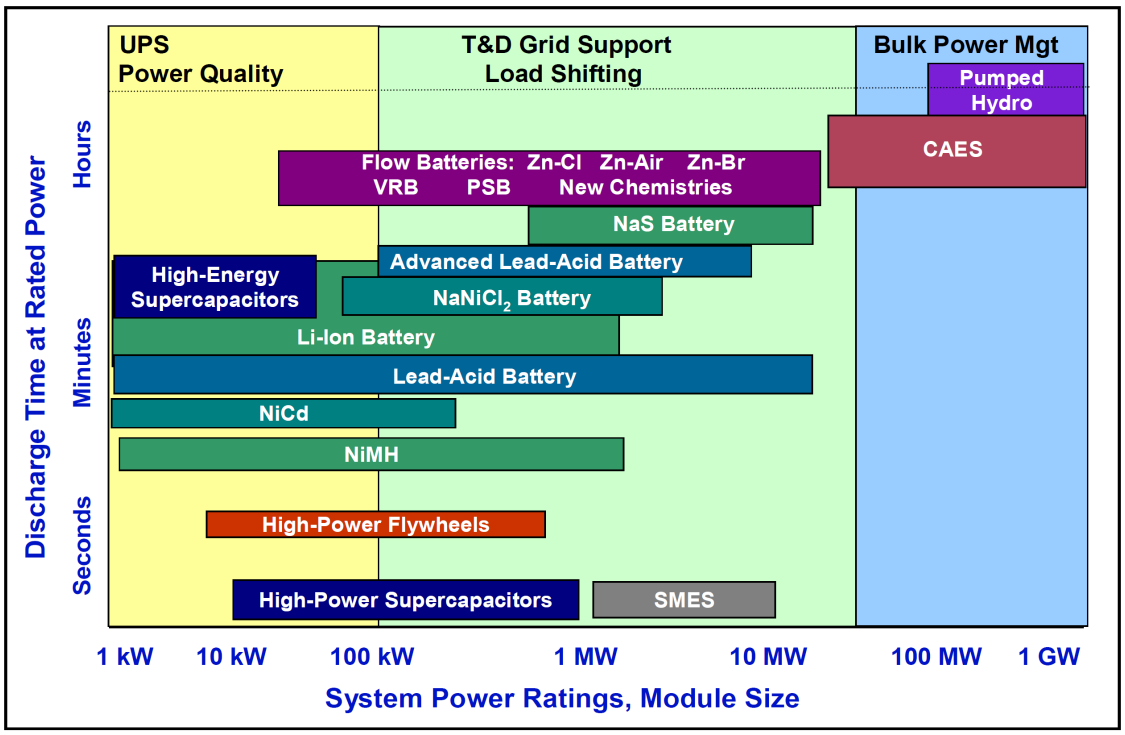

Fig. 2.3 Positioning of battery energy system technologies and their applications in relation to their capacity and duration of rated power discharging according to EPRI [204]

to generate sufficiently accurate prediction results within 10 cycles of the actual RUL at the inspection starting points and within 8.5% relative error [14].

Significant technological advancements and cost reduction have led independent storage providers to invest in energy storage applications. The ownership of storage assets may be different in each country depending on the regulatory framework. Storage systems can be owned by utility companies or independent storage providers, who can either have direct access and trade in the wholesale energy, capacity, balancing and ancillary services markets or have a contractual agreement with a utility company or a third-party company to whom they provide their services. However, network operators are mostly interested in the services that energy storage providers can offer, such as the energy or reserve capacity provided. Therefore, it is possible, in the context of the deregulated energy market for independent and private storage providers to offer services such as peak shaving, load levelling, frequency and voltage control. Ownership of BESS is in fact crucial as it may inhibit healthy competition in the marketplace. OFGEM, the UK regulator, is planning to take action in order to discourage ownership or operation of storage systems as flexibility assets, by utility companies. Flexibility services may also be procured by aggregators emerging in the marketplace that operate a portfolio of multiple smaller-scale storage technologies that act as a single virtual storage provider. Advanced artificial intelligence algorithms, data analytics and machine learning techniques are increasingly playing an important role in managing distributed storage devices in such settings.

The UK has an abundance of independent storage providers, however the business case for optimal storage ownership requires further exploration as the added value and benefits of storage span to the wider range of energy system stakeholders, including consumers,

DNOs and the system regulator. Another trend observed in the UK is the proliferation of Community Energy Storage (CES), mainly placed at the distribution level. CES is a good example of grid-connected, utility-owned or community-owned distributed storage system. Distributed storage systems are modular storage systems that are located at or near end-user homes and businesses.

ESS are expected to be a key enabler for sustainable energy systems. Recent publications in the literature also report the use of another novel enabling technology, the blockchain used to facilitate local energy marketplaces that could lead to renewable energy curtailment reduction and further RES integration. The potential of the technology is discussed in the succeeding section.

2.9 Blockchain technology for RES integration

A potential solution for curtailment mitigation recently reported in the literature, is the development of local energy markets in constrained areas of the grid that aim to alter consumer behaviours in order to match demand to locally produced RES supply and minimise curtailment. The practical implementation of local energy markets is being supported by the advent of novel technologies such as *distributed ledger* or *blockchain* technologies. A recent example is the 'Cornwall Local Energy Market', a £19m project developed by Centrica, that aims to create a virtual marketplace and trading platform for energy and flexibility services, including participation in the wholesale energy market [40]. The local marketplace aims to minimise renewable curtailment in the area, caused primarily by a large number of roof-top PVs connected and saturated grid capacity.

Blockchain is a key factor contributing towards smarter energy management, however blockchain technology is new and its full potential is not yet realised. Hence, an in-depth discussion on the benefits that blockchain could bring in energy applications along with technology limitations and barriers is required. This was achieved in a recent publication by the author of this thesis that thoroughly discussed fundamental principles of blockchain technology and identified promising use cases and applications for the energy sector. Moreover, the study provided a systematic review of 140 research and pilot projects testing the real potential of the technology [10]. The paper took a broader view on the technology's potential and showcased great diversity in potential applications that ranged from decentralised energy trading to Internet of Things (IoT) applications and deployment of EV charging infrastructure. A brief summary of the paper is presented here with focus on applications that could reduce RES curtailment, such as smart local marketplaces and peer-to-peer (P2P) energy trading.

2.9.1 Potential of blockchain technology

Blockchain or distributed ledgers are an emerging technology that has drawn considerable interest from numerous sources, such as energy supply firms, startups, technology developers, financial institutions, national governments and the academic community. Several

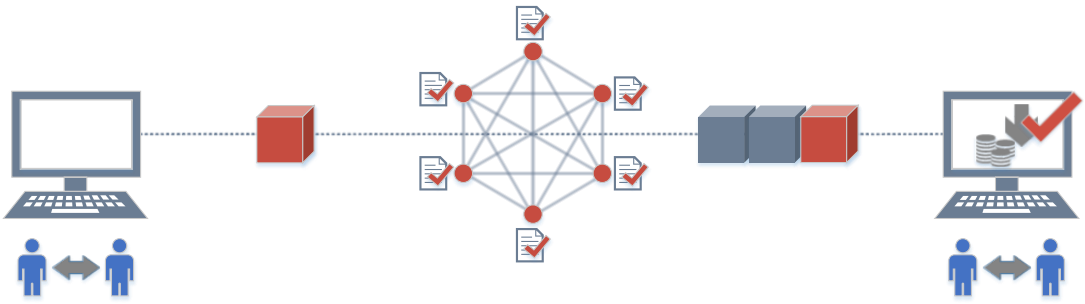

Fig. 2.4 Visual representation of a blockchain transaction: users agree on a transaction which is included in a block, its validity is confirmed by distributed nodes of the network and the block is added to the growing chain of blocks before transaction is confirmed and payments finalised.

studies coming from these backgrounds identify blockchains as having the potential to bring significant benefits and innovation.

Blockchains are shared and distributed data structures or ledgers that can securely store digital transactions without using a central point of authority. More importantly, blockchains allow for the automated execution of smart contracts in peer-to-peer (P2P) networks [239]. They can alternatively be seen as databases that permit multiple users to make changes in the ledger simultaneously, which can result in multiple chain versions. Instead of managing the ledger by a single trusted centre, each individual network member holds a copy of the records' chain. Agreement on the valid state of the ledger is reached with consensus. The exact methodology of how consensus is reached is an ongoing area of research and might differ to suit a wide range of application domains. New transactions are linked to previous transactions by cryptography, which makes blockchain networks resilient and secure (see Fig. 2.4). Every network user can check for themselves if transactions are valid, which provides transparency and trustable, tamper-proof records.

Blockchain technology is primarily known from cryptocurrency applications. While opinions on the long-term future of cryptocurrencies may be divided, several promising applications are being reported in the literature. A report by the UK Government [257] states that blockchains might have the capacity to *'reform our financial markets, supply chains, consumer and business-to-business services, and publicly-held registers'*. Potential applications spread from asset registries and transfer of ownership of hard assets [239] to secure recording of intangible assets. Swan (2015) [239] envisions these assets as any type of information, reputation or online voting systems. Research works from the financial sector discuss blockchain applications in the banking sector and state that blockchain-enabled platforms can facilitate financial transactions between different financial institutions and make payments faster by speeding up confirmation times [93]. Other applications may improve transparency in supply chain records with certification of manufactured products or diamond certification [145]. In fact, the variety of applications proposed is such that Tapscott and Tapscott (2016) [242] *compare blockchains to the advent of the Internet* and state they could prove to be a technological breakthrough, bringing about significant process

optimisation and novel business models. The potential lies on the fact that blockchain or distributed ledger technologies (DLT) can redefine digital trust and can remove intermediaries forming a new paradigm of management that can potentially disrupt traditional forms of governance [130]. The disruptive nature lies on the potential of replacing top-down control with consensus and also in the underlying philosophy of distributed consensus, open source, transparency and community-based decision-making [257]. According to the research institute of the Finnish economy (2016) [155], these characteristics could instigate further societal changes and implications. According to a recent Gartner report [85], blockchain technologies have already surpassed the peak of inflated expectations in the hype cycle and are predicted to be 2-5 years from mainstream adoption.

Along with use cases in various sectors, the potential of blockchains in the energy industry has just started to be realised as shown by the increasing number of startups, pilots, trials and research projects. A survey of the German Energy Agency [34] on the views of energy decision-makers shows that nearly 20% believe that blockchain technology is a game-changer for energy suppliers. The survey was based on the views of 70 executives working in the energy sector including utility companies, energy suppliers, network operators, generators and aggregators. More than half of survey participants plan or have already undertaken initiatives for blockchain innovation. Several energy utility companies have taken interest in exploring the potential benefits of distributed ledger technologies (DLT), as an enabling technology for low-carbon transition and sustainability [156]. Moreover, according to senior consultancy and commercial reports by Deloitte [90] and PWC [201], blockchains have the potential of radically disrupting energy related products and commodities, as they become digital assets that can be traded interoperably.

Early research initiatives and startups indicate that blockchain technology could potentially provide solutions to some of the challenges faced by the energy industry. Requirements for future energy systems can be summarised by three key principles: *decarbonisation*, *decentralisation* and *digitalisation*, with a shift to empower consumers, a pillar for both EU [64] and UK policy [178]. However, the current structure of energy and electricity markets is inadequate to achieving this vision, as small players' participation in the markets is practically excluded and incentives for active consumer participation have so far proved not sufficient. Early blockchain developers are establishing transactional digital platforms that can be completely decentralised and can enable P2P energy trading. They are developing local energy marketplaces and Internet of Things (IoT) applications that can play a significant role in the vision of the smart grid [72, 248]. According to PWC [201], energy firms are increasingly reporting higher energy costs and lower revenues. At the same time utilities face demands for increasing transparency by the regulatory authorities [46]. As a result, any possibility of cost savings and efficiency improvement in the operation of energy systems and markets can prove significant and is worth investigating.

Moreover, potential gains in transparency and competition could benefit other key policy targets related to energy affordability and fuel poverty [101]. According to a UK government report by the Competition and Markets Authority [46], poorly designed tariff prices and lack of mobility in the marketplace have led electricity consumers to

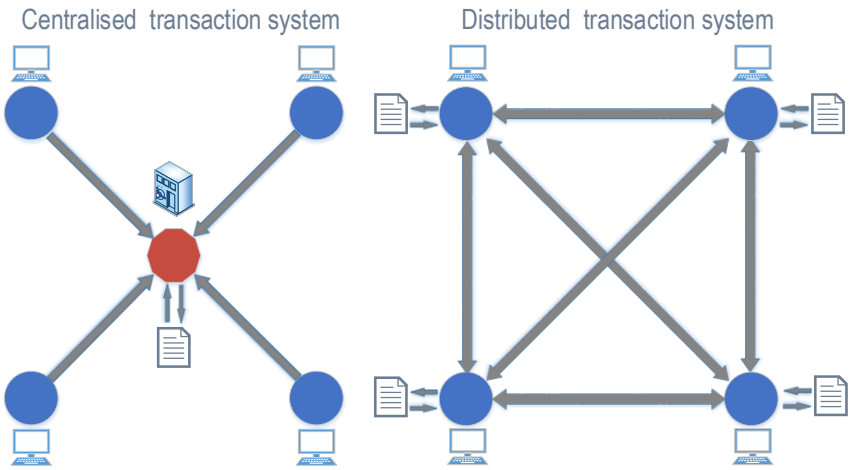

Fig. 2.5 Centralised and distributed transactional platforms: a single trusted authority manages the ledger as opposed to every member holding a copy of the ledger

pay £1.4 billion on average a year in excessive prices for the period 2012-2015. We note that UK retail electricity prices have increased in recent years irrespectively of wholesale electricity prices [35], indicating that there is significant room for improvement. A commercial report by Deloitte [90] states that blockchain-enabled transactional digital platforms could offer operational cost reductions, increased efficiency, fast and automated processes, transparency and the possibility of reducing capital requirements for energy firms. Cost savings potential is not restricted to utilities and can be relevant to energy consumers and prosumers [9], who are facing increasing energy prices and removal of RES incentives, respectively. Solutions promised by blockchains, such as P2P trading in local or consumer-centric marketplaces [196] could potentially lead to cost savings for energy consumers.

A substantial amount of current knowledge on blockchains comes not only from traditional academic sources, such as journals and conference proceedings, but forums, blogs, wikis, white papers and industrial reports. Therefore, an overview of the fundamental principles of blockchain technology is required to determine critical technical characteristics of blockchain systems. The following section distills key information from these sources, to provide the reader with an in-depth understanding of the broad blockchain topic before moving into energy use cases.

2.9.2 Definition and overview of fundamental principles

A blockchain is a digital data structure, a shared and distributed database that contains a continuously expanding log of transactions and their chronological order. The data structure is in other words a ledger that may contain digital transactions, data records and executables. Transactions are aggregated into larger formations, called *blocks*, which are time-stamped and cryptographically linked to previous blocks forming a chain of records that determines the sequencing order of events or the 'blockchain'.

Blockchains run on digital networks. Data transmission in such networks is equivalent to copying data from one place to the other, e.g. in the cryptocurrency domain this is equivalent to copying digital coins from one user's electronic wallet to another's. The principal challenge in digital networks resides in the fact that the system needs to ensure that there is no double-spending. A traditional solution is to use a central point of authority, such as a central bank, who acts as the trusted intermediary between transacting parties and whose job is to store and safeguard the valid state of the ledger and to keep the records up to date. If multiple parties need to write in the ledger at the same time, a central authority also implements concurrency control and consolidates changes in the ledger. In several occasions, central management may not be feasible or desirable, as it introduces intermediary costs and requires network users to trust a third party to operate the system [156]. Centralised systems also have significant disadvantages due to a single point of failure, which renders them more vulnerable to both technical failures and malicious attacks [16].

The primary purpose of blockchain technologies is to remove the need for such intermediaries and replace them with a distributed network of digital users who work in partnership to verify transactions and safeguard the integrity of the ledger. Contrary to centralised systems, every member of the blockchain network holds their own copy of the ledger or can access it in the open cloud (see also Fig. 2.5). As a result, anyone in the network can have access to the historic log of the system transactions and verify their validity, enabling a high level of transparency. If central management is removed, the challenge resides in finding an efficient way to consolidate and synchronise multiple copies of the ledger. The exact process of validation and ledger consolidation varies for different types of blockchains, but in principle, network members compare their versions of the ledger through a process intuitively akin to distributed voting [155], through which consensus on the valid state of the ledger is reached. These validation mechanisms are known as *distributed consensus algorithms*. Collaboration and honest behaviour of distributed nodes is established by game-theoretic incentives or rewards [18]. In fact, it can be very difficult to tamper with blockchains, without a significant part of the network colluding. Consequently, blockchain systems can be secure and tamper-resistant.

Other elements that ensure enhanced security are hash functions and public-key cryptography. *Cryptographic hash functions* are mathematical algorithms or one-way functions that take an input and transform it into an output of specific length, e.g. a series of 256 bits, called the hash output. Their operation relies on the fact that it is extremely difficult to recreate the original input data from the hash output alone (collision resistance). In addition, blockchains use *public-key cryptography* [58], an asymmetric cryptography protocol. Each user holds two cryptographic keys consisting of numeric or alphanumeric characters, a secret private key and a public key, which can be shared with other users in the network. The keys are mathematically related in such a way that information encrypted by one part can only be decrypted by its counterpart. The use of public-private key cryptography ensures authentication, meaning that a transaction is initiated by the source it claims to be from, and authorisation, meaning that actions are performed by users who have the right

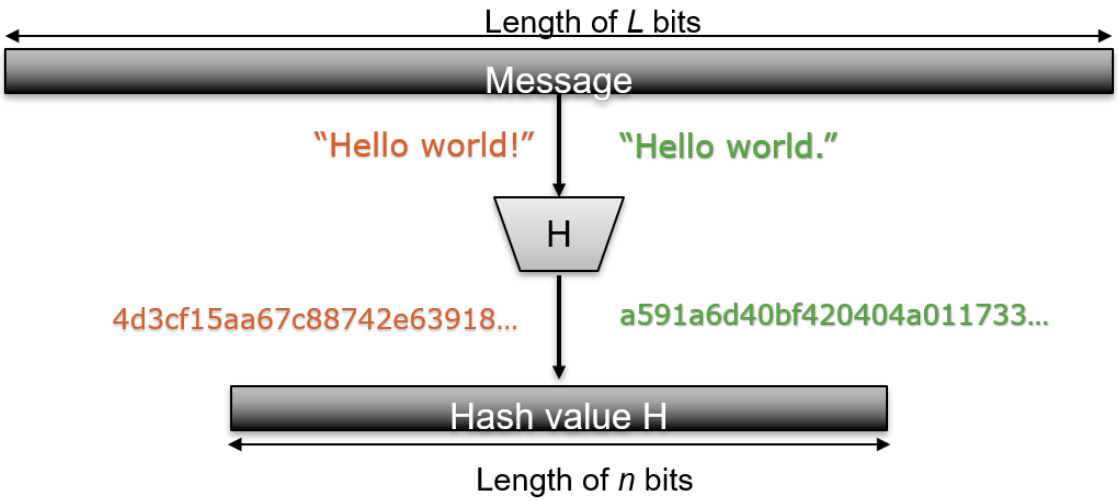

Fig. 2.6 An example of a hash function output for similar original messages

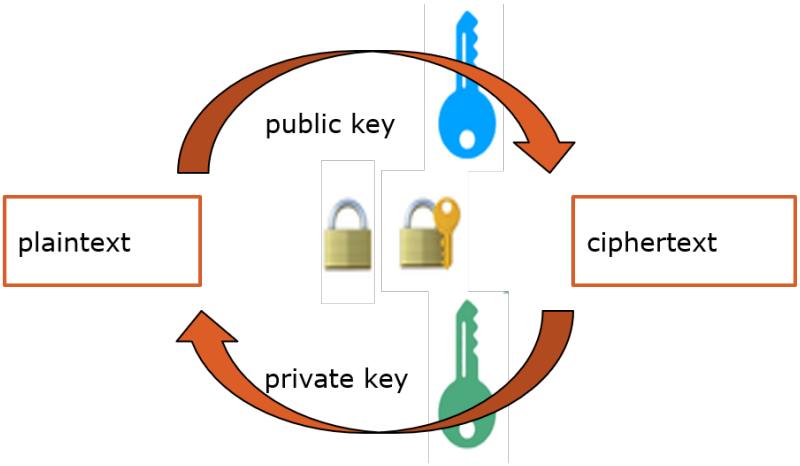

Fig. 2.7 An illustration of the operation of public-key cryptography

to do so. For example, the network can verify the sender's identity, as only the sender's public key can decrypt the original message (encrypted and digitally signed by the sender's private key). A message processed with one's public key can only be decrypted by the intended recipient holding the secret private key. These and other standard communication features such as data validity and security are achieved in blockchain systems by use of P2P communication and advanced cryptographic techniques.

According to the UK Government Office for Science [257], the real potential of blockchain technologies can be fully realised only when combined with *smart contracts*, i.e. user-defined programs that determine the rules of writing in the ledger. Smart contracts are executable programs that make changes in the ledger and can be triggered automatically if a certain condition is met, such as if an agreement between the transacting parties is honoured [239]. Contract terms are recorded in computer language encoding legal constraints and terms of agreement. Smart contracts are self-enforceable and tamper-proof bringing about significant benefits such as removing any intermediaries [90] and reducing transacting, contracting, enforcement and compliance costs [257]. An additional benefit

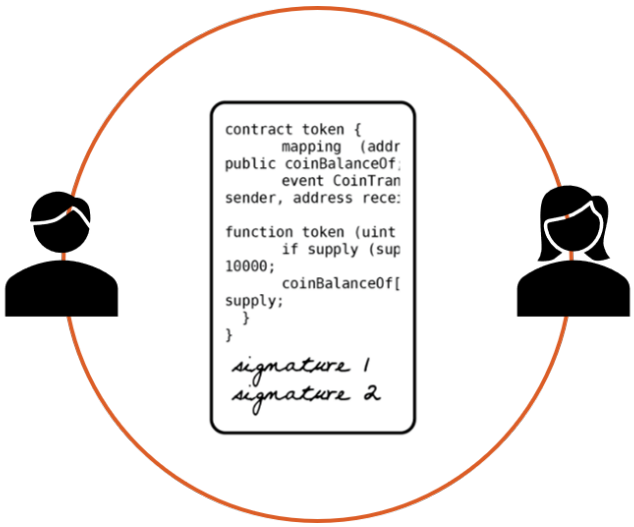

Fig. 2.8 An illustration of a smart contract in a blockchain system

is that low-value transactions can be made cost-efficient, while blockchains can ensure interoperability between transaction systems [93].

Blockchain systems can be classified into different taxonomies according to information access and other criteria. The classification determines at large key properties of blockchain systems. Different system architectures and classifications for blockchain systems are presented in the following section.

2.9.3 Taxonomies of blockchain architectures

A blockchain network or system can follow different rules and system architectures depending on desired operation and specific use case. Blockchain systems typically consist of network *users* and *validators*. User nodes can initiate or receive transactions and hold a copy of the ledger. In addition to read access privileges, validators are responsible for approving modifications of the ledger and reaching consensus throughout the network regarding the valid state of the ledger. Depending on the system configuration, partial or universal access rights and validations rights may apply. All Internet users can join a *public* blockchain system. On the contrary, with *private* blockchains the access is restricted only to authorised participants. *Permissionless* ledgers are completely distributed and censorship-resistant as any member of the network can contribute to the validation of transactions. In contrast, with *permissioned* ledgers only certain validator nodes hold write access rights to modify the blockchain (see Fig. 2.9). With public and permissionless ledgers, users and validators are completely unknown to each other, therefore the collaborative effort and trust required for ledger management is induced by game-theoretic equilibria and rewards. The structure of incentives typically involves spending resources such as computational work, electricity or penalisation that aims to deter selfish behaviour [155]. With private and permissioned ledgers the users' identity is known similarly to know-your-customer practices. Validator nodes are known and trusted to behave honestly, therefore artificial incentives are not required to guarantee the system's operation. Consequently, private and

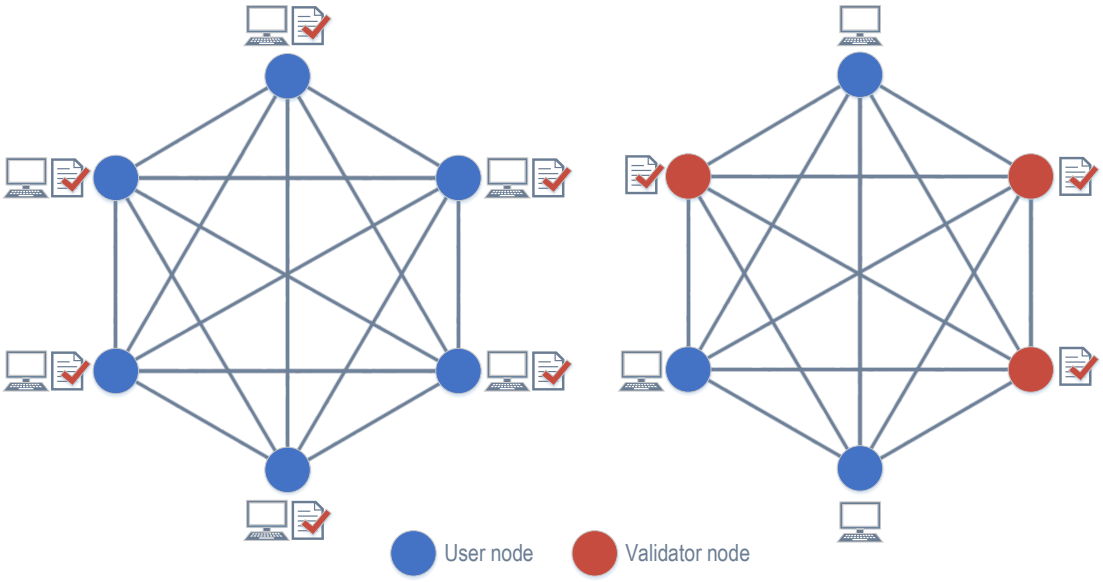

Fig. 2.9 Classification of blockchain architectures, public permissionless ledgers (any user can have join the network and validation process) and private permissioned ledgers (where network access and validation process is restricted to authorised nodes) - figure based on [83]

permissioned ledgers can be faster, more flexible and efficient, however, this comes at the expense of immutability and censorship-resistance [155]. In addition, some ledger architectures can be classified as *consortium* blockchains, i.e. hybrids that stand between public and private blockchains [274].

Blockchains can also be classified according to their development purpose, i.e. in *general purpose* or *specific purpose* blockchains. Typical examples are Ethereum, designed to accommodate a wide range of use cases and applications, and Bitcoin, designed specifically for cryptocurrency transactions, respectively. In terms of governance and protocol rules of the system operation, blockchains can be classified as open-source or closed-source. *Open-source* architectures are open to all network members and can benefit from continuous and transparent peer review, public debate and community decision-making. *Closed-source* blockchains operate similarly to private enterprises, where any changes in the rules of the system operation are decided in private. It is important to understand that one blockchain solution architecture does not fit all applications and use cases, therefore hybrid approaches that lay anywhere in the spectrum between public and private blockchains and have various degrees of centralisation can be explored. The resulting system architecture and the consensus algorithm applied in the system environment are jointly responsible for key performance features, such as speed, scalability and efficiency of the resources spent. A review on different consensus algorithms is presented in the following section.

2.9.4 Distributed consensus algorithms

Existing literature describes many types of distributed consensus algorithms developed, each providing distinctive features, advantages and disadvantages. The method used for

reaching consensus in blockchain networks determines to a large extent key performance characteristics such as scalability, transaction speed, transaction finality, security and spending of resources such as electricity. Broadly speaking, every method requires a procedure for generating and subsequently accepting a block. A block can be generated or proposed by some node in the network, and it encodes a number of transactions (e.g. in a cryptocurrency system, these are monetary transactions between different accounts). Next, a key step is for the proposed block/corresponding transactions to be accepted by network members, a process called *reaching consensus*. Once a block is accepted, it becomes part of the blockchain, and newly generated blocks are cryptographically linked to it. After a time (depending on the algorithm used), the block becomes a permanent part of the blockchain, i.e. it reaches *finality*. Note that finality does not exclude the existence of small statistical chance that the block is reversed, as part of a future fork, occurring by design or as a result of an attack. The chance of reversal decreases with new appended blocks.

Reaching consensus on which blocks/transactions to accept as valid in a distributed system is challenging. Consensus algorithms have to be resilient to failures of nodes, message delays and corrupt messages, as well as unreliable, unresponsive or even deliberately malicious nodes [19]. A large number of approaches for the consensus problem have been proposed. Some authors [69, 105] broadly classify these as *lottery-based* and *voting-based* (although note that some of the more complex consensus approaches have elements that fit into both categories). The most important examples of distributed consensus algorithms used in blockchain systems are presented below[1]:

- **Proof of Work (PoW)**

  In PoW systems, the algorithm rewards participants who solve cryptographic puzzles in order to validate transactions and create new blocks. Validators or miners compete with each other to add a new block in the existing blockchain by solving a cryptographical puzzle of generating a hash output that starts with a number of consecutive zeros in the most significant positions. The method used adds a nonce, i.e. a random number that can only be used once, to the block, and calculates the hash output of the block header. The block header contains information such as the hash of the previous block validated and a special hash of all transactions contained in the block. The goal for all miners is to achieve a hash output that is lower than a specified target. Miners have no way to predict or influence the outcome, so the only feasible action is that of trial and error. This brute-forcing procedure requires computational effort that increases exponentially with the number of trailing zeros. When a correct hash output is found, the block is returned to other nodes in the network and is accepted, if all transactions are valid and unspent, and the successful miner takes a financial reward.

  Other miners accept the newly generated block by starting work on the consecutive block. Crucially, all succeeding blocks contain hash outputs from all preceding blocks. As generation of hash outputs is random and performed in parallel by many

[1] An extensive review of distributed algorithms is presented in a recent publication by the author [10].

miners, multiple chains may appear. In this case, the network stores all resulting chains. Network members eventually abandon all other chains but the longest, which is assumed to have been produced by a network majority of computational power, and therefore is considered to represent the most valid state of the ledger. As a result, malicious attackers are constantly outpaced by the honest part of the network, unless they can control more than 51% of the computational power in the network. In the case of a 51% attack, malicious nodes could potentially rewrite all history of transactions. Breaches in security can be introduced by users, miners, hackers or man-in-the-middle attacks (a detailed discussion of these issues is provided in [170]).

PoW is the distributed algorithm used by the most mature cryptocurrency application, Bitcoin. At first, Bitcoin mining relied on the computing power of standard computers, so anyone could become a miner. Since 2014 however, mining has been dominated by specially designed computer chips, known as application specific integrated circuits (ASICs) [266]. Miners have increasingly joined coalition pools in order to leverage risks and maximise returns. As a result, mining power is continuously becoming more centralized in cartels or 'mining pools'. This has generated a direction of research that uses techniques from game theory and mechanism design to discourage centralised cartels from forming and reduce their influence on the Bitcoin system [75].

PoW strategies have proved they can scale to a large number of users, however transaction rates and finality may not be suitable for certain use cases [195]. Another main criticism point is that PoW is responsible for wasting large amounts of real resources such as electricity. For example, Ethereum's Wiki pages claim that Bitcoin and Ethereum burn over $1 million worth of electricity and hardware costs per day for running their consensus mechanism [69]. Pilkington (2015) [195] cites a media release named the Bitcurrency calculator, which shows that Bitcoin could one day consume up to 60% of global electricity production, equivalent to 13,000 TWh ore equivalent to powering 1.5 billion homes. Other sources report that Bitcoin could consume as much electricity as Denmark [54] by 2020, under the assumption that a single Bitcoin transaction can currently consume 200 kWh of electricity [153]. This cost may not be justified for low value or low-risk transactions where users can be trusted or there are established methods to prevent malicious behaviour [18]. To solve these issues alternative strategies have been proposed, such as a distributed consensus algorithm called proof of stake.

- **Proof of Stake (PoS)**

  PoS replaces computational work with a random selection process, where the chance of successful mining with PoS is proportionally related to the wealth of validators. The probability of generating a block depends on what stake the nodes have invested in the system, i.e. coin ownership [39]. This approach can potentially result to faster blockchains [195] that have much lower electricity consumption and a decreased likelihood of a 51% attack [69]. In addition, there is no need to constantly generate

new coins to incentivise validation. Instead, miners rewards are down only to transaction fees and cannot achieve greater gains by investing in hardware equipment for mining. PoS can make use of game-theoretic mechanism design to prevent collusions and centralisation, often penalising dishonest and malicious behaviour. The main vulnerability of PoS systems is known as the 'nothing at stake' problem or in other words that voting/claiming financial rewards for multiple chains is inexpensive. Several solutions have been proposed such as integrating a punishment mechanism for validators that simultaneously create blocks in multiple chains and automatically deducting coins owned or deposited. Another strategy is to punish validators for creating blocks on the wrong chain, intuitively similarly to PoW, where also validators incur the cost of electricity. Validating nodes are exposed to greater risks in the latter case, but on the other hand, these nodes are not required to be known ahead of time [69]. PoS-based algorithms come in great variety and can be used in public blockchains, where validators are unknown and untrustworthy, or in private/business-oriented settings, where validators form a known set of trusted entities [69].

- **Practical Byzantine Fault Tolerance (PBFT)**

  In trusted or semi-trusted environments, voting-based algorithms such as Practical Byzantine Fault Tolerance (PBFT) can be adequate solutions. In Byzantine fault tolerance[135], nodes transmit votes for block acceptance in a multi-round process, at the end of which validators agree on whether to accept a block as a permanent part of the chain (finality). However, as votes are transmitted through a potentially unreliable network, and some of the validators may be untrustworthy, the consensus voting process requires careful design.

  When a sufficient amount of signatures is collected, transactions are considered valid and consensus is reached. PBFT provides instant finality, as blocks that have been globally verified cannot be reversed. However, the algorithm requires at least 2/3 of the network to behave honestly and messages overhead may increase significantly as the size of the network increases, affecting both speed and scalability [19]. Many variants of BFT-based protocols have been proposed (see [254] for a detailed review) by key developers, such as Hyperledger, the open platform supported by the Linux Foundation [105] and Tendermint [243].

- **Proof of Authority (PoAu)**

  Block generation with PoAu requires granting special permission to one or more members to make changes in the blockchain. For example, one member holding a special key may be responsible for generating all the blocks. Essentially, PoAu can be seen as a modified PoS algorithm, where validators' stake is their own identity. Network members put their trust into authorised nodes and a block is accepted if the majority of authorised nodes signs the block. Any new validators can be added to the system via voting [71]. Although the method represents a more centralised approach,

it is most appropriate for governing or regulatory bodies and is also proving popular with utility companies in the energy sector. The consensus algorithm may be useful in special use cases where security and integrity cannot be put at risk [39]. An example is the Energy Web blockchain that can achieve confirmation time of 3-4 sec and can scale to several thousand transactions per second [65].

Each of these methods presents trade-offs between a set of advantages/disadvantages. Methods that rely on random selection processes scale well to large dimensions. Good scalability means that a system performs well as it grows in scale, for example it can handle an increased number of transactions/blocks within a reasonable time frame and for an increased number of network users/nodes. However, these lottery-based systems may result in multiple chains at different nodes in the network that need to be consolidated and resolved before finality is reached. This can also affect the speed that transactions are recorded in the blockchain. On the contrary, methods based on voting are faster to achieve finality, but may take longer to achieve consensus for a large number of nodes in the network, because nodes need to exchange messages with each other and voting may last for multiple rounds until agreement is reached. This results in a trade-off between scalability and finality/speed [105]. It is worth noting that efforts to improve scalability and speed of transactions are ongoing by the blockchain community. Several solutions have been proposed including sharding (requiring only a subset of nodes to verify transactions) [70], sidechains (only transaction data are stored in the main chain) [26] and utilisation of payment channels (blockchain acts only as a control layer) [197].

Validation and cooperation within the network often requires spending resources, such as computational power or coins. Honest behaviour of validating nodes is assured either by financial rewards or countermeasures that take some form of punishment. Rewards may include direct coin assignment or receiving substantial transaction fees. Punishment may include losing money or deposits. Either way, the incentives' mechanism design reflects a form of resources expenditure, which can be money, computational power, electricity, time, etc. Minimising resources or energy spent forms a significant criteria for evaluating blockchain performance. PoW algorithms for example are known to be energy intensive as they spend significant amounts of energy to validate transactions. While this is a significant concern and wastage of resources needs to be minimised, it is also crucial for not compromising blockchain system security. In fact, the design of validating mechanisms and incentives can determine system vulnerabilities to malicious behaviour, potential cyber-attacks or collusion. This results in a trade-off between security and waste of resources/cost. Some authors argue that incentives and rewards form an integral part of blockchain systems and are required to safeguard their security and integrity [240]. Other authors state that the essence of blockchains is purely informational and process-oriented [195] and see blockchain solutions as a technology that achieves consensus in P2P networks [89].

In addition, distributed consensus strategies are a direct consequence of the trust within the environment blockchain networks operate and their centralisation risks. For example, high cost strategies may be inevitable for public trustless blockchain applications such as Bitcoin, however they may be redundant for private blockchains operating in

Technical features	Permissioned lottery-based	Permissioned voting-based	Permissionless PoW
Scalability	Good	Moderate	Good
Speed	Good	Good	Poor
Finality	Moderate	Good	Poor
Security	Moderate	Moderate	Good
Sustainability	Good	Good	Poor

Table 2.2 Summarised distributed consensus strategies and main characteristics based on [105] and our study findings

trusted environments. Applications of blockchain systems, such as in the corporate world, call for various requirements depending on the specific case under consideration. Several applications require real-time or near real-time transaction clearance and low latency. Other applications need to have good scalability. Traditional PoW approaches support open and censorship-resistant platforms, however they are not suitable for use cases that require immediate transaction finality or high transaction rates. On the other hand, consensus mechanisms developed for private blockchains may become inefficient when scaled to a large number of participants (Table 2.2 provides a summary of key characteristics). A detailed comparison of different algorithms can also be found in [19, 39, 105, 130, 274].

In the following section, blockchain use cases for the energy sector are presented followed by a more detailed discussion on local energy marketplaces and P2P energy trading.

2.9.5 Notable use cases for energy applications

Energy sector decision-makers [34] and utility companies [66] have asserted that blockchains could possibly offer solutions to key challenges that the energy industry is facing. The German Energy Agency [34] claims that blockchain technologies have the potential to improve the efficiency of current energy practices and processes, can accelerate the development of IoT platforms and digital applications and can provide innovation in P2P energy trading and decentralised generation. In addition, they report that blockchain technologies have the potential to significantly improve *current practices* of energy enterprises and utility companies by improving internal processes, customer services and costs [34].

Energy systems are undergoing a transformational change triggered by the advancement of distributed energy resources and information & communication technologies (ICT). One of the main challenges is the emerging decentralisation and digitalisation of the energy system, which requires the consideration, exploration and adoption of novel paradigms and distributed technologies. Due to their inherent nature blockchains could provide a promising solution to control and manage increasingly decentralised complex energy systems and microgrids [130, 162, 173]. Integrating small-scale renewables, distributed generation, flexibility services and consumer participation in the energy market is a demanding task. Some authors [173] argue that blockchains could provide innovative trading platforms where prosumers and consumers can trade interchangeably their energy surplus or flexible demand on a P2P basis. Active consumer participation can be secured and recorded into immutable, transparent and tamper-proof smart contracts. Enabling

such automated trading platforms could be an efficient way of delivering price signals and information on energy costs to consumers [162], simultaneously providing them with incentives for demand response and smart management of their energy needs. Blockchains can enable local energy and consumer-oriented marketplaces or microgrids that aim to support local power generation and consumption [196]. One of the major benefits from this approach is reducing transmission losses and deferring expensive network upgrades. On the other hand, as energy is still delivered through the physical grid, demand and supply need to carefully be managed and controlled to comply with real technical constraints and power system's stability. According to a recently published report by Eurelectric [71], the physical exchange of electricity has so far inhibited larger adoption of blockchains in the energy sector, as opposed to applications in the finance sector. Blockchains can securely record ownership and origins of the energy consumed or supplied. As a result, blockchain solutions could be utilised for smart charging arrangements and sharing of resources, e.g. community storage or microgrids, but also for applications of data storage in smart grids and cybersecurity [172, 174]. A key challenge as volumes of RES continue to increase is maintaining the security of supply and improving network resilience. By facilitating and accelerating IoT applications and enabling more efficient flexibility markets, blockchains could improve network resilience and security of supply [173]. A report by the Research Institute of the Finnish economy [155] argues that blockchains could assure interoperability in smart grid and IoT applications by offering open and transparent solutions. According to Deloitte [90], energy market operations could become more transparent and efficient. As a result, this could improve competition and facilitate consumer mobility and switching of energy suppliers. If cost savings opportunities are realised, we could leverage the technology to improve on fuel poverty and energy affordability issues.

By virtue of advantages offered, blockchains could potentially provide solutions across the energy trilemma: they could reduce *costs* by optimising energy processes, improve energy *security* in terms of cybersecurity, but also act as a supporting technology that could improve security of supply, and finally promote *sustainability* by facilitating renewable generation and low-carbon technology solutions.

To identify potential use cases for the energy sector, a systematic review across 140 research initiatives and organisations that have undertaken blockchain projects for energy applications, was undertaken and presented in great detail in [10]. Projects were classified according to their field activity and application type into eight categories, as shown in Fig. 2.10. Moreover, projects were classified according to the type of distributed consensus algorithm used, as shown in Fig. 2.11. Most of the projects used PoW, especially for preliminary results, however this is expected to change to PoAu or PoS algorithms, as projects move from proof of concept to real-world implementations. According to the field of application, the most popular category was decentralised and P2P energy trading, a potential solution for curtailment. Such schemes and market models are discussed in more detail in the following section.

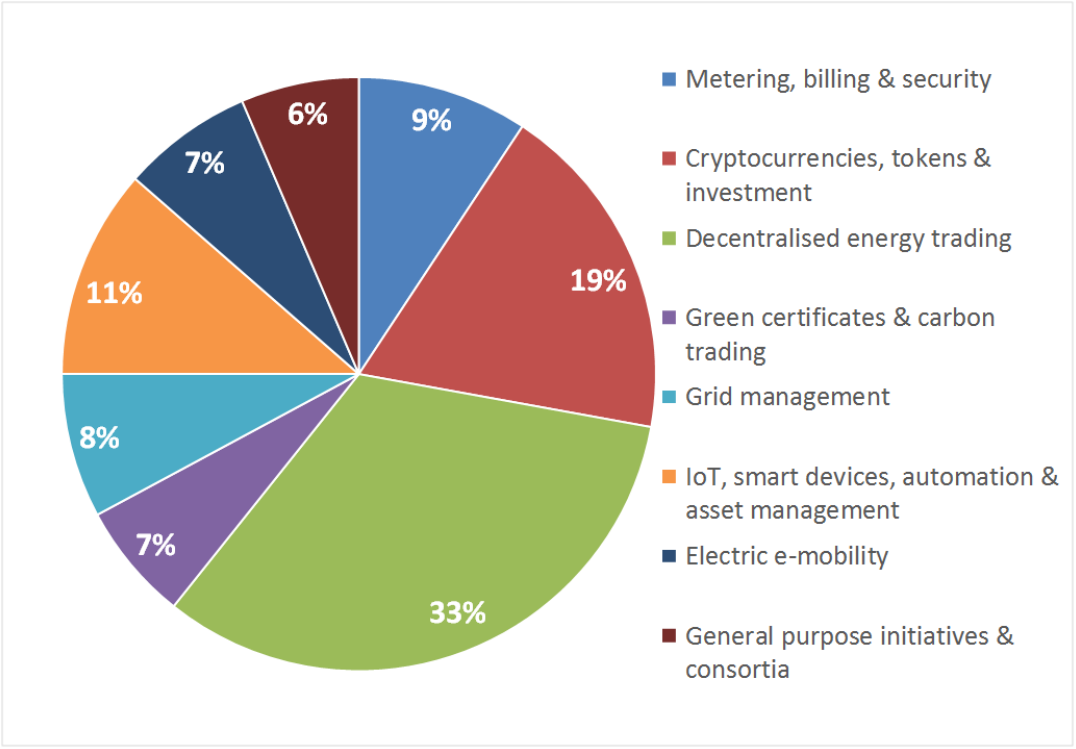

Fig. 2.10 Blockchain use case classification according to their activity field: results derived from a study on 140 blockchain initiatives in the energy sector being pursued by a large number of companies, startups and research institutions

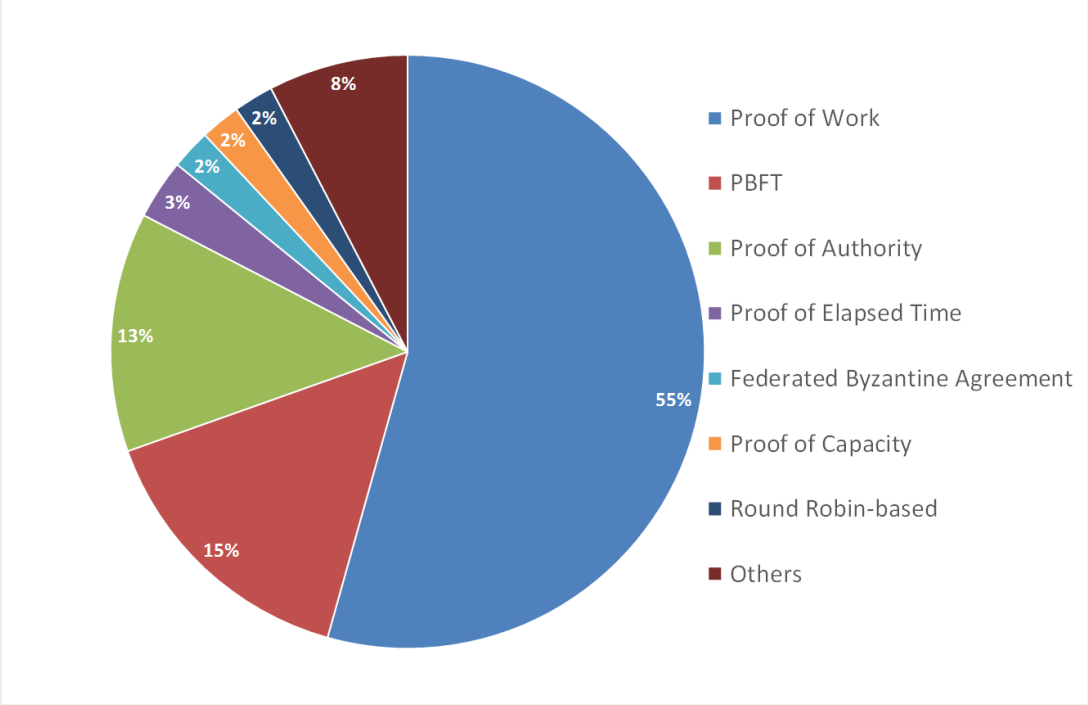

Fig. 2.11 Blockchain use cases in the energy sector according to consensus algorithm used: results derived from a study on 140 blockchain initiatives in the energy sector being pursued by a large number of companies, startups and research institutions

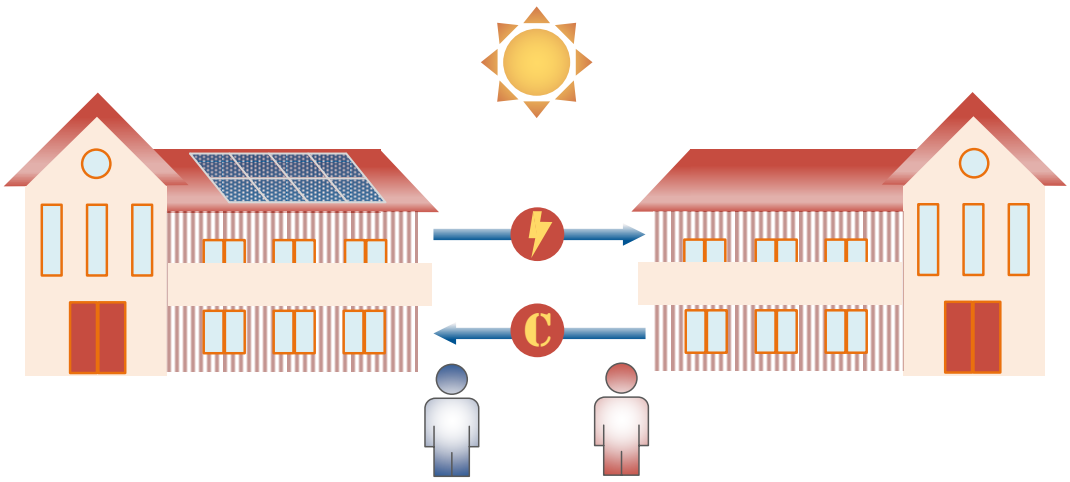

Fig. 2.12 P2P energy trading in local microgrids and community projects

2.9.6 P2P trading and decentralised energy

P2P energy trading and local energy marketplaces represent an application domain where blockchain-enabled systems would fit most naturally, by enabling direct energy trading between energy consumers (energy producers/prosumers and end-consumers), who can use this approach to take control of their generation and demand. Local energy markets and smart energy communities could potentially achieve better matching of RES generation to local demand and have therefore been reported in the literature as a way to tackle curtailment. A recent example is the 'Cornwall Local Energy Market' that aims to create a virtual marketplace and platform for energy trading and flexibility services provision [40]. Moreover, the trading platform aims to minimise renewable curtailment in the area.

In general, local and community energy projects and microgrids are expected to play an increasingly important role in energy systems. According to Berka and Creamer (2018) [27] locally-owned energy projects have a great potential to deliver socio-economic and environmental benefits for the communities involved. In microgrids, distributed generators, storage devices, uncontrollable and controllable loads form an interconnected system that can operate in synchronisation to the main grid or in complete autonomy, if operating in island-mode [152]. From a control point of view, microgrids act as a single system that has distinctive electric boundaries with respect to the main grid [244]. In addition to the formal definition, virtual microgrids can also be considered that can provide aggregate control of supply and demand outside electrical and physical boundaries. Microgrids promote localised energy production and consumption, which may lead to significant distribution and transmission losses reduction [123]. When coupled with sustainable resources, microgrids can enhance further integration of RES [166]. Local microgrids can improve network resilience, provide ancillary services, such as frequency and voltage support, to aging power systems with the potential to defer expensive network

upgrade investment. In addition, they can provide energy services to consumers in the case of grid contingencies.

Efficient microgrid operation on a technical level, such as optimal control strategies and system architectures, has been extensively studied [59, 97, 127, 137, 175, 187, 237]. Trading in microgrid environments at a local level has also been proposed by several researchers that utilise autonomous agents, such as in [134], where a flexible market for coordination of self-interested energy users, suppliers and utilities in a smart grid framework was presented. In [255], security of supply issues and limited network capacity were taken into account. In [29], a market mechanism allocates electricity and heat in microgrids with Combined Heat and Power (CHP). Other autonomous marketplaces for energy trading paradigms in the wholesale market have been developed by the AI community, such as TADA [30] and PowerTac [129]. Local and decentralised energy systems need to overcome significant barriers, such as accounting for a large number of independent and self-interested actors, how to record the energy produced and consumed at different points in the microgrid, but also the issue of coordination between multiple sources and the central energy system so that demand and supply are balanced at all times [130]. An additional challenge that local or community-based energy systems need to overcome is related to social acceptance [253].

In terms of academic research, blockchains in energy markets form a new research area that has just started to be explored. One of the first works to consider the use of cryptocurrencies for P2P energy trading is the work by Mihaylov et al. (2104) [167]. Energy injected into the grid is transformed to a virtual currency (NRGcoins) that enables local energy trading of prosumers. The rate at which coins are produced depends on the supply-demand conditions on the time of injection, so that real cost of energy is reflected in the price. Coins can be traded in exchange markets or used to buy electricity from the grid. Akasiadis and Chalkiadakis (2016) [2] present a cryptocurrency mechanism that is adopted to achieve demand shifting by prosumer coalitions. Local marketplaces rely increasingly on prosumers [9] and consumer participation and engagement [196]. Energy trading for microgrids in the developing world is discussed in [227]. In this work, solar battery units form the validating nodes of the blockchain network. The distributed consensus algorithm considered is proof of stake. A preliminary discussion on the use of blockchains in microgrids can also be found in [130]. Mylrea and Gupta (2017) [173] focus on technical characteristics (security, scalability and speed) of blockchains for distributed energy resources (DER) transaction exchanges and enhanced resilience. Apart from electricity, research work by Al Kawasmi et al. (2015) proposed a local market model to trade carbon emissions [5]. Trading of green certificates was discussed in [109].

Blockchains in local energy markets can incentivise end-consumer participation [162]. As a result, consumers are exposed to the real cost of energy, which might result in more rational energy consumption or suitable price signals for demand response [246]. Self-generating prosumers that have invested in PVs, small wind turbines or CHPs can participate in local energy markets. Until now, prosumers have not had real access to the energy market, which remains a privileged playing field for the institutionalised energy

suppliers [257] due to high associated costs. Incentives for further RES investment, such as FiTs or export fees for selling energy surplus back to the grid are often inadequate or are being removed. Utility companies purchase this surplus at low prices and sell it back to other consumers at standard tariff prices. If prosumers are allowed to sell their surplus directly to other consumers without intermediaries, a potential for energy cost savings emerges for all stakeholders. Prosumers can derive greater benefits from their investment, as profits and value remains within the microgrid and local community. P2P trading in local energy marketplaces can provide socio-economic incentives that promote local renewable generation and therefore might form an alternative incentive for prospective prosumers [162]. Consumers, who cannot afford investing in renewable generation, either due to capital funding or limited space, can buy certified green energy at affordable prices. Emerging platforms indicate that there might be a market for matching consumers to renewable energy suppliers, such as in the case of Piclo and others (see [190] for a detailed review). Often consumers are willing to pay a premium for buying green energy, however currently there is no guarantee about the origin of energy purchased and most likely the energy used by end-consumer is still sourced by the closest fossil-fuel power plant. Current matching platform solutions are intermediaries that act as market access points for RES generating units and demand service providers, however traceability of energy flows is not currently possible. Blockchains on the other hand promise complete transparency on the origins of the energy purchased, such as its type, generating unit and exact location produced [34]. Community energy microgrids based on blockchains essentially enable localised energy trading between consumers, which is recorded in a secure and tamper-proof way.

An important question that local energy marketplaces need to address is the role to be played by the transmission and distribution system operators (TSOs/DSOs) and the Independent System Operators (ISOs). These players own the physical infrastructure of electricity grids and are responsible for system stability. System operator recoup their costs through system maintenance fees, but are also responsible for assuring that the decentralised energy trades agreed between parties can actually take place, given the physical system constraints.

Hence, TSOs/DSOs will have a key role to play in any blockchain implementation. Their potential use of blockchains is twofold: First, they can use blockchains to record more precise use of their network, hence allowing exact collecting of network fees corresponding to each energy transaction. In the case of local energy marketplaces, tariffs or prices set in P2P transactions need to account for grid charges, if the energy is transmitted through the public grid. Second, they can use the information about the P2P transactions recorded in blockchains to better manage the capacity and power flows on their network. This, of course, would require new solutions being developed for managing the system that are able to use the information recorded in the blockchain close to real-time. This is a challenging area requiring further research going forward. In addition, if connected to the main grid, all system users need to collaborate with the system operator and provide forecasts of energy demand and supply. This requirement will also need to apply to any P2P marketplaces.

Individual consumers are not expected to be able to do this, but this could be provided in the future by third-parties such as future energy suppliers or local aggregators. The size of emerging marketplaces and AI and ML algorithms can play a significant role in this respect. In fact, the intersection of blockchain technologies with AI is an emerging research area required to achieve such long-term visions.

In the following section, key conclusions and future outlook on the potential of blockchain technologies, their challenges and market barriers are discussed.

2.9.7 Challenges for blockchain and future outlook

Blockchain projects and research initiatives reviewed in [10] showed that blockchains are a promising technology for a wide area of services and use cases in the energy sector. The large number of established energy companies and utilities that are currently involved in blockchain projects, as well as the investor interest in this area, clearly shows the potential value of this emerging technology for the energy industry. The real long-term value of the technology is however yet to be proven, especially as most initiatives have trialled the technology in relatively small-scale projects that are still in an early development phase. As a result, several questions will need to be answered before mainstream adoption of blockchains in the energy industry is materialised.

First and foremost, blockchain technologies need to prove they can offer the scalability, speed and security required for the proposed use cases. Research efforts on distributed consensus algorithms, which are crucial to achieving these objectives, are still ongoing, however a solution that combines all desired characteristics cannot yet be achieved without significant trade-offs. Early adopters of blockchain technologies face the challenge of selecting the right consensus mechanism and system architecture, without having a clear long-term picture of the advantages and downsides that each approach has to offer. For many applications, including P2P energy trading, blockchain technologies have already passed the proof of concept stage, but require further development to achieve desired operational and performance objectives. Several recent developments, such as the blockchain network developed by the Energy Web Foundation are promising as it can be scaled up to thousands of transactions per second.

Blockchains face additional risks such as possible malfunctions at early stages of development due to lack of experience with large-scale applications. Blockchain ecosystems rely heavily on coding new algorithms, a procedure that can be prone to errors. Security breaches are still highly likely before the technology becomes mature, which could result in bad publicity and delays in acceptance from consumers. Resilience to such attacks is of great importance, especially for applications in critical infrastructure, such as energy systems.

Another important challenge is that blockchain systems have currently high development costs [71]. Blockchains may realise significant cost savings by circumventing intermediaries, however for several use cases, they might not have the competitive advantage against already existing solutions in well-established markets. For example, energy

transactions can be recorded in conventional databases, such as relational databases that are designed to recognise relations between stored items of information [110]. These solutions are already largely available and currently faster and less costly to operate [201], albeit they cannot offer immutability of records or transparency. Blockchain systems may require costly new infrastructure, such as custom ICT equipment and software, the costs of which need to be outweighed by benefits achieved by data integrity, enhanced security and elimination of the need for a trusted intermediary. In the energy sector, smart meters are currently being rolled out without significant computational capabilities, hence integrating the existing smart metering and grid infrastructure with distributed ledgers could come with significant costs.

At present, information in blockchain systems can be transferred for very low costs, but validation and verification of data comes with high hardware and energy costs [201]. Proof of stake or proof of authority algorithms may significantly improve this in the future. In the field of grid communications however, blockchain systems would need to compete with already established solutions such as telemetry, which is not only more mature, but also significantly cheaper technology solution [71].

Significant barriers in the adoption of the technology are relevant both to the regulatory and legal sphere. Regulatory bodies endorse the active participation of consumers in electricity markets [64, 178]. In addition, several policy makers have established supportive measures for local or community energy systems that aim to reduce costs for consumers, promote low-carbon technologies and tackle fuel poverty. Blockchain technologies can support or accelerate such objectives, therefore coordinate well with current regulatory priorities, however regulatory frameworks would need to be amended to allow larger adoption of blockchains. For instance, in general lines current regulatory frameworks do not allow consumer to consumer electricity trading, such as in several P2P energy trading projects. New contract types will be required to describe agreements between prosumers and consumers, especially when counterparties make use of the public grid [201]. Most importantly, a new framework would require new and potentially more flexible electricity tariffs, which are currently heavily regulated. In general, local or microgrid energy markets would need to be integrated with current regulatory practice.

P2P trading platforms are in early stages of development, therefore the scale of their adoption is currently limited. However, they have the potential to radically change established roles of incumbent energy companies, such as energy suppliers or grid operators, who are in most countries are regulated monopolies and own the physical infrastructure. In fact, regulatory bodies have granted special permission to pilot projects trialling such novel marketplaces to examine potential benefits for consumers and energy system operation. Blockchain technologies have started to prove their potential in decentralised microgrids, however they face challenges in balancing, integration with central controls, and coordination with the main grid. Energy trading needs to be reconciled with the system operator practice, and continuous decentralisation may lead to more complex management of energy systems overall. P2P marketplaces and local microgrids may even accelerate grid defection or lead to severe underutilisation of network assets. Such results would call for radical

changes in the way network charges and energy services are offered to consumers. In the case of P2P platforms granting access of consumers to wholesale energy markets, DSO coordination of marketplaces might deliver greater benefits for the consumer, according to a report from Eurelectric [71]. All these issues call for significant regulatory changes and might lead to delays or lack of blockchain adoption.

In addition, regulatory authorities are responsible for setting the rules of consumer data protection. A recent example is the new EU policy on consumer data or General Data Protection Regulation (GDPR). Blockchain system users should be identified to account for their liabilities but at the same time, consumer or commercial sensitive information need to remain confidential, such as the prices agreed between an energy supplier and consumer within a smart contract recorded in a ledger. When information from multiple participants are recorded in shared ledgers, solutions need to be found for data privacy, confidentiality and identity management. Moreover, smart contracts need to be integrated into legal code to ensure compliance with the law and protection of consumers. In a distributed system architecture, it is not always clear who has the legal and technical responsibility for the negative consequences of the actions of different parties. For instance, if a major attack is successfully deployed because of a software or a hardware bug in the system, there is no central authority to which a consumer may address their complaints to, as in current practice. With blockchain systems, trust is put to the technology itself rather than in a known authority.

Finally, another significant factor that might slow blockchain adoption is the lack of standardisation and flexibility. Standards for blockchain architectures need to be developed to allow interoperability between technology solutions. An additional challenge is that once a blockchain system is deployed, any changes in the ruling protocols or code needs to be approved by the system nodes. In blockchain ecosystems, this has historically led to disagreements between developers and multiple system forks. If blockchains are largely adopted in energy systems, these issues may lead to mistrust and fragmentation [71]. Moreover, blockchain adoption might, in some cases, be inhibited by the bad reputation stemming from the early days of Bitcoin and its association with illegal activities - although as blockchains mature, this aspect may become less relevant over time.

In summary, blockchain technologies need to address several issues before achieving larger adoption. One key challenge is that of scalability and cost, while maintaining desired properties of decentralisation and security. Other emerging issues relate to user anonymity, privacy and the governance of blockchain systems, which often goes against traditional practices adopted by governments and industry.

2.10 Key findings

Chapter 2 presented the literature review relevant to the topic of this thesis. At first, a literature survey on renewable curtailment and strategies were presented. Curtailment strategies can be part of ANM schemes being deployed that aim to facilitate renewable energy connections and power system operation at areas of network constraints. Several

works in curtailment have shown that the strategy selected may significantly impact the profitability of generators and moreover may discourage new construction of RES generation plants [7, 20, 125]. Theoretical assessments have been carried out to evaluate curtailment mechanisms. However, effects of curtailment rules in renewable capacity investments, but also in transmission capacity investments were not formalised and require further investigation. These issues are further investigated in the following chapters 3-4. A game-theoretic framework for the study of curtailment and its implications can capture strategic decision-making of low-carbon technology investors. Review of the literature on game-theoretic modelling for network upgrades and generation capacity investments showed a gap in works that jointly consider transmission and generation expansion, while also considering curtailment and line access rules. While other works have studied transmission constraints and congestion, this work aims to study the effect of commercial agreements and curtailment rules in settings of private grid reinforcement by providing a novel formulation in modelling private investment in power network infrastructure, that is increasingly required to further integrate renewable generation. Contributions towards this objective are presented in chapters 5-7. Moreover, a literature survey was conducted on technologies that could minimise curtailment, including energy storage and blockchain technology. The potential of blockchain technology to act as an enabler for P2P local energy marketplaces that would result in better matching of RES supply to demand at a local level was identified. The literature review showed that blockchain technologies could add significant value, however the technology needs to mature and overcome several technical challenges for further adoption and deployment.

Chapter 3

Commercial arrangements and curtailment rules

Chapter 3 focuses on curtailment rules and flexible commercial arrangements between distributed generators and network operators. Literature review on the topic was presented analytically in the previous chapter (Section 2.4). As shown in Chapter 2, part of the renewable capacity installed is subject to generation curtailment, a strategy where generators are granted non-firm grid access (interruptible RES connections) and are required to adjust their production according to the system operator's instructions, due foremost to network constraints, low local demand and/or insufficient distribution or transmission network capacity. Each location's curtailment level (and the curtailment strategy applied) can play a crucial role on the total generation capacity installed, due to their effect on investor decisions, and might therefore discourage future RES investment, as shown in the following sections of this chapter. This work provides the results of a simulation study on three curtailment rules and their impact on the capacity factor of wind generators. This chapter also studies the effect of *spatial wind speed correlation* on the resulting curtailment and impact on lost revenues for distributed generators. The results provide useful insights to DNOs searching to implement smart DG connections and optimal curtailment rules that achieve desired operational objectives and share curtailment between generators in a fair and equitable way. In this vein, a new curtailment strategy is proposed, which is fair and causes minimal disruption to generators.

Parts of the research work presented in Chapter 3 were published in peer-reviewed scientific papers [8, 12].

3.1 Research contributions

Research works on the topic of curtailment rules and PoAs were presented in detail in Chapter 2 and Section 2.4. Generation curtailment rules and flexible commercial strategies are deployed by network operators to deal with curtailment issues caused by network congestion or excess renewable generation capacity. With respect to the literature

presented in the previous section, the research work undertaken throughout the duration of this thesis advances the state of the art in the following points.

As seen in Chapter 2, a large number of commercial and academic studies [20, 23, 49, 62, 126] have discussed issues around the application of curtailment strategies, with main focus on their technical, legal and regulatory implications. However, few research works have focused on their effects on the profitability of RES generators. Along with other financial incentives provided to renewables, such as the level of the guaranteed feed-in-tariff (FiT) price or the strike price agreed with the Contracts of Difference (CfD) scheme, the curtailment rule selected in the PoAs and the curtailment level are key factors that affect the investors decision-making on future projects. Our work specifically focuses on the impact of different rules on the viability of RES investments and the decision-making of investors about future generation expansion.

The main threads found in the literature are LIFO rules which do not affect existing generation, Pro Rata rules that share curtailment equally amongst all generators, or Market-based rules that require the establishment of a curtailment market. These rules were discussed in [6] with regards to their risk allocation and social optimality, rather than their effect on the viability of RES investments, which is the focus of this work. Specifically, this dissertation focuses on the most representative PoAs, LIFO, Pro Rata and Rota. A new type of strategy, called Fractional Round Robin (FRR), which guarantees equal curtailment for generators of unequal rated capacity, is also proposed.

Similar to [126], the analysis takes a direct approach in quantifying the effects of most commonly used PoAs to the capacity factor of wind generators by virtue of simulations. In addition, our work demonstrates how wind speed spatial correlation affects the resulting curtailment and how different PoAs affect the frequency of curtailment events, providing useful insights to DNOs regarding the most efficient strategy. Correlation should not be ignored as most generators responsible for a particular grid constraint have geographical proximity and therefore correlated power outputs, resulting in a greater impact on the resulting curtailment. In addition, results shown in this work formally prove that fair strategies can maximise the total generation capacity installed at a single location.

In summary the research contributions of this work that advance the state of the art are:

- A simulation analysis on widely used curtailment rules, as found by the literature survey presented in Chapter 2, was developed. The results of the study demonstrate the impact of three curtailment rules on the profitability of RES investments by showing the long-term effects the rules have on the capacity factor of wind generators.

- A new round-robin rule is proposed that guarantees fair distribution of curtailment amongst generators, while minimising individual generator's disruption and individual number of curtailment events.

- The feasibility of the new rule is shown by simulation results that demonstrate how the newly proposed rule compares to commonly-used curtailment strategies. The results achieve a comparative evaluation by the criteria of fairness and social optimality, profitability of investments and renewable resource spatial correlation.

- Finally, the effect of curtailment on the RES capacity installed at a single/particular location is formalised. Specifically, this thesis proves that fairness or equal sharing of curtailment makes more efficient use of the available network capacity by maximising the total generation capacity built at a single location.

The following sections present in detail the models developed for the analysis and their underlying assumptions.

3.2 Curtailment rules analysis

In Section 3.2, the attention is drawn to curtailment rules and the presentation of the methods developed in this thesis for the assessment of their potential effects on the profitability of renewable generation projects.

3.2.1 Analysis for prevailing curtailment rules

While a larger number of curtailment rules is summarised and reviewed in Table 2.1 and Chapter 2, in this work we focus our attention on three main schemes frequently applied in commercial projects in the UK and other countries, namely:

- *LIFO:* Early connections have a clear market advantage. The LIFO rule was selected by Scottish and Southern Energy (SSE) in two occasions as being transparent, simple to implement and not affecting existing generators ('Orkney Smart Grid' and NINES).

- *Rota:* Generators are curtailed on a rotational basis or at a predetermined rota specified by the system operator. An early example of the Rota rule applied in a practical setting in the United States by Xcel Energy can be found in [216].

- *Pro Rata or Shared Percentage:* Curtailment is shared equally between all non-firm generators, proportionally to the rated capacity or actual power output of the generators. Pro Rata was the favourite choice for UK Power Networks and was applied to generators participating in the FPP project.

To illustrate the effects and operation of these frequently used schemes, a simple network of three wind generators of different rated capacities $P_{N_1} = 7$ MW, $P_{N_2} = 2$ MW and $P_{N_3} = 3$ MW was considered, where the subscript denotes the chronological order of their connection to the power grid or the ANM scheme. For simplicity, we assume there is no export capability and the demand is constant and equal to 6 MW. At a given time t, if all generators are producing their nominal output power, the total renewable production is equal to $P_{G,t} = \sum_i P_{G_{i,t}} = \sum_i P_{N_i} = 12$ MW. Given that the available power output exceeds the required demand, generation curtailment is enabled. The total power curtailed is therefore equal to $P_{C,t} = 6$ MW. How curtailment is applied in practice to wind generators depends on their technology type. For pitch-controlled wind turbines or models

that permit advanced power electronics control mechanisms, curtailment can be achieved by modifying the wind turbine's control system, in order to accept a power output set point, as defined by the system operator. For wind turbines that rely on stall control for limiting the rotor power, curtailment may only be achieved by shutting down completely one or more wind turbines from the multiple wind turbines that consist the wind farm. The allocation of the power curtailed to the renewable generators depends on the curtailment scheme selected:

- With LIFO, 6 MW are curtailed by the the last generator connected to the power system. In our example, this leads to the third and second generator completely curtailed and the first generator curtailed by 1 MW.

- When Rota is implemented, the generators are curtailed one after the other, resulting in 6 MW curtailed by the first generator. Other generators are not affected. When the next curtailment event occurs, the second generator is curtailed, but as this is not sufficient, the third generator is also completely curtailed and 1 MW is curtailed by the first generator. In the next event, the second generator is first to be curtailed and so on.

- By contrast, with Pro Rata, curtailment is allocated proportionally to each generator's output. In other words, curtailment is distributed evenly among the generators according to their nominal capacity or actual power output (equal in the example considered). The power curtailed at time t from generator i is found by the following equation:

$$P_{C_i,t} = \frac{P_{C,t}}{P_{G,t}} P_{G_i,t} \tag{3.1}$$

  This results in:

  - Generator (1): $P_{C_1,t} = \frac{P_{C,t}}{P_{G,t}} P_{G_1,t} = \frac{6}{12} 7 = 3.5$ MW
  - Generator (2): $P_{C_2,t} = \frac{P_{C,t}}{P_{G,t}} P_{G_2,t} = \frac{6}{12} 2 = 1$ MW
  - Generator (3): $P_{C_3,t} = \frac{P_{C,t}}{P_{G,t}} P_{G_3,t} = \frac{6}{12} 3 = 1.5$ MW

  power curtailed, respectively.

The curtailment rules have various effects on generators, system operators and consumers. As imposed curtailment reduces the energy produced by generators, it causes a reduction of the capacity factor (CF) of renewable projects, and therefore results in lost revenues. Financial implications have the potential to discourage, in the long term, the generation capacity investment at the location where ANM is applied, which may lead to inefficient use of potential renewable and network capacity resources.

From the example above, it can concluded that the LIFO scheme discriminates according to the order of connection. Thus, LIFO may disincentivise future renewable development and makes inefficient use of the transmission capacity available. The Rota

scheme follows a simple approach, which does not take into account the generators' size or their actual contribution to the network constraint. This results in disproportionate losses of revenue, especially for smaller sized generators. Finally, Pro Rata shares curtailment equally and is 'fair' [1] however, all participating generators are curtailed at all times when curtailment is required, leading to increased disruption. For this reason, Pro Rata might not always be desirable and might be technically preferable to curtail a larger amount of power from one generator than smaller amounts from all generators when a curtailment event occurs. For the reasons above, an equivalent Rota-type curtailment strategy is proposed in this work, called Fractional Round Robin (FRR). FRR is presented in detail in the following section.

3.2.2 FRR curtailment strategy

In this section, a new Rota-type curtailment rule called *Fractional Round Robin* (FRR) is proposed. With FRR, the power curtailed is distributed sequentially on a rotation basis, according to the number of rated capacity units installed, so that larger generators are chosen proportionally more times and in direct relation to their size. Prior knowledge of the curtailment order reduces the uncertainty of short-term power output prediction of a generator, therefore any disruption to individual generators minimised. In more detail and following the same illustrative example as in the previous section:

- Similarly to the Rota strategy, at first 6 MW will be curtailed by the first generator. The generator will be first to be curtailed in all future events, up until a quota equal to its rated capacity is reached. Therefore, in the subsequent curtailment event, 1 MW is curtailed by the first generator and the remaining 5 MW are curtailed by the second and third generator. This means that on average, every 12 times a curtailment of 6 MW is needed, the first generator will be curtailed 7 times, the second 2 times and the third 3 times. In fact if multiple curtailment events are considered, the probabilities of generators being curtailed in this example are equal to:
  - Generator (1):

$$\frac{P_{G_1,t}}{P_{G,t}} = \frac{7}{12}$$

  - Generator (2):

$$\frac{P_{G_2,t}}{P_{G,t}} = \frac{2}{12}$$

  - Generator (3):

$$\frac{P_{G_3,t}}{P_{G,t}} = \frac{3}{12}$$

[1] As we show in the following sections, 'fairness' is significant as fair schemes maximise the generation capacity built at a single location [8].

Moreover, for a sufficiently long period of time (i.e. many years and like the typical lifetime of a wind turbine) or for multiple curtailment events, the curtailment imposed to generators under FRR converges to the proportional curtailment rate achieved with Pro Rata.

As shown by the illustrative example, the curtailment strategy chosen can affect significantly the power production of the generators, the energy produced, the revenue earned and therefore the actual viability of the investment. Some strategies are fair in the way they deal with network constraints and allocation of amongst generators (Pro Rata, Fractional Round Robin), while others offer a significant market advantage to certain generators. To further elaborate on the effects of the rules, a simulation process was developed to show how different rules affect the CF of wind generators.

3.2.3 Simulation analysis

In this section, we turn our attention on the effects' quantification of the selected curtailment strategy. Several prior works have discussed the effect of applied curtailment strategies on the installation of generation capacity. In [126], the influence that several curtailment strategies have on the CF of wind generators based in Orkney, Scotland is examined. It is shown that LIFO leads to lower CF for 'later' connections, when compared to Pro Rata and Rota. Therefore LIFO might discourage investment in new generation capacity [125]. In fact, a related study by UK Power Networks observed that the most important factor affecting the decision-making process of a new investor, especially when a LIFO scheme is applied, is the CF of the last generator connected [68]. A LIFO scheme discourages new investment by shutting out newer entrants, essentially leading to inefficient use of the grid capacity available.

Based on the example network presented in the previous section, we implemented a simulation process, in the course of one year, to compute the capacity factors of the wind generators, under different schemes. However, since network constraints are usually applicable to a particular geographical area of the grid, where wind conditions may be similar, generator power outputs present a level of spatial correlation, which is a significant factor for resulting curtailment levels at this area. To model correlation, we apply the technique developed by Früh (2015) [84]. First of all, we generate 8760 wind speed data points $u_{rand,i}$ for $i = 1...3$ generators. Data points come from *random* and independent samples of three Weibull distributions (one for each generator), using the typical UK values of $c = 9$ m/s and $k = 1.8$. Wind speed at the first generator's location ia set as a reference u_{Ref}, in order to produce random, yet cross-correlated wind data series u_i for each generator's location, by the following equations:

$$u_i(t) = c_r \cdot u_{Ref}(t) + (1 - c_r) \cdot u_{rand,i}(t) \tag{3.2}$$

$$c_r = \frac{1}{\pi} \cdot \arccos(1 - 2r) \tag{3.3}$$

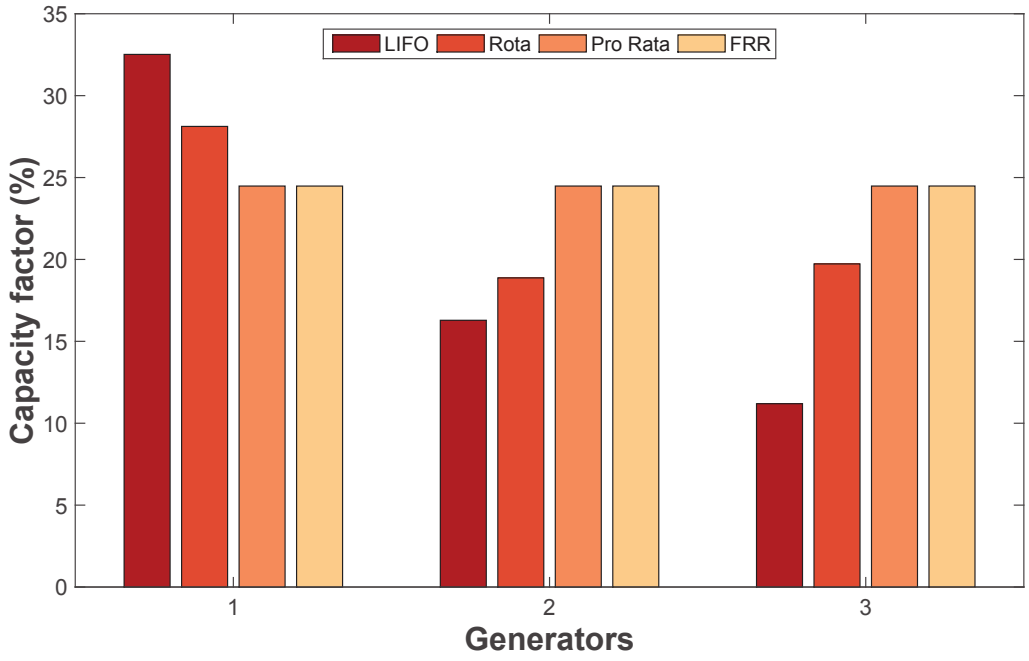

Fig. 3.1 Curtailment mechanisms effects on the CF of wind generators under LIFO, Rota, Pro Rata and FRR

where r is the Pearson's correlation coefficient. The data series are then converted to power outputs, using a generic model of a wind turbine[2]. If the aggregate power at time t exceeds the power demanded, then curtailment is required, which is allocated to the generators according to the strategy imposed.

Fig. 3.1 shows the CF results for each generator under the four different schemes for conditions of perfect correlation ($r = 1$). LIFO clearly favours 'early' connections, while the third generator suffers a reduction of 67.4%. Rota can disadvantage smaller-sized generators. On the contrary, Pro Rata produces equal CF reduction for all generators, while FRR produces similar results to Pro Rata, as expected.

A measure of fairness is the variance of the average CF for each strategy. In Fig. 3.2 we illustrate for $r = 1$, this variance with the average number of curtailment events required. LIFO presents a poor performance with respect to fairness, as opposed to Pro Rata, which requires the largest number of curtailment events. The results show that FRR has similar fairness properties to Pro Rata, but also reduces significantly the number of curtailment events per generator. Finally, Rota is fairer than LIFO and requires the smallest number of curtailment events than all other schemes.

Finally, as shown in Fig. 3.3 the required total curtailment increases as we proceed from no correlation to perfect correlation, resulting in lower CFs.

In the following sections, we determine an upper level of tolerable curtailment at a single location with network congestion, which enables renewable capacity investment to be profitable. Moreover, we examine which types PoAs can be used to maximise the capacity installed at this location.

[2]Based on the power curve of Enercon E44 commercial wind turbine.

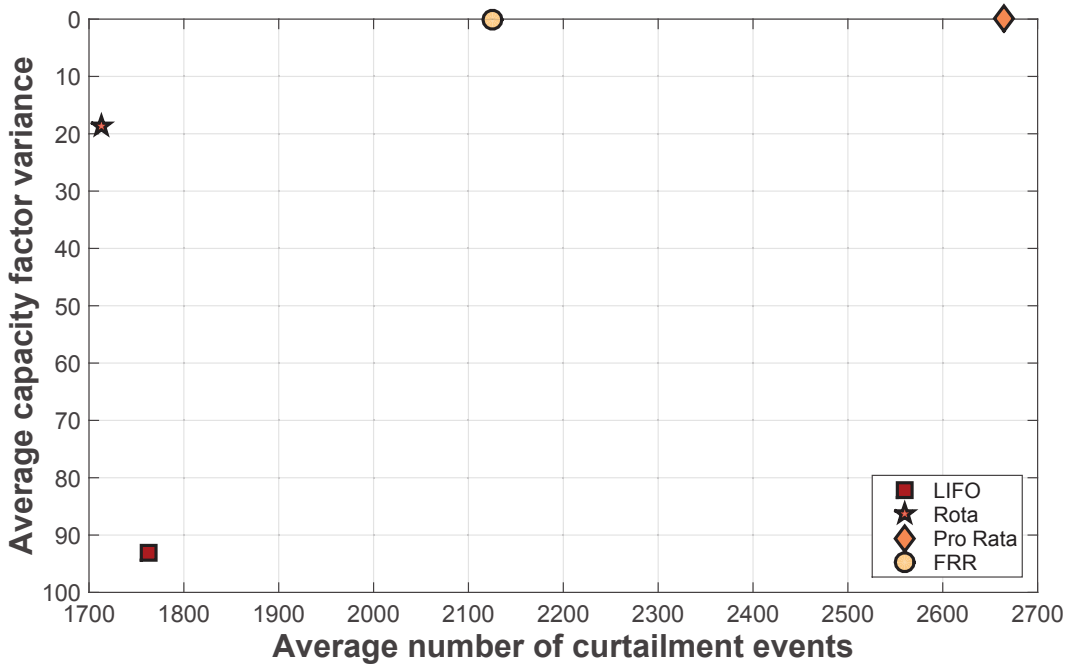

Fig. 3.2 Fairness under different curtailment schemes

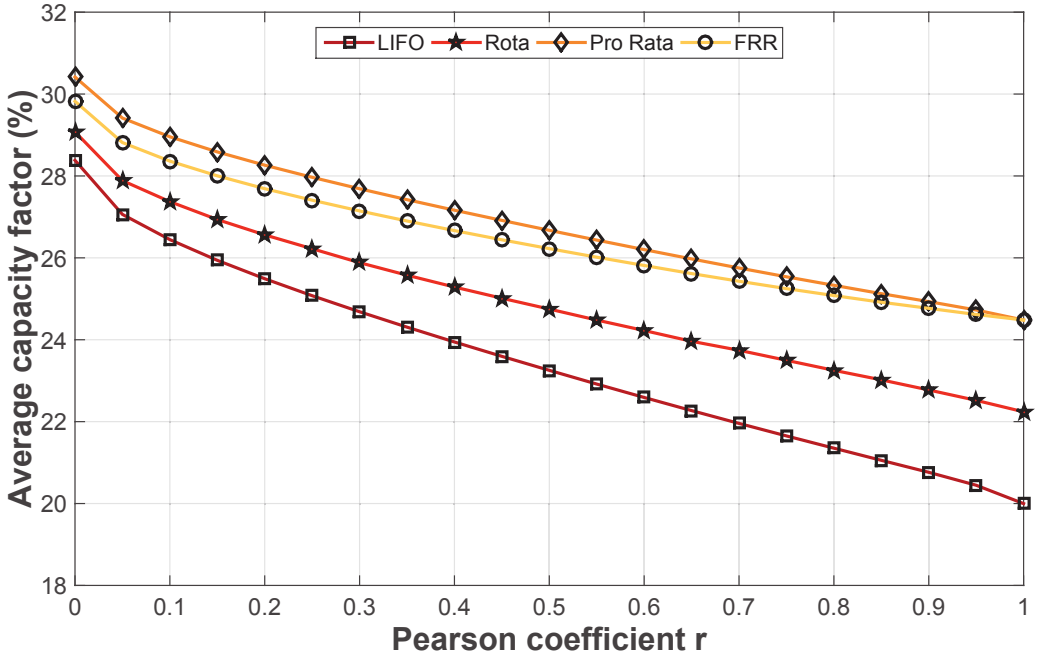

Fig. 3.3 Correlation effects on average CF under different curtailment schemes

3.3 Generation capacity at a single location

Consider n renewable generators $\langle P_{N_1}, P_{N_2}, ..., P_{N_i}, ..., P_{N_n} \rangle$ at a single location of the distribution network with network constraints. Generator i is expected to produce $\mathbb{E}(E_{G_i,t})$ energy units at time t and according to the available resource on site location, when no curtailment is considered. It is important to note that while for a particular period such as an hour or a day the expected generation is uncertain, for the overall lifetime of a renewable project (typically 20-25 years), total expected generation can be estimated with relatively high certainty from the weather and wind patterns at a particular location.

As this is the case in many countries, it can be assumed that the energy generated by RES units generates revenue at a constant price, such as the FiT price for smaller capacity generators or the CfD price for larger capacity generators, denoted here as p_G [180] or *generation tariff price*. Curtailment of the power/energy production is imposed in the region due to network constraints. The expected curtailed energy units are denoted as $\mathbb{E}(E_{C_i})$.

The term $\mathbb{E}()$, which symbolises the 'expected' value of the variable under consideration, will be omitted from this point on, in order to simplify the notation. Hence, from this point on this thesis, expected energy generated will be denoted by $E_{G_i,t}$, and $E_{C_i,t}$ will represent the expected energy curtailed.

With respect to the i-th generator, the cost of per unit of expected generation c_{G_i}[3] is defined as:

$$c_{G_i} = \frac{I_{G_i} + M_{G_i}}{E_{G_i}} \tag{3.4}$$

where I_{G_i} is the installation cost of the renewable energy plant (initial investment), M_{G_i} is the operation and maintenance cost and E_{G_i} the expected generation throughout the duration of the project lifetime. When subscript t is omitted, the variable under consideration refers to the project lifetime and is equal to the sum of energy produced at all time intervals t.

We will also define a new parameter, useful for the analysis, which measures and quantifies the curtailment imposed to each generator. We define the *curtailment rate* of i generator CR_i, as the ratio of expected curtailment [4] to expected generation, over the project lifetime:

$$CR_i = \frac{E_{C_i}}{E_{G_i}} \tag{3.5}$$

Curtailment rate CR_i is computed as the average of all $CR_{i,t}$ over a longer time horizon equal to the project lifetime (e.g. all hourly time periods over the project lifetime). The curtailment rate of generator i at time interval t is denoted as $CR_{i,t}$ and by definition is

[3] No depreciation was considered.

[4] In real-world settings and over a large time horizon, such as the project lifetime, curtailment may change significantly due to numerous external factors. For example, curtailment may increase if additional RES generation is installed in the area or if demand is reduced. On the other hand, curtailment may decrease if grid reinforcement takes place. Such externalities and possibilities are ignored in this study and expected curtailment is estimated based on current grid conditions.

equal to the ratio of expected curtailment over expected generation at time t:

$$CR_{i,t} = \frac{E_{C_i,t}}{E_{G_i,t}} \tag{3.6}$$

By definition the curtailment rate represents the percentage change of the CF of a renewable generator, when comparing production with and without curtailment. For example, a curtailment rate of 5%, is directly interpreted as a 5% reduction of the CF, compared to the CF value when no curtailment is required. Moreover, when $CR_i = 0$ there is no curtailment, so all potential energy is produced and absorbed by the power system. On the other hand, if $CR_i = 1$ all potential generation is curtailed. Combining the latest statements, the curtailment rate CR_i is subject to the following condition:

$$0 \leq CR_i \leq 1 \tag{3.7}$$

This parameter is crucial for the profitability of renewable investment projects, not only for already established projects, but also for investment decisions on future renewable capacity (see analysis in the following section).

3.3.1 Renewable generator profitability

The curtailment rate is a key parameter that determines the profitability of a renewable project. The relation between CR_i and the viability of the investment is formalised in the following Lemma.

Lemma 3.3.1. *A generation capacity investment is viable, if and only if the curtailment rate of i generator CR_i is smaller or equal to a threshold τ_{G_i}*

$$CR_i \leq \tau_{G_i} \tag{3.8}$$

where

$$\tau_{G_i} = 1 - \frac{c_{G_i}}{p_G} \tag{3.9}$$

Proof. When no curtailment is required, the profit equation of i generator is equal to the revenue earned from energy production minus the cost of energy or power generation $\Pi_i = E_{G_i} \cdot p_G - E_{G_i} \cdot c_{G_i} \geq 0$. Likewise, the profit function Π of generator i, when part of renewable production is curtailed, is given by $\Pi_i = (E_{G_i} - E_{C_i}) \cdot p_G - E_{G_i} \cdot c_{G_i} \geq 0$. Dividing the latter by $E_{G_i} \cdot c_{G_i}$:

$$\left(1 - \frac{E_{C_i}}{E_{G_i}}\right) \cdot \frac{p_G}{c_{G_i}} - 1 \geq 0$$

Substituting from the definition of the curtailment rate Eq. (3.5):

$$(1 - CR_i) \cdot \frac{p_G}{c_{G_i}} - 1 \geq 0$$

By rearranging, the proof is concluded:

$$CR_i \leq 1 - \frac{c_{G_i}}{p_G} = \tau_{G_i}$$

□

The curtailment rate determines the profitability of i generator. Specifically, the curtailment rate cannot exceed a *threshold* τ_{G_i} that depends on the ratio of the generation cost c_{G_i} over the energy production selling price p_G. The smaller the generation cost with respect to the generation tariff price, the larger amounts of curtailment a generator is willing to accept.

Relaxing further Eq. (3.3.1), we assume that all n generators at a single location have equal access to land and type of technology, therefore their marginal costs of generation can be assumed equal. In this occasion, the threshold for investment viability can express the tolerable curtailment at a single specific location.

Proposition 3.3.2. *For a single location, if all generators have equal marginal costs then:*

$$CR_i \leq 1 - \frac{c_G}{p_G} = \tau_G \tag{3.10}$$

Proposition 3.3.2 shows that the curtailment rate at a certain location can not exceed a location-specific threshold that depends on the quantitative relation of the generation cost with the selling generation tariff price. The lower the ratio the higher the amounts of curtailment that can be tolerated by generators at this location.

The curtailment rate is directly linked to the capacity factor of a renewable project. As shown in Section 3.3, CF depends on the curtailment strategy used. The strategy selected remains under the control of the network operator and regulator, who play the role of the mechanism designer. Hence, a natural question to ask is *which curtailment rule maximises the local generation capacity?* Generation capacity needs to be maximised in order to also maximise the utilisation of network assets before installing new grid capacity. This question is of interest in itself, but it also plays a key role in modelling investment decisions of grid expansion, as shown in Chapter 4.

3.3.2 Curtailment rule for generation capacity maximisation

The analysis so far showed that the viability of a RES investment depends on the curtailment rate and consequently on the curtailment strategy chosen by the system operator. As shown below, the generation capacity at a single location is maximised when curtailment is distributed evenly between all generators.

To prove this, a perfectly competitive setting is assumed, in which no generator has the market power to influence the price equilibrium. Using assumptions of competitive equilibrium analysis (and more specifically Cournot equilibrium analysis [47]), any investor or 'player' is able to install an additional generation unit, as long as the marginal profit exceeds the marginal cost. As discussed in Section 3.3.1, since this is a single location

setting (e.g. an island or some other remote location) where renewable resources and access to available technology are roughly equal for all players, we can safely assume marginal costs are also the same. Moreover, the decision to invest takes into account whether the curtailment rate exceeds a certain location-dependent threshold τ_G, as in Eq. (3.10). Given these assumptions, the curtailment strategy selected by the system operator, can affect the total generation capacity installed.

Lemma 3.3.3. *In a perfectly competitive equilibrium setting, the local generation capacity installed is maximised under proportional curtailment strategies that distribute curtailment evenly among generators of the same technology type.*

Proof. The problem of maximising the generation capacity installed is equivalent to maximising the total energy generated at a single location and it can be formulated as the optimisation problem

$$\max\left(\sum_{i=1}^{n} E_{G_i}\right) = max(E_{G_1} + ... + E_{G_i} + ... + E_{G_n}) \tag{3.11}$$

subject to a set of n constraints (one for each generator), as derived from Lemma 3.3.1:

$$\frac{E_{C_i}}{E_{G_i}} \leq \tau_G, \forall i = 1 \dots n \tag{3.12}$$

Expected curtailment E_{C_i} is equal to the energy it could be generated, minus the energy demand actually required, $E_{C_i} = E_{G_i} - E_{D_i}$. Furthermore, total generation purchased from renewable sources at this location (or exported at another location) is bounded across all the n generators to some quantity E_D (total demand), where $E_D = \sum_{i=1}^{n} E_{D_i}$. The constraints in Eq. (3.12), can hence be written as $E_{G_i} \leq \frac{E_{D_i}}{1-\tau_G}, \forall i = 1 \dots n$. The initial maximisation target can be decomposed without loss of generality into n individual maximisation problems, therefore $\max\left(\sum_{i=1}^{n} E_{G_i}\right) = \sum_{i=1}^{n} \max\left(E_{G_i}\right)$, and given the set of n constraints, will be maximised when all the constraints are equal, i.e. $E_{G_i} = \frac{E_{D_i}}{1-\tau_G}, \forall i = 1 \dots n$. Expressed back in terms of curtailment rate, the solution of the problem is given when all curtailment rates CR_i of generators are equal to each other and to threshold τ_G:

$$\frac{E_{C_1}}{E_{G_1}} = \frac{E_{C_2}}{E_{G_2}} = ... = \frac{E_{C_i}}{E_{G_i}} = ... = \frac{E_{C_n}}{E_{G_n}} = \tau_G \tag{3.13}$$

Essentially, this condition will be satisfied by proportional or 'fair' curtailment strategies, i.e. those mechanisms which allocate equally the demand or curtailment imposed. □

In summary, fair curtailment mechanisms can lead to the maximum generation capacity being installed at a specified location. Such fair rules can be expressions of either Pro Rata or FRR type of strategy.

3.4 Discussion and concluding remarks

Chapter 3 presented work on generation curtailment and curtailment rules. A literature review on the topic of curtailment rules was presented in Chapter 2. In this chapter, we focused on the study of most frequently used curtailment rules, such as LIFO, Rota and Pro Rata, and showed how curtailment is allocated according to these rules. In agreement to previous works published in the field, it was found that LIFO favours early connections, Rota might disfavour smaller size generators, while Pro Rata requires simultaneous intervention to all generators participating in the scheme. To satisfy the criteria of even distribution of curtailment and minimising generator disruption, a new rule called FRR was proposed. A simulation analysis, including all four curtailment strategies, showed that FRR has similar effects on the CF of generators, as Pro Rata. Such effect is achieved with reduced disruption for generators, as shown by the average number of curtailment events per generator. The results also showed how curtailment strategies affect the CF of generators, and consequently the viability of their investment. Under the LIFO scheme, the CF of the last generator was severely reduced. Pro Rata or FRR on the other hand, allow more capacity to be built. In addition, the simulation analysis showed how CF is affected with regards to the wind speed spatial correlation. It was found that CF reduction is linked to higher correlation. This highlights the importance of geographical dispersion of RES resources, when possible, in order to minimise curtailment. In addition, combination of different RES technologies and diversification of resources could also minimise required curtailment. This was not studied in this thesis, since the work focused on a single technology type (wind power), but is of great interest for future works.

Afterwards, the work focused on the curtailment effects on decisions about investment in renewable generation capacity. In particular, we showed that a renewable project can be profitable if the curtailment rate is smaller than a threshold that depends on the economic parameters of the investment, and more specifically, on the ratio of the generation cost to the selling tariff price. If marginal costs of generation at a single location are equal, this threshold is the same for all generators and can characterise the location. Moreover, under perfect competition analysis assumptions, it was proved that fair curtailment rules such as Pro Rata and FRR can be selected by network operators and regulators in order to maximise the generation capacity built at a single location. The generation capacity is maximised when generators are curtailed at their maximum acceptable curtailment rate.

In real-world applications, some RES generators might have been installed in earlier time periods and therefore might have larger generation costs. For example, in general, similar technology solutions tend to be become cheaper over time. On the other hand, renewable incentives and financial premiums have gradually decreased with time and in some occasions they have been totally stripped off. Moreover in practice, RES investors may not have perfect knowledge of the market or access to all the technology solutions available. In other words, the assumption of equal marginal costs may not hold in most practical settings. A proportional curtailment scheme, such as Pro Rata or FRR, does not consider the real marginal cost of generation, which can be estimated with good accuracy,

but normally it is not publicly known, as it is considered private information. Curtailment with proportional rules is distributed evenly, however cheaper generators should be able to tolerate larger amounts of curtailment. A method for dealing with curtailment more efficiently is moving towards establishing a market for curtailment and required flexibility. This would allow curtailment allocation according to real generator costs. A market-based solution is compliant with the overall vision towards deregulated electricity markets, hence market solutions are of great interest for future work consideration.

Chapter 3 studied the effect of curtailment on generation capacity and profitability of RES projects. The following chapter focuses on how curtailment and line access rules affect transmission capacity investments, such as installing new distribution and transmission lines or reinforcing existing ones.

Chapter 4

Transmission capacity game with distributed generation

Chapter 4 studies the problem of how line access and curtailment rules applied influence the decision to reinforce existing transmission lines or build new transmission capacity. In the context of this thesis, transmission capacity may refer to distribution/transmission lines installed by independent investors. A game-theoretic modelling approach is used to study the network upgrade investment and to model strategic interactions between transmission and generation capacity investors. Two separate cases are considered to model different agent behaviours, one with myopic players, who are not able to react to other players' strategies, and one with strategic players, where each agent is able to estimate and forecast the opponents' behaviour and is able to adjust his own actions according to his individual beliefs. As shown in Chapter 4, the network upgrade problem can be modelled as a Stackelberg game between a *private investor (leader)*, who builds additional grid capacity and new renewable generation capacity, and *local renewable investors (follower)*. Following average-case assumptions, an analytical solution of the Stackelberg game equilibrium was formulated. These assumptions are relaxed in the following chapters, where equilibria are found by empirical game-theoretic approaches.

Parts of the work presented in Chapter 4 were published in peer-reviewed scientific publications [8] and [12].

4.1 Research contributions

A literature review on game-theoretic modelling in network upgrades and generation capacity investments was analytically presented in Chapter 2. With respect to the scientific publications found in the literature review, the main contribution of this work relates to the use of game-theoretic and microeconomic models to the problem of transmission and generation expansion, while also considering curtailment and line access rules. Other works have studied transmission constraints and congestion, but the work presented in this thesis aims to study the effect of flexible commercial agreements and curtailment rules with private grid reinforcement. More specifically, the effects of curtailment rules

on low-carbon technology investors' decision-making about additional generation and transmission capacity are studied. The methods developed provide a useful tool to network operators that seek to incentivise privately funded grid capacity investment projects and sustainable low-carbon technologies.

In summary, the research contributions of the work presented in Chapter 4 that progress beyond the state of the art are:

- First, a two-location model was developed that studies the interaction between two players, a line investor and local generators[1]. The model output is the determination of the optimal generation capacities installed by the players, which maximise at the game equilibrium, their utility functions, i.e. their profits. The model follows a hierarchical, two-stage Stackelberg game formulation.

- Next, a market model is developed for optimal decision-making with regards to investments on generation capacity and grid upgrades at regions that are already experiencing significant volumes of curtailment. This model is analysed for two sets of underlying assumptions, in the case of *myopic* agents that take decisions without a foresight to the future, and in the case of *strategic* agents, where players have the ability to forecast their opponents' behaviour and take this into account when making their own decisions. While other works have studied network upgrades in areas with grid constraints and congestion, to the best of our knowledge, this work is one of the first to study the effect of commercial agreements and curtailment rules in settings of private grid reinforcement. This work provides a novel formulation in modeling private investment in grid capacity investments that is required to further integrate renewable generation.

- As a first approach, a simple model based on average and expected values of renewable production and demand is studied. In the Stackelberg game formulation, the line investor is the leader, as he has the first mover advantage and builds the transmission line. Investors' decision variables constitute renewable generation capacities they need to install in order to maximise their profit. Decisions on optimal (and interdependent) renewable capacities built by investors, affect the resulting curtailment and profitability of projects and can be determined in the equilibrium of the Stackelberg game. Average-case analysis assumptions and expected values approach allowed for an analytical, closed-form solution of the problem and a preliminary examination of the Stackelberg game equilibrium properties.

- Equilibrium results of the leader-follower game are examined for a wide range of cost parameters. A feasible range of suitable charges for transmission is identified allowing both transmission and generation capacity investments to be profitable. The game-theoretic models developed enable network operators to bridge the knowledge

[1] Note here that players or agents are considered gender-neutral, however by convention male forms such as *'he'* and *'his'* are used when referring to a single player.

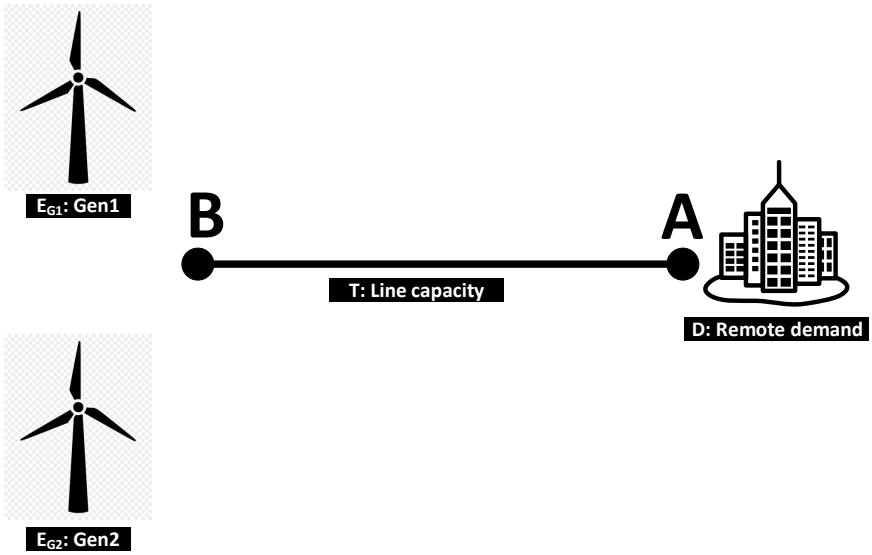

Fig. 4.1 A simplified model schematic of the two-node, two-player network assumed: RES generation capacity built by the line investor E_{G_1} and RES generation capacity built by local generators E_{G_2} are connected at location B, while demand D is located at A

gap of incentivising privately funded grid infrastructure, especially in settings where multiple generators can share their grid access and use the same transmission line.

- Finally, the theoretical models are demonstrated in practice, based on realistic assumptions from a network upgrade project in the UK. The practical application aims to showcase the value of the models in real-world settings with the ambition that this work can easily be replicated and applied to other cases and locations, where potential renewable production and demand are not co-located.

The following sections present in greater detail the models developed for studying the network expansion game .

4.2 Transmission capacity game

The effects of curtailment and line access rules on transmission capacity investment projects were studied in the context of a two-location game, the main features of which are described in detail below (see also Fig. 4.1):

- **Location A** is a net consumer of D power demand. Location A can be thought of as a mainland location with industry or significant population density. Meeting the demand at location A would require energy produced and imported from different locations. In practice, some generation capacity might be operating at A, part of which could also be renewable generation. In this case, the net demand D would be equal to generation at A minus the actual demand at A. However here, for simplicity, location A is assumed to be a net consumer node, with a net power demand of D and net energy demand of E_D.

- On the contrary, **location B** is assumed to be a net energy producer node and can be thought of as a location where RES resources are favourable, for example such as a remote region rich in wind resource. In practical settings, there would be some local demand and supply considered here negligible. Nevertheless, due to plentiful resources, high renewable generation potential and relative proximity to A, renewable investors would be interested in installing new renewable generation capacity at B, especially if a transmission link was carried out between the A-B locations.

In addition, we consider two different types of investors or players, who intend to install renewable generation capacity at B:

- *Player 1* is a private investor willing to install a *new transmission line T* between locations A-B *and renewable generation capacity* with a rated capacity of P_{N_1}. Installing P_{N_1} leads to potential energy generation of E_{G_1} over a larger time horizon. Player 1, also called the **'line investor'**, can be a merchant-type or a utility company, who is granted with a license to build the line. Note here that in reality, investments on network assets are usually performed by DNOs or DNO-approved partners that have the technical expertise to carry out such projects.

- *Player 2* represents all other, than the line player, investors, i.e. local renewable generators at location B. Local RES generators are keen to install a *generation capacity* of P_{N_2}, which can produce E_{G_2} energy units, over a large time horizon. This second player, also called **'local generators'**, can be thought of as investors from the local community, who do not have the technical/financial capacity to build a line, but may have access to cheaper land, find it easier to get community approval to build turbines etc., hence may have a lower per-unit generation cost c_{G_2} [2]. Recall here that the per-unit generation cost is defined as the cost per unit of expected generation (see Eq. (3.4), and depends on the renewable energy plant's capital cost of installation, on operation and maintenance costs and on expected generation over the duration of the project. Individual behaviour of local renewable investors is considered negligent and too small to have a great effect in the emerging game. In this model formulation, local generators are considered to act as a single entity and in this context c_{G_2} is the weighted average generation cost of local players. The aggregated actions of local generators can and do exert some market power in the outcome of the game.

Moreover, it is assumed that players or agents are rational, and are able to take initiative and act in order to maximise their own utility function (in this work profit functions were assumed hence agents seek to maximise their profits), and they have perfect knowledge about the parameters of the game including opponent's costs. Note that similar assumptions are typical in game-theoretic formulations, although they may not always be representative of real-world situations.

[2]Note that in Scotland, or other countries such as Denmark, local groups often act together to make land available and invest in RES projects. Community Energy Scotland (CES) is an umbrella organisation of such groups, supporting more than 300 community-owned projects in Scotland.

The transmission line of capacity T can transport energy generated by both player types. In fact, the line investor is granted the license to build the power line, as long as it provides access to local generators, who do not possess the market power or financial means to build the line themselves. This 'common access' principle is opposed to traditional practices, when a renewable generator usually builds and pays for a 'single access' line with a capacity large enough to meet his own needs. Instead, under a common access principle, private investors are incentivised to build larger capacity lines that grant access to other competing generators, who need to pay a transmission fee of p_T for the energy transported through the line.

The power line's cost or transmission cost is denoted as C_T and is equal to:

$$C_T = I_T + M_T \tag{4.1}$$

where I_T represents the costs related to building the power line, summarised as initial investment required for transmission, and M_T the costs related to operation and maintenance of the power line. Note here the difference between the generation cost c_G defined in Eq. (3.4), which is divided by the expected generation, whereas C_T, defined in Eq. (4.1), refers to the total transmission cost over the project lifetime. The parameters are denoted with a small and capital letter, respectively, to highlight this difference.

Energy curtailed, either because of RES overproduction when compared to the actual demand or because the transmission capability of the line is exceeded, is denoted as E_{C_1} and E_{C_2}, i.e. the energy curtailed by the line investor and the energy curtailed by local generators.

A question of interest in the transmission game is how curtailment and line access rules affect the decision to build the power line. To answer this question, we consider two separate models, distinguished by how local investors respond to the line player's actions. In the first model (Section 4.2.1), we study the effect of curtailment on the line investor's decision to build the line, but assuming the local players do not react to this line being built, by building extra capacity themselves. In this model, local generators are considered 'myopic' as they do not adapt their actions or strategy after the line is built. This assumption cannot hold in realistic settings, where investors carefully and strategically consider competitor actions and even the possibility of future demand growth. A study on more realistic assumptions and strategic players is shown in the second model (Section 4.2.2), where local investors react to the additional line capacity built by installing new renewable generation capacity. In this occasion and under the 'common access' principle, the decisions rely interdependently on both player actions. The agents' decision-making process can be informed by modelling as a Stackelberg game, as shown in the following sections.

4.2.1 Game with myopic players

This model setting studies how curtailment might affect the installation of new transmission capacity. More specifically, the model allows for an inference of the decision to build the

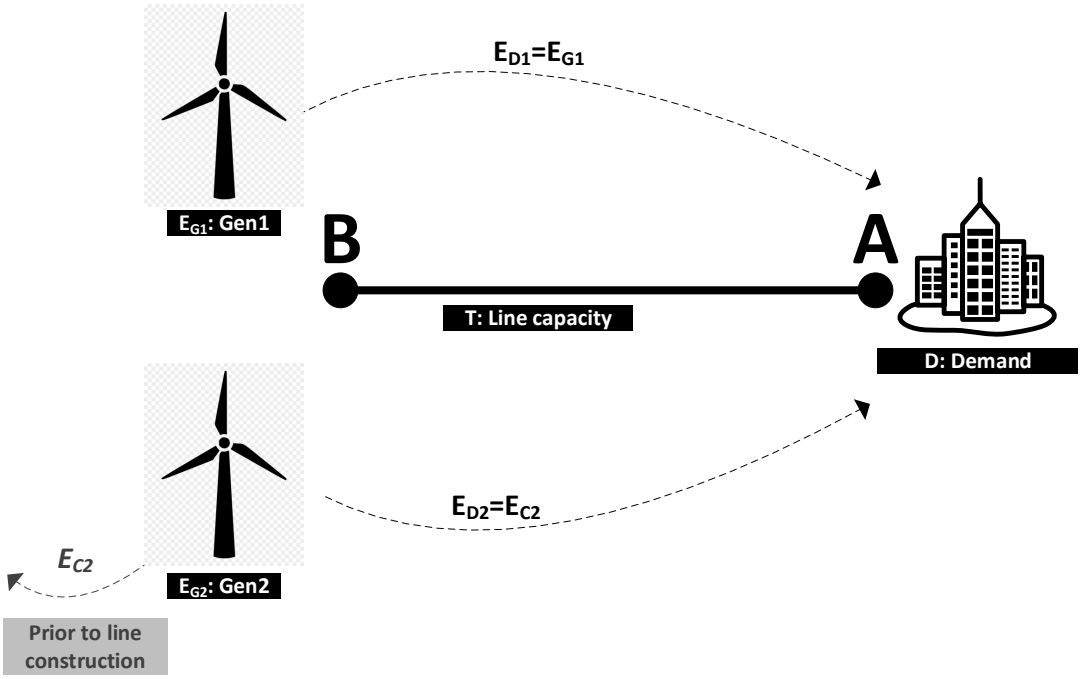

Fig. 4.2 Model schematic of the game with myopic players: RES generation capacity built by the line investor E_{G_1} and RES generation capacity built by local generators E_{G_2} are connected at location B, while demand D is located at A

transmission link A-B in relation to the curtailment rate and more concretely, how the curtailment rate relates to the viability of the transmission capacity investment. Recall here, the curtailment rate was introduced in Eq. (3.5) and is equal to the ratio of expected curtailment to expected generation over the project lifetime.

To study these effects, it is assumed that local generators, motivated by advantageous renewable resources potential, have already built significant amounts of RES generation capacity at location B, *prior* to the installation of the line. Generation by local producers exceeds at times the local demand or cannot be absorbed by the power grid because of technical limitations and network constraints. As a result, power production is curtailed by E_{C_2} energy units.

The line investor is interested in building a transmission line that links A-B and some renewable generation capacity of its own. The transmission link can export the line investor's renewable production E_{G_1} and the energy previously curtailed by already installed capacity of local generators E_{C_2}. A model schematic is shown in Fig. 4.2. Recall here that local generators are considered myopic and cannot react to the line being built by installing additional generation capacity to the one already installed at B. Moreover, as generation capacity installed by local generators exists prior to the line's construction, it is assumed that local producers take priority when serving local demand at B and can only export E_{C_2} via the transmission line.

Under these assumptions, the decision to build the power line depends on the curtailment rate at location B, as shown in the following lemma.

Lemma 4.2.1. *At an area already experiencing curtailment, a transmission capacity investment is viable if and only if the curtailment rate of local generators CR_2 (before the line is built) is greater or equal to a threshold τ_T*

$$CR_2 \geq \tau_T \tag{4.2}$$

where

$$\tau_T = \frac{C_T - E_D \cdot (p_G - c_{G_1})}{c_{G_1} \cdot E_{G_2}} \tag{4.3}$$

Proof. Assuming that the demand at A is much larger than local demand at B, the line investor will install a line with a transmission capacity that satisfies demand at A, and with the ability to transport the energy generated by own renewable assets E_{G_1}, and the energy previously curtailed by local generators E_{C_2}. In other words:

$$E_D = E_{G_1} + E_{C_2} \tag{4.4}$$

The line investor has two streams of revenue, the curtailed energy produced by local generators and the energy generated from additional capacity installed at B:

$$\Pi_1 = E_{C_2} \cdot p_T + E_{G_1} \cdot (p_G - c_{G_1}) - C_T \geq 0$$

By rearrangement, the profit function is:

$$E_{C_2} \cdot p_T + E_{G_1} \cdot (p_G - c_{G_1}) \geq C_T \tag{4.5}$$

From equations Eq. (4.4) and Eq. (4.5):

$$E_D \cdot (p_G - c_{G_1}) + E_{C_2} \cdot (p_T - p_G + c_{G_1}) \quad \geq \quad C_T$$

$$E_{C_2} \geq \frac{C_T - E_D \cdot (p_G - c_{G_1})}{(p_T - p_G + c_{G_1})} \tag{4.6}$$

The latter Eq. (4.6) divided by the expected energy of local generators at location B, prior to the line installation, E_{G_2}[3], is equal to the curtailment rate at location B:

$$\frac{E_{C_2}}{E_{G_2}} \geq \frac{C_T - E_D \cdot (p_G - c_{G_1})}{(p_T - p_G + c_{G_1}) \cdot E_{G_2}} \tag{4.7}$$

$$CR_2 \geq \frac{C_T - E_D \cdot (p_G - c_{G_1})}{(p_T - p_G + c_{G_1}) \cdot E_{G_2}} \tag{4.8}$$

For local generators, curtailed energy before the line installation is essentially wasted. Recall that (see Lemma 3.3.1), the local generators' renewable capacity investment is still profitable, as long as $CR_2 \leq \tau_{G_2}$. This means that the line investor can actually impose a

[3] Note here, this does not include the new generation capacity of the line investor.

large transmission fee to local generators. By definition, $p_T \leq p_G$ however, the line investor can charge a fee that approaches the selling price $p_T \to p_G$, in order to maximise its own profits. Local generators would be willing to accept such a fee, as long as they are better off and can increase their own profit, even by a marginally small amount. Considering this in Eq. (4.8), we derive the desired conclusion.

$$CR_2 \geq \frac{C_T - E_D \cdot (p_G - c_{G_1})}{c_{G_1} \cdot E_{G_2}} = \tau_T \tag{4.9}$$

□

As shown by Lemma 4.2.1, the viability of a new transmission capacity investment depends on the curtailment rate at the location of renewable producers prior to the line being installed. Specifically, the curtailment rate has to be larger or equal to a threshold τ_T that depends on the demand served at mainland, the local generators' capacity, the cost parameter of the line, the line investor's generation cost and the selling tariff price. Note that the threshold does not depend on the cost of generation of local producers. In addition, the line investor can take full advantage of the curtailed energy of other producers, as long as he is able to charge a slightly lower transmission fee than p_G. In real-world settings, the transmission fee needs to be agreed between RES investors, hence, local generators might find this difficult to accept, resulting in a better negotiated price[4].

Model assumptions also considered that local investors cannot react by increasing their own generation capacity, once the line gets built. Even in this simple non-strategic setting, it can be seen that the volume of curtailed energy is a key factor for the decisions regarding the installation of new transmission line. Conclusions from this section can be utilised in areas experiencing high curtailment rates, however in practice, when building a transmission line, additional generation investment from other stakeholders is anticipated. In practice, the decision of the line investor must include an element of 'strategic foresight' to include the reaction of other investors or even demand growth in location A, when deciding whether or not to build the line. Models in these lines can be formulated and studied as Stackelberg game models formed between the line investor and local generators, and are presented in the following section.

4.2.2 Game with strategic players

In the previous section, decision of local players did not consider the interplay of the transmission line in future generation capacity investment decisions, instead, the line investor would build the line, only if enough renewable generation existed to use it. In this

[4]A relevant setting in game theory is the 'ultimatum game'. The game is played by two players, who need to agree on the allocation of a monetary sum between the players. One of the two players makes an offer to his opponent on how the reward should be split. Crucially, the second player can only accept or reject this offer. If agreement is not reached, then the reward is lost and no player makes any gains. A theoretic analysis of the game dictates an advantageous position of the first player. A very low offer would in principle be accepted by the second player, as long as it creates some profit. However, experimental results undertaken have repeatedly shown a significant deviation from pure theoretical results that also depends on the participants' social values and norms.

section, we turn our attention to a much more relevant case when both types of investors are strategic, meaning both the line investor and local renewable producers critically make up their decisions by reasoning about each other's actions. Local generators are able to react to the new line built and the line investor can anticipate this reaction in order to reach optimal decisions.

The strategic interaction formed between the line investor and local generators can be formulated as a hierarchical, two-stage, Stackelberg game [252]. In Stackelberg games, one player has the market power to influence the equilibrium result. Here, the line investor has a 'first mover' advantage, as only he can build the grid infrastructure, which is expensive and technically challenging and only a limited set of investors (such as DNO-approved or DNO themselves), have the technical expertise and regulatory approval to carry it out. Both players are self-interested and take decisions that would maximise their utility functions i.e. maximise their profits. The line investor installs E_{G_1} capacity and the transmission line T. By building the line, the line investor will elicit a reaction from other renewable generation investors, and must take into this reaction when considering their own investment decision. Local generators react to the line being built by installing additional generation capacity themselves. For simplicity, we can safely assume there is no renewable capacity installed at location B prior to the construction of the transmission line and therefore local generators' capacity can produce E_{G_2}. Recall here that E_{G_i} represents the expected energy units which could be produced over the project lifetime, according to the resource on the site's location of i generator, without encountering curtailment, while E_{C_i} is the amount of available energy lost through curtailment under the adopted Principle of Access (PoA), as explained in Chapter 3. A schematic of the model is shown in Fig. 4.3.

As the line is shared among the players under a 'common access' principle, profit functions and therefore decisions on optimal generation capacities built are interdependent. The line investor has two potential streams of revenue, one from own production and one from the energy produced by other investors or local generators, transported through the transmission line. The line investor's costs are related to the installation and operation of the generation capacity (generation cost c_{G_1}) and the installation of the power line C_T.

$$\Pi_1 = (E_{G_1} - E_{C_1})p_G - E_{G_1}c_{G_1} + (E_{G_2} - E_{C_2})p_T - C_T \tag{4.10}$$

Similarly, local generators' profits depend only on the energy they produce with some generation cost c_{G_2} and then transmit through the power line at an access charge of p_T:

$$\Pi_2 = (E_{G_2} - E_{C_2})(p_G - p_T) - E_{G_2}c_{G_2} \tag{4.11}$$

Each player has to decide on his strategy, namely how much generation capacity should one build. In the above expressions, profits as defined in Eq. (4.10) and Eq. (4.11) are functions of the players' own strategies, i.e. the rated capacity they install. Incurred curtailment E_{C_i} however, is a function of both players' strategies. Therefore, the line investor or (*leader*) can assess and evaluate the reaction of other investors, to determine his strategy, namely the level of renewable capacity to be installed, with the ultimate goal to

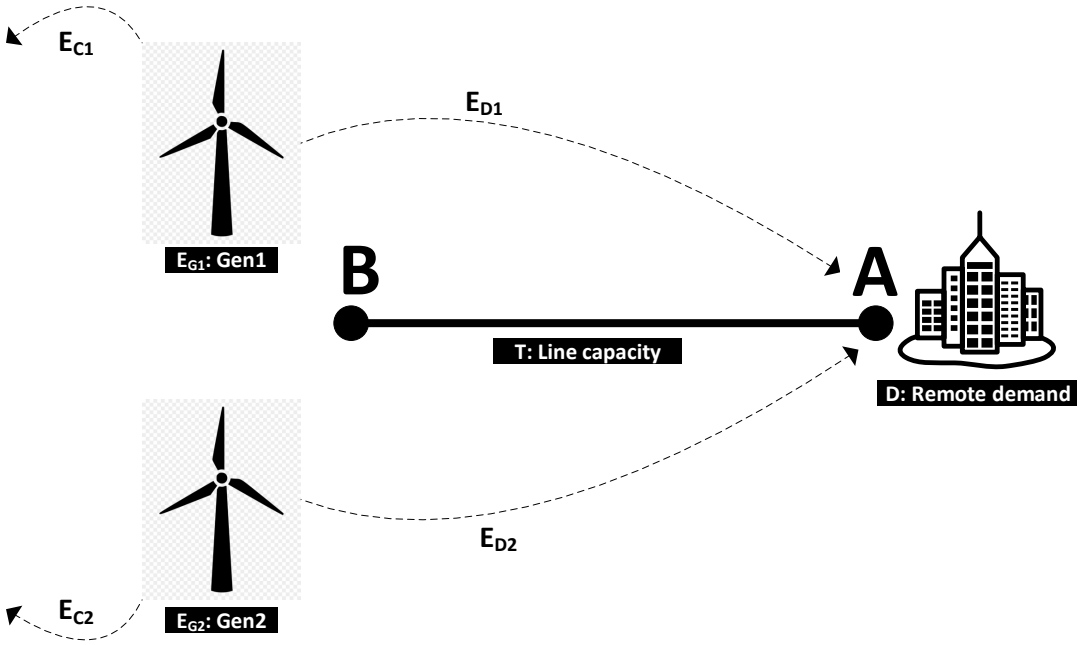

Fig. 4.3 Model schematic of the game with strategic players: RES generation capacity built by the line investor E_{G_1} and RES generation capacity built by local generators E_{G_2} are connected at location B, while demand D is located at A

influence the equilibrium results and maximise his profits Π_1. Local investors (*followers*) can only act after observing the leader's strategy and aim to maximise their profit Π_2. Taking these into consideration, the equilibrium of the game can be found by a well-known technique in game-theoretic modelling called *backward induction*.

First of all, the leader estimates the best response of local generators, for every possible strategy action. In other words, for every possible E_{G_1}, the follower chooses to install renewable capacity that produces E_{G_2} and maximises his profit Π_2. Hence, the local generators' best response is described as:

$$E^*_{G_2} = \underset{E_{G_2}}{\arg\max}\, \Pi_2(E_{G_1}, E_{G_2}) \tag{4.12}$$

Crucially, the renewable generation capacity installed by the follower will also be a function of the generation capacity installed by the line investor.

Afterwards, the leader selects from the follower's best responses, to build $E^*_{G_1}$ that maximises his profit Π_1. Given the best response capacity built by the followers $E^*_{G_2}$, the line investor's best response is:

$$E^*_{G_1} = \underset{E_{G_1}}{\arg\max}\, \Pi_1(E_{G_1}, E^*_{G_2}) \tag{4.13}$$

The line investor decides to install $E^*_{G_1}$. At a second stage, the follower observes this strategy and decides his generation capacity, according to its best response, i.e. maximising his own profit, as anticipated and predicted by the leader. The solution of this process

is the Stackelberg equilibrium of the transmission investment game $(E^*_{G_1}, E^*_{G_2})$, which corresponds to (Π^*_1, Π^*_2) profits and satisfies both Eq. (4.12) and Eq. (4.13).

The network access arrangements and curtailment rules play here a crucial role for the determination of the market equilibrium formed. We examine, in the following sections, the effects of two representative curtailment rules, a LIFO-based rule and a proportional, fair rule, which can be represented by either Pro Rata or FRR type of rules.

LIFO Scheme

Here, we study the results of the transmission capacity installed when a LIFO curtailment rule is implemented.

Lemma 4.2.2. *The transmission investment game between the line investor and local generators, when a LIFO curtailment strategy is implemented, results in the following expected generation capacities and profits at equilibrium:*

$$E^*_{G_1} = E_D \tag{4.14}$$

$$E^*_{G_2} = 0 \tag{4.15}$$

$$\Pi_1{}^* = (p_G - c_{G_1}) \cdot E_D \tag{4.16}$$

$$\Pi_2{}^* = 0 \tag{4.17}$$

Proof. The transmission line capacity is bound by the demand at mainland A, therefore total generation capacity at location B installed by both players $(E_{G_1} + E_{G_2})$, cannot exceed E_D. Under a LIFO scheme, any generation capacity built exceeding the demanded energy has to be curtailed. Therefore:

$$E_{G_1} + E_{G_2} = E_D \tag{4.18}$$

Moreover, since $E_{C_1} = E_{C_2} = 0$, the profit functions defined in Eq. (4.12) and Eq. (4.13) can be simplified as below:

$$\Pi_1 = p_T \cdot E_D + (p_G - p_T - c_{G_1}) \cdot E_{G_1} - C_T \tag{4.19}$$

$$\Pi_2 = (E_D - E_{G_1}) \cdot (p_G - p_T - c_{G_2}) \tag{4.20}$$

Under a LIFO scheme the line investor (who acts first) is protected from any curtailment, therefore has the absolute market advantage to build all generation capacity that satisfies the demand E_D himseld and maximise his profits. Local investors would suffer all curtailment in the LIFO scheme, as they represent 'late' connections and have low priority, hence there is no incentive for them to invest in new generation capacity. This concludes the proof. □

In a LIFO curtailment strategy setting, the line investor has the absolute market advantage, as LIFO always protects the line investor from any curtailment. This is not the case under proportional curtailment rules that share curtailment equally between generators. This case is examined in the following section.

Pro Rata or FRR Scheme

The main difference from LIFO, is that Pro Rata or FRR rules are imposed to all generators, regardless of their order of connection. Therefore, more total capacity $E_G = E_{G_1} + E_{G_2}$ than the energy demanded at A can potentially be installed, as long as the curtailment rate or energy curtailed, allows the investments to be profitable. The total energy curtailed is equal to the expected generation minus the expected demand:

$$E_C = E_G - E_D \tag{4.21}$$

The curtailment rate at location B is given by:

$$CR = \frac{E_C}{E_G} \tag{4.22}$$

Combining Eq. (4.21) and Eq. (4.22):

$$CR = 1 - \frac{E_D}{E_{G_1} + E_{G_2}} \tag{4.23}$$

Using the curtailment rate from Eq. (4.23), the general profit functions of the players, defined in Eq. (4.10) and Eq. (4.11) as functions of both players energy outputs i.e. $\Pi(E_{G_1}, E_{G_2})$, can be written as:

$$\Pi_1 = p_G \cdot E_{G_1} \cdot (1 - CR) + p_T \cdot E_{G_2} \cdot \frac{E_D}{E_{G_1} + E_{G_2}} - C_T - E_{G_1} \cdot c_{G_1} \tag{4.24}$$

By rearrangement:

$$\begin{aligned} \Pi_1 &= \left(\frac{p_G \cdot E_D}{E_{G_1} + E_{G_2}} - c_{G_1} \right) \cdot E_{G_1} \\ &+ \frac{p_T \cdot E_D}{E_{G_1} + E_{G_2}} \cdot E_{G_2} - C_T \end{aligned} \tag{4.25}$$

Respectively, the profit function of the follower is:

$$\Pi_2 = (p_G - p_T) \cdot (1 - CR) \cdot E_{G_2} - c_{G_2} \cdot E_{G_2} \tag{4.26}$$

After rearranging:

$$\Pi_2 = \left[\frac{(p_G - p_T) \cdot E_D}{E_{G_1} + E_{G_2}} - c_{G_2} \right] \cdot E_{G_2} \tag{4.27}$$

Estimation of the game equilibrium with backward induction requires the determination of the players' best responses. First of all, the best response of local generators is estimated for a given E_{G_1}.

Proposition 4.2.3. *Given the generation capacity of the leader E_{G_1}, the best response of the follower, which maximises his profit is equal to:*

$$E^*_{G_2} = \sqrt{\frac{(p_G - p_T)\cdot E_D \cdot E_{G_1}}{c_{G_2}}} - E_{G_1} \tag{4.28}$$

Proof. As already stated the value of E_{G_2} which maximises the profit of the follower is:

$$E_{G_2}{}^* = \underset{E_{G_2}}{argmax}\, \Pi_2$$

Setting as zero the partial derivative of Π_2 in Eq. (4.27), with respect to E_{G_2}:

$$\frac{\partial \Pi_2}{\partial E_{G_2}} = 0 \tag{4.29}$$

$$\frac{(p_G - p_T)\cdot E_D \cdot E_{G_1}}{(E_{G_1} + E^*_{G_2})^2} = c_{G_2} \tag{4.30}$$

By solving the above for E_{G_2}, the desired equation is derived. □

As shown above E_{G_2} is a function of E_{G_1}, i.e. $E_{G_2} = E_{G_2}(E_{G_1})$. By a similar analysis as above, the best response of the leader is found. The leader only needs to consider local generators' strategies that correspond to the follower playing his best response.

Proposition 4.2.4. *Given the output of the follower $E^*_{G_2}$, the best (i.e. profit-maximising) response of the leader is:*

$$E^*_{G_1} = \frac{(p_G - p_T)\cdot c_{G_2} \cdot E_D}{4 \cdot {c_{G_1}}^2}$$

Proof. The value of E_{G_1}, which maximises the profit of the follower is:

$$E_{G_1}{}^* = \underset{E_{G_1}}{argmax}\, \Pi_1$$

Substituting Eq. (4.28) in Eq. (4.25) gives:

$$\Pi_1 = \sqrt{(p_G - p_T)\cdot E_D \cdot c_{G_2} \cdot E_{G_1}} + p_T \cdot E_D - c_{G_1} \cdot E_{G_1} - C_T \tag{4.31}$$

Setting as zero the partial derivative of Π_1 with respect to E_{G_1}:

$$\frac{\partial \Pi_1}{\partial E_{G_1}} = \sqrt{(p_G - p_T)\cdot c_{G_2} \cdot E_D} - 2 \cdot c_{G_1} \cdot \sqrt{E_{G_1}} \tag{4.32}$$

Finally, setting the latest equation equal to zero gives the stated expression. □

The Stackelberg equilibrium game needs to satisfy both best response equations. The result is shown below.

Lemma 4.2.5. *The transmission investment game between the line investor and local generators with Pro Rata, results in expected generation at Stackelberg equilibrium:*

$$E^*_{G_1} = \frac{(p_G - p_T)\cdot c_{G_2}\cdot E_D}{4\cdot {c_{G_1}}^2} \tag{4.33}$$

$$E^*_{G_2} = \frac{(p_G - p_T)\cdot (2\cdot c_{G_1} - c_{G_2})\cdot E_D}{4\cdot {c_{G_1}}^2} \tag{4.34}$$

and associated profits

$${\Pi_1}^* = \frac{(p_G - p_T)\cdot c_{G_2}\cdot E_D}{4\cdot c_{G_1}} + p_T\cdot E_D - C_T \tag{4.35}$$

$${\Pi_2}^* = \frac{(2\cdot c_{G_1} - c_{G_2})^2\cdot (p_G - p_T)\cdot E_D}{4\cdot c^2_{G_1}} \tag{4.36}$$

Proof. Replacing Proposition 2 in Eq. (4.28), the optimum output of local generators $E^*_{G_2,B}$ is found, i.e. (4.34). Finally, substituting the energy outputs at equilibrium Eq. (4.33) and Eq. (4.34) in (4.25) and (4.27), we derive the equilibrium profits ${\Pi_1}^* = \max \Pi_1$ and ${\Pi_2}^* = \max \Pi_2$. □

By adding up Eq. (4.33) and Eq. (4.34), it can be observed that the total generation installed at B depends on the energy demand, the transmission fee and the line investor's generation cost, as shown below:

$${E_G}^* = E^*_{G_1} + E^*_{G_2} = \frac{(p_G - p_T)E_D}{2c_{G_1}} \tag{4.37}$$

Note here that Eq. (4.37) does not depend on c_{G_2}.

Finally note that a curtailment scheme is required, if and only if the total generation capacity exceeds the net demand at A, i.e. $E_{G_1} + E_{G_2} > E_D$ (otherwise there is no strategic interaction and no game, as both players can sell all their generated power). This constraint yields the following condition, which must hold for the setting to actually be game-theoretic (and for the analysis to be relevant):

$$c_{G_1} < \frac{p_G - p_T}{2} \tag{4.38}$$

In addition, the follower's generation cost needs to be smaller or equal to the difference of the selling tariff price minus the transmission fee to satisfy the rationality criteria:

$$c_{G_2} < p_G - p_T \tag{4.39}$$

The latter derives from the requirement that Eq. (4.26) is positive when no curtailment is imposed, i.e. $CR = 0$. By Eq. (4.39) is concluded that the follower can only make a profit, if the followers generation cost is below $(p_G - p_T)$.

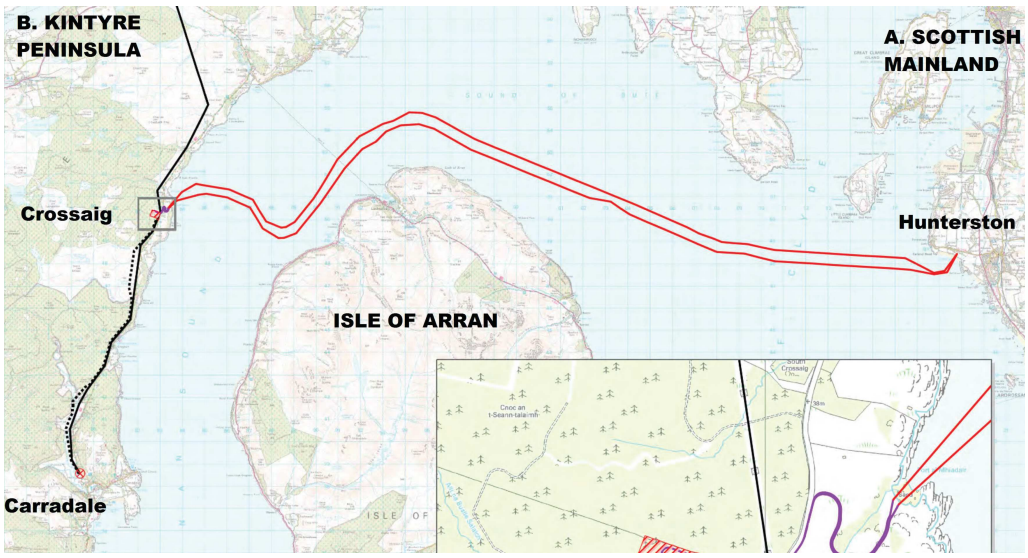

Fig. 4.4 Hunterston-Kintyre project map: Power line connecting Scottish mainland (high demand area) to the Kintyre peninsula (high renewable generation capacity) [235]

In the following section, the theoretical analysis results of the game with strategic players and Pro Rata are applied to a practical example based on realistic figures from a grid reinforcement project located in the western coast of Scotland.

4.3 Practical application example

In this section, we apply the theoretical Stackelberg model stated in the previous section (c.f. Lemma 4.2.5), to a practical example based on a grid reinforcement project in the UK, the Kintyre-Hunterston link. The project attracted considerable attention (being a national consultation exercise) from both the National Grid (the UK's system operator) and the responsible DNO for this particular region, Scottish Southern Energy (SSE).

The power grid in the Kintyre peninsula was originally designed and built to serve a typical rural area of low local demand. Wind energy development quickly led to substantial volumes of renewable investment in the region. RES capacity in the region was estimated to be up to 454 MW by 2015. Future renewable connections in this area were estimated to exceed 793 MW. SSE, the regional DNO, proceeded to a grid reinforcement project that aimed to connect the Kintyre peninsula to the Scottish mainland, in the location of Hunterston, partially via a sub-sea link (see Fig. 4.4).

More analytically, the grid reinforcement project consisted of:

- Subsea cable installation works north of Arran and the installation of 2×220 kV of 240 MVA HVAC subsea cables at a distance of 2×41 km from Crossaig to the existing substation at Hunterston
- New substation $132/220$ kV built in Crossaig

- Power line upgrade over a distance of 13 km of 132 kV double circuit overhead line between Carradale and the Crossaig substation and dismantling of the existing overhead line
- Integration works to the existing substation in Hunterston

The project estimated the creation of 150 MW additional renewable capacity [235] with an estimated cost of £230m. Note here that the capacity of network upgrades and associated costs are largely determined by the rating, distance and characteristics of the connection route. Underground cables and sub-sea interconnenctors have higher costs than overhead power lines. For high voltage power lines e.g. 275 kV and 400 kV, underground cables are reportedly 8 times more expensive than overhead lines, costing an additional £10m per km [163].

Apart from facilitating renewable generation, the project also aimed to increase the security of supply by increasing the export capability to the mainland grid. According to a Sinclair Knight Merz (SKM) study, the grid reinforcement project is expected to deliver significant value to consumers, since the project costs are lower than the projected costs for congestion management, estimated at £18m per annum. SKM estimated the net lifetime benefit of the project at £520m [232].

Realistic figures based on the Kintyre-Hunterston project were used for the practical demonstration of the game-theoretic models developed in this thesis, starting from the application of the Stackelberg game equilibrium results, as shown in the following section.

4.4 Practical demonstration results for analytical solution

Based on the Kintyre-Hunterston project figures, a simplified two-node network is considered. Scottish mainland, where the Hunterston substation is located, represents the high demand location A and the Kintyre peninsula represents the high renewable generation or location B. The mainland energy demand met by generation in Kintyre, equals the energy transmitted through the power line. With the majority of investment being wind projects, the total energy demand is estimated as $E_D = 9,198,000$ MWh, which corresponds to 150 MW of wind capacity, with a typical CF of 35% and 20 years project lifetime. Moreover, it is assumed that the energy generated by renewable production can be sold for a constant generation price, reflecting financial support mechanisms for renewable generation. Such support mechanisms are usually technology-specific and depend on the RES capacity built. Typical support mechanisms in the UK are feed-in-tariff prices, usually granted to smaller scale generators or CfD schemes designed to supplement and minimise RES generator exposure to volatile wholesale electricity market prices. For the practical example analysis a generation price of $p_G = £74.30/\text{MWh}$ was assumed, equivalent to the support mechanism in the UK available at the time of study, such as the revenue generated by a medium sized wind turbine with a feed-in tariff and export fee of £2.52/kWh and

	Scenario 1	Scenario 2	Scenario 3-a	Scenario 3-b
c_{G_1}	$0.14p_G : 0.02p_G : 0.37p_G$	$0.30p_G$	$0.26p_G$	$0.20p_G$
c_{G_2}	$0.30p_G$	$0 : 0.02p_G : 0.74p_G$	$0.20p_G$	$0.26p_G$
p_T	$0.26p_G$	$0.26p_G$	$0 : 0.02p_G : 0.48p_G$	$0 : 0.02p_G : 0.60p_G$

Table 4.1 Summary of cost parameters considered in scenarios for the analysis of the transmission capacity game with distributed generation (in all scenarios the generation price remained fixed at $p_G = £74.3/\text{MWh}$ and the transmission cost at $C_T = £230m$

$£4.91/\text{kWh}$[5], respectively [180]. Based on the Kintyre-Hunterston project figures, the transmission cost of the line was assumed equal to $C_T = £230m$.

Finally, the following scenarios were considered in order to study the effect of different cost parameters to equilibrium results. In each scenario, the cost parameter under examination varies, while other parameters remain fixed. All parameters are shown in relation to p_G for easier interpretation of results. For each scenario, the range of the 'free' parameter (fixing the others) is determined from the constraints in Eq. (4.38) and Eq. (4.39). A summary of cost parameters for each scenario is provided at Table 4.1.

4.4.1 Scenario results

To study the equilibrium results, we assume the following set of assumptions. In each case or *scenario*, all parameters remain fixed except the parameter under study. Each scenario aims to study the effects of a financial parameter to the game equilibrium results. Three main scenarios were assumed:

- *Scenario 1: Varying line investor's generation cost:* In this scenario, local generators' cost and transmission fee are set equal to $c_{G_2} = 0.30p_G$ and $p_T = 0.26p_G$, respectively. The parameter under examination, varies from $c_{G_1} = 0.14p_G$ to $0.37p_G$. The equilibrium results for the optimal generation capacity installed and players' profits are shown in Fig. 4.5 and Fig. 4.6, respectively. We make sure Eq. (4.39) conditionality is respected (in this occasion c_{G_1} has to be smaller than $0.37p_G$ and within the accepted range for the model to be relevant). The energy generation at equilibrium in Fig. 4.5, shows that c_{G_1} has to be larger than $0.15p_G$ for local generators to be able to build any renewable generation capacity ($E_{G_2} \geq 0$). Fig. 4.5, shows that the total capacity build at location B drops as the c_{G_1} value increases. Moreover, local producers' capacity exceeds that the line investor's capacity when $c_{G_1} \geq c_{G_2}$). Players build the same generation capacity when $c_{G_1} = c_{G_2} = 0.30p_G$.

[5]Note here that in the UK the feed-in-tariff mechanism is no longer valid for new onshore wind developments since March 2019. Depending on the RES capacity built, RES generators can generate revenue from the electricity sold either through Power Purchase Agreements (PPAs) with energy suppliers, through participate in wholesale electricity markets and support by CfD schemes. For simplicity, a constant revenue stream was assumed based on a medium wind turbine, valid at the initial time of this study, shown also in the Appendix. Full information on the feed-in-tariff support mechanism can be found on Ofgem's website: https://www.ofgem.gov.uk/environmental-programmes/fit/fit-tariff-rates

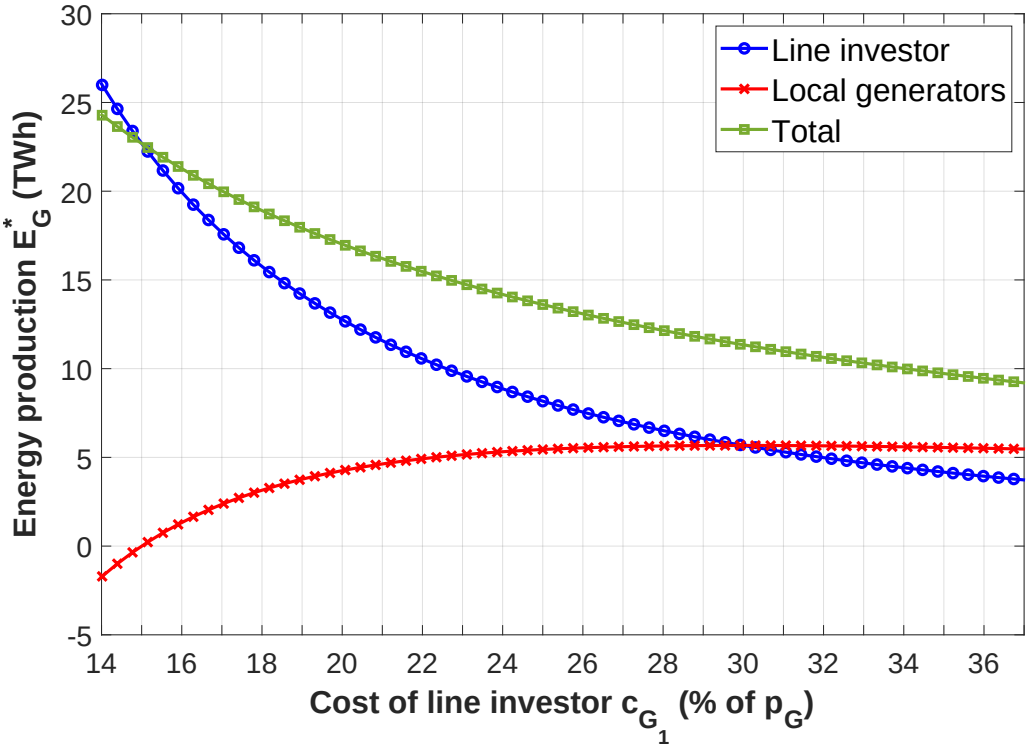

Fig. 4.5 Scenario 1: Effects of line investor's generation cost on energy production

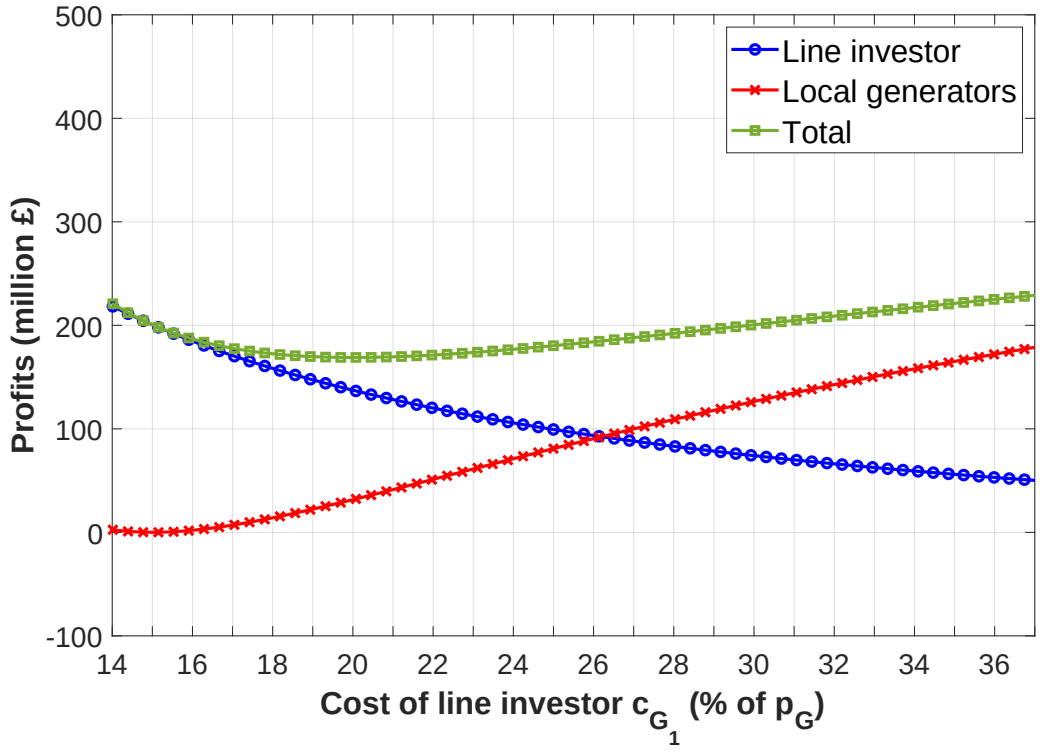

Fig. 4.6 Scenario 1: Effects of line investor's generation cost on profits

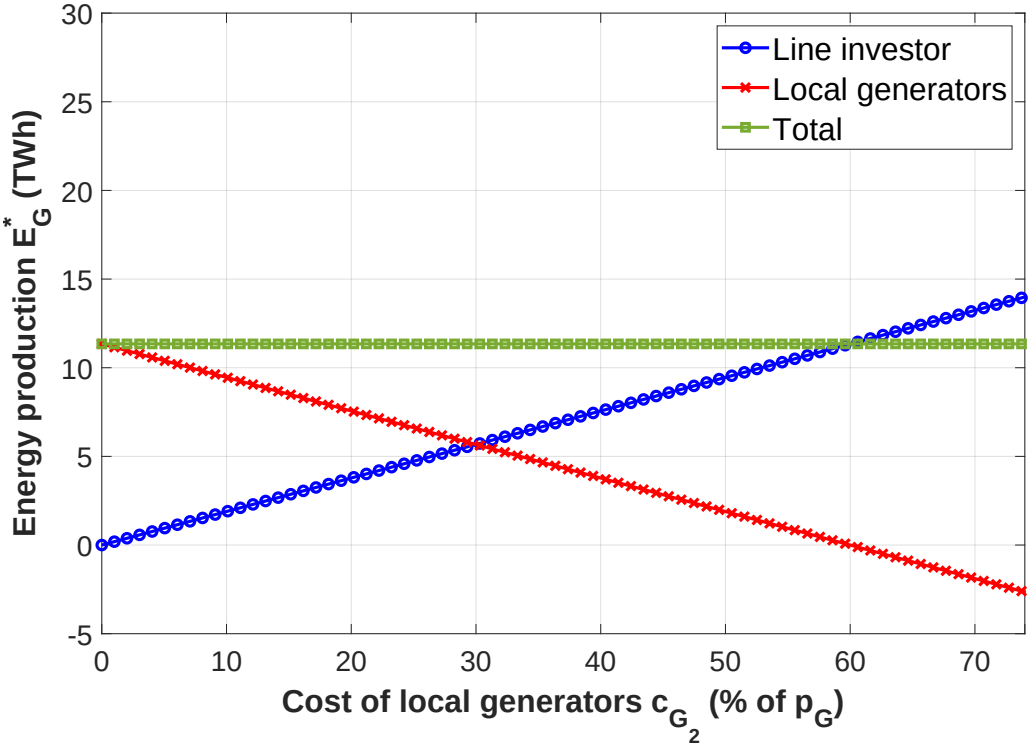

Fig. 4.7 Scenario 2: Effects of local generators generation cost on energy production

Profit functions present a similar behaviour, with higher profits when generation capacity is high, and lower profits when installed generation capacity is low. Profits are equalised for $c_{G_1} = 0.26p_G$, as shown in Fig. 4.6.

- *Scenario 2: Varying local generators' cost:* In this scenario, the line investor's generation cost is $c_{G_1} = 0.30p_G$ and the transmission fee is $p_T = 0.26p_G$, while the local generators' cost varies from $c_{G_2} = 0$ to $0.74p_G$. Results are shown in Fig. 4.7 and Fig. 4.8. In this setting, Eq. (4.38) conditionality demands that $c_{G_2} < 0.74p_G$. In fact, Fig. 4.7 shows that $c_{G_2} < 0.60p_G$ for local generators to install any renewable generation capacity at B ($E_{G_2} \geq 0$). Also, it can be seen that the total generation capacity at location B is constant and independent of the local producers generation cost c_{G_2}. In addition, total generation capacity exceeds the generation demand at location A, assumed equal to $E_D = 9,198,000$ MWh. The generation capacity of local generators is larger than the capacity of the line investor at location B, when $c_{G_2} < c_{G_1}$. The two players build equal capacity, when generation costs are equalised $c_{G_1} = c_{G_2}$. Profit functions follow similar a behaviour as in Scenario 1 and are equalised for $c_{G_2} = 0.34p_G$, as shown in Fig. 4.8.

- *Scenario 3: Varying transmission fee:* For this scenario, two cases are examined with different assumptions on the relation of players' costs of generation.

  In the first case, the line investor's generation cost is $c_{G_1} = 0.26p_G$ and the local generators' cost is equal to $c_{G_2} = 0.20p_G$. The transmission fee varies from 0 to $0.48p_G$, as derived by the prerequisite condition in Eq. (4.38). Results are shown

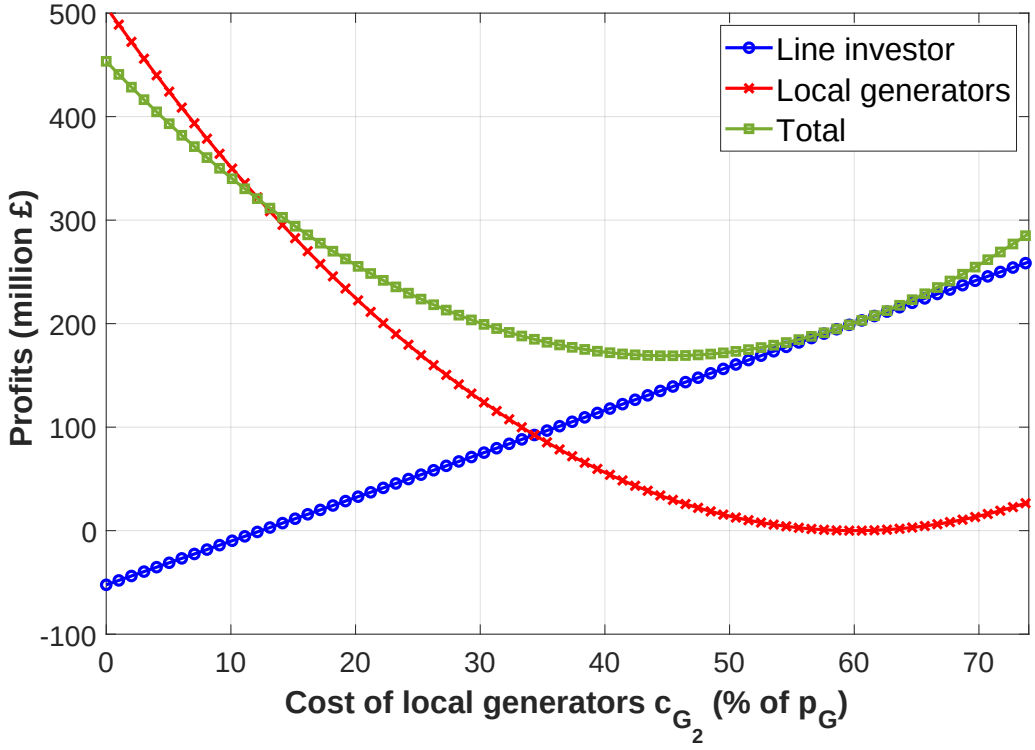

Fig. 4.8 Scenario 2: Effects of local generators generation cost on profits

in Fig. 4.9 and Fig. 4.10. In the second case, the line investor's generation cost

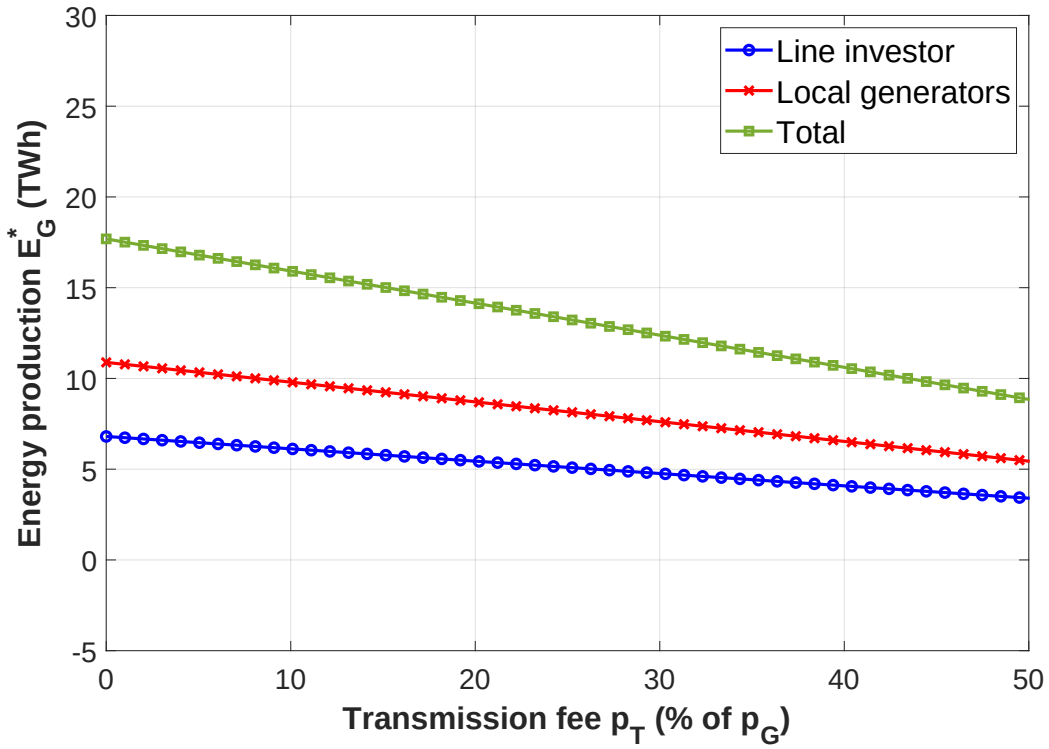

Fig. 4.9 Scenario 3-a: Effects of transmission fee on energy production for $c_{G_1} > c_{G_2}$

is $c_{G_1} = 0.20 p_G$ and the local generators' cost is equal to $c_{G_2} = 0.26 p_G$. The

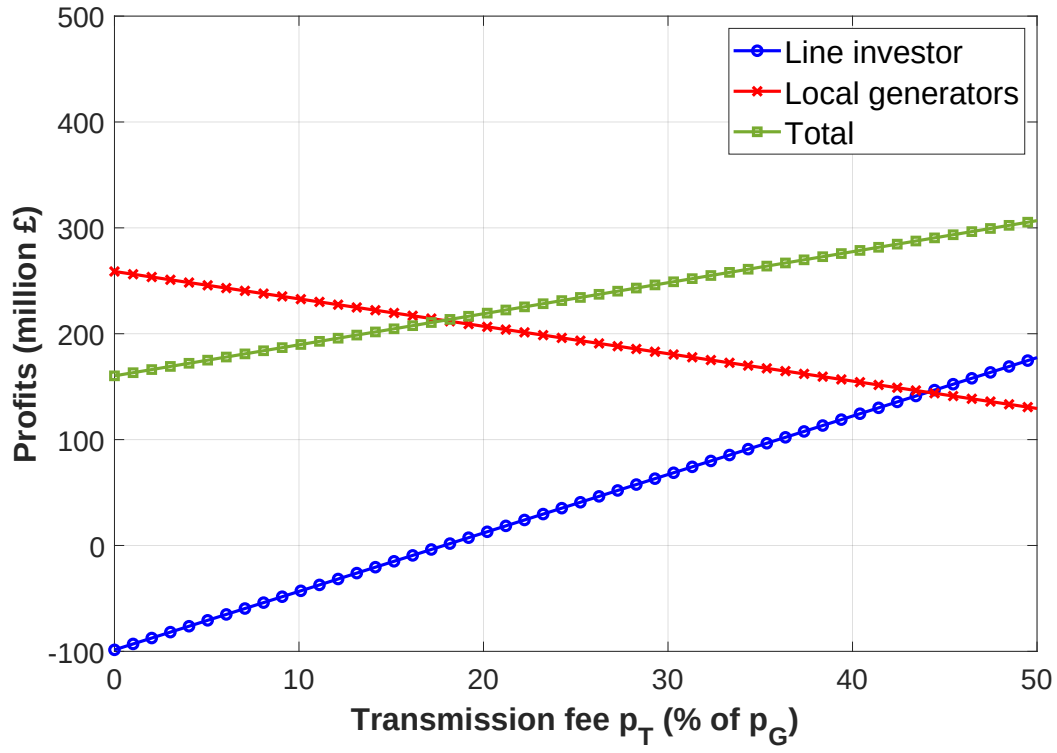

Fig. 4.10 Scenario 3-a: Effects of transmission fee on profits for $c_{G_1} > c_{G_2}$

transmission fee varies from 0 to $0.60p_G$, as derived by the prerequisite condition in Eq. (4.38). Results are shown in Fig. 4.11 and Fig. 4.12.

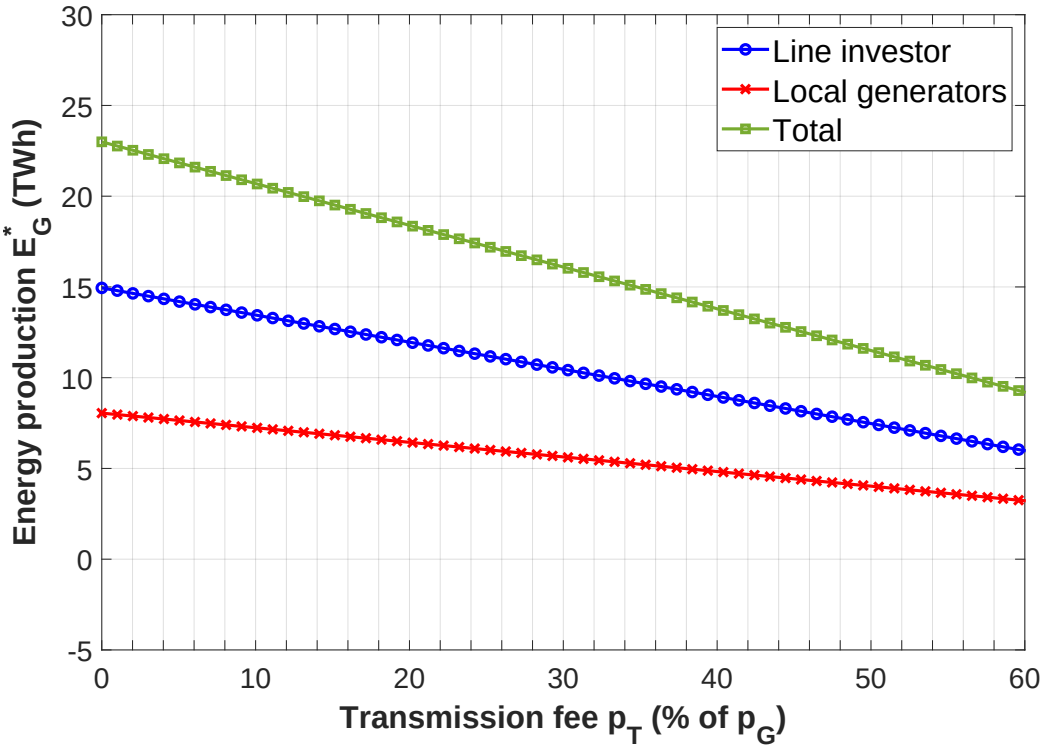

Fig. 4.11 Scenario 3-b: Effects of transmission fee on energy production for $c_{G_1} < c_{G_2}$

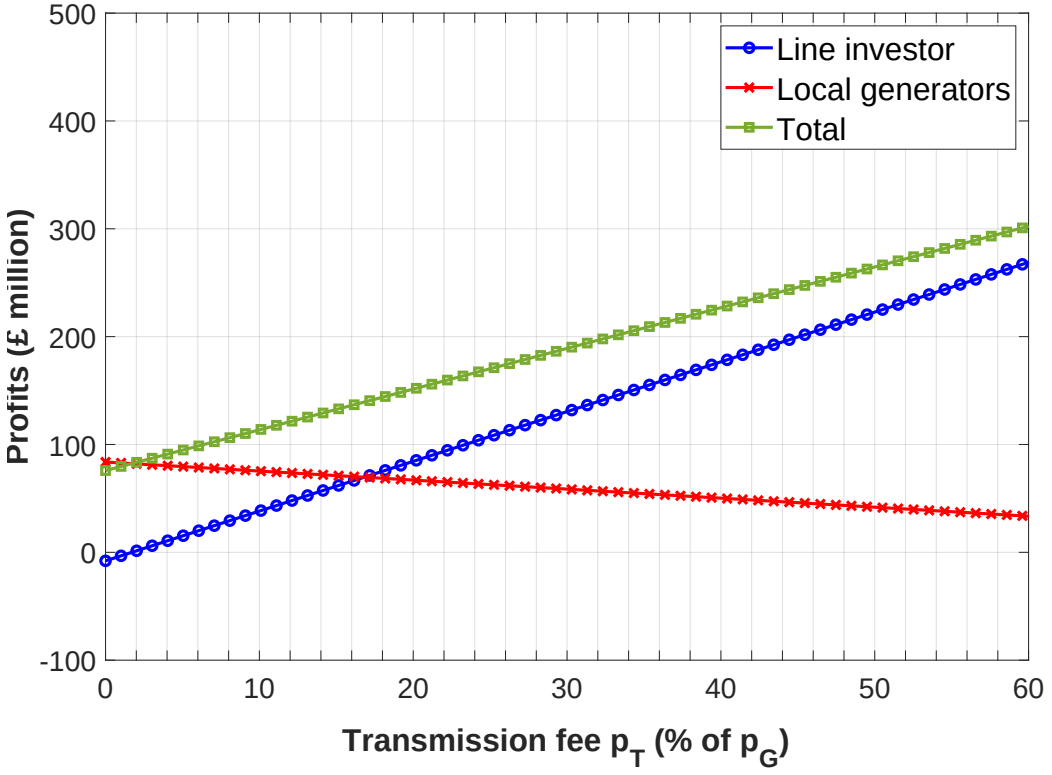

Fig. 4.12 Scenario 3-b: Effects of transmission fee on profits for $c_{G_1} < c_{G_2}$

Total generation capacity at location B decreases as p_T increases, as seen in both cases (see Fig. 4.9 and Fig. 4.11). When $c_{G_1} > c_{G_2}$, local generators build more generation capacity than the line investor ($E_{G_2} > E_{G_1}$). The opposite is valid when $c_{G_1} < c_{G_2}$, i.e. the line investor builds more generation capacity than local generators ($E_{G_1} > E_{G_2}$).

For small values of p_T, the line investor may not make any profit ($\Pi_1 < 0$), as seen in Fig. 4.10 and Fig. 4.12. Fig. 4.10 shows that a positive profit for the line investor is achieved for $p_T \geq 0.18 p_G$. On the other hand, in Fig. 4.12, it is shown that positive profits can be achieved for a much smaller transmission fee $p_T \geq 0.02 p_G$. However, as the transmission fee p_T increases, the line investor's profit also increases, as he benefits from charging a higher price for the energy transmitted through the line. When $c_{G_2} > c_{G_1}$, the line investor builds more capacity than other local producers at B, therefore profit figures are significantly improved (see a comparison between Fig. 4.10 and Fig. 4.12). On the contrary, local generators see diminishing profits, as transmission fee grows.

4.4.2 Discussion of results

Given a certain generation tariff price p_G, the feasibility of the transmission capacity game depends directly on the generation cost c_{G_1} (see Fig. 4.5) and the transmission fee p_T (see Fig. 4.9 and Fig. 4.11).

If the line is built and access to demand is therefore granted, it sets up a level of total feasible generation investment at B which, combined with a proportional access rule, leads to larger volumes of capacity being built than the actual demand (see Fig. 4.5 and Fig. 4.7), as long as the curtailment rate is kept under reasonable levels and renewable investment projects are viable. Recall here that from Eq. (4.37), total production or generation capacity installed at the game equilibrium depends on the demand at location A E_D, the transmission fee p_T and the line investor's generation cost c_{G_1}. E_D determines an upper level for the total generation that can be built at location B. By increasing the capacity beyond this level, production could not be absorbed by the mainland grid, leading to unacceptable levels of curtailment, hence, the investments would not be profitable. When p_T is increased, total generation capacity is expected to decrease, as shown in Fig. 4.9 and Fig. 4.11. Finally, optimal generation is inversely proportional to the line investors generation cost c_{G_1}. Note that the total level of generation does *not* depend on the generation costs of local investors, since they cannot act without the existence of the line (see Fig. 4.7).

For all scenarios, the comparative relation between c_{G_1} and c_{G_2} determines how the exportable level of generation capacity, defined by the upper level of demand in A, is shared among the two players. Cheaper generation has an advantage in all three scenarios sets of results (c.f. Fig. 4.5-4.11), although as the graphs show, the dependency is not necessarily linear. The players install equal generation capacities when $c_{G_1} = c_{G_2}$.

Profit equations depend on the generation capacity installed by each player and the transmission fee. The relation between the profits and the generation capacity built presents positive correlation. For the line investor the larger the transmission charges, the higher the profits, while local generators experience lower profits as p_T increases. In practice, local generators may have smaller generation costs than the line investor due to cheaper access to land and permit approval for final RES development. Consequently, results shown in Fig. 4.9 and Fig. 4.10 tend to represent real-world settings in a more accurate fashion.

Another conclusion is that transmission charges, agreed by the line investor and an independent regulatory authority, have to be set within a specific range. Low values of p_T may lead to transmission investment being aborted, somewhat larger values might theoretically be sufficient to achieve profitability for the line investor, however, hide the risk of 'free-riding' from local investors, who benefit from the leader's investment at cost much less than to leader's himself. What the result in Fig. 4.10 shows is that there exists a range in which p_T can be set such as to assure the line gets built (i.e. when the leader's profits are above 0 – in this case, transmission charges need to be at least £13/MWh), but also not discourage other local renewable investors. If the value of the transmission fee is set too high, then this will prevent local producers from investing in renewable energy, as their profit diminishes with increasing transmission fee. The line investor can react by building the generation capacity himself. When $c_{G_1} > c_{G_2}$, this would lead to the renewable capacity being built by more expensive generation. In the second case of Scenario 3, transmission charges need to be at least £2/MWh) to allow any profit for the line investor, as shown in Fig. 4.12. On the other hand, if the value of the transmission fee is set too high, then this will prevent other RES producers to invest in further generation,

as their profit diminishes with increasing transmission fee. The line investor can react by building the generation capacity himself, but up to the level of decreasing total generation capacity as p_T values increase.

4.5 Concluding remarks

Chapter 4 studied how line access and curtailment rules can affect investment decisions on new transmission capacity being built. Two agent settings were explored, myopic and strategic agents.

In areas already experiencing high curtailment, the transmission line investment is viable if and only if the curtailment rate (prior to the line construction) is higher than a threshold τ_T. Moreover, it was shown that the line investor is able to charge in this occasion a very expensive transmission fee, the theoretical limit of which can approach p_G. The reason being that curtailed energy is anyway wasted energy for local generators, who would be willing to accept high charges, as long as they are (even marginally) better off. It can be argued that in real-world situations, the model would have limited application, as it presupposes high curtailment rates and high levels of generation capacity already built. Furthermore, high charges for transmission might not be in practice accepted by local producers, resulting in higher prices potentially reached through negotiation.

The analysis for strategic agents was performed for two cases of curtailment rules, LIFO and Pro Rata/FRR. For the latter case, the work shows that network infrastructure such as building new transmission/distribution lines can be built under a 'common access' principle, where a private investor is granted a license to build the line, subject to the condition he grants network access to other competing generators, who pay a transmission fee for the energy transported through the line.

Such shared-capacity line models can also be used settings, where power line infrastructure is privately-owned. For example, a large investor, who is financially capable of funding a power line and required equipment to get connected to the main distribution network, can also grant access to other smaller generators or demand consumers[6], either on a permanent arrangement or temporarily until their own project connection infrastructure works are completed. In such a case, the line-sharing rules are arranged privately through commercial agreements between RES investors. Transmission charges are also dictated in private contracts. Grid infrastructure is managed privately up to the point of connection with the DNO-owned network. As per normal procedures, the power coupling point needs to comply with technical and regulatory rules. There are several observations here that need to be noted. First, an investor would agree in sharing his grid access if there is spare capacity on the line already installed, in which occasion a LIFO scheme would make more sense. Second, these synergies are more likely to happen in cases when RES

[6]One example of a privately owned distribution network that is connected through a single point of connection to the DNO-owned network is the eco-village of Findhorn, in the north of Scotland. The community owns a private distribution network that connects residential consumers, commercial consumers and a wind park. More information on Fidhorn can be found here: https://www.ecovillagefindhorn.com/

projects have complementary natures and resources are not perfectly correlated, resulting in unsynchronised use of the line. Finally, in real-world settings, investments on larger capacity lines, in expectation that other generators might connect and use the line, may come at significant costs and hide large risks.

The work presented in Chapter 4 examined the combined effects of curtailment strategies and line access rules on network expansion. One aspect our study highlights is that regulatory authorities who seek renewable facilitation can promote grid infrastructure expansion, not only by providing subsidies or technical support, but by allowing 'common access' rules, as a tool to attract private investment and improve the profitability of line investors.

The Stackelberg game equilibrium results also show that there is a range of acceptable transmission charges that the line investor can impose. If the transmission fee is too small, then it is not profitable for the line investor to construct the power line. On the other hand, if the transmission fee is set too high, then the local producers are prevented from any feasible renewable investment.

The assumptions in the model presented in Chapter 4 allowed for an analytical closed-form solution of the game. However, the model does not take into account the stochastic nature of wind resources nor the variability of demand. This would allow for more accurate estimation of the incurred curtailment and equilibrium results. These issues are further explored in Chapter 5. The following chapter improves this work, by formalising the Stackelberg game solution as a stochastic problem and by utilising real wind speed and demand data for the estimation of the game equilibrium.

Chapter 5

Transmission capacity game with stochastic generation

Chapter 5 presents an extension of the model developed in Chapter 4. The model presented in Chapter 4 followed an approach based on average or expected values of RES resources and demand over a large time horizon equal to the project lifetime. In practice however, expected curtailment depends on variable renewable resources and their relation to the power demand. The model developed in this chapter takes into account the stochastic nature of RES resources, such as wind speed, and the variability of the demand. The first part of Chapter 5 provides the theoretical foundations of the extended model leading to the estimation of the Stackelberg game equilibrium. The theoretical formulation and analysis requires knowledge of the distributions of the wind resource and demand for the locations under study. However, even when distributions can be inferred by available historic data, incurred curtailment, which depends jointly on the wind resource at each investor's location and demand, cannot always be computed analytically. The same holds for the Stackelberg game equilibrium estimation process. This limitation can be avoided by using an empirical and algorithmic approach that directly utilises available historic data, such as wind speed and demand data. As previously, the Kintyre-Hunterston grid reinforcement project was used to demonstrate a practical and empirical solution approach for equilibrium estimation.

The stochastic model and parts of the work presented in Chapter 5 were published in a peer-reviewed journal article [13].

5.1 Research contributions

Research work presented in Chapter 5 builds on the game-theoretic model of Chapter 4 and work published in [8, 12]. More specifically, the model focuses on the two-location Stackelberg game, formed between the line investor (leader) and local generators (follower) when a transmission line is installed, the use of which is shared by both players under a 'common access' principle. Most crucially, any curtailment incurred is also shared equally

between the players following the principle of a fair curtailment scheme, such as Pro Rata or FRR.

Relevant publications to the work presented here were discussed in Chapter 4. In addition to those works, most relevant to the model presented in this chapter is the work from Anaya & Pollitt [7]. They provided a cost-benefit analysis, which compared traditional connections i.e. network upgrades to smart interruptible connections, however their results were based on static assumptions of the generation mix and curtailment levels. The results from the work presented in this chapter are based on hourly data of RES resources and demand. In more detail, the specific contributions of the work presented in Chapter 5 that advance the state of the art are:

- Work published in [8, 12] and Chapter 4 followed assumptions on expected generation and curtailment that led to a closed form solution of the Stackelberg game equilibrium. The model presented in Chapter 5 extends previous work by developing a stochastic game formulation and by formulating a theoretical analysis of the game. The analysis can be used to estimate the equilibrium of the leader-follower game when distributions of RES resources and demand are known, and curtailment can be computed directly from these distributions. However, in practice this is difficult to achieve without the use of an empirical or algorithmic solution.

- An algorithmic approach that utilises real renewable resource and demand data is shown. This empirical solution dictates how curtailment can be computed in practical settings and captures stochastic variation of wind resources and variability of demand in the equilibrium results. This forms a new solution concept that is based on empirical or simulation analysis for payoff estimation. Similar approaches can be used in various settings with RES generation analysis, as a generic way to estimate payoff functions and game equilibria. Moreover, we show a data analysis approach for estimation of wind power generation and demand.

- Next, the algorithmic approach is applied to a practical application based on realistic assumptions from the Kintyre-Hunterston grid reinforcement project in Western Scotland. Real wind speed measurements and demand data that spanned over the course of 17 years were used for equilibrium estimation and determination of optimal generation capacities built by players along with their associated profits at the equilibrium of the game. An additional contribution of the work is the wind speed data analysis process and estimation of wind power generation presented in this chapter.

5.2 Stackelberg game with stochastic generation and variable demand

This section investigates the combined effects of fair curtailment strategies, such as Pro Rata or FRR, and 'common access' line rules on grid reinforcement and renewable generation capacity installed.

Similarly to the model introduced in Chapter 4, a two-location model is assumed, where a transmission line is built between locations A-B. The line investor installs renewable generation capacity at B, equal to a rated capacity of P_{N_1}, and a local player, who represents the local renewable generators at B, installs P_{N_2}. The demand at location A is represented as D. Note here that D represents the demand at location A, while P_D represents the demand that is served by RES generators located in the area of high renewable generation or B. Demand served by the renewable capacity of the leader or line investor is denoted as P_{D_1} and demand served by local generators/investors is denoted as P_{D_2}. If a larger time horizon is assumed, generation and curtailment can be expressed in energy terms, i.e. E_{G_i} represents the generation, E_{C_i} the curtailed energy and E_{D_i} the demand served by the i player. A simple schematic of the model is shown in Fig. 5.1.

With respect to profits, the line investor earns revenue from the energy generated by his own capacity and serves demand at A or E_{D_1}, and the energy generated by local generators and transmitted through the line or E_{D_2}. The line investor incurs the renewable capacity installation cost and the cost of building the line. Local investors earn revenue when serving demand E_{D_2} and pay a cost for building the renewable generation capacity at B. For each player, the demand served is equal to the potential generation minus the curtailment incurred:

$$E_{D_1} = E_{G_1} - E_{C_1} \tag{5.1}$$

and

$$E_{D_2} = E_{G_2} - E_{C_2} \tag{5.2}$$

The profit functions for the line investor and local generators can be expressed as in Eq. (4.10) and Eq. (4.11), respectively. The equations are repeated here for the convenience of readers:

$$\Pi_1 = (E_{G_1} - E_{C_1})p_G - E_{G_1}c_{G_1} + (E_{G_2} - E_{C_2})p_T - C_T$$

$$\Pi_2 = (E_{G_2} - E_{C_2})(p_G - p_T) - E_{G_2}c_{G_2}$$

Similarly to the analysis presented in Section 4.2.2, the estimation of the Stackelberg game equilibrium, answers the research question of the optimal generation capacities that players need to install, in order to maximise their profits, given that the line investor has a first mover advantage over smaller generators and investors at B. A player's strategy action is the rated capacity he can install (P_{N_i}). Therefore, the research question can be rephrased as *'Which are the optimal rated capacities players install at the equilibrium of the game, so that profits are maximised?'* The Stackelberg game equilibrium can be found by backward induction, where the line investor first estimates the local generators best

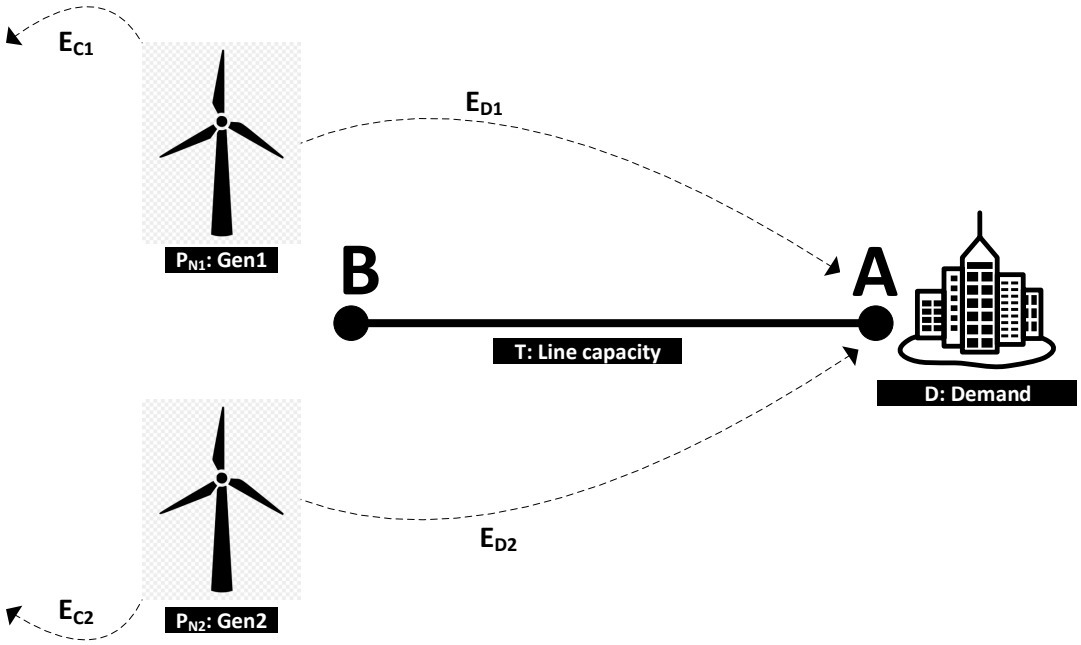

Fig. 5.1 Model schematic of the game with stochastic generation and variable demand: RES generation capacity built by the line investor PN_1 and RES generation capacity built by local generators P_{N_2} are connected at location B, while demand D is located at A

response for every possible action taken. Hence for every P_{N_1}, the follower's best response action is:

$$P^*_{N_2} = \arg\max_{P_{N_2}} \Pi_2(P_{N_1}, P_{N_2}) \tag{5.3}$$

Next, the line investor selects from the follower's best responses $P^*_{N_2}$, the strategy that maximises his own profit:

$$P^*_{N_1} = \arg\max_{P_{N_1}} \Pi_1(P_{N_1}, P^*_{N_2}) \tag{5.4}$$

The game equilibrium $(P^*_{N_1}, P^*_{N_2})$ must satisfy both Eq. (5.3) and Eq. (5.4).

Note here that profit functions refer to a longer time horizon and are expressed in energy terms over this time period. Crucially, however, energy quantities depend on the rated capacities installed by players i.e. E_{G_i} can be expressed as a function of P_{N_i}, and in the case when curtailment is shared equally between players (Pro Rata or FRR type of curtailment strategy), curtailment E_{C_i} can be expressed as a bivariate function of both players' strategies (P_{N_1}, P_{N_2}). Generation and curtailment depend on the wind resource at the project's location and variable demand. As a result, it is possible to derive expressions of these quantities with respect to known distributions of renewable resources and demand, as shown in the following theoretical analysis. First, a theoretical formulation of the model is shown for a single player, to ease understanding, and next, the formulation is extended for the two-player game.

5.2.1 Single player analysis

This section shows how generation and curtailment quantities in the general profit equations can be expressed as functions of a player's strategy, namely the rated capacity he chooses to install. To ease understanding, a single player i or generator is at first assumed. The per unit or normalised power that can be generated by the player, if no curtailment is required, is defined as a stochastic variable $x_i = P_{G_i}/P_{N_i}$, where P_{G_i} is the actual power output of generator i, and P_{N_i} is the rated capacity. Crucially, x_i depends directly on the renewable resource, such as the wind speed distribution, and a generator's power generation curve. The generation or power curve describes the relation of the power output to the renewable resource available. The largest power output a generator can produce is equal to its rated capacity, therefore x_i is bounded in the region $x_i \in [0,1]$. If x_i follows a probability distribution function $f(x_i)$, then $\int_0^1 f(x_i)dx_i = 1$. By definition, the expected generation, when curtailment is not considered, is equal to:

$$\mathbb{E}(P_{G_i}) = \mathbb{E}(x_i) \cdot P_{N_i} = \int_0^1 x_i P_{N_i} f(x_i) dx_i \tag{5.5}$$

Curtailed power depends on the power that can be generated, given the wind resource, and the actual demand at the mainland location. Assuming D_t is the demand at time t, which can be predicted with great accuracy from historic demand [158, 159] and weather data available, generation curtailment is required for all t that generation exceeds the demand $P_{G_i} - D_t > 0$ or expressed in relation to the normalised power output, for all t that $x_i > D_t/P_{N_i}$. In practice, the time interval t can be defined as a reasonable time step, e.g. one hour or any other suitable metric that can easily coordinate with the resolution of available historic data, either wind speed or demand data.

The expected power curtailed (for time interval t) can then be expressed as the difference between the conditional expectation of the power generated minus the demand, under the condition that generation exceeds that demand, multiplied by the probability that the power generated exceeds the demand. In other words, the expected curtailment is equal to the expected value of the generation given that generation exceeds the demand (a posteriori expectation) minus the power demanded times the probability that generation exceeds the demand:

$$\mathbb{E}(P_{C_i,t}) = [\mathbb{E}(P_{N_i} \cdot x_i \,|_{P_{N_i} \cdot x_i > D_t}) - D_t] \cdot \int_{\frac{D_t}{P_{N_i}}}^1 f(x_i) dx_i \tag{5.6}$$

The conditional expectation, as in the first term of the previous equation, is by definition equal to:

$$\mathbb{E}(P_{N_i} \cdot x_i \,|_{P_{N_i} \cdot x_i > D_t}) = \frac{\int_{\frac{D_t}{P_{N_i}}}^1 P_{N_i} x_i f(x_i) dx_i}{\int_{\frac{D_t}{P_{N_i}}}^1 f(x_i) dx_i} \tag{5.7}$$

By combining the latest equations, the expected curtailment can be expressed as:

$$\mathbb{E}(P_{C_i,t}) = \int_{\frac{D_t}{P_{N_i}}}^{1} P_{N_i} x_i f(x_i) dx_i - D_t \int_{\frac{D_t}{P_{N_i}}}^{1} f(x_i) dx_i \tag{5.8}$$

Eq. (5.5) and Eq. (5.8) represent the expected power generated and curtailed at t, respectively. For a longer period of time, e.g. equal to the project lifetime, the total energy produced is equal to $E_{G_i} = \sum_t \mathbb{E}(P_{G_{i,t}}), \forall t$, as derived by (5.5). In a similar fashion, by Eq. (5.8) the energy curtailed is given by the summation of the expected curtailment for each t, hence $E_{C_i} = \sum_t \mathbb{E}(P_{C_{i,t}}), \forall t$. A similar theoretical analysis can be applied in a two-player setting as shown in the following section.

5.2.2 Two player analysis

This section estimates the expected power produced and curtailed for a setting comprising two players. Let's assume two types of generators, the leader (player 1) and follower (player 2), both located at an area of favourable RES potential B, but at different sub-regions of this location. The wind resources at these sub-regions differentiate from each other, but experience a degree of spatial correlation, due to the proximity of the locations. The generators aim to satisfy the same aggregate demand at A.

Following the same intuition as in the previous section, production of players can be modelled as correlated stochastic variables x_i, where x_1 and x_2 follow a joint probability distribution function $f(x_1, x_2)$, which satisfies the property $\int_0^1 \int_0^1 f(x_1, x_2) dx_2 dx_1 = 1$. A joint probability distribution is required to model the correlation between wind resources, e.g. wind projects deployed at proximate areas (sub-regions of B) are most likely characterised by simultaneous time periods of high and low wind speeds. The aggregate expected power that can be generated by both players if no curtailment takes place is equal to:

$$\mathbb{E}(P_G) = \int_0^1 \int_0^1 (x_1 P_{N_1} + x_2 P_{N_2}) f(x_1, x_2) dx_2 dx_1 \tag{5.9}$$

Following the same analysis as in Section 5.2.1, production needs to be curtailed at times when generation exceeds demand or for all t that $x_1 P_{N_1} + x_2 P_{N_2} - D_t > 0$. By rearrangement, the latter results in $x_2 > \dfrac{D_t - x_1 P_{N_1}}{P_{N_2}}$. Total expected curtailment is equal to the expected generation, given that generation exceeds the demand (a posteriori expectation) minus the power demanded, and multiplied by the probability that generation exceeds the demand:

$$\mathbb{E}(P_{C,t}) = [\mathbb{E}(x_1 P_{N_1} + x_2 P_{N_2} \mid_{x_1 P_{N_1} + x_2 P_{N_2} > D_t}) - D_t] \cdot \int_0^1 \int_{\frac{D_t - x_1 P_{N_1}}{P_{N_2}}}^{1} f(x_1, x_2) dx_2 dx_1 \tag{5.10}$$

By definition, the conditional expectation of generation during a curtailment event (i.e. when RES oversupply occurs) is equal to:

$$\mathbb{E}(x_1P_{N_1}+x_2P_{N_2}\,|_{x_1P_{N_1}+x_2P_{N_2}>D_t}) = \frac{\int_0^1 \int_{\frac{D_t-x_1P_{N_1}}{P_{N_2}}}^1 (x_1P_{N_1}+x_2P_{N_2})f(x_1,x_2)dx_2dx_1}{\int_0^1 \int_{\frac{D_t-x_1P_{N_1}}{P_{N_2}}}^1 f(x_1,x_2)dx_2dx_1} \tag{5.11}$$

Combining the last two equations, the expected curtailment at time interval t can be expressed as:

$$\mathbb{E}(P_{C,t}) = \int_0^1 \int_{\frac{D_t-x_1P_{N_1}}{P_{N_2}}}^1 (x_1P_{N_1}+x_2P_{N_2})f(x_1,x_2)dx_2dx_1 - D_t\int_0^1 \int_{\frac{D_t-x_1P_{N_1}}{P_{N_2}}}^1 f(x_1,x_2)dx_2dx_1 \tag{5.12}$$

Eq. (5.9) and Eq. (5.12) represent the *aggregate* expected power generated and curtailed at t, respectively. If a longer time period is assumed, the total energy produced by both players is equal to $E_G = \sum_t \mathbb{E}(P_{G_t}), \forall t$, as derived by Eq. (5.9). Moreover, the total energy curtailed is equal to the summation of curtailment for all t and is equal to $E_C = \sum_t \mathbb{E}(P_{C_t}), \forall t$, where P_{C_t} is given by Eq. (5.12).

The general profit functions (as in Eq. (4.10) and Eq. (4.11)), however, require expressions for *individual* production and curtailment. The energy production by a single player i, when curtailment is not required, is equal to $E_{G_i} = \sum_t x_i P_{N_i} = \sum_t \mathbb{E}(P_{G_{i,t}}), \forall t$ as in Eq. (5.5). The energy curtailed by i player is equal to $E_{C_i} = \sum_t P_{C_{i,t}}, \forall t$. Assuming the implementation of a curtailment strategy that shares curtailment evenly between generators, and according to their actual power output at the time of curtailment, the power curtailed by i player during a curtailment event t is given by:

$$P_{C_{i,t}} = \frac{x_{i,t}P_{N_i}}{x_{i,t}P_{N_i}+x_{-i,t}P_{N_{-i}}} \cdot P_{C,t} \tag{5.13}$$

where $-i$ denotes other players or opponents. As shown in Chapter 3, such 'fair' curtailment strategies lead to approximately equal CF reduction, in the long term. Therefore, the energy curtailed by each player throughout a longer time horizon can be approximated based on Eq. (5.13) as:

$$E_{C_i} = \frac{E_{G_i}}{E_{G_i}+E_{G_{-i}}}E_C \tag{5.14}$$

This concludes the analysis, as profits can be expressed as functions of the players' strategies. Specifically, E_{G_i} is a function of P_{N_i} and crucially, E_{C_i} is a function of both players' strategies or generation capacities the players may install (P_{N_1}, P_{N_2}). The equilibrium of the Stackelberg game can be found following the procedure and best response estimations, as in Eq. (5.3) and Eq. (5.4).

The theoretical analysis shown here, requires knowledge of historic data on wind resources and demand. Moreover, a solution of the Stackelberg game equilibrium requires

solving the integral expressions and estimation of distribution functions. In the following section, we show how the methodology can be applied in a practical setting, such as the Kintyre-Hunterston grid reinforcement project.

5.3 Theoretical analysis application to a practical setting

The previous section presented the theoretical analysis of the leader-follower game and the equilibrium emerging from the strategic interactions of the players in this game. Application of the theoretical results requires the utilisation of historic data on wind resource and demand, in order to accurately estimate the probability distribution functions required for generation and curtailment estimation.

A practical application of the theoretical results is shown here based on realistic assumptions of a real grid reinforcement project in the UK, the installation of the Kintyre-Hunterston link. In a similar fashion to previous analysis, Hunterston is assumed to be the location of high demand (Location A) and Kintyre the location of high renewable potential (Location B). Moreover, it is assumed that both players may install new renewable generation capacity at B, albeit in different sub-regions of B. Equilibrium estimation requires the analysis of available wind speed data and demand at the two-location setting.

5.3.1 Wind resource data analysis

The analysis is based on wind speed datasets containing historic data on UK mean wind speed, which were obtained by the Met Office Integrated Data Archive System (MIDAS) [164]. The data analysis process in Section 5.3.1 describes the steps followed to analyse the wind speed data and estimate the wind power generation data. Datasets contain observations on mean wind speed collected by numerous weather stations across the UK. In order to accurately represent the wind resource at the two sub-regions at location B, two weather stations were selected from the MIDAS repository. Located in the Kintyre peninsula, the data collected from the station with ID 908 are used to model the production of the renewable capacity installed by the line investor. The weather station with ID 23417, located in Islay and approximately 44 km away, is used to model renewable production by local generators. The criteria for station selection were based on their availability of data, alignment across the same period of time and their proximity, so that a degree of spatial wind speed correlation can be captured by the model. The weather stations selected have common available data across a 17-year time period, from 1999 to 2015. The duration of the time period is approximately equal to a typical project lifetime of a renewable development, which is usually around 20 years.

Wind speed observations u_a consist of hourly data entries of mean wind speeds, computed as the hourly average across 10-min measurements, measured at anemometer height z_a. Let the wind speed historic data be represented by $u_{a,i}$, where $i = 1$ denotes the wind resource of the line investor and $i = 2$ denotes the wind speed at the local generators' project location. Observations are measured at an anemometer height of $z_a = 10$ m for

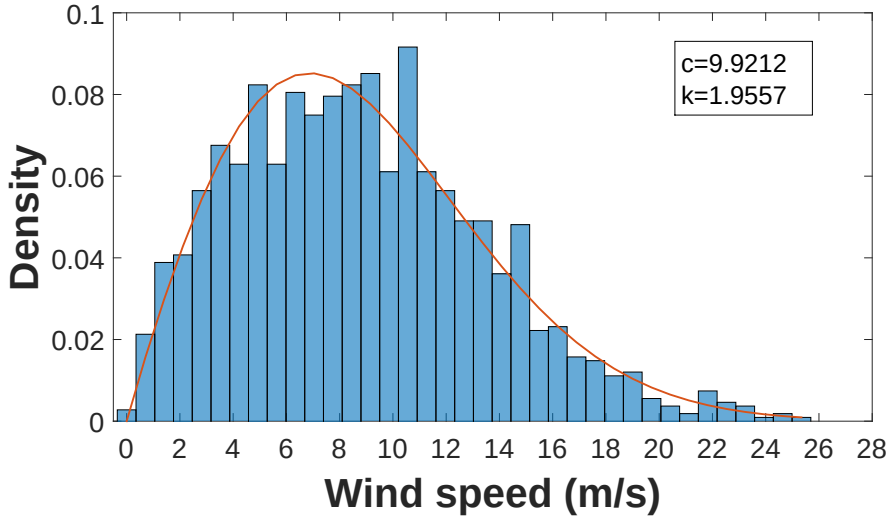

Fig. 5.2 Wind speed histogram and best Weibull fit 9:00 in Autumn (local generators' location)

both stations and are rounded to the nearest knot (1 kn = 0.5144 m/s). Data is already preprocessed and cleaned by the dataset provider. To improve on the alignment of available data across the two weather stations, any missing data for a shorter than a 6 hr duration were replaced by a linear interpolation of the nearest available wind speeds, rounded to the nearest knot. This practice is not expected to introduce a large error, as large variation of wind speeds is unusual within short periods of time. In addition, the data interpolated represent a small part of the total observations available. Any missing data of a larger duration were removed from both players datasets and were not taken into consideration for the analysis.

The first step for the data processing was to extrapolate wind speed observations u_a taken by the measuring equipment at weather stations to the wind turbine's hub height. A logarithmic shear profile is used to estimate the wind speed at hub height w:

$$w = u_a \frac{\log z_h/z_o}{\log z_a/z_o} \tag{5.15}$$

where w is the wind speed extrapolated at hub height, u_a is the wind speed at anemometer height, z_a the anemometer height, z_h the hub height and z_o the surface roughness of the environment where measurements were taken. A typical wind turbine was considered, such as the Enercon E82[1] with 2.05 MW rated capacity, cut-in wind speed of 3 m/s, cut-out wind speed of 28 m/s, a rated wind speed of 13 m/s at which the turbine is able to generate its nominal power output and a hub height of $z_h = 85$ m. Moreover, similarly to other works [84, 260], the surface roughness was chosen to be short grass, which represents a typical environment for the weather stations and therefore a suitable value for the parameter z_o was chosen as $z_o = 30$ mm.

[1]http://www.enercon.de/en/products/ep-2/e-82/

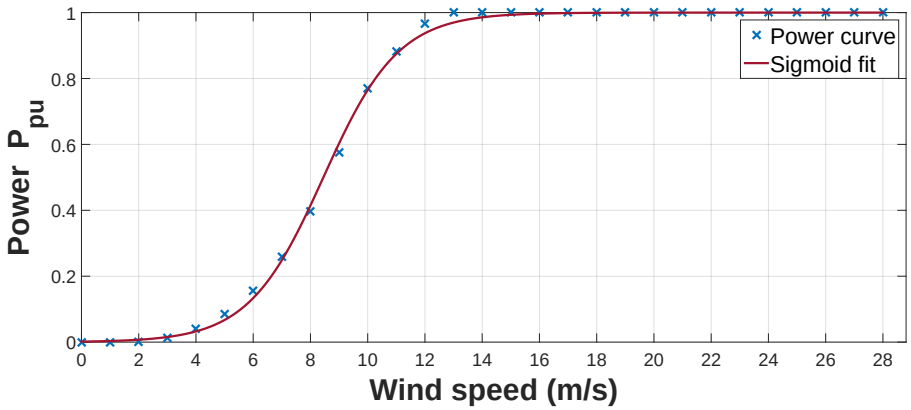

Fig. 5.3 Power curve of Enercon E82 and best Sigmoid fit function

Weibull distributions are often used to represent actual wind speed distributions and are commonly used in the literature. Typical examples from wind speed forecasting papers include [61, 245]. Using the extrapolated values of wind speeds at hub height, derived from Eq. (5.15), and at each player's location, the probability distribution function of w wind speed can be approximated by a Weibull distribution with a shape factor k and a scale factor c:

$$f(w,c,k) = \frac{k}{c}\left(\frac{w}{c}\right)^{(k-1)} e^{-\left(\frac{w}{c}\right)^{k}} \tag{5.16}$$

To achieve greater accuracy, different Weibull distributions may be assumed that capture hourly and seasonal variations of wind speed. Wind conditions depend highly on the time of day and season. Assuming 24 hours and 4 seasons, a total of 96 Weibull distributions were generated, one for every hour $(1-24)$ and season $(1-4)$. It is assumed that hour 1 refers to 00:00 and hour 24 to 23:00, March, April and May refer to Spring, June, July and August to Summer, September, October and November to Autumn and December, January and February refer to Winter. Fig. 5.2 shows the wind speed histogram and best fit of a Weibull distributions for 09:00 in Autumn at the location of the local generator's renewable project. The parameters of the Weibull distributions are found by use of the 'fitdist' function in MATLAB.

Given the wind speed w, renewable production can be estimated by use of a generic power curve. The power curve represents the relation of wind speed at hub height with the power output of a wind turbine. Several values of the power curve are known by the wind turbine manufacture, as shown in Fig. 5.3 for the E82 wind turbine. The power output is normalised according to maximum power output of the turbine achieved under nominal conditions $P_{pu} = P/P_N$. The intermediate values can be approximated by a sigmoid function with parameters $\alpha = 0.3921$ m/s and $\beta = 16.4287$ m/s found by the 'fitdist' MATLAB function (see Fig. 5.3):

$$f(w,\alpha,\beta) = \frac{1}{1+e^{-\alpha(w-\beta)}} \tag{5.17}$$

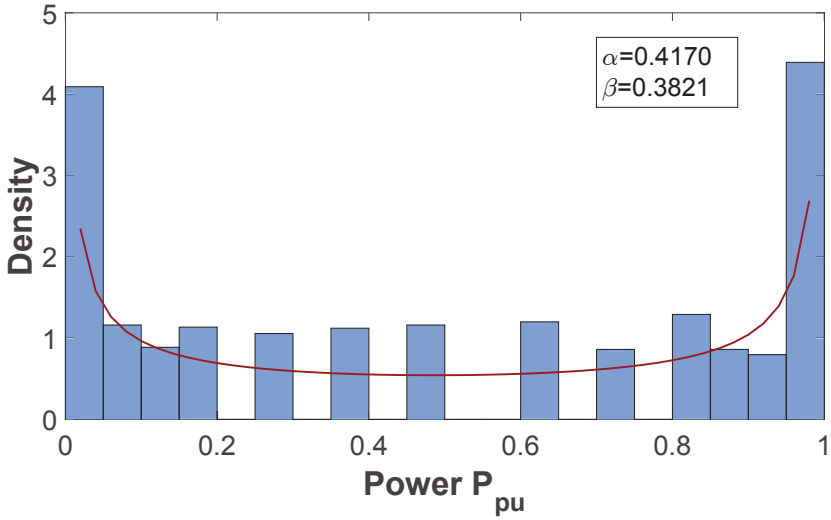

Fig. 5.4 Power output histogram and best fit Beta curve 9:00 in Autumn (local generators' location)

As seen in Fig. 5.3, generation is negligible for very low wind speeds and equal to maximum output for higher values than the nominal wind speed. In the intermediate area, generation varies with the third power of the wind speed.

The normalised power output is bounded in the closed interval $[0,1]$ and can be represented by a standard Beta probability distribution function. A similar approach is followed in numerous works such as in [76, 84, 259]. 96 standard beta distributions can be generated from the wind speed Weibull distributions and power curves, one for every hour and season:

$$f(x_i) = \frac{1}{B(a,b)} x_i^{a-1}(1-x_i)^{b-1} \tag{5.18}$$

where

$$B(a,b) = \frac{\Gamma(a)\Gamma(b)}{\Gamma(a+b)} \int_0^1 t^{a-1}(1-t)^{b-1} dt \tag{5.19}$$

Fig. 5.4 shows the histogram and best Beta fit, found by function 'fitdist' in MATLAB, at 09:00 hour, in Autumn. Note here, the discreteness in the available observations (datasets obtained by the MIDAS repository are discrete values of wind speed, rounded to the nearest knot), combined with the fact that for wind speeds lower than the nominal, wind speed generation varies with the third power of the wind speed, may create empty bins in the power output histogram.

Aggregate power production of both players captures correlation between wind resources and can be represented by the joint probability distribution of power outputs. Note here that correlated outputs mean that the aggregate power output from both players is not equal to a two-dimensional Beta distribution. If there are sufficient wind speed measurements for both players locations, then the joint probability distribution can be estimated directly from the available data. For example, Fig. 5.5 shows the joint generation histogram at 09:00 hour in Autumn. Most observations are concentrated at zero power output (no wind) or close to rated power (wind equal to or above nominal). Moreover,

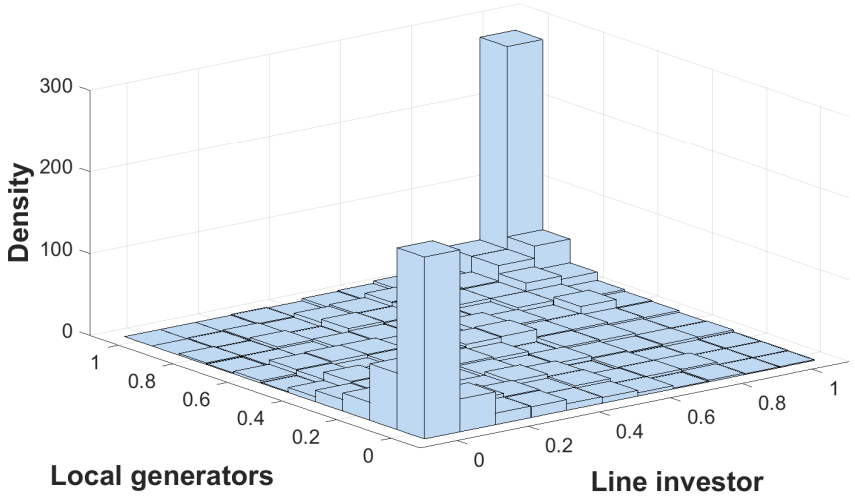

Fig. 5.5 Joint power output histogram at 09:00 in Autumn

many observations appear around the diagonal, which indicates partial correlation between the outputs generated by each player.

Results from such an analysis can feed into Eq. (5.9) and Eq. (5.12) to compute expected generation and curtailment. However, a similar analysis is required also for the demand data, shown in the following section. Note here that analytical expressions of the joint distributions and consequently solutions and calculation of integrals are difficult to achieve. To overcome such challenges an empirical approach based on simulations can be used to compute expected generation and curtailment, as shown in the following sections.

5.3.2 Demand data analysis

The analysis is based on the UK National Demand data obtained by the UK's system operator, i.e. National Grid [2]. The data used for the study span from 2006 to 2015. The observations include national demand data in half-hourly settlement intervals. The national demand is the sum of generation, as recorded by operational metering managed by the National Grid, plus the estimated embedded generation from wind/solar generators, plus imports from interconnectors linked to the Great Britain system. Actual demand may differ from this estimation, as some demand is not visible to the system operator, due to embedded generation or microproduction that is connected to low-voltage and distribution networks. Half-hourly demand data were averaged to create hourly data that have the same granularity as wind speed data. Fig. 5.6 shows the hourly average of the UK national demand data and yearly variation for a 10-year period. As shown in Fig. 5.6, the demand is low during the night and presents a morning and an afternoon peak in coordination with human activities throughout the day.

UK national demand data were analysed in a similar manner to wind speed data in separate distributions for every hour and season. The demand at location A was taken

[2]http://www2.nationalgrid.com/UK/Industry-information/Electricity-transmission-operational-data/Data-Explorer/

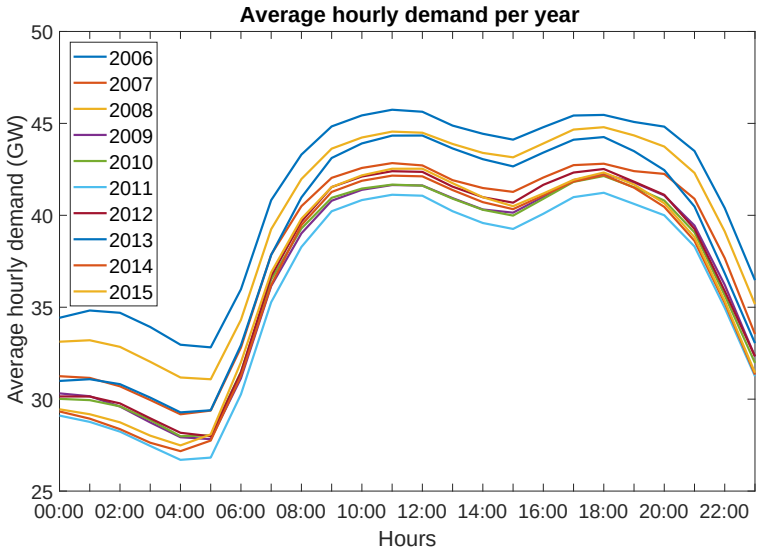

Fig. 5.6 Hourly average of the UK national demand and variation across different years

to be equal to the average national demand for every hour and season, scaled down by a factor, such that peak load would be equal to the capacity of the power line, assumed to be 150 MW. Fig. 5.7 shows the average seasonal demand at location A as well as the minimum and maximum hourly demand. Fig. 5.8 summarises the seasonal effect on the average hourly demand.

From the demand distributions and joint power distributions, expected generation and curtailment can be found as in Eq. (5.9) and Eq. (5.12). However, it is clear that analytical solutions of the expected generation and curtailment are difficult to compute. These challenges can be overcome by following an empirical simulation approach that can significantly simplify the computation of expected generation and curtailment. The proposed solution is presented in the following section.

5.4 Empirical approach for equilibrium estimation

When sufficient data is available, an empirical approach based on simulation analysis can be useful for equilibrium estimation. This section describes the methodology applied based on a data analysis and simulation approach. Hourly wind speed data w_i from each player's location and average demand per hour and season D (as in Fig. 5.8) were used for the following analysis.

The general methodology steps are shown in Fig. 5.9. The first step deals with the evaluation and processing of the available data. Next, determination of a feasible strategy space for both players is required. Recall here that a strategy action is the generation capacity a player can install, namely P_{N_i}. A player can choose to install generation capacity within the bounds of zero capacity $P_{N_i} = 0$ and a maximum capacity $P_{N_{max}}$ above which any player would not achieve any profit. The feasible strategy or action space is defined as $\langle P_{N_1}, P_{N_2} \rangle = \langle 0 : \delta P_N : P_{N_{max}}, 0 : \delta P_N : P_{N_{max}} \rangle$, where δP_N is the incremental generation capacity that a player can build. For every possible combination of actions from the

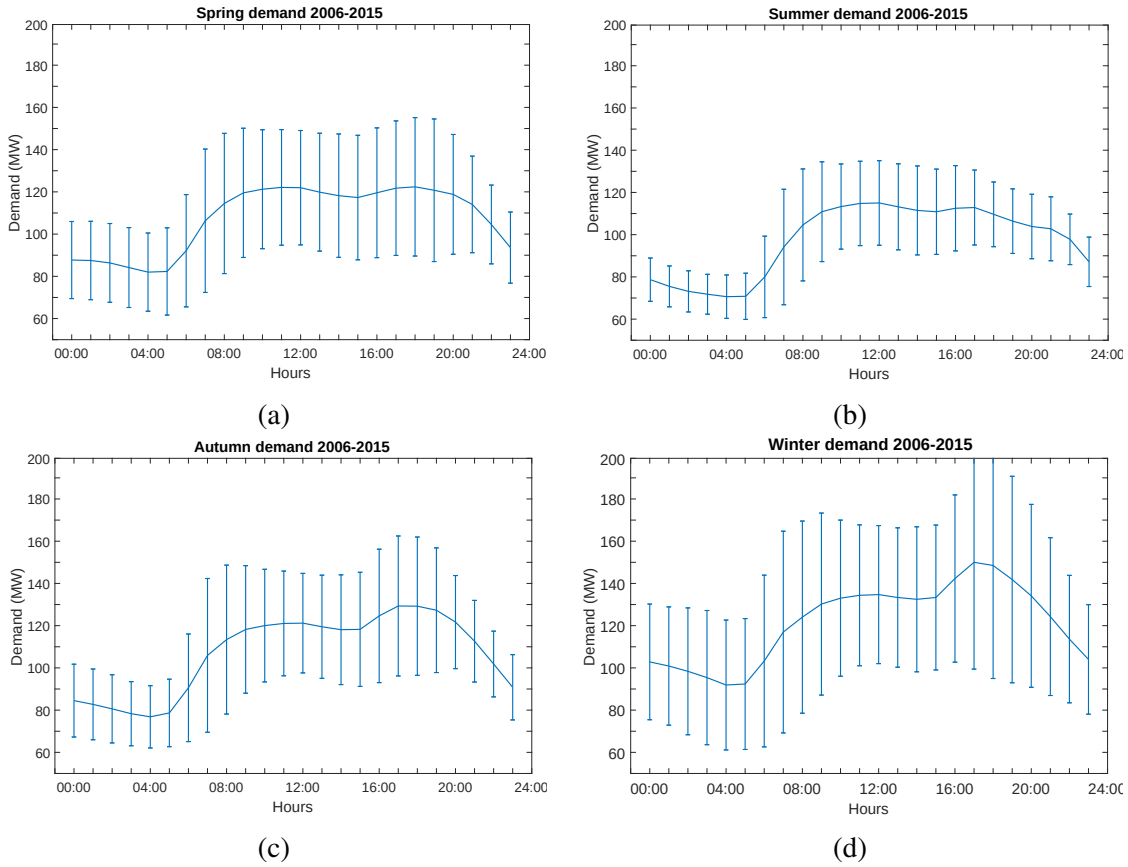

Fig. 5.7 Seasonal average demand with minimum and maximum values during (a) Spring (b) Summer (c) Autumn and (d) Winter

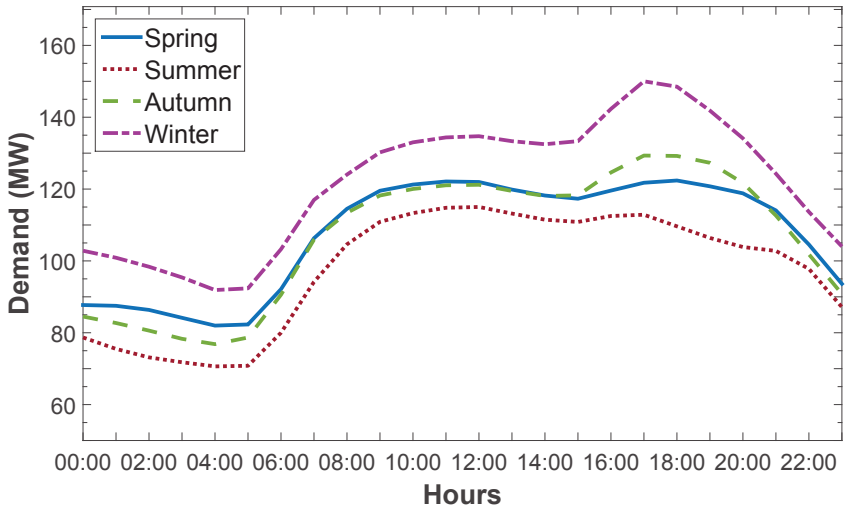

Fig. 5.8 Hourly average demand per season

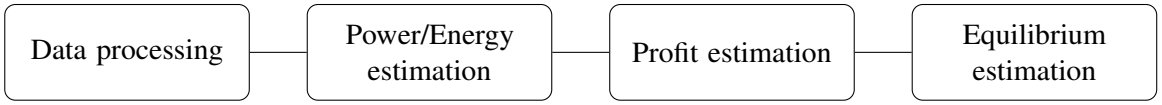

Fig. 5.9 Summarised methodology steps for transmission capacity game with stochastic generation

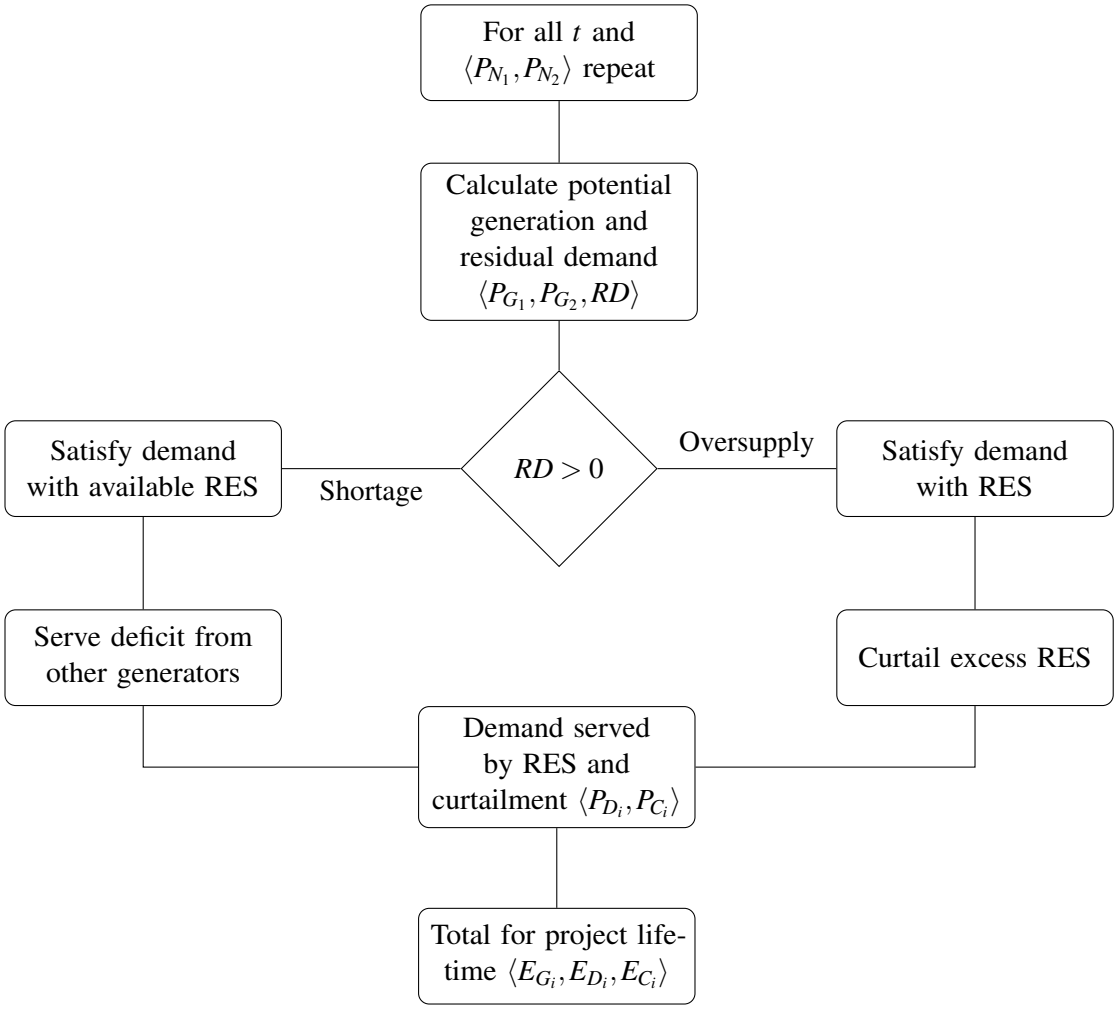

Fig. 5.10 Power and energy estimation flow chart

Algorithm 1 POWER & ENERGY ESTIMATION

$P_{N_{max}}$ ▷ max rated capacity in search space
$P_{N_i} \leftarrow [0 : \delta P_N : P_{N_{max}}]$ ▷ strategy space i=1,2 player
α, β ▷ power curve sigmoid parameters
for all $P_{N_1} \in \{0, ..., P_{Nmax}\}$ **do**
  for all $P_{N_2} \in \{0, ..., P_{Nmax}\}$ **do**
    for all t
      $P_{G_i}^{(t)} \leftarrow \frac{1}{1+e^{-\alpha(w_i^{(t)}-\beta)}} \cdot P_{N_i}$ ▷ i player generation
      $RD \leftarrow D - (P_{G_1} + P_{G_2})$ ▷ residual demand
      if $RD > 0$ **then** ▷ no curtailment
        $P_{D_i} \leftarrow P_{G_i}$
        $P_{C_i} \leftarrow 0$
      else
        $P_{C_i} \leftarrow -\frac{P_{G_i} \cdot RD}{P_{G_1} + P_{G_2}}$ ▷ curtailment gen i
        $P_{D_i} \leftarrow P_{G_i} - P_{C_i}$ ▷ actual demand served
      end
    end
  end
end
$E_{G_i}(P_{N_i}) \leftarrow \sum_t P_{G_i}$ ▷ total gen i
$E_{D_i} \leftarrow \sum_t P_{D_i}$ ▷ total demand served i
$E_{C_1}(P_{N_1}, P_{N_2}) \leftarrow \sum_t P_{C_1}$ ▷ total curt 1
$E_{C_2}(P_{N_1}, P_{N_2}) \leftarrow \sum_t P_{C_2}$ ▷ total curt 2
return $(E_{G_1}, E_{G_2}, E_{C_1}, E_{C_2}, E_{D_1}, E_{D_2})$ ▷ $E_{D_i} = E_{G_i} - E_{C_i}$

strategy space of $\langle P_{N_1}, P_{N_2} \rangle$, potential generation (no curtailment) P_{G_i}, curtailed power P_{C_i} and actual power used to serve the demand P_{D_i} are estimated for all t under a fair curtailment rule such as Pro Rata or FRR. The total energy production and curtailment over a larger time horizon and project duration is given by the summation of the estimated quantities for all t. The procedure is shown in Fig. 5.10 and in greater detail in Algorithm 1.

Energy quantities of expected curtailment and generation are estimated. Profits are computed for different cost parameters, as shown in Algorithm 2.

The next step is to estimate the Stackelberg game equilibrium, by backward induction, as in Algorithm 3. In more detail, the equilibrium is estimated from the normal form of the Stackelberg game. Profits or expected payoffs are computed for every possible action in the strategy space $\langle P_{N_1}, P_{N_2} \rangle$. The algorithmic procedure is shown in Fig. 5.11. For every P_{N_1} i.e. for every row in Fig. 5.11, the rated capacity $P_{N_2}^*$ is found that maximises the follower's profits Π_2^*. In other words the follower's best response is found for every P_{N_1}. Line investor profits that correspond to the follower's best responses are also recorded. Next, from this set of recorded solutions, the leader selects to install $P_{N_1}^*$ that maximises his own profit. The pair $(P_{N_1}^*, P_{N_2}^*)$ constitutes the equilibrium of the game.

Algorithm 2 PROFIT ESTIMATION

p_G, p_T ▷ generation tariff, transmission fee
C_T ▷ cost of line
c_{G_i} ▷ i player's generation cost
for all $P_{N_1} \in \{0, ..., P_{N_{max}}\}$ **do**
    for all $P_{N_2} \in \{0, ..., P_{N_{max}}\}$ **do**
        $\Pi_1 \leftarrow (E_{G_1} - E_{C_1})p_G - E_{G_1}c_{G_1} +$
            $(E_{G_2} - E_{C_2})p_T - C_T$
        $\Pi_2 \leftarrow (E_{G_2} - E_{C_2})(p_G - p_T) - E_{G_2}c_{G_2}$
    end
end
return (Π_1, Π_2)

Algorithm 3 STACKELBERG EQUILIBRIUM ESTIMATION

for all $P_{N_1} \in \{0, ..., P_{N_{max}}\}$ **do** ▷ best response gen 2
    $\Pi_2^* \leftarrow \max_{P_{N_2}} \Pi_2(P_{N_1}, P_{N_2})$
    $P_{N_2}^* \leftarrow \arg\max_{P_{N_2}} \Pi_2(P_{N_1}, P_{N_2})$
end
$\Pi_1^* \leftarrow \max_{P_{N_1}} \Pi_1(P_{N_1}, P_{N_2}^*)$ ▷ best response gen 1
$P_{N_1}^* \leftarrow \arg\max_{P_{N_1}} \Pi_1(P_{N_1}, P_{N_2}^*)$
return $\Pi_1^*, \Pi_2^*, P_{N_1}^*, P_{N_2}^*$

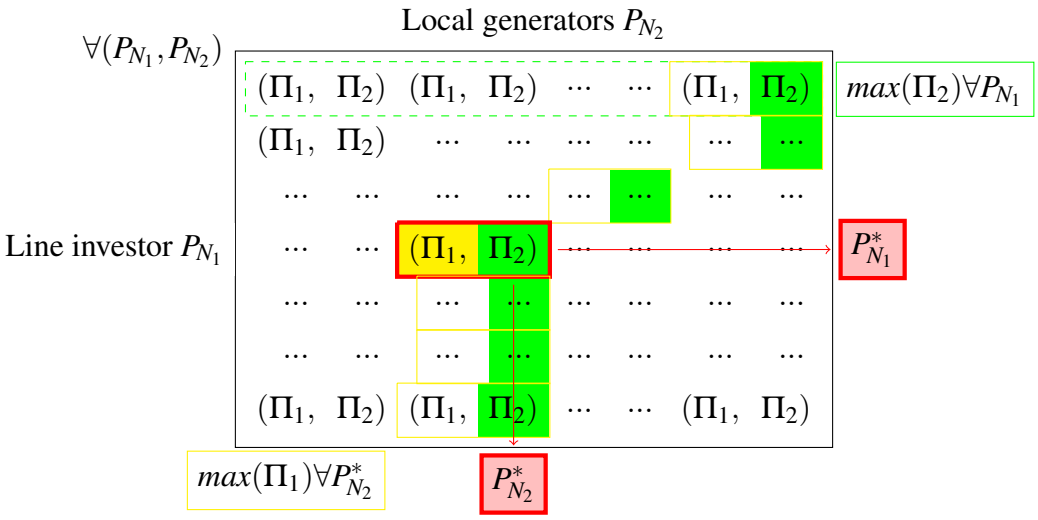

Fig. 5.11 Stackelberg game equilibrium estimation process

In the next section, we provide the solutions of the empirical and algorithmic approach for varying parameters and discuss the main findings of the practical example application based on the Kintyre-Hunterston project.

	Scenario 1	Scenario 2	Scenario 3
c_{G_1}	$0.14p_G : 0.02p_G : 0.50p_G$	$0.30p_G$	$0.26p_G$
c_{G_2}	$0.30p_G$	$0.06p_G : 0.02p_G : 0.52p_G$	$0.20p_G$
p_T	$0.26p_G$	$0.26p_G$	$0 : 0.02p_G : 0.76p_G$

Table 5.1 Summary of cost parameters considered in three scenarios for the analysis of the transmission capacity game with stochastic generation (in all scenarios the generation price remained fixed at $p_G = £74.3/\text{MWh}$ and the transmission cost at $C_T = £230m$)

5.4.1 Scenario assumptions

One of the first assumptions to consider is defining a feasible search space that includes all possible action strategies of both players. Based on several trial runs, the upper limit of the solution search space was set as $P_{N_{max}} = 415$ MW. Note here that $P_{N_{max}}$ is larger than the line capacity (150 MW) divided by the minimum CF experienced by any player at all hours and seasons, to guarantee that all feasible solutions are included in the search space. Moreover, the incremental generation capacity a generator can install is set to $\delta P_N = 0.5$ MW, therefore the solution search space was defined as $[P_{N_1}, P_{N_2}] = [0 : 0.5 : 415, 0 : 0.5 : 415]$. All possibilities were considered, even the case where demand is served by a single player.

For every action in the feasible strategy space $\langle P_{N_1}, P_{N_2} \rangle$, we estimate the power generated and curtailed for both players under a fair curtailment rule such as Pro Rata or FRR (Algorithm 1). For example, for a specific pair of $\langle P_{N_1}, P_{N_2} \rangle$, we estimate the power generated at each hour given the wind speed, and estimate the power curtailed given the demand. Next, we estimate the aggregate power generated and curtailed by each player for the time period of 17 years and therefore derive the energy that would have been generated (if no curtailment) and the energy curtailed, as the summation of $145,077$ valid data points (hours in the 17 years that wind speed and demand data are available). Next, the profits can be estimated (see Algorithm 2), if cost parameters are known (c_{G_1}, c_{G_2}, p_T). The procedure is repeated for all strategies in the search space and the results describe the normal form of the Stackelberg game. Finally, the equilibrium of the game is found as shown in Fig. 5.11.

Different scenarios are used to study the interplay between the Stackelberg equilibrium solution and varying cost parameters (c_{G_1}, c_{G_2}, p_T). Similar to the analysis presented in Chapter 4, the selling tariff is set equal to $p_G = £74.3/\text{MWh}$. All other cost and tariff parameters are expressed as a percentage of p_G for easier representation of the results. Varying one cost parameter at a time, while other parameters remain constant, three different scenarios emerge. Scenario 1 shows how the equilibrium results depend on the generation cost of the line investor, Scenario 2 shows the dependence on local generators' cost and Scenario 3 shows the dependence on the transmission fee. The step size of varying parameters is set equal to $0.02p_G$ for all scenarios considered. Precise values of cost parameters considered are summarised in Table 5.1.

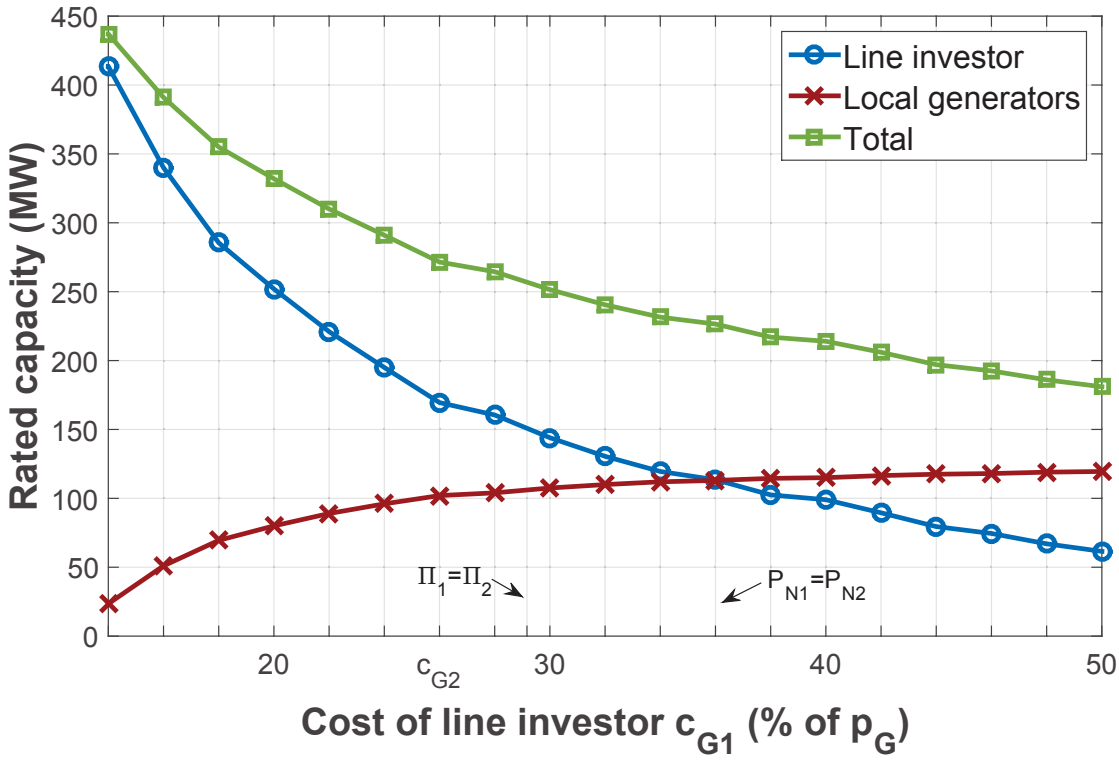

Fig. 5.12 Scenario 1: Generation capacity installed and dependence on the line investor's generation cost

5.4.2 Scenarios results

Scenario 1: Varying c_{G_1}

The first scenario shows how the equilibrium results depend on the line investor's generation cost c_{G_1}. Other cost parameters remain fixed at $c_{G_2} = 0.30p_G$ and $p_T = 0.26p_G$, while c_{G_1} varies from $0.14p_G$ to $0.50p_G$.

Fig. 5.12 shows the generation capacity installed by the players for varying generation costs of the line investor. Fig. 5.13 shows the profits at equilibrium and Fig. 5.14 shows the energy that could have been generated and the energy curtailed. Total generation capacity decreases as c_{G_1} increases with other parameters remaining equal (Fig. 5.12). For low leader's generation cost, the line investor installs more generation capacity leading to larger profits. However as c_{G_1} increases, less capacity is installed by the line investor. This leads to decreasing profits. At $c_{G_1} \simeq 0.292p_G$ the profits of the players become equal (Fig. 5.13). From $c_{G_1} \simeq 0.292p_G$ to $0.36p_G$, the line investor continues to install more capacity up to $c_{G_1} \simeq 0.36p_G$, where players install equal generation capacity (Fig. 5.12).

Scenario 2: Varying c_{G_2}

The second scenario shows how the equilibrium results depend on the local generators' generation cost c_{G_2}. Other cost parameters remain fixed with $c_{G_1} = 0.30p_G$ and $p_T = 0.26p_G$, while the local generators' cost varies from $c_{G_2} = 0.06p_G$ to $0.52p_G$.

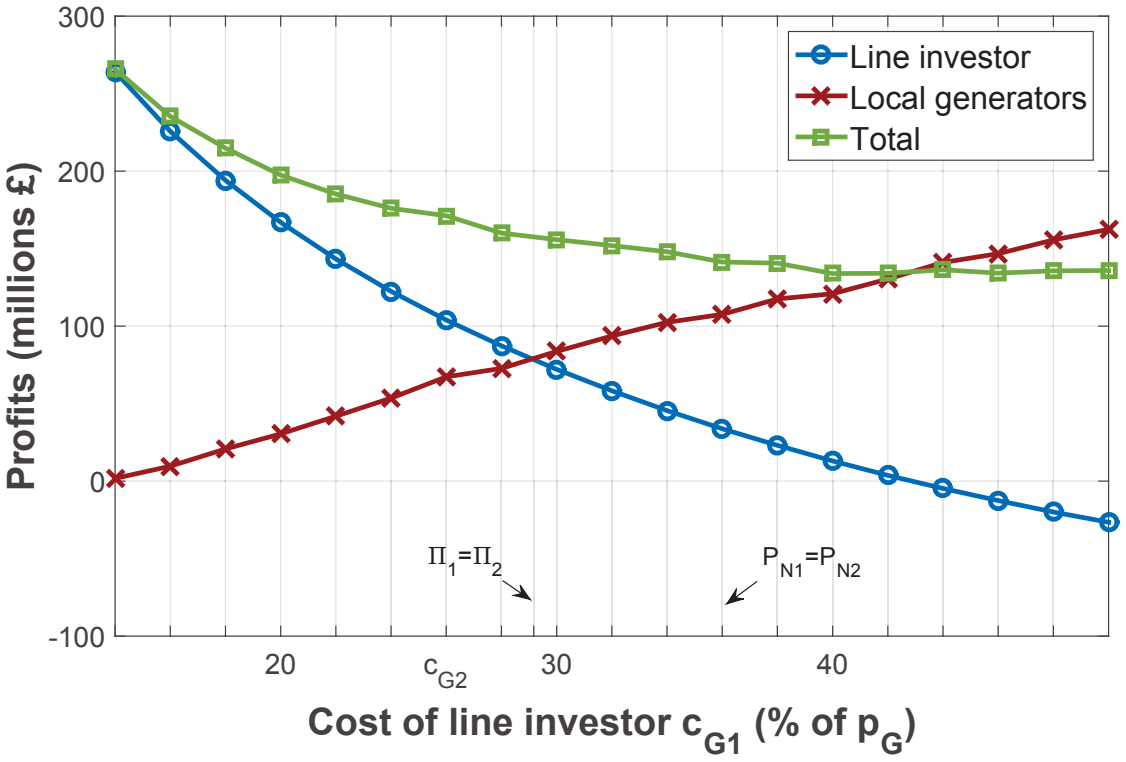

Fig. 5.13 Scenario 1: Profits and dependence on the line investor's generation cost

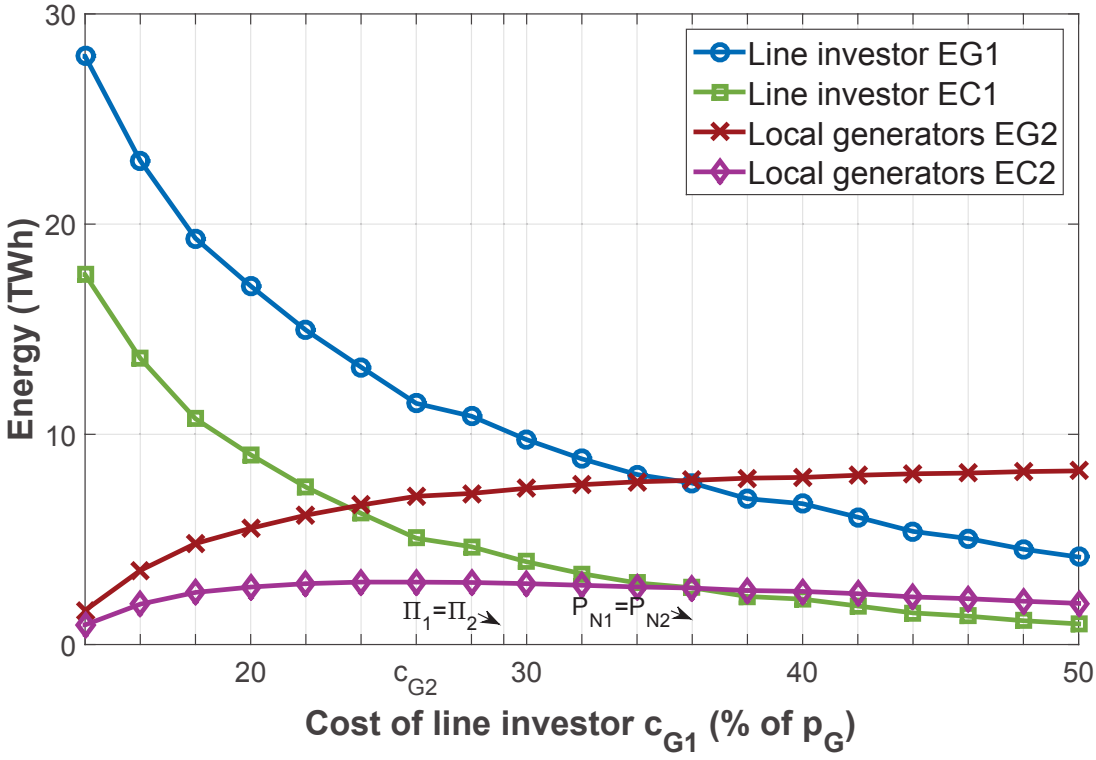

Fig. 5.14 Scenario 1: Energy generated and curtailed and dependence on the line investor's generation cost

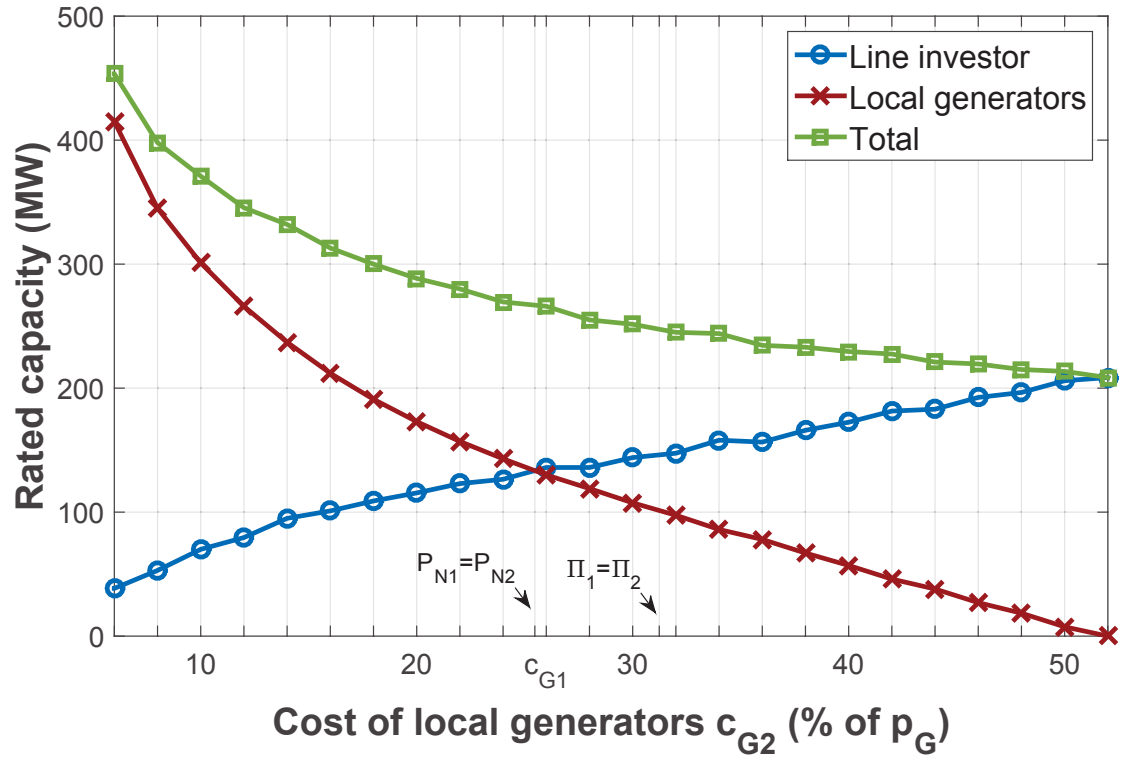

Fig. 5.15 Scenario 2: Generation capacity installed and dependence on the local generators' generation cost

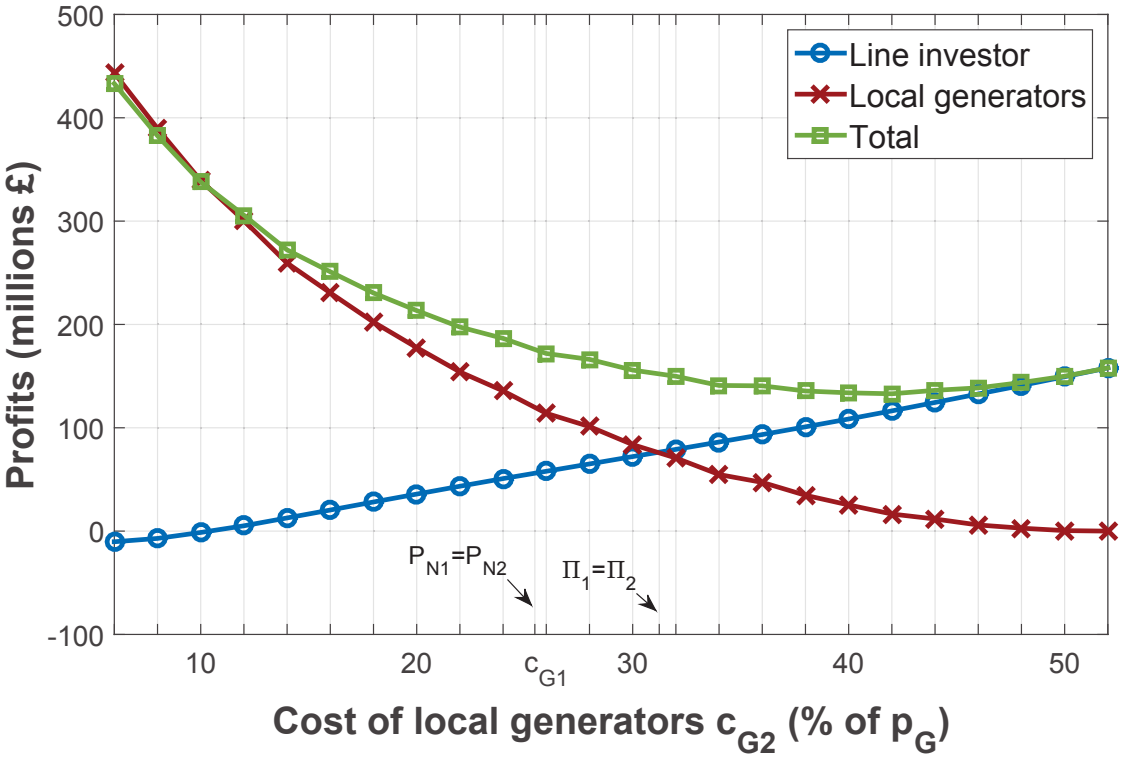

Fig. 5.16 Scenario 2: Profits and dependence on the local generators' generation cost

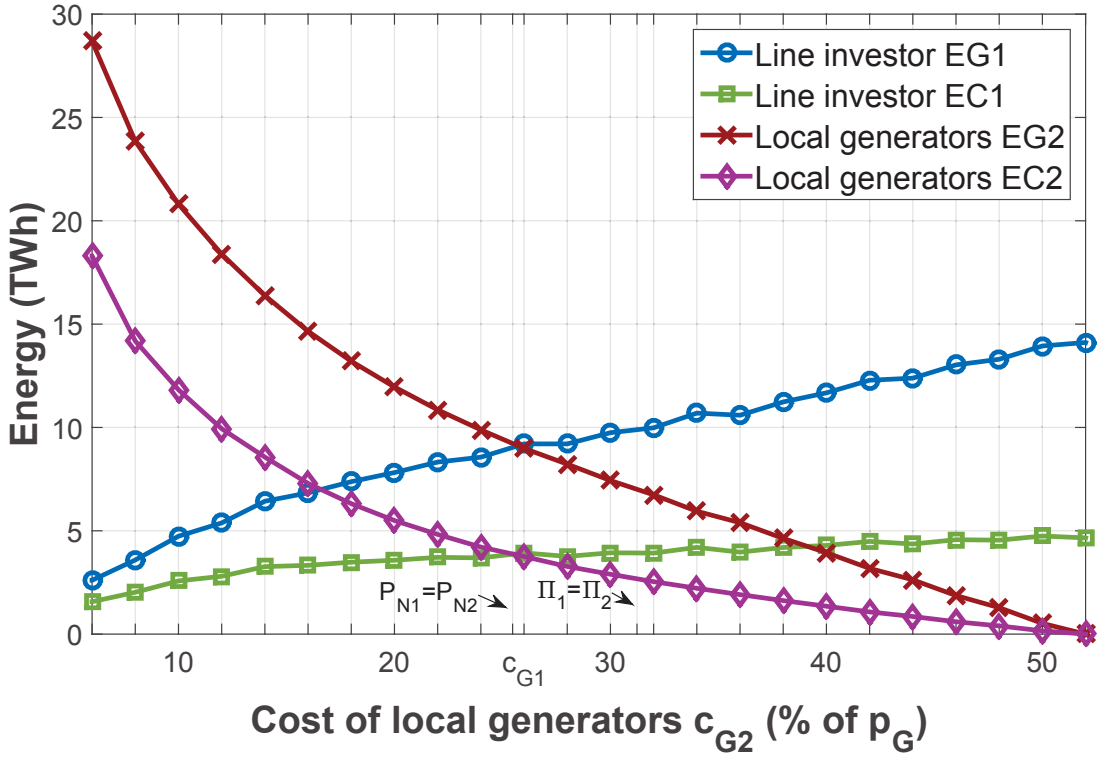

Fig. 5.17 Scenario 2: Energy generated and curtailed and dependence on the local generators' generation cost

Fig. 5.15 shows the generation capacity installed by the players for varying generation costs of the local generators. Fig. 5.16 shows the profits at equilibrium and Fig. 5.17 shows the energy that could have been generated and the energy curtailed. The total generation capacity installed decreases as c_{G_2} increases due to the reduction of P_{N_2} installed, as shown in Fig. 5.15. We can observe two critical points, $c_{G_2} \simeq 0.255 p_G$ where players install equal generation capacities $P_{N_1} = P_{N_2}$ (Fig. 5.15) and $c_{G_2} \simeq 0.312 p_G$, where profits for both players are equal $\Pi_1 = \Pi_2$ (Fig. 5.16). For $c_{G_2} < 0.255 p_G$, local generators install more generation capacity than the line investor. For $c_{G_2} = 0.255 p_G$ to $0.312 p_G$ although $P_{N_1} > P_{N_2}$ (Fig. 5.16), the leader's profit is lower, due to the additional cost of installing the line C_T. If c_{G_2} increases further, then local generators decrease their installed capacity, which eventually leads to equal profits and sequentially to the leader's overcoming the follower's profit (Fig. 5.16).

Scenario 3: Varying p_T

The third and last scenario shows how the equilibrium results depend on the transmission charges imposed p_T. Other cost parameters remain fixed with $c_{G_1} = 0.26 p_G$ and $c_{G_2} = 0.20 p_G$, while the transmission fee varies from $p_T = 0$ to $0.76 p_G$.

Fig. 5.18 shows the generation capacity installed by the players for varying generation costs of the local generators. Fig. 5.19 shows the profits at equilibrium and Fig. 5.20 shows the energy that could have been generated and the energy curtailed.

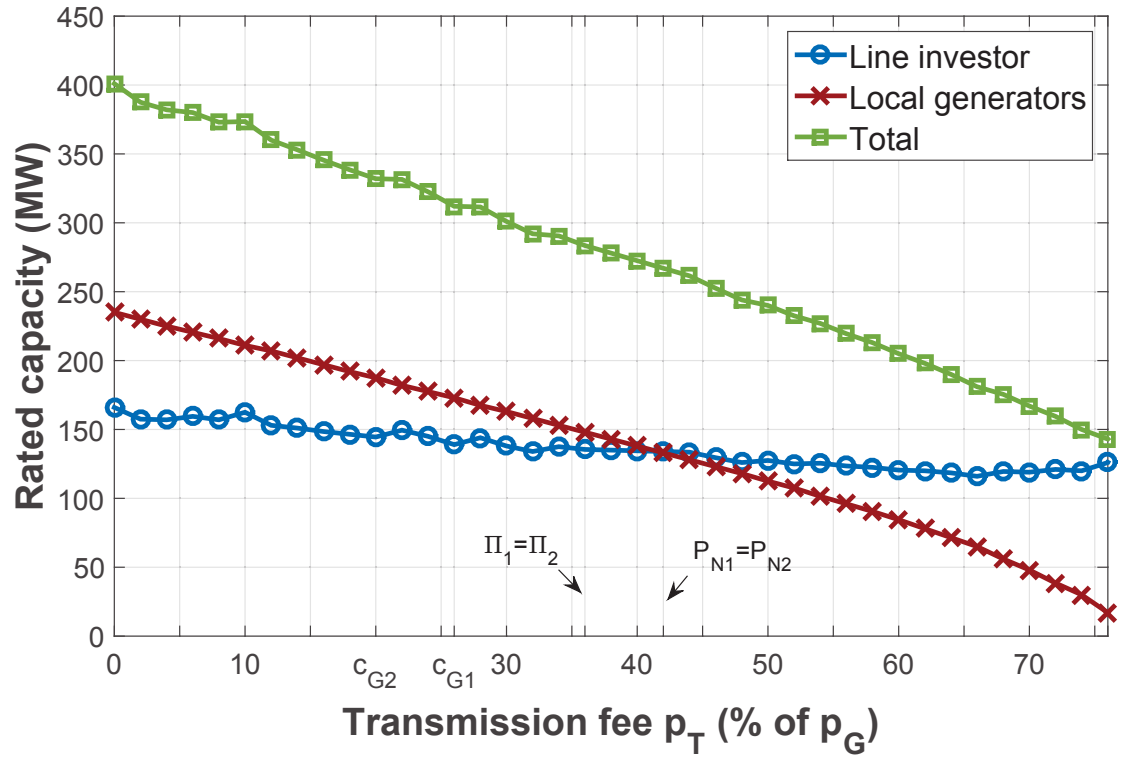

Fig. 5.18 Scenario 3: Generation capacity installed and dependence on the transmission fee

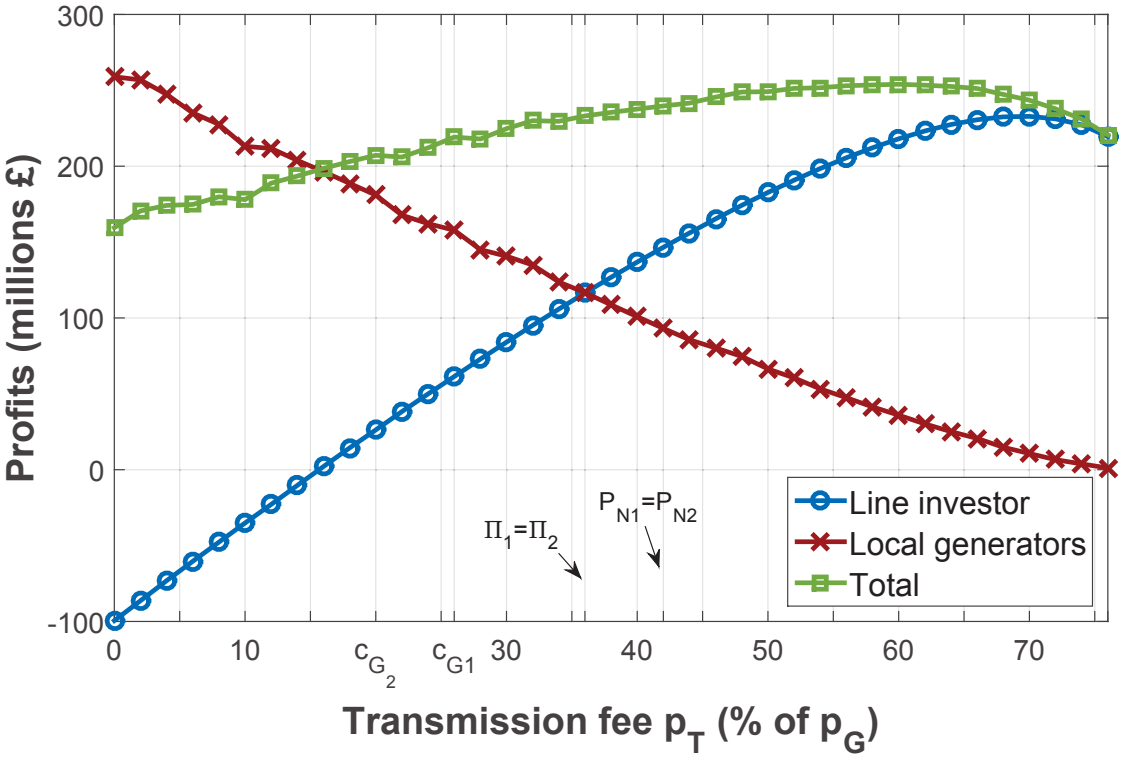

Fig. 5.19 Scenario 3: Profits and dependence on the the transmission fee

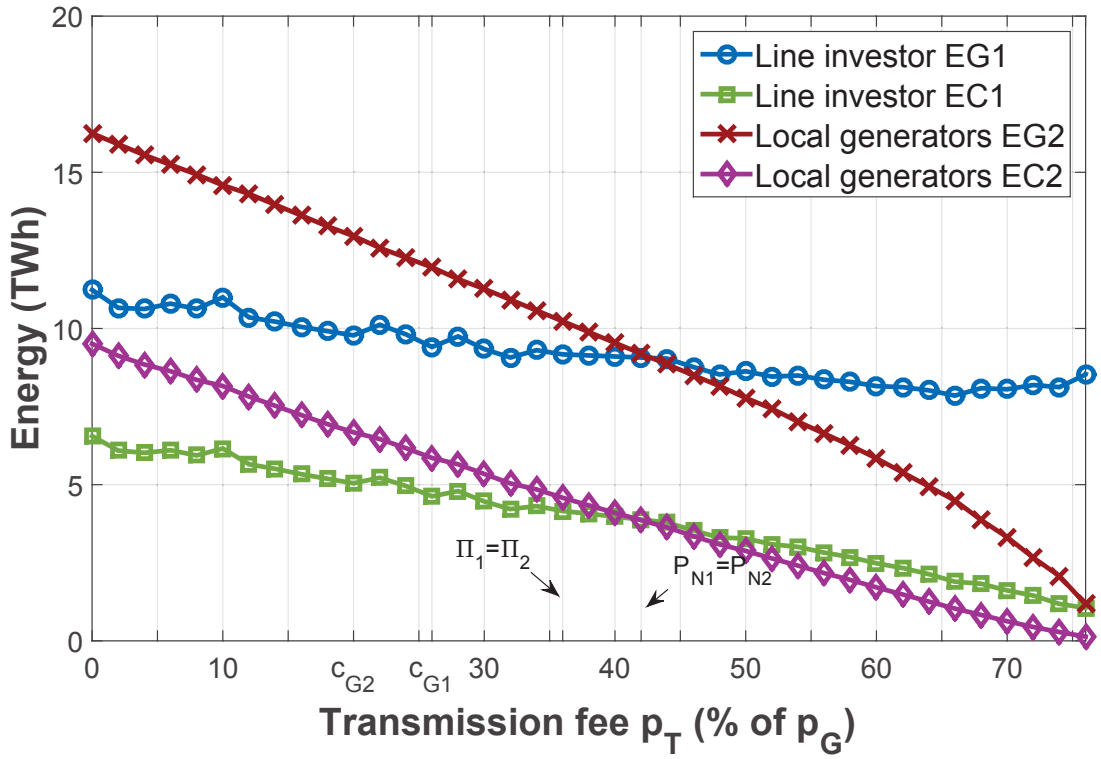

Fig. 5.20 Scenario 3: Energy generated and curtailed and dependence on the transmission fee

The total generation capacity decreases as p_T increases, due to local generators installing less capacity. The leader's generation capacity is relatively constant with varying p_T. Note here that the leader may react to the decreasing capacity of the local generators as p_T increases, both by decreasing or increasing their own built capacity, as p_T increases (Fig. 5.18).

When the transmission fee is $p_T < 0.42 p_G$, followers install more capacity as a result of the transmission fee and cheaper generation cost. However, as p_T increases, the revenues drop for local generators, who install less P_{N_2}, up to $p_T \simeq 0.42 p_G$ where players install equal capacities (Fig. 5.18). Local generators have larger profits until $c_{G_2} \simeq 0.36 p_G$ where profits break even, mainly due to the high power line installation cost C_T (Fig. 5.19).

For this setting, the transmission fee needs to be at least $p_T \simeq 0.15 p_G$. Charging a transmission fee below this amount would make it uneconomical for the line investor to install the line, given the expected response by local generators. Morever, the line investor needs to install roughly as much generation capacity as local generators to achieve similar profit, in this scenario. In contrast, if p_T is set too high, it is not feasible for local generators to invest in renewable energy at this location (Fig. 5.20).

5.4.3 Discussion of results

As shown in the results, for every set of cost (c_{G_1}, c_{G_2}) and revenue parameters (p_T, p_G), there is an upper limit of total generation capacity being installed at Location B, which is equal to the sum of rated capacities installed by each player. In all sets of scenarios,

the total capacity installed decreases as the tested parameter value increases (Fig. 5.12, Fig. 5.15 and Fig. 5.18). Each player installs less capacity as their generation cost increases, while the other player benefits by increasing their capacity (Fig. 5.12 and Fig. 5.15). The cost of local generators has a larger impact on the capacities installed for both players, as shown by comparing Fig. 5.12 and Fig. 5.15, as local generators face the additional cost of transmission charges. Profits have similar behaviour to the generation capacities built in Scenarios 1 and 2, while in Scenario 3, the line investor's profit increases because of larger revenues from transmission (Fig. 5.19). Note here that the players profits are not equal when $P_{N_1} = P_{N_2}$ (which over a long time window means $E_{G_1} \simeq E_{G_2}$ and $E_{C_1} \simeq E_{C_2}$ as shown when comparing Fig. 5.12 with Fig. 5.18, or Fig. 5.13 with Fig. 5.19 and Fig. 5.14 with Fig. 5.20), because of transmission charges p_T, but also because of different generation costs and C_T.

If the followers' generation cost is much smaller than the line investor's (assuming for example that local generators might have access to cheaper land or favourable licensing approval), then the line investor will need to charge a high transmission fee to have positive earnings (Fig. 5.19). On the other hand, if the leader's cost is much smaller, the generation capacity will mostly be installed by the line investor, as there is no room for profitable investment of other renewable producers. Moreover, in Scenario 3 it is shown that the followers' generation capacity decreases as p_T increases, but this does not always result in the leader increasing their own capacity (see Fig. 5.20). Estimating the best response is a complex procedure which depends on the curtailment imposed and varying demand. In a similar way, if we assume that local generators increase their installed capacity, it is possible for the line investor to slightly increase their own generation capacity, as this strategy move may minimise the profit losses incurred, as long as the increased cost of installing the additional generation capacity units leading to larger energy curtailed is counter-balanced by the revenues generated by satisfying a larger demand at times when no curtailment occurs.

As shown in Scenario 3, $p_T \simeq 0.15 p_G$ is the minimum value of the transmission fee that allows profit for the line investor. Similarly, if the transmission fee is set too high, then local investors will not invest in renewable generation, as their profit diminishes with increasing transmission fee. As p_T is set by the system regulator, this method determines a feasible range that allows both transmission and generation investments to be profitable (Fig. 5.19).

The model developed in this work can study grid reinforcement projects performed by private investors, who aim to maximise their profits instead of typical cost minimising techniques or maximising social welfare objectives, that exist when network upgrade is performed by the system operators. Typical settings, where this model can be applied in practice, include numerous locations where demand and generation are not co-located. Finally, the model developed offers good insights to the strategic game formed between the players, for varying cost parameters. Conclusions can be reached either directly on real data measurements or their distributions.

5.5 Concluding remarks

The work in Chapter 5 showed how private network upgrades developed for RES integration can lead to a leader-follower game between the line investor and local generators. Curtailment and line access rules play a key role in the strategic game, the equilibrium of which can be used to determine optimal generation capacities installed in such settings and their associated profits. The model developed can capture the stochastic nature of renewables and the variation in demand. A method for estimation of the game equilibrium was presented and also it was shown how optimal capacities installed at the equilibrium of the game depend on players' generation costs and the transmission fee. Most crucially, the latter can be used by regulators to assess a feasible range for the transmission fee, that allows both network upgrade and local renewable generation investments being realised. A methodology for the equilibrium of the game that utilises real data, both on the supply and demand side, was developed and applied to an example case in Western Scotland. The practical application used a big dataset analysis that spanned over the course of 17 years.

However, a challenge that needs to be addressed is that often data for a large time period, may not be available or may present significant gaps. In addition, the approach shown in Chapter 5 follows a single-shot analysis for equilibrium estimation and decision-making. To improve on these issues, in the following chapter, a method that generates useful data for simulation analysis was developed that draws samples from historic observations and is based on Gibbs sampling. This also allows for multiple iterations of the equilibrium estimation that reduces uncertainty on future decisions.

Chapter 6

Gibbs sampling for multiple simulation of possible future events

Work presented in Chapter 5 utilised real data over a 17-year time period to estimate the equilibrium of the Stackelberg game. However, in most occasions real data that span over such long periods might not be available. Even when data is available, such as for shorter time periods like one year, data may not be clean or may have significant gaps. A solution to such issues is to find a methodology that can generate multiple series of data from available historic observations. To do so, we follow a Markoc Chain Monte Carlo (MCMC) methodology that is based on a particular case of the Metropolis-Hasting algorithm, and more specifically, Gibbs sampling. This method allows for equilibrium estimation across several time series of synthetic wind speed and demand, and therefore can reduce the uncertainty in the decision-making process, as opposed to getting results only by following a single-shot approach. The methodology suggested is shown in the following sections. Work presented in Chapter 6 was published in a peer-reviewed study [11].

6.1 Research contributions

Work presented in Chapter 4 consisted one of the first research works to introduce Stackelberg game formulations in settings that combine decision-making about network reinforcements, renewable generation and line access rules. The model however did not take into account the stochastic nature of the primary renewable resources or variability in demand. The model presented in Chapter 5 improved on this work and utilised real data to evaluate and estimate the equilibrium results. This approach however consists of a single-shot approach, where the equilibrium is estimated once and is based on the historic observations available. Utilisation of MCMC methods or Gibbs sampling to generate data based on historic observations allows modelling multiple renewable investment scenarios that reduce the uncertainty of future generation and demand.

Models presented in previous Chapters are extended here by developing a principled framework, based on game-theoretic and state-of-the-art sampling techniques, i.e. Markov Chain Monte Carlo (MCMC). MCMC is a class of methods for simulation of stochastic

processes. More specifically, a MCMC is a class of methods in which one can simulate draws that are slightly dependent and approximately from the posterior distribution [94]. Gibbs sampling can be thought of as a particular case of the Metropolis-Hastings algorithm used for MCMC [82].

The Gibbs sampler uses the conditional distributions as proposal distributions with acceptance probability equal to 1 [87] and can be easily implemented in various applications when conditional distributions are available. In general, iterative samplers are an attractive option when drawing samples from high dimensional multivariate distributions due to their inexpensive cost per iteration and small computer memory requirements [82].

Using this technique we can generate, from historic data, observations that are dependent. Wind data samples from the project locations form a Markov chain (MC). Sampled data are then used for simulation analysis. Several authors used MCMC for modelling of wind speeds or wind power outputs [189, 265]. This creates a framework that allows modelling multiple renewable investment scenarios that reduce the uncertainty of future generation and demand. Multiple scenarios are required to model uncertainty regarding future events.

In more detail, the main contributions of the work are:

- A new methodology that generates observations from renewable resource data is developed. While historic data, such as wind speeds may be available, they might have considerable gaps and joint distributions cannot be expressed in simple, closed-form equations. For this reason we develop a MCMC methodology (Gibbs sampling) that can draw samples from available data and run multiple scenarios of potential futures.

- We establish a methodology that can determine optimal generation capacity investments through use of real demand and wind speed data. This work is one of the first to combine Stackelberg equilibria to a large-scale realistic game with MCMC techniques. Our model designates players' actions, depending on RES output correlation and expected curtailment, and studies the cost parameters effects on the equilibrium of the game.

- The model is applied and validated through a practical application based on realistic assumptions of a grid reinforcement project in Britain.

In the following sections, the Gibbs sampling methodology is presented.

6.2 Gibbs sampler

In practical settings the joint distribution of stochastic renewable resources is often unknown, but historic data may be available. In addition, due to the interdependency in resulting curtailment and multiple parameters a closed-form solution is difficult to find and cannot be expressed analytically. In Chapter 5, an empirical algorithm was presented utilising real data for the computation of the game equilibrium solution on a single-shot

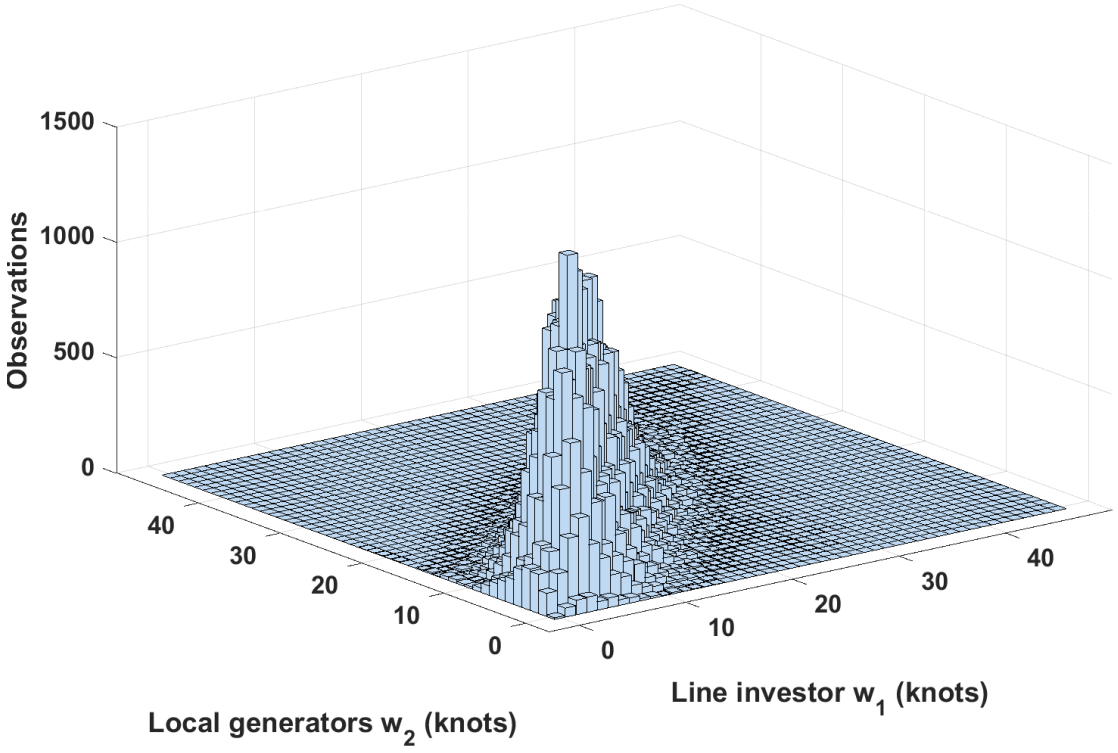

Fig. 6.1 Histogram of available wind speeds at project's location

basis. However, in real-world applications large-scale data may not be available or may experience important gaps. In this chapter, we show how we can utilise real data to simulate scenarios that approximate the real distribution with a state-of-the-art MCMC technique called the Gibbs sampler.

The Gibbs sampler uses the conditional distributions as proposal distributions with acceptance probability equal to 1 [87]. Using this technique one can generate, from historic data, observations that are dependent. Wind data samples from the project locations form a Markov Chain (MC). We can experiment with the length of the chain or *sampling size n* and we can repeat the process for multiple MCs or *number of realisations N*. In practice, n and N need to be determined in such a way that the resulting MC converges to the real distribution, is ergodic and computationally efficient. Ergodicity means that all possible states of the MC can be visited and are independent of the starting state [87]. In other words, the resulting MC after Gibbs sampling is applied, needs to converge to the real distribution. The satisfaction of these criteria depends on the sampling size n and the number of realisations of the experiments N. Longer and multiple runs are possible, but this is computationally expensive and therefore the right balance must be found.

In previous chapters, we showed that an empirical approach can be used to estimate the equilibrium of the Stackelberg game formed between the line investor and the local generators. A challenging issue that inhibits the analysis is the estimation of the joint probability distribution of wind speeds and subsequently the players' generation outputs. Fig. 6.1 presents the histogram of the wind speeds at each project's location for the practical example demonstration of the Kintyre-Hunterston project. Fig. 6.1 shows that

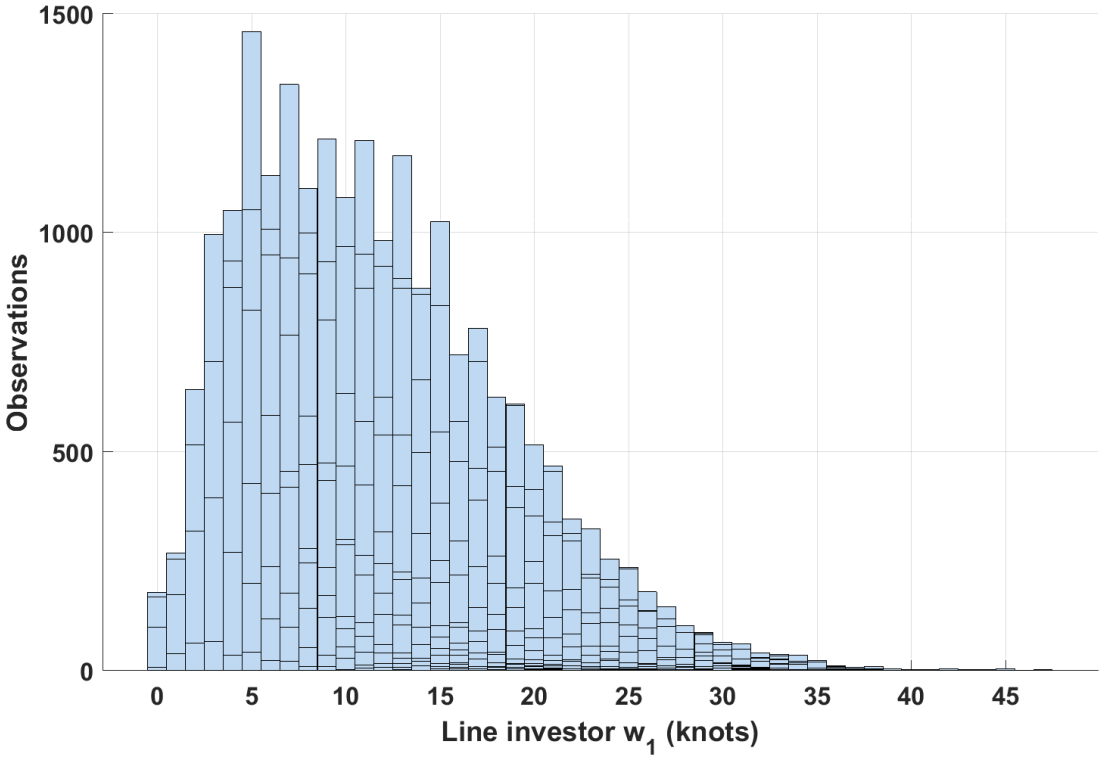

Fig. 6.2 Line investor view derived by joint wind speed histogram

a mathematical expression for the joint distribution of wind speeds is difficult to find. However, prior knowledge of the joint distribution is available. For example, the individual wind speed distributions can be approximated by a Weibull distribution, as shown in Fig. 6.2 and Fig. 6.3.

If wind speeds were independent, the joint distribution could be approximated by a bivariate Weibull distribution, however in our occasion the two distributions experience some level of correlation, shown by the fact that the majority of observations occur around the diagonal at Fig. 6.1, and therefore this assumption cannot hold. Crucially, the individual distributions for each player exhibit a degree of correlation due to similar weather patterns in neighbouring locations. In practice, this means that the joint distribution is not explicitly known, but we can generate data from the joint distribution if sufficient historic observations and wind speed measurements are available.

The technique of Gibbs sampling can be used to generate large datasets of wind speed at each project location, which next can be used to simulate multiple scenarios of different future events. The methodology applied in the practical example application is summarised in Algorithm 4. The ultimate goal is to generate synthetic data series (time series) of wind speeds at each RES project location and demand. These data form a Markov Chain (MC), where each sample represents a state and future states (samples) depend on the condition of the previous state.

The method starts with the wind speed observations for each player's project location denoted as w_i. Wind speed historic observations are shown in Fig. 6.4. From available historic data (Line 4 in Algorithm 4), a joint distribution table of wind speed observations

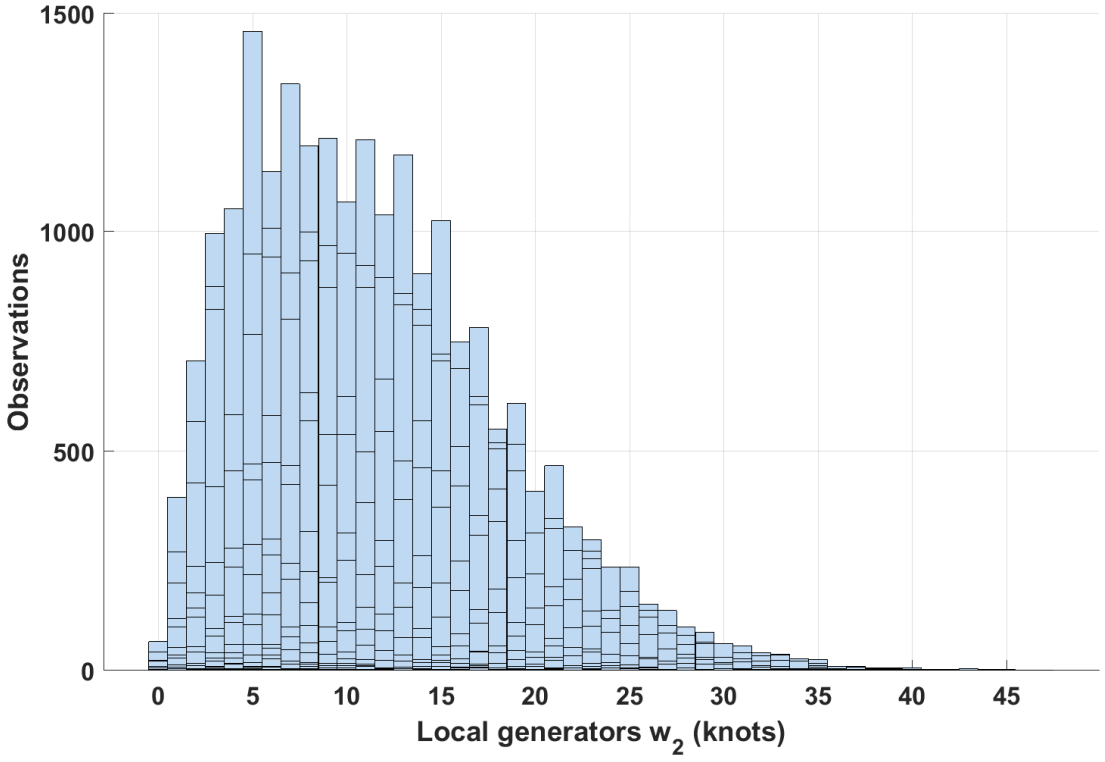

Fig. 6.3 Local generators view derived by joint wind speed histogram

Algorithm 4 GIBBS SAMPLING

w_1,w_2,D ▷ wind speed 1,2, power demand
n ▷ sampling size
t_{burn} ▷ burn-in period (samples ignored)
$\langle w_1^{(k)}, w_2^{(k)}, D^{(k)} \rangle$, $k \in \{1,2,...,k_{max}\}$ ▷ historic data
$F(w_1, w_2)$ ▷ wind distribution from data
$G\left(D, \frac{w_1 + w_2}{2}\right)$ ▷ demand cond. distrib. on mean wind
$t \leftarrow 1$[1]
$\langle w_1^{(t)}, w_2^{(t)}, D^{(t)} \rangle \leftarrow sample(w_1, w_2, D)$ ▷ initialise
repeat
    $w_2^{(t+1)} \leftarrow sample\ F(w_2 \mid_{w_1^{(t)}})$
    $w_1^{(t+1)} \leftarrow sample\ F(w_1 \mid_{w_2^{(t+1)}})$
    $D^{(t+1)} \leftarrow sample\ G\left(D \mid_{\frac{w_1^{(t+1)} + w_2^{(t+1)}}{2}}\right)$
    $t \leftarrow t + 1$
until $t > n$
return $\langle w_1^{(t)}, w_2^{(t)}, D^{(t)} \rangle$, $t \in \{t_{burn}, t_{burn} + 1, ..., n\}$

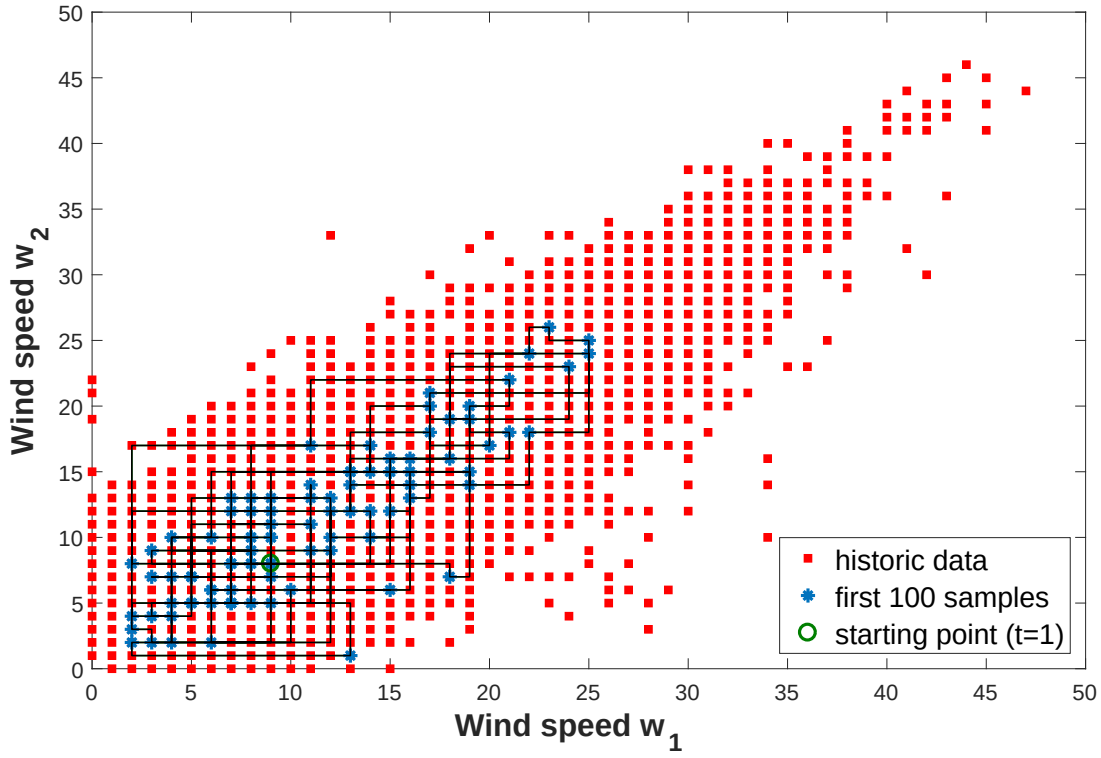

Fig. 6.4 An illustration of the Gibbs sampling technique

is created. More specifically, for every wind speed w_1, we record the subset of w_2 wind speeds, and vice versa (Line 5 in Algorithm 4). These subsets correspond to the distribution of w_2 conditional on w_1, and vice versa, and can be used to estimate future states of the MC. Different subsets are shown in Fig. 6.4.

Note here that in practice the probabilities for certain combinations of wind speeds can be low (e.g. it is unlikely to have extremely high wind at one location and low wind speed to a proximal location), therefore some subsets can be sparse. Sparsity of several subsets is caused by the joint effect that some observations represent rare events and correlation. We overcome this difficulty by merging sparse bins of rare events and outliers, and ensure ergodicity of the MC.

The MC is initialised by randomly selecting a sample from the joint distribution table (Line 8 in Algorithm 4). An example with a starting point of $\langle w_1^{(1)}, w_2^{(1)} \rangle = \langle 9, 8 \rangle$ is shown in green color in Fig. 6.4. The Gibbs sampler can be used to generate n samples via an iterative procedure. Each iteration step involves replacing the value of one variable by a value selected randomly by the conditional $F(w_i \mid_{w\_i^{(t)}})$. In the example shown in Fig. 6.4, since $w_1^{(1)} = 9$, a random sample is drawn from $F(w_2 \mid_{w_1^{(1)}=9})$, equal to $w_2^{(2)} = 6$. In Fig.6.4 this corresponds to moving vertically from the starting point. Next, we randomly draw a sample from $F(w_1 \mid_{w_2^{(2)}}) = 6$, equal to $w_1^{(2)} = 7$. This corresponds to moving horizontally in Fig. 6.4. The new state is $\langle w_1^{(2)}, w_2^{(2)} \rangle = \langle 7, 6 \rangle$, shown in Fig. 6.4 in blue color. The process is repeated for n samples. The procedure for $n = 100$ samples is shown in Fig. 6.4 to facilitate understanding.

Table 6.1 Sampling results for $N = 100$ realisations and an increasing number of sampling size n

Sample size	$\bar{w}_1$	$\sigma_{\bar{w}_1}$	WCI $\bar{w}_1$	ME $\bar{w}_1$	$\bar{w}_2$	$\sigma_{\bar{w}_2}$	WCI $\bar{w}_2$	ME $\bar{w}_2$	$\bar{D}$	$\sigma_{\bar{D}}$	WCI $\bar{D}$	ME $\bar{D}$
$n = 1,000$	12.1321	0.6569	0.2607	18.91%	12.2297	0.6226	0.2470	17.61%	108.5722	0.7859	0.3119	2.63%
$n = 5,000$	12.0853	0.2903	0.1152	6.65%	12.1762	0.2797	0.1110	6.47%	108.6271	0.3395	0.1348	1.49%
$n = 10,000$	12.0929	0.2262	0.0897	4.63%	12.1842	0.2187	0.0869	4.36%	108.6000	0.2403	0.0953	1.03%
$n = 50,000$	12.1125	0.0874	0.0347	2.02%	12.2028	0.0857	0.0340	1.97%	108.5979	0.1033	0.0410	0.73%
$n = 100,000$	12.1155	0.0631	0.0251	1.28%	12.2075	0.0602	0.0239	1.16%	108.5954	0.0663	0.0263	0.70%
$n = 200,000$	12.1065	0.0441	0.0175	0.80%	12.1986	0.0427	0.0169	0.76%	108.5915	0.0453	0.0180	0.62%
$n = 500,000$	12.1049	0.0272	0.0108	0.68%	12.1968	0.0262	0.0103	0.62%	108.5930	0.0288	0.0114	0.57%

Table 6.2 Sampling results for $n = 5,000$ sampling size and an increasing number of realisations N

Realisations	$\bar{w}_1$	$\sigma_{\bar{w}_1}$	WCI $\bar{w}_1$	ME $\bar{w}_1$	$\bar{w}_2$	$\sigma_{\bar{w}_2}$	WCI $\bar{w}_2$	ME $\bar{w}_2$	$\bar{D}$	$\sigma_{\bar{D}}$	WCI $\bar{D}$	ME $\bar{D}$
$N = 100$	12.0850	0.2774	0.0840	6.64%	12.2017	0.2671	0.0809	6.01%	108.5703	0.3037	0.0919	1.34%
$N = 170$	12.1120	0.2217	0.0879	5.35%	12.1812	0.2145	0.0851	5.15%	108.6275	0.3279	0.1301	1.26%
$N = 500$	12.0867	0.2709	0.0476	7.22%	12.1764	0.2618	0.0460	7.16%	108.5932	0.3052	0.0536	1.47%
$N = 1,000$	12.1097	0.2764	0.0343	8.20%	12.2025	0.2666	0.0331	7.57%	108.5949	0.3198	0.0397	1.47%
$N = 5,000$	12.1044	0.2793	0.0155	9.06%	12.1966	0.2717	0.0151	8.81%	108.5951	0.3244	0.0180	1.58%
$N = 10,000$	12.1032	0.2754	0.0108	9.41%	12.1956	0.2672	0.0105	8.60%	108.5917	0.3268	0.0128	1.70%
$N = 50,000$	12.1022	0.2787	0.0049	9.87%	12.1943	0.2707	0.0048	9.26%	108.5901	0.3241	0.0057	1.70%

Hourly demand data D were also used to generate the synthetic data series. Demand is randomly selected by the conditional distribution of demand over the average wind speed (Line 12 in Algorithm 4). When demand D is included, a single sample refers to time interval t and can be displayed as the tuple $\langle w_1^{(t)}, w_2^{(t)}, D^{(t)} \rangle$. The procedure is cycled through the variables forming n samples of $\langle w_1^{(t)}, w_2^{(t)}, D^{(t)} \rangle$, $t \in \{1, 2, ..., n\}$. Each sample represents a state of the MC, where future states depend on the previous state. Note here that the resulting MC forms a data series of samples that depend on values at the previous state, but samples are not time-dependent. This is sufficient to accurately estimate energy generated and curtailed as the summation of power generated and curtailed over a longer time horizon. However, if other energy system assets such as energy storage devices are introduced, their operation depends on the time variable. Hence, the method would not produce suitable results for such an analysis. This issue is addressed by modifying the Gibbs sampling technique in Chapter 7, where energy storage is introduced.

To ensure that the MC converges, we run Algorithm 4 for several sampling sizes n (small, moderate, large) and repeat the procedure for N realisations. Results are shown in Tables 6.1 and 6.2. Table 6.1 shows results for $N = 100$ realisations and different sample sizes $n = 1,000 - 500,000$. Table 6.2 on the other hand repeats the Gibbs sampling procedure for a varying number of realisations $N = 100 - 50,000$ and a fixed sampling size of $n = 5,000$.

If χ is the variable under consideration, then the table columns represent the mean of the sampling distribution of the sample mean $\bar{\chi}$, the standard deviation of the sampling distribution of the sample mean $\sigma_{\bar{\chi}}$, most commonly known as standard error of mean, the width of the 95% confidence interval (WCI) and the maximum error (ME) of the sample mean, when compared to the mean of the original distribution derived from historic data. The mean values of the original distribution derived from the historic data are $\mu_{w_1} = 12.1029$, $\mu_{w_2} = 12.1950$ and $\mu_D = 108.1830$.

As shown in Algorithm 4, n samples are drawn by the original distribution. Note here that the expressions of n samples or n sampling size are equivalent. For example, for w_1, the Gibbs sampler is used and n samples are derived. Every time the sampling procedure is performed, the sample mean is estimated as the mean value across n samples $\overline{w_{1_{(N)}}} = \frac{\sum_{i=1}^{n} w_{1,i_{(N)}}}{n}$. The process is repeated N times. From the frequency distribution of the sample means after N realisations, also known as the sampling distribution of the sample mean, the mean of sample means can be estimated as the average of all sample mean values across N realisations, i.e. $\bar{w}_1 = \frac{\sum_{i=1}^{N} \overline{w_{1_{(N)}}}}{N}$. In addition, from the sampling distribution, the standard deviation of the sampling distribution of the sample mean can be estimated $\sigma_{\bar{w}_1} = \frac{\sum_{i=1}^{N} \left(\overline{w_{1_{(i)}}} - \bar{w}_1\right)^2}{\sqrt{N}}$. This is alternatively known as the standard error of the mean. The table columns also show the width of the 95% confidence interval (WCI) of the sampling distribution and the maximum error (ME) of the sample means, when compared to the mean of the original distribution. The latter is an indication of the largest deviation of the sample means derived for N realisation from the real mean of the original distribution.

According to the central limit theorem, the mean of sample means follows a normal distribution $(\bar{w}_i, \sigma_{\bar{w}_1})$. As the sampling size n increases, the mean of the sample means converges to the mean of the original distribution and the standard error decreases (Table 6.1). Therefore, a large sample size is a key factor that allows accurate representation of the original distribution. The other aspect to investigate is the effect of the number of realisations or repetitions of the sampling procedure. Crucially, each realisation uses a different starting point. Table 6.2 shows that a relative small number of realisations is sufficient for the sampling procedure. More realisations (large N) means smaller width of the confidence interval. However, in all occasions the maximum error increases as N increases, due to a potential effect from the different and random starting point. The MC formed need to be independent of the starting state, therefore a common approach is not to include the initial samples of the sampling algorithm. To deal with such issues, a burn-in or warm-up period of 20% of samples is adopted, to make sure that our results are independent off the starting state [87]. This is shown in Line 15 in Algorithm 4 with the adoption of t_{burn}.

Appropriate selection of suitable n and N is crucial when considering practical applications of Gibbs sampling. Computational limitations dictate that a balance needs to be found between multiple shorter runs (large N and small n) and one-shot longer runs (small N large n) [87]. The results from Table 6.1 and 6.2 show that for the MC to converge to the original distribution, a large n is required, but N can be chosen to be relatively small. For this reason and driven by computational limitations, for the Stackelberg equilibrium estimation and further analysis a sampling size of $n = 50,000$ with a burn-in period of $10,000$

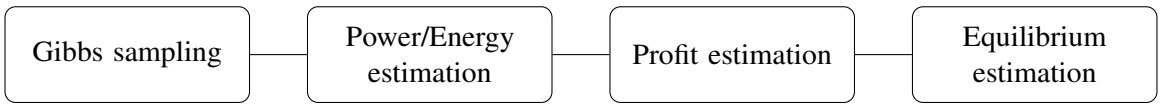

Fig. 6.5 Summarised methodology steps

samples (i.e. 40,000 data points were used for the analysis) and $N = 170$ realisations were selected.

6.3 Stackelberg equilibrium estimation

The estimation of the Stackelberg equilibrium is similar to the procedure presented in Chapter 5. The Gibbs sampler is used to generate data series of wind speeds and demand. Next, data is used to estimate the power generated at each t and the energy values for a larger time horizon (see Algorithm 1). The maximum feasible strategy action for a single player was set equal to $P_{N_{max}} = 500.5$ MW and the incremental capacity to $\delta P_{N_i} = 0.5$ MW. For every possible combination of the rated capacities installed (P_{N_1}, P_{N_2}), the power generated and curtailed for each player on an hourly basis was estimated. Next, the aggregate energy generated and curtailed by each player was estimated as the summation of 40,000 data points. After energies were estimated, profit equations were computed for each possible P_{N_1}, P_{N_2} and varying cost parameters (c_{G_1}, c_{G_2}, p_T), as in Algorithm 2. Finally, the last step is to estimate the generation capacities built $(P^*_{N_1}, P^*_{N_2})$ and profits (Π^*_1, Π^*_2) at the equilibrium of the game, as in Algorithm 3. The steps are summarised in Fig. 6.5.

The process in Fig. 6.5 can be repeated several times (here for $N = 170$ realisations). Recall here, that every realisation corresponds to a completely different MC, which allows for multiple runs of the Stackelberg game equilibrium estimation. Simulation results are shown in the following section.

6.3.1 Results for varying realisations N

The methodology described in the previous section is executed for several runs or realisations. Every realisation represents a completely different MC generated. For a given set of cost parameters $c_{G_1} = 0.30 p_G$, $c_{G_2} = 0.28 p_G$, $p_T = 0.26 p_G$ and $p_G = £74.3/\text{MWh}$ and several realisation runs $N = 170$, the equilibrium of the Stackelberg game is estimated. Rated capacities built at the equilibrium of the game by the players are shown in Fig. 6.6. The results are satisfactory and show a 10 MW range in the estimated solutions for optimal rated capacities. Fig. 6.7 shows the players' profits at the equilibrium of the Stackelberg game. Similarly to the generation capacities solutions, profit results are satisfactory and do not present a wide range.

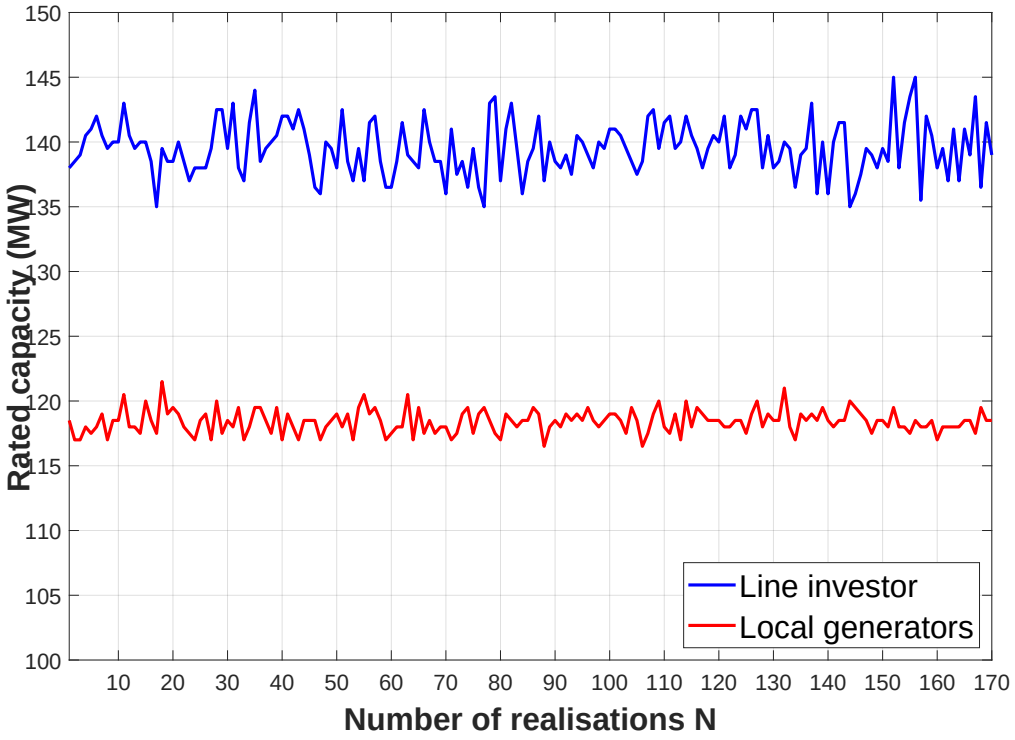

Fig. 6.6 Optimal generation capacities of each player for several realisations ($c_{G_1} = 0.30p_G$, $c_{G_2} = 0.28p_G$, $p_T = 0.26p_G$ and $p_G = £74.3/\text{MWh}$)

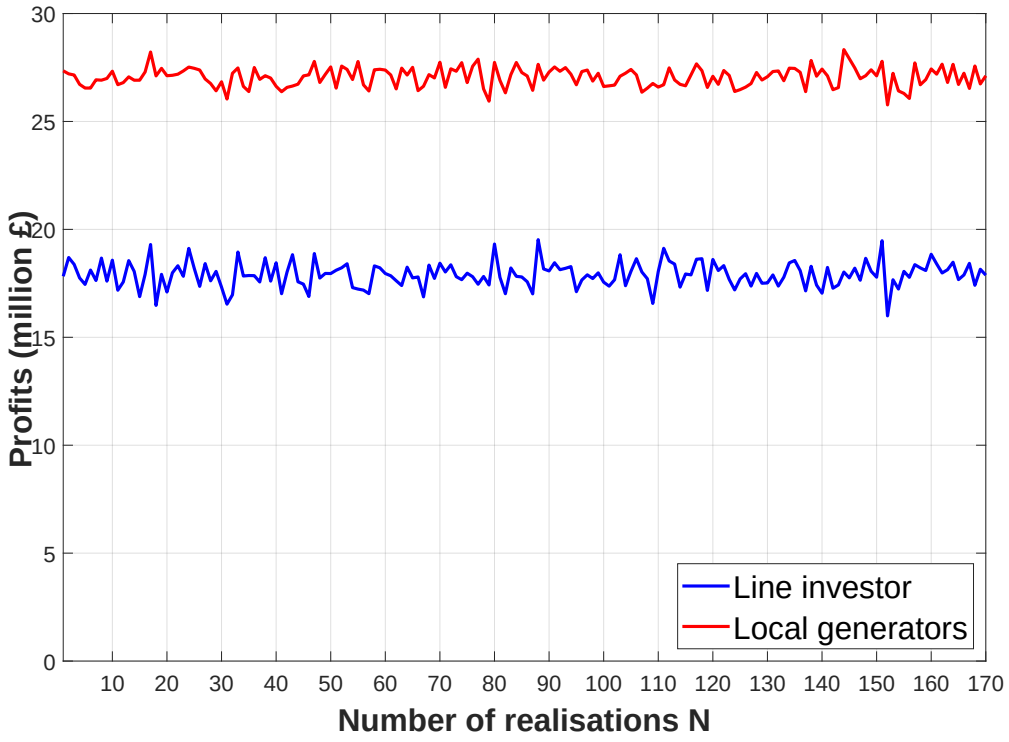

Fig. 6.7 Optimal profits of each player for several realisations ($c_{G_1} = 0.30p_G$, $c_{G_2} = 0.28p_G$, $p_T = 0.26p_G$ and $p_G = £74.3/\text{MWh}$)

	Scenario 1	**Scenario 2**	**Scenario 3-a**
c_{G_1}	$0.16p_G : 0.02p_G : 0.68p_G$	$0.30p_G$	$0.26p_G$
c_{G_2}	$0.30p_G$	$0.08p_G : 0.02p_G : 0.54p_G$	$0.20p_G$
p_T	$0.26p_G$	$0.26p_G$	$0 : 0.02p_G : 0.80p_G$

Table 6.3 Summary of cost parameters considered in scenarios for the analysis of the transmission capacity game with Gibbs sampling (in all scenarios the generation price remained fixed at $p_G = £74.3/\text{MWh}$)

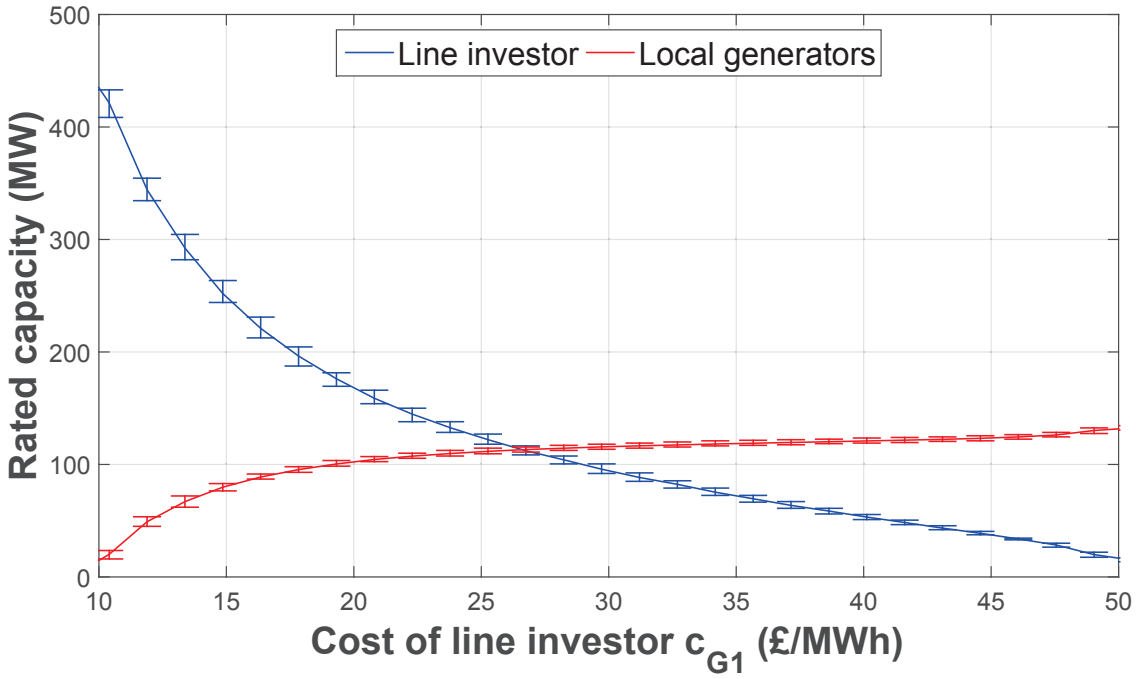

Fig. 6.8 Scenario 1: Generation capacity installed at equilibrium and dependence on the line investor's generation cost

6.3.2 Cost parameter scenario results

Similarly to previous analyses in Chapter 4 and Chapter 5, we study how the equilibrium results depend on varying cost parameters. Simulations were executed in a state-of-the-art and high-performance computing facility, funded by EPSRC (Cirrus UK National Tier-2 HPC Service at EPCC (http://www.cirrus.ac.uk) and the University of Edinburgh (EP/P020267/1)) with MATLAB software environment and 36 parallel workers. The exact cost parameter assumptions are shown at Table 6.3.

Scenario 1: Varying c_{G_1}

The first scenario shows how the equilibrium results depend on the line investor's generation cost c_{G_1}. The line investor's generation cost varies from $c_{G_1} = 0.16 \ldots 0.68p_G$, while other cost parameters remain constant and equal to $c_{G_2} = 0.30p_G$ and $p_T = 0.26p_G$.

Fig. 6.8 shows the generation capacity installed by the players for varying generation costs of the line investor. Fig. 6.9 shows the profits at equilibrium. The results show the

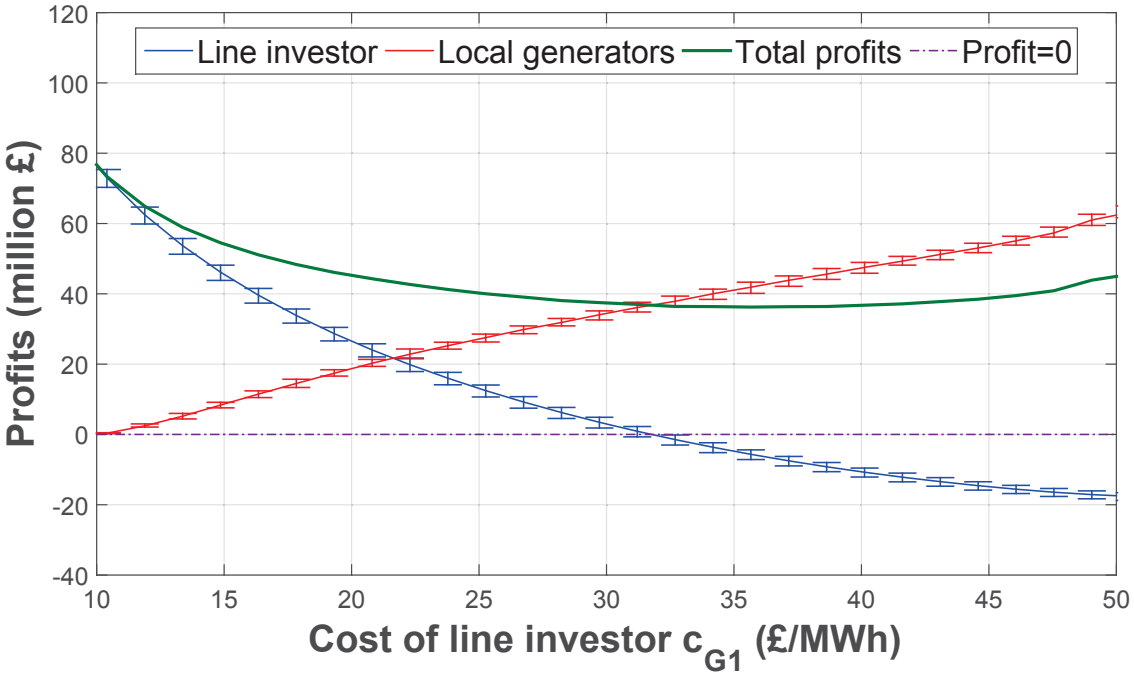

Fig. 6.9 Scenario 1: Profits at equilibrium and dependence on the line investor's generation cost

average equilibrium solution and min-max solutions found for $N = 170$ realisations of the simulation procedure.

Scenario 2: Varying c_{G_2}

The second scenario shows how the equilibrium results depend on the local generators' generation cost c_{G_2}. Other cost parameters remain fixed $c_{G_1} = 0.30 p_G$ and the transmission fee is $p_T = 0.26 p_G$, while the local generators' cost varies from $c_{G_2} = 0.08 \ldots 0.54 p_G$.

Fig. 6.10 shows the generation capacity installed by the players for varying generation costs of the local generators. Fig. 6.11 shows the profits at equilibrium.

Scenario 3: Varying p_T

The third and last scenario shows how the equilibrium results depend on the transmission charges imposed p_T. Other cost parameters remain fixed with $c_{G_1} = 0.26 p_G$ and $c_{G_2} = 0.20 p_G$, while the transmission fee varies from $p_T = 0$ to $0.80 p_G$.

Fig. 6.12 shows the generation capacity installed by the players for varying generation costs of the local generators. Fig. 6.13 shows the profits at equilibrium.

6.3.3 Discussion of results

In all sets of scenarios, the total capacity installed by all players decreases as the tested parameter value increases. Each player installs less capacity as their generation cost increases, while the other player benefits by increasing their capacity. The cost of local generators has a larger impact on the capacities installed for both players. Profits have

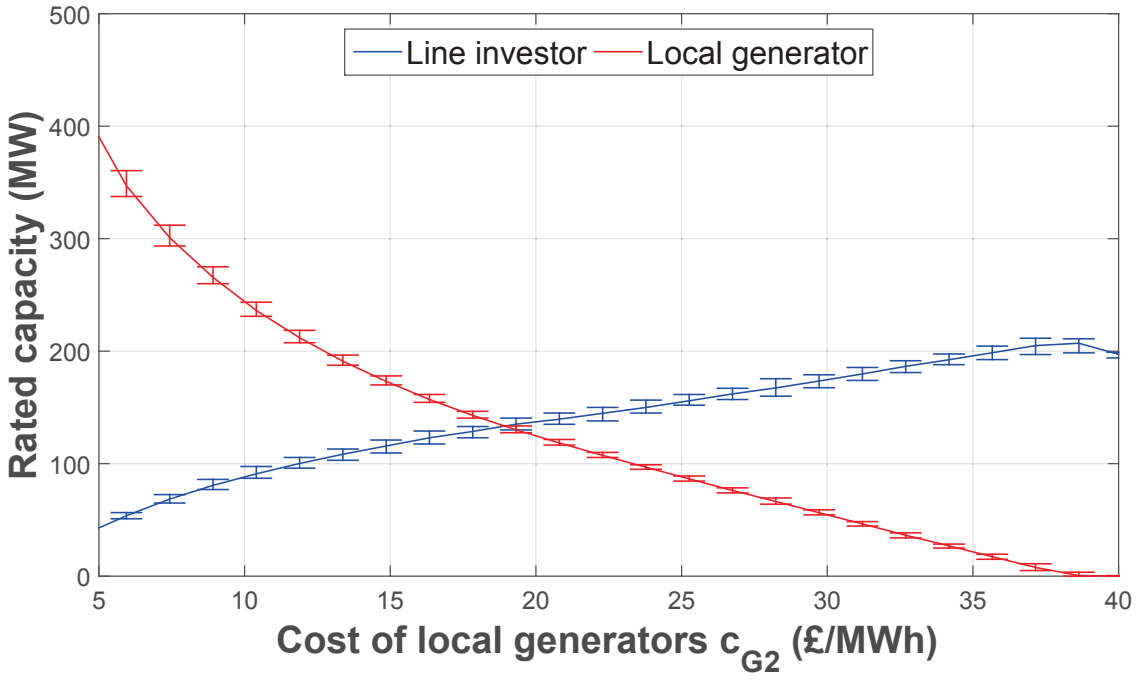

Fig. 6.10 Scenario 2: Generation capacity installed at equilibrium and dependence on the local generators generation cost

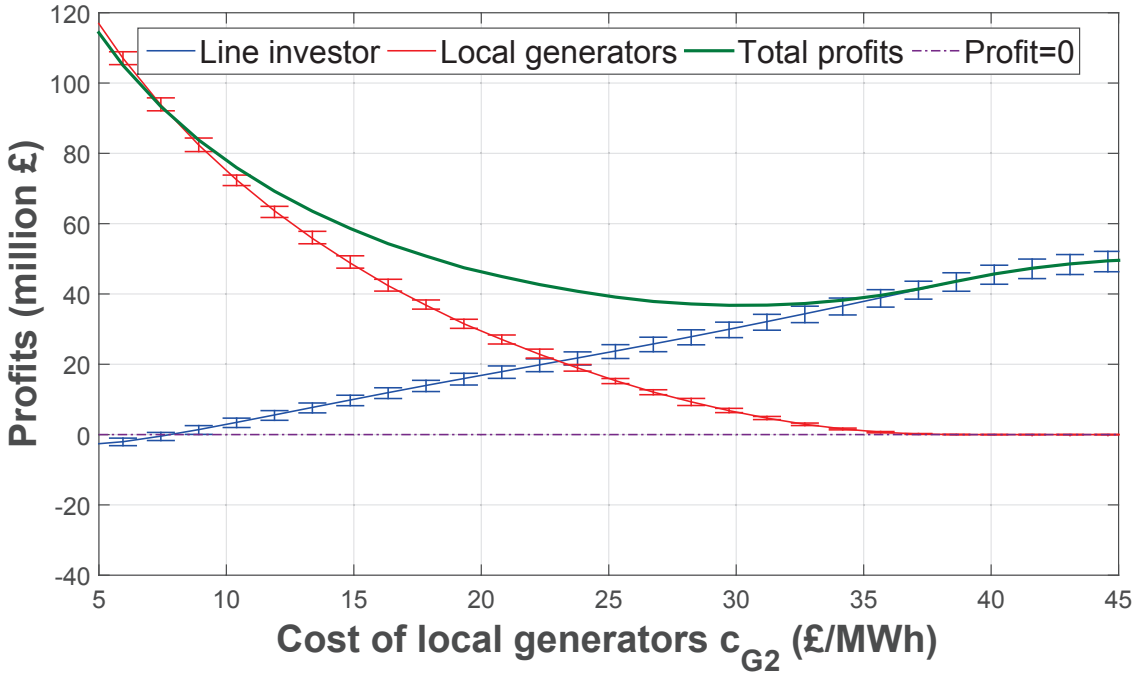

Fig. 6.11 Scenario 2: Profits at equilibrium and dependence on the local generators generation cost

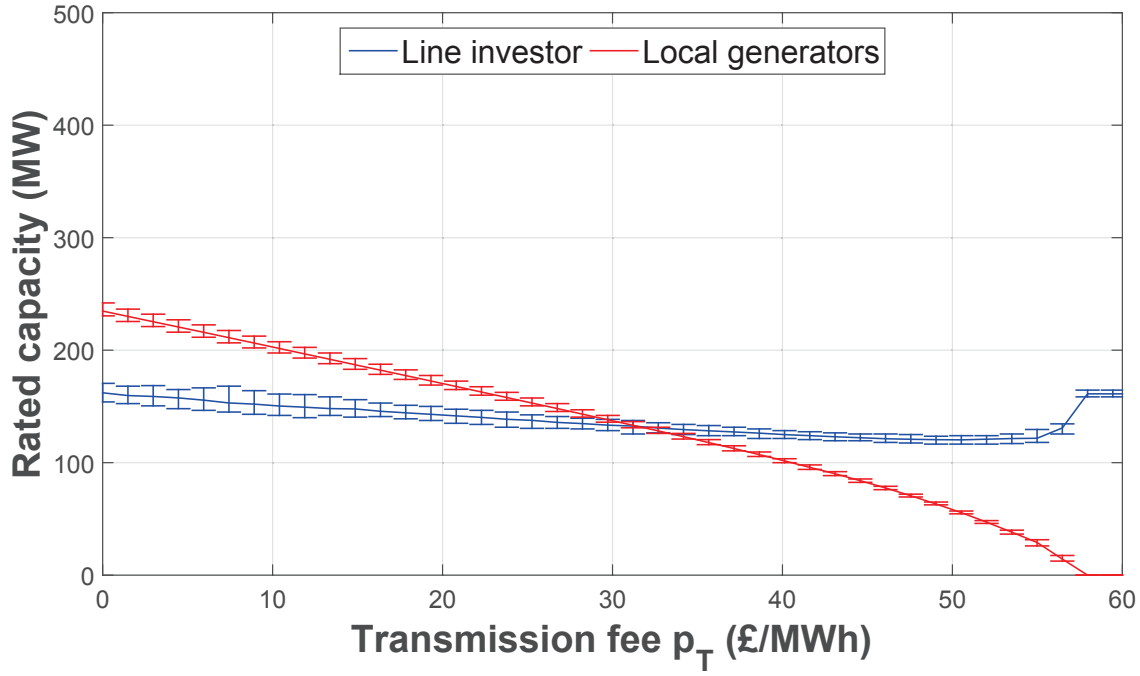

Fig. 6.12 Scenario 3: Generation capacity installed at equilibrium and dependence on the transmission fee

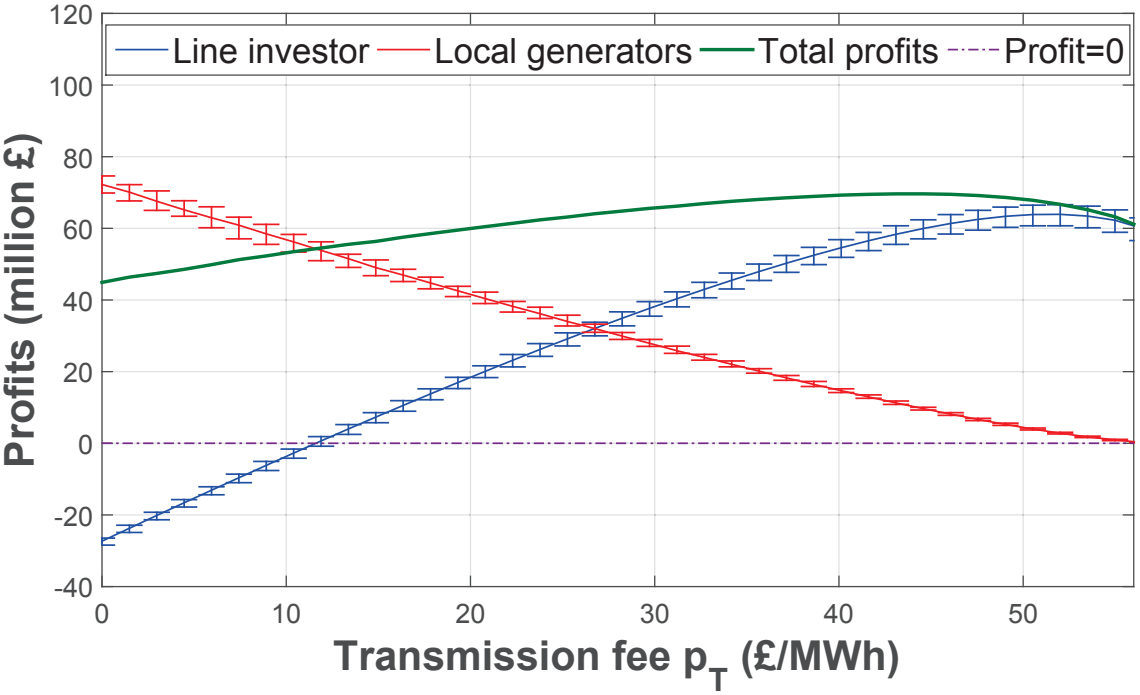

Fig. 6.13 Scenario 3: Profits at equilibrium and dependence on the transmission fee

similar behaviour to the optimal rated capacities, but local generators face the additional cost of transmission charges. If the followers' generation cost is much lower than the line investor's (assuming for example that local generators might have access to cheaper land), the line investor needs to charge a high transmission fee to have positive earnings. On the contrary, if the leader's cost is much lower, the generation capacity will mostly be installed by the line investor, as there is no room for profitable investment from local renewable producers. As shown in Scenario 3, $p_T \simeq 0.16 p_G$ or $\simeq$ £12MWh is the minimum value of transmission charges that allows profit for the line investor. Similarly, if the transmission fee is set too high, then it is not profitable for local investors to invest in renewable generation. As p_T is set by the system regulator, the methodology can be useful to determine a feasible range of charges that allows both transmission and generation investments to be profitable.

6.4 Concluding remarks

Chapter 6 extended the analysis of the Stackelberg game for multiple runs. It was shown how when real historic data is available, MCMC and Gibbs sampling can be used to simulate multiple future scenarios and reduce the uncertainty of the investment decisions. Equilibria solutions from multiple iterations, do not show great variance from the average solution. Moreover, optimal generation capacities and profits at equilibrium displayed similar behaviour to results shown in Chapter 5.

Energy storage can represent a promising solution to reduce curtailment. In Chapter 7, we extend the analysis of the game and show that if an independent storage player is introduced, the model evolves into a Stackelberg game between the line investor (leader), and local low-carbon technology investors, i.e. local generators and energy storage player (followers). Local generators and storage share the available capacity by playing a Cournot game. The Gibbs sampling procedure developed for Chapter 6 creates samples that are independent of the time component. This technique is adequate for analysing the game with generation, transmission and demand, however when energy storage is added to the game, a modified Gibbs sampling procedure is required and this is presented in Chapter 7.

Chapter 7

Transmission capacity game with energy storage

In Chapter 6, Gibbs sampling and MCMC techniques were used to simulate multiple future scenarios for estimation of the Stackelberg game equilibrium. The methodology developed achieved a reduction in uncertainty with regards to generation and transmission capacity investments in locations with network constraints and high generation curtailment. In this chapter, we turn our attention to developing a new model that incorporates energy storage, as a way to partially avoid and reduce curtailment. In this context, the model presented in Chapter 7 consists of three different player types: a line investor, local generators and an independent energy storage player, who is willing to install energy storage capacity that reduces curtailment. The model aims to determine optimal capacities installed by players at the equilibrium of the game. In this setting, the line investor has a first mover advantage over all other players. Local generators and the energy storage provider are players, who compete for the available capacity in the network. It is shown here that a Cournot game can describe competition and strategic behaviour of local investors. This leads to a bilevel game-theoretic model that can be described as a Stackelberg-Cournot game between the leader (line investor) and all other local investors (local generators and storage player). In addition, results from work in Chapter 7 aim to evaluate the contribution of energy storage in improving the energy system's operation and aim to study the evolution of the game-theoretic model. This is achieved by comparing the operation of the energy system before and after the introduction of the storage player.

7.1 Research contributions

The models presented in previous chapters considered only generation and transmission capacity investment decisions and did not include energy storage. However, energy storage can reduce curtailment and can play a significant role in the dynamics of the resulting game. Energy storage can store excess energy from renewable generators that can be used for later use. Moreover, energy storage can defer expensive network reinforcement and

help with the integration of large volumes of renewable generation at a particular location, as shown by the literature review conducted in this work (Section 2.8 in Chapter 2).

In more detail, the research contributions of this work to the state of the art are:

- Previous work is extended by developing a model that consists of three player types: the line investor, local generators and an independent storage player. A game-theoretic model (Stackelberg-Cournot game) is applied to study this formulation. It is shown that optimal transmission, generation and storage capacities installed by players can be determined at the equilibrium of the Stackelberg-Cournot game. At a first level, the line investor, who has the first mover advantage, decides the transfer capability of the transmission line and the RES capacity to be installed. At a second level, local generators and the energy storage player decide on generation and storage capacities, respectively, by playing a Cournot game.

- An algorithmic approach is introduced to determine the capacities built by each player (transmission capacity built by the line investor, generation capacity built by the line investor and local generators, and storage capacity built by the storage player) and corresponding profits at the equilibrium of the game. The approach shown here is an example of empirical game-theoretic modelling applied in energy systems with distributed generation and energy storage.

- A practical application of the models is shown by use of realistic figures based on the Kintyre-Hunterston network upgrade project. Previous modelling approaches are extended also by considering local demand at the location of high renewable generation B (previously considered negligible).

In the following section, the general framework of the Stackelberg-Cournot game is analytically discussed along with the model assumptions.

7.2 Game-theoretic model with energy storage

The objective of the extended model presented in Section 7.2 is to assess the value of energy storage investments, which can be used to minimise renewable curtailment. In models presented in previous chapters, despite the installation of transmission capacity, a percentage of available RES generation is still curtailed at times, due to renewable oversupply or the inability of the power system to absorb the excess energy produced. In fact, it is shown in previous chapters that RES investors may tolerate some curtailment, as long as their investments are still profitable. However, the energy curtailed is essentially wasted. If energy storage is introduced to the system, part of the otherwise curtailed energy can generate revenue and value for investors and the energy system overall. More specifically, a three-player game-theoretic model is assumed that consists of a line investor, local generators and a third independent storage player, who can purchase from RES investors excess energy that would otherwise have been curtailed. As a result, RES generators could potentially install more generation capacity than previously, because

they can now earn some additional revenue from selling their excess energy to storage. Moreover, curtailment may be reduced. In Chapter 7, we investigate these issues and the dynamics of the game when energy storage is added to the system and study how profit equations are affected after storage comes into play. Model assumptions with regards to energy storage are presented in the following section.

7.2.1 Energy storage model

The behaviour and operation of energy storage is described by a generic model suitable for a wide range of energy storage devices and technology types.

An energy storage investor installs a system of S storage energy capacity at a favourable location for renewable generation or location B. The storage investor aims to purchase energy from renewable generators at B, at times when there is an oversupply of RES production and when renewable energy cannot be used to satisfy the energy demand.

During its operation, the storage device needs to follow several operational constraints. The energy stored in the storage device at time t depends on the previous state and is given by the following equation:

$$E_{S,t} = E_{S,t-\delta t}(1 - s_{dch}) + \left(P_{ch,t}\eta_{ch} - \frac{P_{dch,t}}{\eta_{dch}} \right) \delta t \tag{7.1}$$

where:

$E_{S,t}$ is the energy stored in the storage device at time t

δt is the duration of time between two consecutive time intervals used in the analysis

$E_{S_{t-\delta t}}$ is the energy stored in storage device at time $t - \delta t$ i.e. in the previous state or simulation step

s_{dch} is the storage system's self-discharge rate, i.e. the energy lost when the storage system is at idle state (this quantity varies significantly for different technology types and is usually given in a percentile form per month of stored energy lost, which can easily be transformed into energy lost per time interval t of analysis)

$P_{ch,t}$ is the charging power at t

$P_{dch,t}$ is the discharging power at t

η_{ch} is the charging efficiency, which accounts for the energy losses during the charging process, and

η_{dch} is the discharging efficiency, which accounts for the energy losses during the discharging process of the storage system.

The energy stored at time t in the storage device is often represented by the State of Charge (SOC) and is calculated as a percentile of the storage capacity:

$$SOC_t = \frac{E_{S,t}}{S} 100\% \tag{7.2}$$

The minimum SOC allowed is a limitation to the storage device operation that needs to be accounted for. For example, useful lifetime and capacity of battery energy storage systems

is significantly reduced, when the battery is operated at small SOC or equivalently when the battery is frequently discharged beyond a certain Depth of Discharge DOD. The depth of discharge DOD_t at time t is directly linked to SOC_t and is equal to:

$$DOD_t = 1 - SOC_t \tag{7.3}$$

As a result, energy storage system's operation is usually bounded between a safe minimum state of charge and a maximum that is equal to the storage capacity:

$$SOC_{min} \leq SOC_t \leq SOC_{max} \tag{7.4}$$

where $SOC_{max} = 100\%$. The equation above can also be expressed in DOD terms:

$$DOD_{min} \leq DOD_t \leq DOD_{max} \tag{7.5}$$

where $DOD_{min} = 0$ (equivalent to SOC_{max}) and $DOD_{max} = 1 - SOC_{min}$.

Moreover, there are power constraints on the energy storage operation that restrict the maximum power that can be charged to or discharged from the energy storage device:

$$0 \leq P_{ch,t} \leq P_{ch_{max}} \tag{7.6}$$

$$0 \leq P_{dch,t} \leq P_{dch_{max}} \tag{7.7}$$

The analysis in this work focused on battery energy storage systems (BESS), such as Lithium-ion batteries, increasingly being reported as one of the most promising technologies for integration of RES technologies in electricity grids. For battery storage systems, the following simplifying assumptions hold:

- Energy losses due to self-discharge can safely be ignored, hence $s_{dch} = 0$. Self-discharge losses represent a very small percentage of the energy lost over a month and can be ignored for battery systems. On the other hand, if other technology types were to be considered such as flywheels that store energy in the form of kinetic energy, self-discharge losses can be significant and should not be ignored.

- The round-trip efficiency η_{rt} can be defined, which represents the energy losses in a full cycle, i.e. it includes losses during both charging and discharging. This parameter is usually known from technical specification sheets given by battery manufacturers. Without loss of generality, it can be assumed that charging and discharging efficiencies are equal and therefore $\eta_{ch} = \eta_{dch} = \sqrt{\eta_{rt}}$.

By adopting these simplifying assumptions Eq. (7.1) can be rewritten as:

$$E_{S,t} = E_{S,t-\delta t} + r_t \eta \delta t \tag{7.8}$$

where:

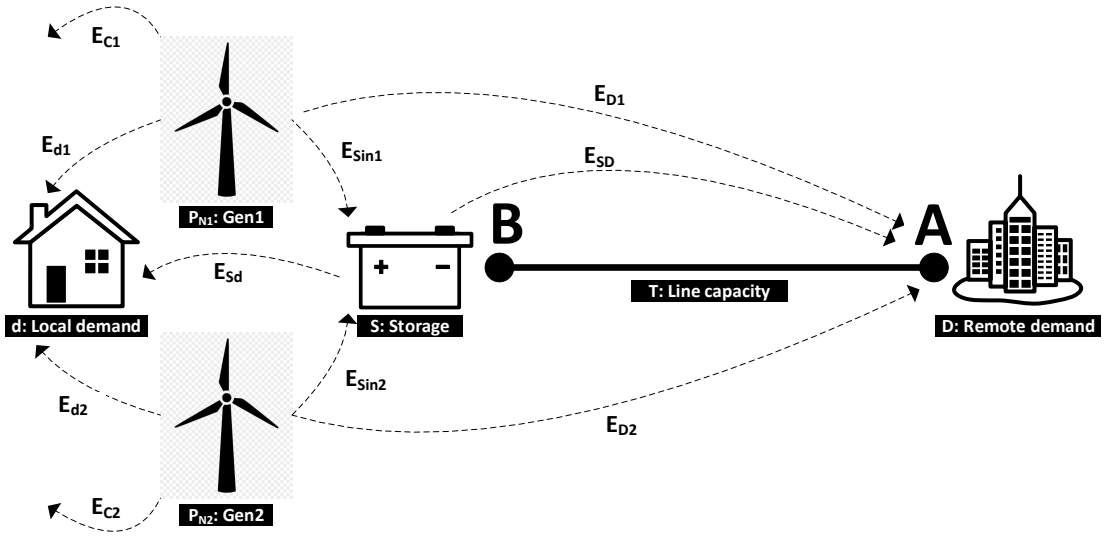

Fig. 7.1 Model schematic of the game with three players: a line investor, local generators and a storage investor: RES generation capacity built by the line investor P_{N_1}, RES generation capacity built by local generators P_{N_2}, storage capacity S and local demand d are connected at location B, while demand D is located at A

r_t is the power charged or discharged from the storage device, i.e. when $r_t > 0$ then $r_t = P_{ch,t} > 0$, else when $r_t < 0$ then $r_t = -P_{dch,t} < 0$ and

η represents the efficiency and is given by:

$$\eta = \begin{cases} \dfrac{1}{\eta_{dch}} = \dfrac{1}{\sqrt{\eta_{rt}}}, & \text{if } r_t < 0 \\ \eta_{ch} = \sqrt{\eta_{rt}}, & \text{if } r_t > 0 \end{cases} \tag{7.9}$$

In the following section, the three-player game-theoretic model is introduced and model assumptions are discussed.

7.2.2 Three-player Stackelberg-Cournot game

Similar to previous work presented in chapters 4-6, we consider two locations, location A representing a location with high energy demand requirements, and location B representing a location with high renewable potential. The demand at location A is denoted as D. In this model, we also consider some local demand at B, denoted as d. Three type of investors are involved in the game:

- Player 1 or the **'line investor'**, who is interested in building P_{N_1} *renewable generation capacity* at location B and a *transmission line* of capacity T that links A to B[1].
- Player 2, also called **'local generators'**, represents all small-scale generators at location B, who install *renewable generation capacity* of P_{N_2}.

[1]Note here that players or agents are considered gender-neutral, however by convention male forms such as *'he'* and *'his'* are used in this thesis when referring to a single player.

- Player 3, also called the **'storage investor'** is a third, independent storage player, who builds *storage capacity S* at location B.

The model schematic of the game is shown in Fig. 7.1, along with the energy flows between energy system components installed by the players.

Following a similar notation to previous work, first the potential energy production E_{G_i} is defined, which depends on the RES resource at each project's location and the installed generation capacity P_{N_i}. Renewable generators can serve either local demand d at B or remote demand D at A via the transmission line. Part of E_{G_i} is used to serve the local demand at B and is equal to E_{d_i}. Another part flows through the transmission line to serve demand D and is equal to E_{D_i}. Demand D represents the remote demand at location A, which can be served when the transmission line capacity T is taken into consideration. In other words, if demand at A is represented by a generic demand profile of P_L, then:

$$D = \begin{cases} P_L, & \text{if } P_L < T \\ T, & \text{otherwise} \end{cases} \tag{7.10}$$

In addition, renewable generators can sell excess energy that cannot be absorbed locally or transferred by the transmission line to the storage system S installed at B. The energy sold to storage by i player is denoted as $E_{S_{ini}}$. Finally, part of the renewable production is curtailed, either because it cannot serve any of the demand (D or d) or cannot be stored in the energy storage system (e.g. the energy storage system may already have reached full capacity). This energy is essentially wasted and is equal to E_{C_i}. Taking all possible energy flows for renewable energy production, the following must hold for the line investor and local generators, respectively:

$$E_{G_1} = E_{d_1} + E_{D_1} + E_{S_{in1}} + E_{C_1} \tag{7.11}$$

$$E_{G_2} = E_{d_2} + E_{D_2} + E_{S_{in2}} + E_{C_2} \tag{7.12}$$

Similarly, the energy stored in the storage system can be used to serve demand d at location B or D at A. These are denoted as E_{S_d} and E_{S_D}, respectively. Hence, local demand d at B can be served directly from renewable generators E_{d_1} and E_{d_2}, from storage E_{S_d} or other sources from the main grid that are external to the system under study, denoted as $E_{d_{oth}}$. This results in the total energy demand at location B equal to:

$$E_d = E_{d_1} + E_{d_2} + E_{S_d} + E_{d_{oth}} \tag{7.13}$$

In a similar manner, remote demand D located at A is served by any combination of renewable production generators E_{D_1} and E_{D_2}, storage E_{S_D} or other sources in the main power system $E_{D_{oth}}$, therefore:

$$E_D = E_{D_1} + E_{D_2} + E_{S_D} + E_{D_{oth}} \tag{7.14}$$

Note here that Eq. (7.11) - (7.14) are valid for energy flows at t, but also hold for energies in a larger time period, such as an annual period, the project lifetime or the sum of energies over all t in a larger time period. Total energy quantities referring to a larger time horizon and tariff prices determine the players' profit equations. Similar to the analysis in previous chapters, every player's objective function is to maximise their own profit.

Renewable energy production used to serve the demand (local or remote) is sold at a fixed price equal to p_G. Renewable energy traded with the energy storage system is sold for a tariff price equal to p_S. Energy transported through the transmission line originating from local generators or the storage investor needs to pay a transmission fee of p_T. In addition, renewable generation installation costs c_{G_i} in £/MWh, as defined in Eq. (3.4). The line investor can build a power line with a transmission cost of c_T in £/MW per unit of transmission capacity installed. Note that c_T refers to the transmission cost per unit of line capacity installed and is different than C_T, defined in Eq. (4.1), which refers to the total transmission cost over a larger time period. Finally, the storage player also incurs a cost of c_S in £/MWh per unit of storage capacity installed.

Crucially, when energy storage is introduced, the model evolves into a *Stackelberg-Cournot game*. The line investor is the leader of the game, as he moves first by building the transmission line T and renewable generation capacity P_{N_1} at B. The line investor's profits however, depend also on the investment capacity decisions taken by local generators and the storage investor. In the context of the game, the line investor needs to decide how much generation capacity P_{N_1} and transmission capacity T to install to maximise his profit. Local generators and the storage investor share the available capacity at location B by playing a Cournot game. Local generators determine how much generation capacity they need to install P_{N_2}, and the storage investor needs to decide the storage capacity S that maximises his own profit.

Profit equations for each player are determined from the total energy quantities, price and cost parameters. The profit of the line investor is equal to:

$$\Pi_1 = (E_{d_1} + E_{D_1})p_G + (E_{D_2} + E_{S_D})p_T + E_{S_{in1}}p_S - c_{G_1}E_{G_1} - c_T T \tag{7.15}$$

Line investors' revenues stem from selling energy to serve the demand (local and/or remote) for which he earns p_G, from the energy transmitted through the transmission line (originating from local generators or the storage investor) charged with p_T, and from the energy sold to the storage system, charged with p_S. On the other hand, the line investor incurs costs related to the installation and operation of renewable generation capacity c_{G_1} and costs related to the installation of the transmission capacity c_T.

Local generators earn p_G per unit of demand served (local or remote) and p_S for the energy sold to storage. The costs incurred by local generators are the energy production costs c_{G_2}, and the cost for energy transmitted through the power line p_T:

$$\Pi_2 = (E_{d_2} + E_{D_2})p_G + E_{S_{in2}}p_S - c_{G_2}E_{G_2} - E_{D_2}p_T \tag{7.16}$$

Similarly, the storage player earns p_G when serving the local and/or remote demand. The storage investor pays p_S for the energy purchased by the renewable generators, p_T for the energy transported through the transmission line and c_S for installing energy storage capacity of S:

$$\Pi_3 = (E_{S_d} + E_{S_D})p_G - (E_{S_{in1}} + E_{S_{in2}})p_S - E_{S_D}p_T - c_S S \tag{7.17}$$

Note here that the energy purchased by storage from renewable generators would otherwise be wasted, meaning that the storage player can negotiate a low tariff price p_S with the line investor and local generators. Essentially, the storage investor can purchase energy from renewable producers at very low prices, therefore increasing the profitability of storage investments in the region.

Similarly to the analysis presented in Section 4.2.2, the estimation of the Stackelberg-Cournot game equilibrium answers the research question of the optimal strategies that players adopt, in order to maximise their profits, given that the line investor has a first mover advantage over local investors at B [2]. The game equilibrium can be found by *backward induction*. At the first level, the line investor estimates the Cournot game equilibrium, determined by the joint actions of local generators and the storage player, for every possible action taken by the leader $\langle P_{N_1}, T \rangle$. For a given $\langle P_{N_1}, T \rangle$, the Cournot game equilibrium can be found by the intersection of the local investors best responses. Local generators' best response needs to account for all possible actions of the storage player, i.e. for every S, the best response of local generators is given by:

$${P_{N_2}}^{\#} \leftarrow \arg\max_{P_{N_2}} \Pi_2(P_{N_2}, S)|_{\langle P_{N_1}, T \rangle} \tag{7.18}$$

$$BR_2 \leftarrow (P_{N_2}^{\#}, S)|_{\langle P_{N_1}, T \rangle} \tag{7.19}$$

Similarly, the storage investor's best response needs to account for all possible actions of local generators and is given by:

$$S^{\#} \leftarrow \arg\max_{S} \Pi_3(P_{N_2}, S)|_{\langle P_{N_1}, T \rangle} \tag{7.20}$$

$$BR_3 \leftarrow (P_{N_2}, S^{\#})|_{\langle P_{N_1}, T \rangle} \tag{7.21}$$

The Cournot game equilibrium solution is given by the intersection of the local investors best responses:

$$(P_{N_2}, S)^{\dagger} = intersect(BR_2, BR_3)|_{\langle P_{N_1}, T \rangle} \tag{7.22}$$

[2]The Stackelberg-Cournot game represents a static game, as optimal decisions on strategy actions are estimated one-off, as opposed to a repeated game.

Next, the line investor selects from the set of Cournot game equilibria to build (P_{N_1}, T) that maximises his profit:

$$(P_{N_1}, T, P_{N_2}, S)^* \leftarrow \underset{(P_{N_1}, T)}{\arg\max}\, \Pi_1(P_{N_1}, T, (P_{N_2}, S)^\dagger) \tag{7.23}$$

The equilibrium of the Stackelberg-Cournot game is equal to $(P^*_{N_1}, T^*, P^*_{N_2}, S^*)$.

Energy quantities in Eq. (7.15) - Eq. (7.17) represent the sum of energy quantities over a larger time horizon. To estimate this, we first need to estimate the energy flows (or power flows) for each t in the time horizon under consideration. The power flows are determined by a control mechanism that is used to define priorities over available suppliers and demand. The control scheme used in the energy system is presented in detail in the following section along with an algorithmic approach for the analysis of the Stackelberg-Cournot game.

7.3 Algorithmic approach for Stackelberg-Cournot game analysis

An algorithmic approach is developed for the estimation of the Stackelberg-Cournot game equilibrium. Profit equations required for the game equilibrium estimation depend on the sum of energy flows or power flows for each t. The power flows are determined by a control mechanism that is used to define priorities over available suppliers and demand, analysed in the following section.

7.3.1 Control scheme for power flow estimation

In this section, the control scheme that defines the energy flows and priorities in the two-location system is presented. The control scheme used in the energy system is shown in the flowchart depicted in Fig. 7.2.

Recall here, the line investor needs to decide how much generation capacity P_{N_1} and transmission capacity T he needs to install. Local generators need to estimate P_{N_2} and the storage investor S, so that their profits are maximised. For any combination of possible $\langle P_{N_1}, T, P_{N_2}, S\rangle$ and each t, the power flows are determined by the control algorithm logic presented in Fig. 7.2 and more analytically in Algorithm 5.

In summary, for each time step t in the simulation process, the residual demand (total demand minus potential RES production) is estimated. When there is a *shortage of renewable supply*, the control algorithm estimates the energy storage discharge. The power discharged by the storage system cannot be larger than the maximum power that can be discharged at t. In addition, the storage system's state of charge is not allowed to exceed SOC_{min}. In the next step, available supply from all three players, is used to serve the local demand on a Pro Rata basis. Local demand is prioritised over remote demand due to reduced energy losses, but also because of transmission charges imposed to local generators and the storage investor. The remaining renewable generation and power from

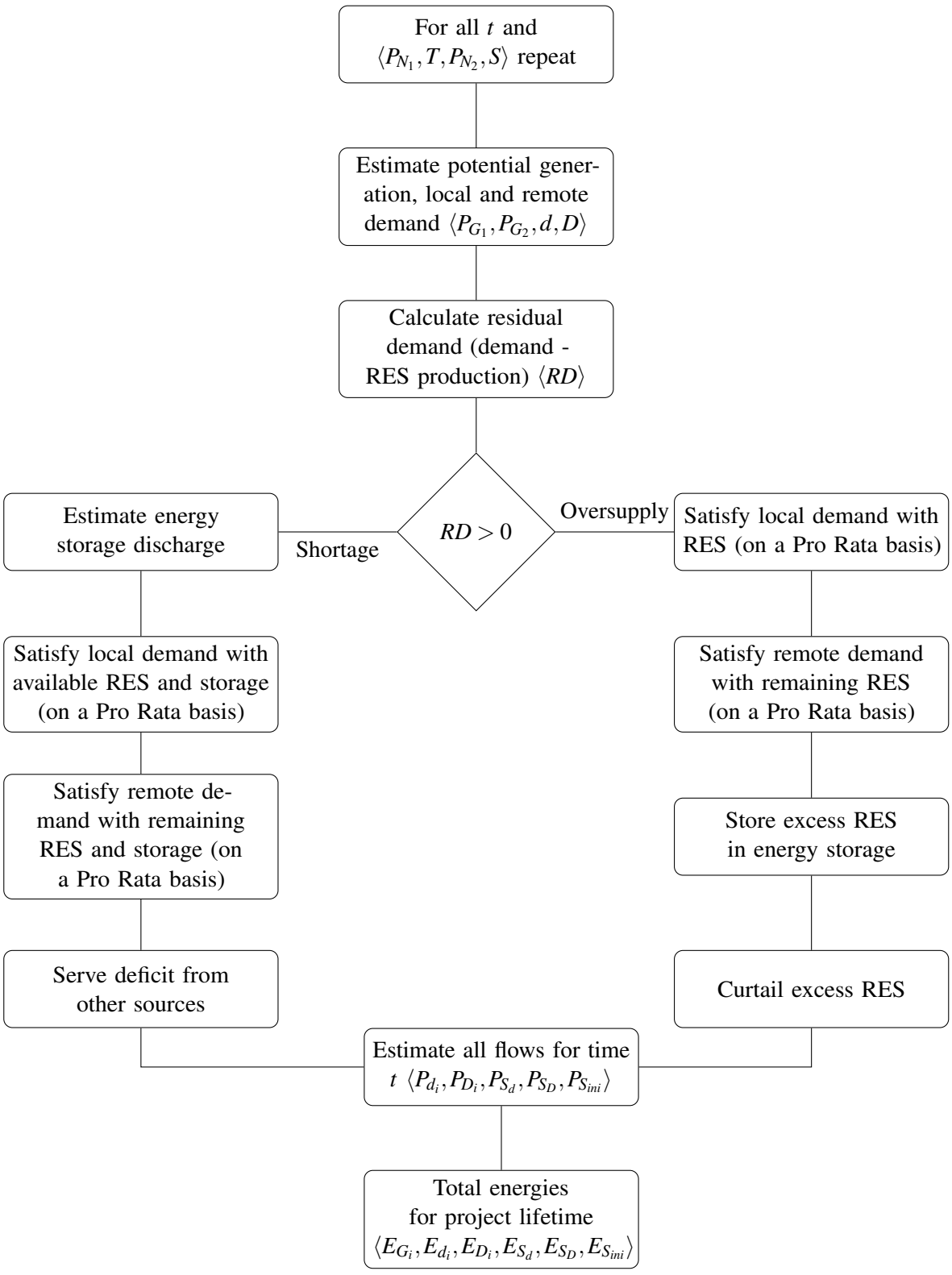

Fig. 7.2 Flowchart summarising control algorithm logic to derive energy flows estimation

the storage system is used to serve the remote demand. If there is any deficit, the remaining power required to fully serve the demand is served by other sources in the system. On the other hand, when there is an *oversupply of renewable production*, renewable generators serve the local and remote demand on a Pro Rata basis. Any excess energy is stored in the storage system, as long as the state of charge does not exceed its nominal value and maximum charging power constraints are not violated. Any excess generation that cannot be stored in the storage tank is curtailed.

Energy flows for each t are estimated by Algorithm 5 and total energy quantities for the period under examination are given by the summation of energy flows for all t. The next step is to calculate the profits of the players for given cost parameters and all possible combinations of $\langle P_{N_1}, T, P_{N_2}, S \rangle$. The procedure is summarised in Algorithm 6. Profit estimation is followed by the actual determination of the Stackelberg-Cournot game equilibrium. The methodology developed is discussed in the following section.

7.3.2 Stackelberg-Cournot game estimation

When energy storage is introduced, the game evolves into a Stackelberg-Cournot game between the line investor (leader) and local generators and storage player (followers). The solution of the Stackelberg-Cournot game is found by backward induction and is summarised in Algorithm 7. Recall here that the strategy actions of each player are: the line investor chooses his renewable generation capacity P_{N_1} and transmission capacity T, local generators choose their renewable energy capacity P_{N_2} and the storage investor chooses the storage capacity to be installed S. The objective of all players is to maximise their profits. In order to do so, the line investor needs to anticipate the reaction of other investors to his own actions i.e. to building the transmission line and renewable generation capacity at B. Hence, the line investor needs to compute for every possible strategy $\langle P_{N_1}, T \rangle$), the equilibrium solution of the Cournot game played between local generators and the storage investor.

For every given $\langle P_{N_1}, T \rangle$, local generators estimate their best response to all possible strategies of the storage player. In other words, local generators estimate the renewable capacity they need to install ${P_{N_2}}^{\#}$ for every possible storage capacity S, for every given $\langle P_{N_1}, T \rangle$. This is the best response of local generators to the storage capacity being built. At the same time, the storage investor estimates his best response to the renewable generation capacity built by local generators. For every possible P_{N_2}, the storage investor estimates the quantity of storage capacity he needs to build $S^{\#}$ to maximise his own profit Π_3.

The Cournot game equilibrium solution between local generators and the storage investor is given by the intersection of the best responses $(P_{N_2}, S)^{\dagger}$. A Cournot solution is found for all possible strategies of the line investor and the line investor's profits Π_1 are computed. The line investor then estimates the optimal generation and transmission capacity that maximises his profit Π_1, throughout the set of all Cournot game equilibria. This concludes the backward induction process followed by the line investor to select his optimal strategy. The line investor then installs $(P^*_{N_1}, T^*)$. Local generators and the storage

Algorithm 5 POWER & ENERGY ESTIMATION

$P_{N_{max}}$ ▷ max rated capacity in search space
$P_{N_i} \leftarrow [0 : \delta P_N : P_{N_{max}}]$ ▷ generation capacity strategies i=1,2 player
$T \leftarrow [0 : \delta T : T_{max}]$ ▷ transmission capacity strategy
$S \leftarrow [0 : \delta S : S_{max}]$ ▷ storage capacity strategy
α, β ▷ power curve sigmoid parameters
$x_{G_i}^{(t)} \leftarrow \dfrac{1}{1+e^{-\alpha(w_i^{(t)}-\beta)}}$ ▷ i player normalised generation
P_L ▷ demand profile
for all $\langle P_{N_1} \in \{0,...,P_{Nmax}\}, T \in \{0,...,T_{max}\}\rangle$ **do**
    for all $P_{N_2} \in \{0,...,P_{Nmax}\}$ **do**
        for all $S \in \{0,...,S_{Nmax}\}$ **do**
            for all t
                $P_{G_1} \leftarrow x_{G_1} \cdot P_{N_1}$ ▷ generation 1 player
                $P_{G_2} \leftarrow x_{G_2} \cdot P_{N_2}$ ▷ generation 2 player
                $S_0 \leftarrow \dfrac{S}{2}$ ▷ initial storage state
                $S_{min} \leftarrow SOC_{min} \cdot S$ ▷ minimum SOC
                γ ▷ ratio of local to remote demand
                $d \leftarrow \gamma P_L$ ▷ local demand
                $D \leftarrow \begin{cases} P_L, & \text{if } P_L < T \\ T, & \text{otherwise} \end{cases}$ ▷ remote demand
                $RD \leftarrow d + D - (P_{G_1} + P_{G_2})$ ▷ residual demand
                if $RD > 0$ **then** ▷ shortage of RES generation
                    if $RD > P_{dch_{max}}$ **then** ▷ check maximum discharge rate
                        $P_{dch} \leftarrow P_{dch_{max}}$ ▷ discharge at max rate
                    else
                        $P_{dch} \leftarrow RD$ ▷ discharge power
                    end
                    $from\_store \leftarrow E_{S_t}(1 - s_{dch}) - \dfrac{P_{dch}}{\eta_{dch}}$ ▷ storage state no constraints
                    if $from\_store > S_{min}$ **then** ▷ no violation of min SOC
                        $E_{S_{t+1}} \leftarrow from\_store$ ▷ update storage state
                    else
                        $E_{S_{t+1}} \leftarrow S_{min}$ ▷ min storage state
                        $P_{dch} \leftarrow (E_{S_t}(1 - s_{dch}) - S_{min})\eta_{dch}$ ▷ update power discharged
                    end
                    if $P_{G_1} + P_{G_2} + P_{dch} >= d$ **then** ▷ supply exceeds local demand
                        $P_d \leftarrow d$ ▷ local demand satisfied
                        $P_{d_1} \leftarrow \dfrac{P_{G_1} \cdot P_d}{P_{G_1} + P_{G_2} + P_{dch}}$ ▷ served by generator 1
                        $P_{d_2} \leftarrow \dfrac{P_{G_2} \cdot P_d}{P_{G_1} + P_{G_2} + P_{dch}}$ ▷ served by generator 2
                        $P_{S_d} \leftarrow \dfrac{P_{dch} \cdot P_d}{P_{G_1} + P_{G_2} + P_{dch}}$ ▷ served by storage
                    else
                        $P_d \leftarrow P_{G_1} + P_{G_2} + P_{dch}$ ▷ local demand satisfied
                        $P_{d_1} \leftarrow P_{G_1}$ ▷ served by generator 1
                        $P_{d_2} \leftarrow P_{G_2}$ ▷ served by generator 2
                        $P_{S_d} \leftarrow P_{dch}$ ▷ served by storage
                    end

$P_{D_1} \leftarrow P_{G_1} - P_{d_1}$ ▷ remote demand served by generator 1
$P_{D_2} \leftarrow P_{G_2} - P_{d_2}$ ▷ remote demand served by generator 2
$P_{S_D} \leftarrow P_{dch} - P_{S_d}$ ▷ remote demand served by storage
$P_D \leftarrow P_{D_1} + P_{D_2} + P_{S_D}$ ▷ total remote demand
$P_{d_{oth}} \leftarrow d - P_d$ ▷ local demand served by other sources
$P_{D_{oth}} \leftarrow D - P_D$ ▷ remote demand served by other sources
$P_{S_{in}} = P_{S_{in_1}} = P_{S_{in_2}} = 0$ ▷ renewable generation to storage
$P_C = P_{C_1} = P_{C_2} = 0$ ▷ RES generation curtailed
else ▷ oversupply of RES generation
$P_{d_1} \leftarrow \frac{P_{G_1} \cdot d}{P_{G_1} + P_{G_2}}$ ▷ local demand served by generator 1
$P_{d_2} \leftarrow \frac{P_{G_2} \cdot d}{P_{G_1} + P_{G_2}}$ ▷ local demand served by generator 2
$P_{D_1} \leftarrow \frac{P_{G_1} \cdot D}{P_{G_1} + P_{G_2}}$ ▷ remote demand served by generator 1
$P_{D_2} \leftarrow \frac{P_{G_2} \cdot D}{P_{G_1} + P_{G_2}}$ ▷ remote demand served by generator 2
if $-RD > P_{ch_{max}}$ **then** ▷ check max charge rate
$P_{ch} \leftarrow P_{ch_{max}}$ ▷ charge at max rate
else
$P_{ch} \leftarrow -RD$ ▷ update charge power
end
$to\_store \leftarrow E_{S_t}(1 - s_{dch}) + P_{ch}\eta_{ch}$ ▷ storage state no constraints
if $to\_store <= S_{max}$ **then** ▷ no violation of max storage capacity
$E_{S_{t+1}} \leftarrow to\_store$ ▷ update storage state
$E_{S_{in}} \leftarrow P_{ch}$ ▷ charging power
else ▷ storage capacity is exceeded
$E_{S_{t+1}} \leftarrow S_{max}$ ▷ update storage
$E_{S_{in}} \leftarrow \frac{S - E_{S_t}(1 - s_{dch})}{\eta_{ch}}$ ▷ in storage
end
$P_{S_{in_1}} \leftarrow \frac{P_{G_1} \cdot P_{ch}}{P_{G_1} + P_{G_2}}$ ▷ in storage from gen 1
$P_{S_{in_2}} \leftarrow \frac{P_{G_2} \cdot P_{ch}}{P_{G_1} + P_{G_2}}$ ▷ in storage from gen 2
$P_C \leftarrow RD - P_{S_{in}}$ ▷ total power curtailed
$P_{C_1} \leftarrow \frac{P_{G_1} \cdot P_C}{P_{G_1} + P_{G_2}}$ ▷ power curtailed from gen 1
$P_{C_2} \leftarrow \frac{P_{G_2} \cdot P_C}{P_{G_1} + P_{G_2}}$ ▷ power curtailed from gen 2
$P_{S_d} = P_{S_D} = 0$ ▷ demand served by storage
$P_{d_{oth}} = P_{D_{oth}} = 0$ ▷ demand served by other sources
end
end
end
end
end
$\langle E_{G_i}, E_{d_i}, E_{D_i}, E_{S_d}, E_{S_D}, E_{S_{ini}} \rangle \leftarrow \langle \sum_t P_{G_i}, \sum_t P_{d_i}, \sum_t P_{D_i}, \sum_t P_{S_d}, \sum_t P_{S_D}, \sum_t P_{S_{ini}} \rangle$
return $\langle E_{G_i}, E_{d_i}, E_{D_i}, E_{S_d}, E_{S_D}, E_{S_{ini}} \rangle$ ▷ total energies

Algorithm 6 PROFIT ESTIMATION

p_G, p_T, p_S ▷ generation tariff, transmission fee, storage fee
c_T ▷ transmission capacity cost
c_{G_i} ▷ i player's generation cost
for all $\langle P_{N_1} \in \{0,...,P_{Nmax}\}, T \in \{0,...,T_{max}\}\rangle$ **do**
  for all $P_{N_2} \in \{0,...,P_{Nmax}\}$ **do**
    for all $S \in \{0,...,S_{Nmax}\}$ **do**
      $\Pi_1 \leftarrow (E_{d_1} + E_{D_1})p_G + (E_{D_2} + E_{S_D})p_T + E_{S_{in1}}p_S - c_{G_1}E_{G_1} - c_T T$
      $\Pi_2 \leftarrow (E_{d_2} + E_{D_2})p_G + E_{S_{in2}}p_S - c_{G_2}E_{G_2} - E_{D_2}p_T$
      $\Pi_3 \leftarrow (E_{S_d} + E_{S_D})p_G - (E_{S_{in1}} + E_{S_{in2}})p_S - E_{S_D}p_T - c_S S$
    end
  end
end
return $\langle \Pi_1, \Pi_2, \Pi_3 \rangle$

Algorithm 7 STACKELBERG-COURNOT EQUILIBRIUM ESTIMATION

for each $\langle P_{N_1}, T\rangle \in \langle \{0,...,P_{Nmax}\}, \{0,...,T_{max}\}\rangle$ **do**
  for each $S \in \{0,...,S_{max}\}$ **do**
    $\Pi_2^{\#} \leftarrow \max_{P_{N_2}} \Pi_2(P_{N_2}, S)|_{\langle P_{N_1}, T\rangle}$ ▷ local generators best response
    ${P_{N_2}}^{\#} \leftarrow \arg\max_{P_{N_2}} \Pi_2(P_{N_2}, S)|_{\langle P_{N_1}, T\rangle}$
  end
  $BR_2 \leftarrow (P_{N_2}^{\#}, S)|_{\langle P_{N_1}, T\rangle}$
  for each $P_{N_2} \in \{0,...,P_{Nmax}\}$ **do**
    $\Pi_3^{\#} \leftarrow \max_{S} \Pi_3(P_{N_2}, S)|_{\langle P_{N_1}, T\rangle}$ ▷ storage best response
    $S^{\#} \leftarrow \arg\max_{S} \Pi_3(P_{N_2}, S)|_{\langle P_{N_1}, T\rangle}$
  end
  $BR_3 \leftarrow (P_{N_2}, S^{\#})|_{\langle P_{N_1}, T\rangle}$
  $(P_{N_2}, S)^{\dagger} = intersect(BR_2, BR_3)|_{\langle P_{N_1}, T\rangle}$ ▷ Cournot game equilibrium
end
$\Pi_1^* \leftarrow \max_{(P_{N_1}, T)} \Pi_1(P_{N_1}, T, (P_{N_2}, S)^{\dagger})$ ▷ line investor best response
$(P_{N_1}, T, P_{N_2}, S)^* \leftarrow \arg\max_{(P_{N_1}, T)} \Pi_1(P_{N_1}, T, (P_{N_2}, S)^{\dagger})$
$(P_{N_1}, T, P_{N_2}, S)^* = (P_{N_1}^*, T^*, P_{N_2}^*, S^*)$ ▷ game equilibrium
return $\langle \Pi_1^*, \Pi_2^*, \Pi_3^*, P_{N_1}^*, T^*, P_{N_2}^*, S^* \rangle$

player observe the leader's strategy and respond by installing their best responses and Cournot game solution $P^*_{N_2}$ and S^*.

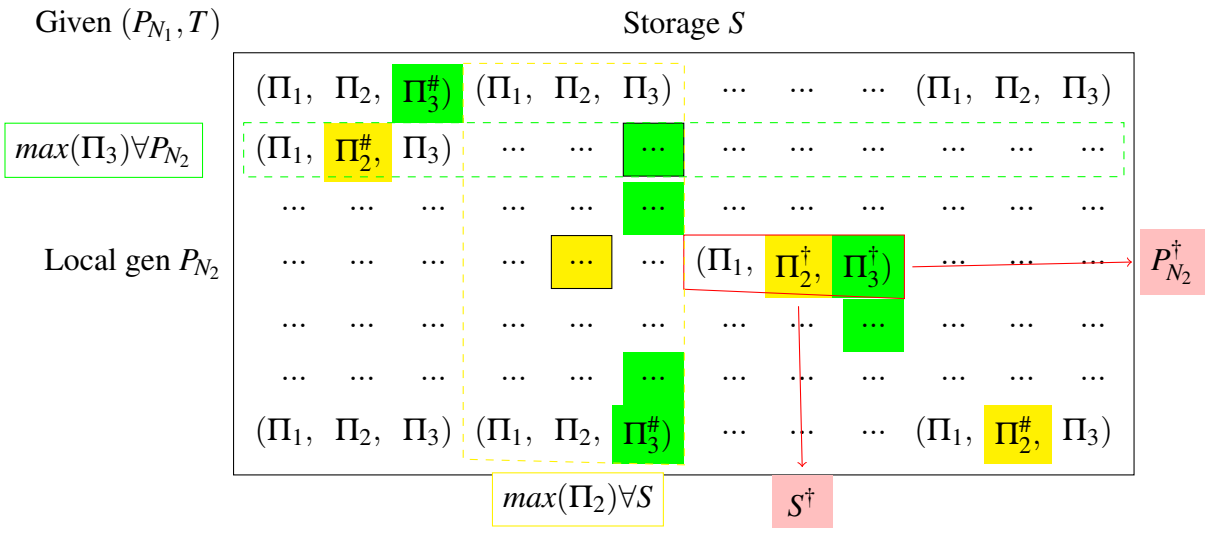

Fig. 7.3 Cournot game equilibrium estimation process from normal form of the game

The the game equilibrium estimation in practice is achieved from the normal form of the Stackelberg-Cournot game. Profits represent the players' expected payoffs and are computed for every possible action in the strategy space $\langle P_{N_1}, T, P_{N_2}, S\rangle$.

The normal form of the Cournot game given a line investor's strategy (P_{N_1}, T) is shown in Fig. 7.3. The figure shows the local investors payoff matrix and the procedure followed to determine the players best responses. The best response of local generators to the installation of storage capacity S corresponds to finding P_{N_2} that maximises profit Π_2 i.e. finding the maximum Π_2 at each column (shown in yellow color). Respectively, finding the best response of the storage player for every possible strategy coming from the local generators is equal to finding the maximum Π_3 at every row of the payoff matrix (shown in green). The equilibrium solution of the Cournot game lies in the intersection of the followers best responses (shown in pink color).

The strategies that implement this solution $(P_{N_2}, S)^\dagger$ are estimated for all possible actions in the line investor's strategy space. The leader computes the followers' payoff matrix for every P_{N_1}, T, finds their best responses, estimates the Cournot game equilibrium and from this set equlibria selects the optimal payoff strategy that maximises his own profit. Cournot game equilibria are shown in Fig. 7.4. From the set of Cournot solutions, the line investor selects the optimal strategy that maximises Π_1. The equilibrium of the Stackelberg-Cournot game is $\langle P^*_{N_1}, T^*, P^*_{N_2}, S^*\rangle$ (encircled by a red box in Fig. 7.4).

An application of the methods developed for the estimation of the Stackelberg-Cournot game equilibrium is shown in the following section. The empirical analysis was based on realistic assumptions based on the project for network reinforcement between Hunterston and the Kintyre peninsula in the western coast of Scotland.

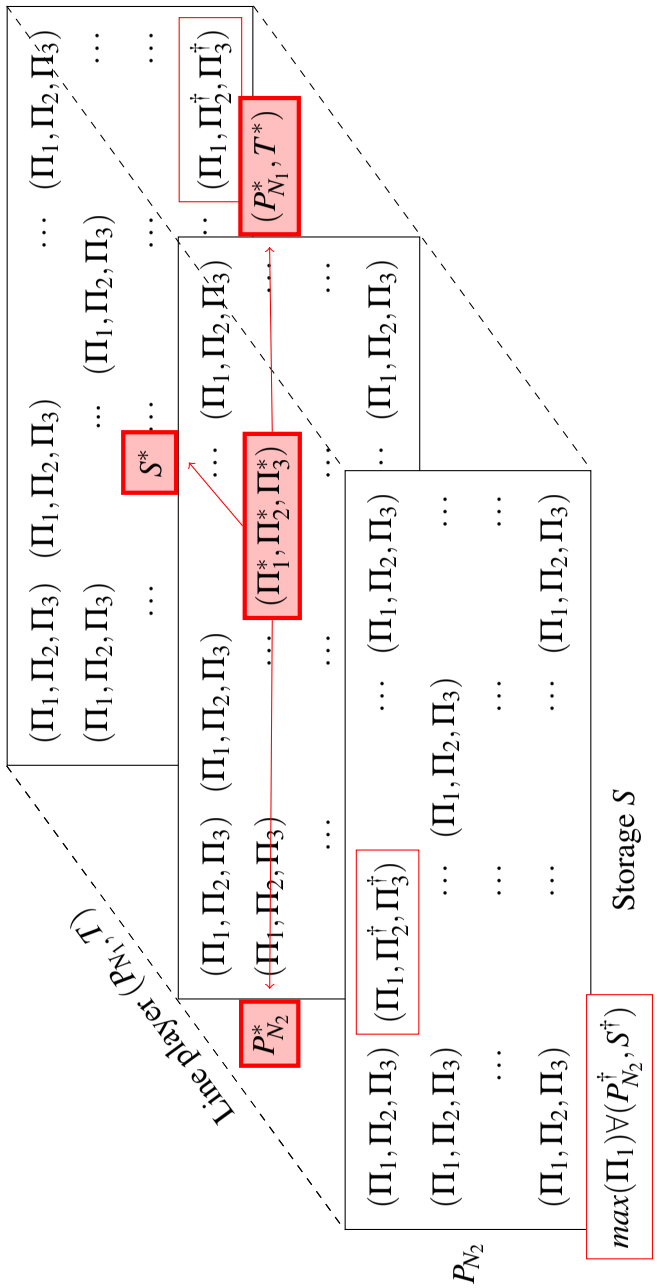

Fig. 7.4 Stackelberg-Cournot game equilibrium estimation

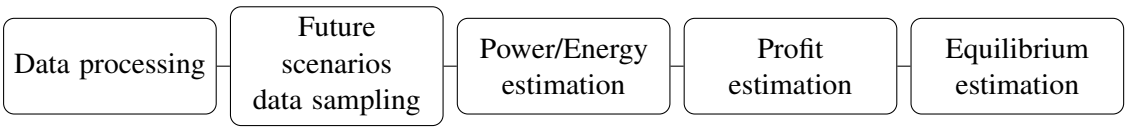

Fig. 7.5 Summarised methodology steps for transmission capacity game with energy storage

7.4 Practical application of algorithmic approach

This section elaborates on the three player game equilibrium estimation of the emerging Stackelberg-Cournot game using realistic assumptions based on the Kintyre-Hunterston grid reinforcement project. The procedure and methodology steps followed are summarised in Fig. 7.5. In summary, at first, historic data are collected and processed. Next, we sample future energy scenarios through a modified Gibbs sampling technique, which is similar to the sampling procedure presented in Chapter 6, but also preserves time dependency of resulting samples, in order to account for the introduction of energy storage and its time-dependent operation. For each scenario, power and energy flows in the system are estimated. Next, total energies are used to compute profits of players for a combination of different strategies and cost parameters. Once profits are available, the equilibrium of the game can be estimated. The steps followed for the simulation analysis are discussed in detail in the following sections.

7.4.1 Model assumptions

In more detail, the first step of the analysis is to collect historic data on wind resources and demand at locations of main demand (Location A) and high renewable potential (Location B). We assume that location B is represented by the Kintyre peninsula and location A by Hunterston. Wind speed data were collected from the UK Met Office and the MIDAS dataset. Two weather stations were identified in the area of interest, the weather station with ID 908 was used to model the renewable production and capacity installed by the line investor, and the weather station with ID 23417 was selected to represent renewable production by local generators. ID numbers refer to the UK Met Office database. As for the demand data, UK National Demand data over the 2006-2015 period were used. For additional information on data used, the reader is referred to Section 5.3 of Chapter 5.

Second from historic data, we can generate or sample multiple future scenarios by utilising a Gibbs sampling or MCMC technique, which is suitable for the analysis with energy storage. The Gibbs sampler used for the analysis of the transmission game with storage is shown in Algorithm 8. Historic data refer to mean wind speed data at location B for all players that invest in renewable generation capacity w_1, w_2, and historic demand data from which a generic demand profile is determined P_L[3]. To preserve time dependency and capture seasonal variations, demand data was classified into hour-season distributions.

[3]Recall here that P_L represents a generic demand profile derived from historic data, while D represents the remote demand that can be served by renewable and storage investors, when also accounting for the capacity of the transmission line T, as shown in Eq. (7.10).

For example, $G(P_{L_{h=1,s=4}})$ represents the distribution of demand from $0:00-00:59$ in Winter. Preserving the time dependency is crucial for transmission capacity game with energy storage, as the storage system sizing depends heavily, not only on the magnitude of demand, but also on the actual demand shape with time. Optimal sizing for storage usually follows a typical daily cycle that depends on demand, wind power and their interdependencies. Demand, however, follows a daily pattern and shape which depends on time. This time dependency needs to be preserved, otherwise peaks and valleys may appear more frequently after sampling, which might lead to undersizing of storage capacity required for the application. In previous models (without storage), such as in Chapter 6, time dependence preservation of demand was not required for the estimation of curtailment, but this is a crucial factor when storage is incorporated in the model.

Wind speeds larger than 48 knots were considered outliers and therefore were removed from the datasets. Moreover, only data that reside in common time periods were used to construct the joint distribution of wind speeds. Conditional distributions of players' wind speeds were found as follows: wind speed data were grouped into bins with a step of 1 knot e.g. $[0,1),[1,2),...,[47,48)$. Available wind speed measurements from which the dataset is constructed are rounded into the nearest knot. This means that the first bin corresponds to wind speeds equal to 1 knot and so on. Historic wind speed data are recorded in pairs $\langle w_1, w_2 \rangle$. For every possible value of w_1, all w_2 values were recorded and grouped together. The procedure created 48 bins that contain w_2 wind speed data conditional on w_1 values. As expected, several bins are sparse. For example, very high wind speeds are rare and therefore bins might have a limited number of elements. To ensure the Markov Chain after the utilisation of the Gibbs sampler is ergodic, several bins were merged into forming bins with a larger number of elements. The bins merged into larger bins were the following $[39^{th},40^{th}]$, $[41^{th},42^{th},43^{th}]$ and $[44^{th},45^{th},46^{th},47^{th},48^{th}]$. A similar procedure was followed to derive the distribution of the local generators wind speed conditional on the wind speed of the line investor.

The sampling procedure for wind speeds is initialised by randomly selecting a pair of wind speeds. This represents the initial state of the MC of wind speeds generated. Subsequent states of the MC $w_i^{(t+1)}$ were generated by replacing the value of the wind speed by a randomly selected value from the conditional $F(w_i \mid_{w\_i^{(t)}})$. Demand sampling followed a procedure that preserved the time dependency. At first, a random sample was drawn from the demand distribution for $h=1$, $s=4$, i.e. 1am winter time. The consecutive sample was drawn from the demand distribution for $h=2$ and $s=4$. The values of h and s are alternated to form a time series of demand data that contains n samples.

Similarly to the analysis in Chapter 6, to ensure that the sampling procedure is independent of the starting condition, a burn-in period was adopted and the first 20% of the data generated were not included in the simulation procedure. The final length of data included in the analysis was equal to a duration of a year. A yearly analysis was performed in this model, for the reason that inclusion of storage introduced additional computational requirements that made simulations time-consuming and demanding. Safe conclusions

can be drawn, even if a single year is assumed, as seasonal and hourly variations are still accounted for. The procedure is summarised in Algorithm 8.

Algorithm 8 GIBBS SAMPLING

w_1,w_2,P_L ▷ wind speed 1,2, power demand
n ▷ number of samples
t_{burn} ▷ burn-in period (samples ignored)
$\langle w_1^{(k)}, w_2^{(k)}, P_L^{(k)} \rangle$, $k \in \{1,2,...,k_{max}\}$ ▷ historic data
$F(w_1, w_2)$ ▷ wind distribution from data
$G(P_{L_{h,s}})$ ▷ demand distribution (hour-season)
$t \leftarrow 1$
$\langle w_1^{(t)}, w_2^{(t)} \rangle \leftarrow sample(w_1, w_2)$ ▷ initialise wind
$\langle P_L^{(t)} \rangle \leftarrow sample(P_{L_{h,s}})$ ▷ initialise demand ($h = 1$,$s = 4$)
repeat
    $w_1^{(t+1)} \leftarrow sample\ F(w_1 \mid_{w_2^{(t)}})$
    $w_2^{(t+1)} \leftarrow sample\ F(w_2 \mid_{w_1^{(t+1)}})$
    $P_L^{(t+1)} \leftarrow sample\ G(P_{L_{h,s}})$
    $t \leftarrow t + 1$
until $t > T$
return $\langle w_1^{(t)}, w_2^{(t)}, P_L^{(t)} \rangle$, $t \in \{t_{burn}, t_{burn} + 1, ..., n\}$

Wind speed data generated by the Gibbs sampler are used to estimate the per unit power output of wind generators installed by the line investor and local generators. The conversion from wind speed to power output data was based on a generic power curve[4] and a sigmoid function approximation.

Demand samples were used to estimate local and remote demand. For the three player game, it was assumed that location B has some local demand which is significantly smaller than the remote demand, but follows the same shape and pattern as the UK demand profile. For simplicity, we assumed in the experimental analysis that the demand d is a portion $\gamma \simeq 20\%$ of the demand P_L.

Power and energy flows were estimated every $\delta t = 1$hr and for the duration of one year. Costs of the transmission line and the energy storage system were adjusted to represent the cost for a single year. For example, as in the analysis in previous chapters, the total cost of a transmission line of $T = 150$ MW capacity was assumed to be $C_T = £230$m for a period of 20 years. Dividing the total cost by the capacity of the line and the years results in an annual transmission cost per unit of transmission capacity installed c_T. Similarly for the storage system, an annual storage cost per unit of energy storage capacity installed was derived as the ratio of the total storage cost divided by a useful lifetime of 10 calendar years. After 10 years, we assume the energy storage system has exceeded its useful lifetime and is substituted with a new storage system.

Energy storage system parameters were based on typical values for Lithium-ion batteries. The battery storage system was limited to an operational range of $SOC_{min} = 20\%$

[4]Parameters derived by a 2.05 MW Enercon E82 wind turbine: http://www.enercon.de/en/products/ep-2/e-82/

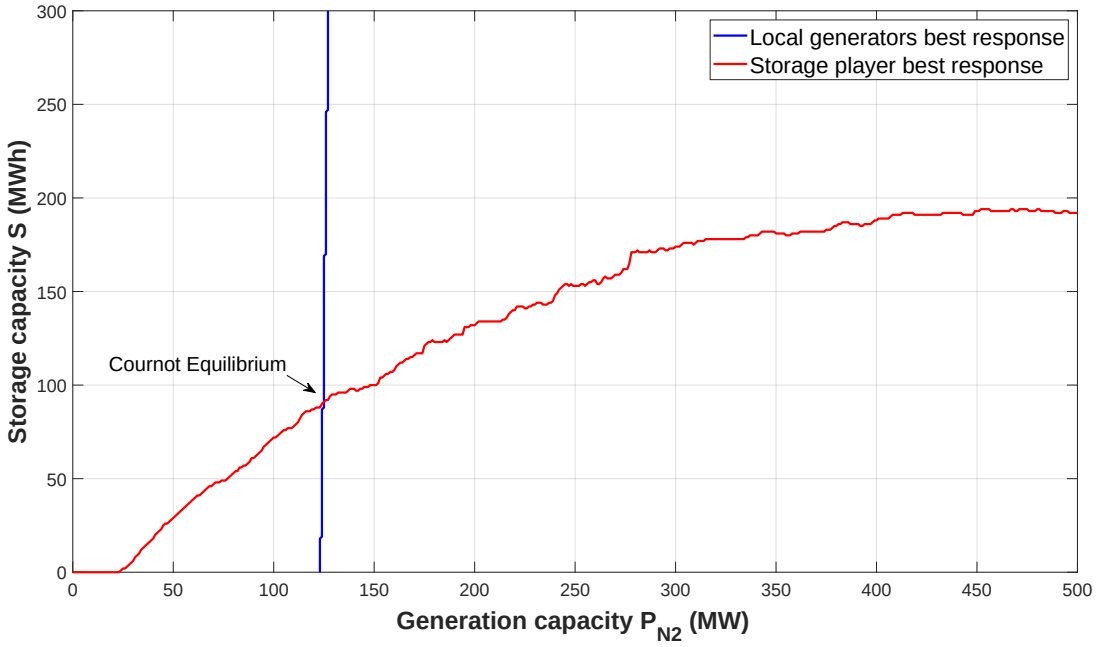

Fig. 7.6 Cournot game: Best responses of local generators and storage investor for $\langle P_{N_1}, T \rangle = \langle 100, 100 \rangle$ and $c_{G_1} = c_{G_2} = p_T = 0.30 p_G$, $p_S = 0.10 p_G$

and $SOC_{max} = 100\%$. The round-trip efficiency was assumed $\eta_{rt} = 0.81$ leading to a charging and discharging efficiency of $\eta_{ch} = \eta_{dch} = 0.9$. Charging and discharging rates were assumed equal to a 1 MW/1 MWh rate (normalised for the storage nominal capacity S). This means that the battery can charge/discharge from/to $SOC = 0\% - 100\%$ to $SOC = 100\% - 0\%$ in $\delta t = 1\ hr$. Note here that in reality, the useful lifetime of battery storage systems is greatly affected by the DOD and charging/discharging rates. Although technically possible, often battery storage systems are limited to lower rates in order to increase their useful lifetime. Considerations about such costs were not assumed in this work. Instead, a useful lifetime of 10 calendar years was assumed, after which the storage system is replaced. Annual costs were adjusted to represent this assumption. Moreover, c_S was assumed to follow a linear approach with the storage capacity installed. In real-world settings large-scale energy storage may have a lower per unit cost due to economies of scale.

The search space and potential strategies of players were assumed to be $P_{N_{max}} = 500$ MW with an incremental capacity of $\delta P_N = 1$ MW. Potential strategy actions for transmission capacity were assumed equal to $T = [0, 75, 100, 125, 150, 175]$ MW and for the storage system $S_{max} = 300$ MWh with $dS = 1$ MWh.

The Stackelberg-Cournot game equilibrium was estimated as follows. For every possible strategy action of the line investor $\langle P_{N_1}, T \rangle$, the local generators P_{N_2} and the storage player S, aggregated energy quantities were estimated on an annual basis from the hourly energy flows, as derived by the control algorithm 5. Next, for different combination of cost parameters and tariff prices, profits were estimated and the normal form of the Stackelberg-Cournot game (payoff matrix) was constructed (see Fig. 7.3). For every $\langle P_{N_1}, T \rangle$, the solution of the Cournot game was found. As shown by Fig. 7.3, the Cournot

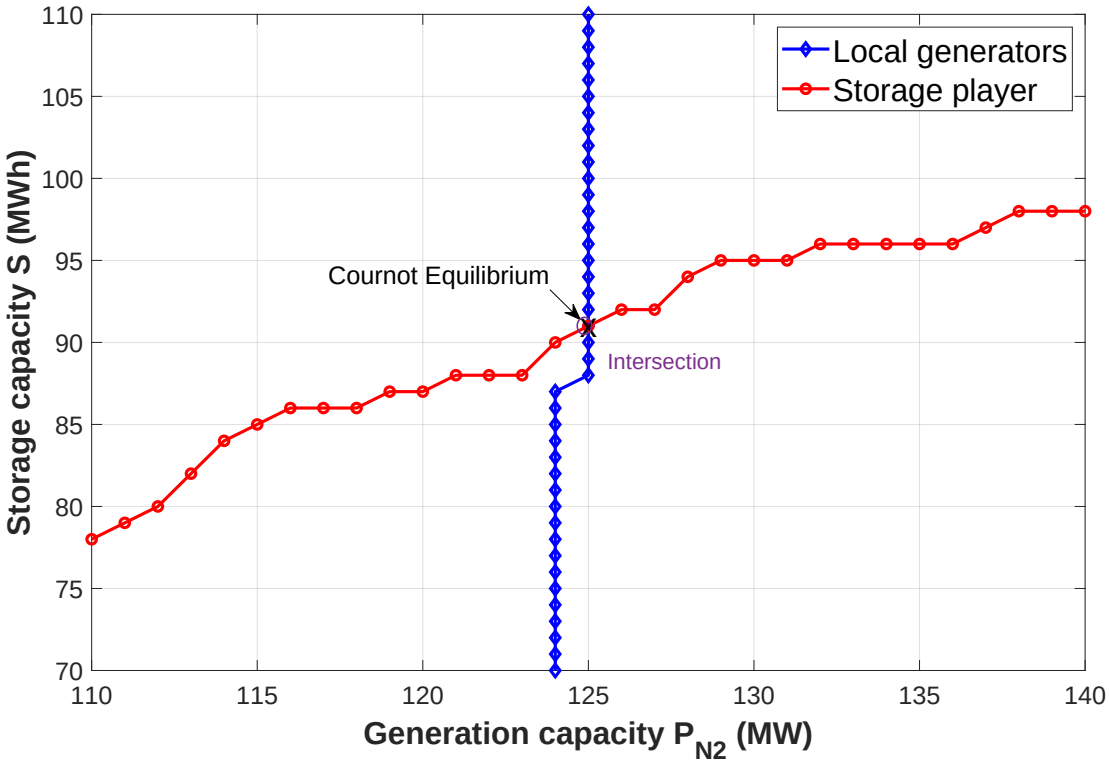

Fig. 7.7 Empirical equilibrium estimation: single intersection point for $\langle P_{N_1}, T \rangle = \langle 100, 100 \rangle$ and $c_{G_1} = c_{G_2} = p_T = 0.30 p_G$, $p_S = 0.10 p_G$

equilibrium is found by the intersection of the local generators and the storage player best responses (Line 12 of Algorithm 7). A practical example of local investors best responses and the Cournot game equilibrium is shown in Fig. 7.6.

Due to the discreteness of data and search space for equilibrium estimation in the empirical approach, the players' best responses are vectors of pair elements (or arrays). For example, local generators best response is equal to a vector of $(P^{\#}_{N_2}, S)$, with S being all potential strategies for the storage investor (see Line 6 of Algorithm 7). Respectively, storage player's best response is equal to a vector of $(P_{N_2}, S^{\#})$, with P_{N_2} being all potential strategies for local generators (see Line 11 of Algorithm 7). The intersect function (Line 12 of Algorithm 7) represents the intersect function between two arrays and returns the data that are common in both arrays BR_2 and BR_3. As such, the following cases were observed during the simulation procedure:

- The search for an intersection between the local generators and storage investor best responses returns exactly one intersection point $(P_{N_2}, S)^{\dagger}$. In this case, the single point is the Cournot game equilibrium between the local generators and the storage player (see Fig 7.7).

- The search for an intersection returns multiple (two) intersection points. In this case, the Cournot game equilibrium is assumed to be the average of the intersection points (see Fig. 7.8).

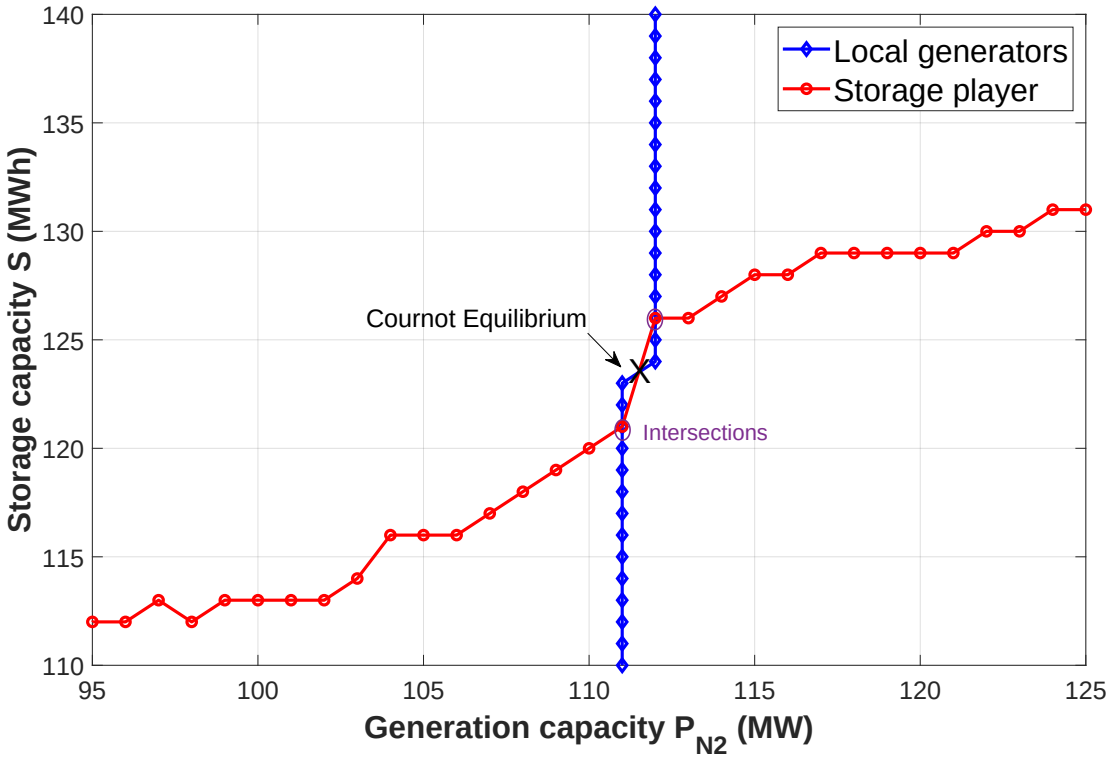

Fig. 7.8 Empirical equilibrium estimation: multiple intersection points for $\langle P_{N_1}, T \rangle = \langle 181, 100 \rangle$ and $c_{G_1} = c_{G_2} = p_T = 0.30 p_G$, $p_S = 0.10 p_G$

- Finally, the search for intersection may lie in a point in-between of the best responses recorded. In this case, the empirical algorithm finds the intersection of the lines formed by the best response curves (intersection of multiple line segments). The solution is considered to be the Cournot game equilibrium between the local generators and the storage investor (see Fig. 7.9).

Note here, the cases above only occur because the method for estimation of the equilibrium is empirical and based on real large-scale data, rather than analytically derived by abstract mathematical functions, like in other studies. On completion of the estimation of all Cournot equilibria for each $\langle P_{N_1}, T \rangle$, we search for the Cournot equilibrium that maximises the profit of the line investor. The solution is the equilibrium of the Stackelberg-Cournot game.

7.4.2 Computational requirements

In the previous section, the numerical assumptions on key parameters of the game were presented. With regards to the algorithmic approach followed in the simulation analysis, a few remarks should be made about the computational resources required:

- The potential strategies for all players lead to $501 \times 301 \times 3006$ potential combinations of strategies, where 501 are the possible P_{N_2} local generators strategies, 301 the possible S storage investor's strategies and $501 \times 6 = 3006$ possible $\langle P_{N_1}, T \rangle$ line investor's strategies. This leads to more than 450 million potential combinations.

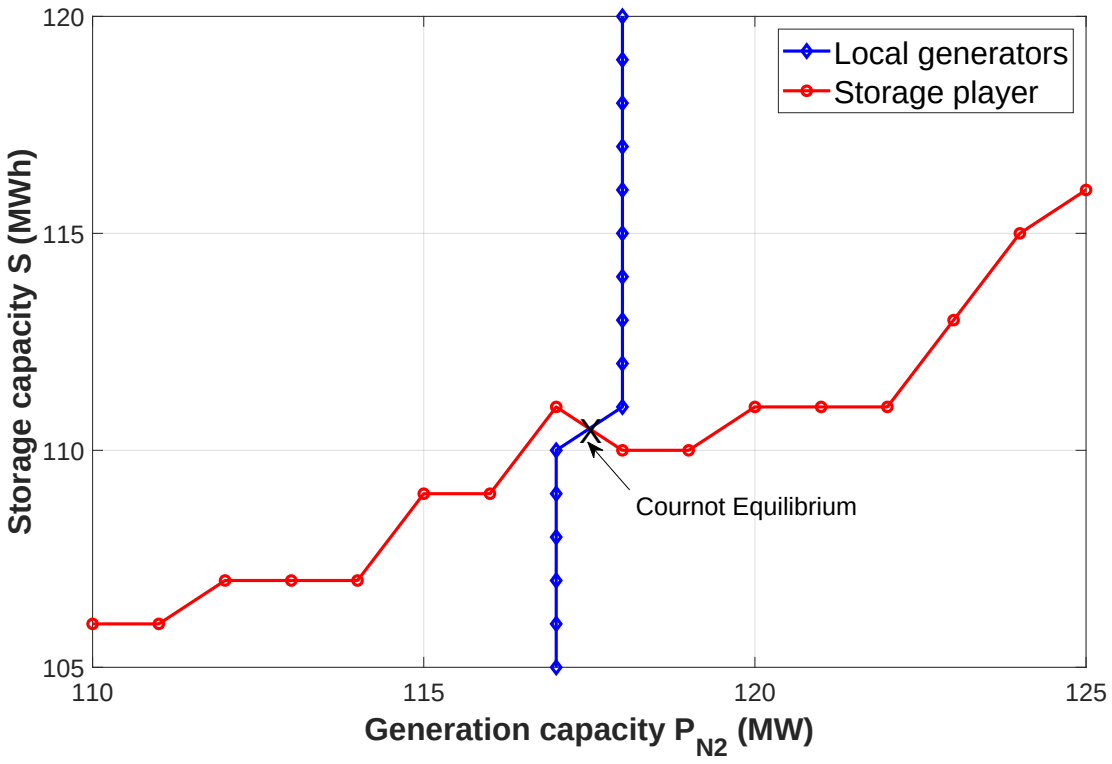

Fig. 7.9 Empirical equilibrium estimation: no intersection point (illustration based on $\langle P_{N_1}, T \rangle = \langle 100, 100 \rangle$ and $c_{G_1} = 0.28 p_G$, $c_{G_2} = p_T = 0.30 p_G$, $p_S = 0.10 p_G$)

- Moreover, for every strategy above, the control algorithm needs to estimate the hourly energy flows and quantities on an annual basis (vectors of a magnitude of 8760). While results from different strategy actions are independent from each other, and therefore calculations can be carried out and executed simultaneously with the use of parallel computing, the storage element, however, does not allow any further use of parallel computing, especially for the estimation of the hourly energy flows. Hourly energy flows depend on previous states of the system (current state of charge depends on the state of charge of the previous time step). Independent simulations for all possible strategies were executed in a state-of-the-art and high-performance computing facility, funded by EPSRC (Cirrus UK National Tier-2 HPC Service at EPCC (http://www.cirrus.ac.uk) and the University of Edinburgh (EP/P020267/1)). The simulations were executed with MATLAB software environment and were split into 36 parallel workers.

- For a given set of financial parameters, the payoff matrix dimensions are $501 \times 301 \times 3006$, where 501 are the possible P_{N_2} strategies, 301 the possible S strategies and $501 \times 6 = 3006$ possible $\langle P_{N_1}, T \rangle$ strategies. However, for each scenario (presented in the following sections) at least 51 combinations of cost parameters were estimated, increasing further the computational requirements of the work.

In the following section, the Stackelberg-Cournot game is analysed under different scenarios and cost parameters.

	Scenario 1	Scenario 2	Scenario 3	Scenario 4	Scenario 5
c_{G_1}	$0.10p_G : 0.02p_G : 0.70p_G$	$0.30p_G$	$0.36p_G$	$0.36p_G$	$0.36p_G$
c_{G_2}	$0.30p_G$	$0.10p_G : 0.02p_G : 0.70p_G$	$0.30p_G$	$0.30p_G$	$0.30p_G$
p_T	$0.30p_G$	$0.30p_G$	$0.10p_G : 0.02p_G : 0.90p_G$	$0.30p_G$	$0.30p_G$
p_S	$0.10p_G$	$0.10p_G$	$0.10p_G$	$p_S = 0 : 0.02p_G : p_G$	$0.10p_G$
c_S	15,000	15,000	15,000	15,000	$0.30c_S : 0.05c_S : 1.60c_S$

Table 7.1 Summary of cost parameters considered in scenarios for the analysis of the transmission capacity game with energy storage (in all scenarios the generation price remained fixed at $p_G = £74.3/\text{MWh}$ and the per unit transmission cost at $c_t = £76,666.67/\text{MW}$)

7.5 Scenario results

The following scenarios were considered to study the Stackelberg-Cournot game formed between low-carbon technology investors. The scenarios examine the dependence of the equilibrium results on the line investor's generation cost c_{G_1}, the local generators' cost c_{G_2}, the transmission fee p_T, the storage tariff price p_S and finally dependence on the actual cost of storage c_S. For each scenario, the cost variable under study varies while all other parameters remain fixed. A summary of all cost parameters for each scenario is provided at Table 7.1.

The time horizon for the simulation analysis is equal to one calendar year. The introduction of energy storage resulted in high computational requirements that restricted the analysis in a single year, a sufficient time period for the purpose of the analysis, as hourly energy calculations on an annual basis take into consideration seasonal and hourly variations of generation and demand. RES generation and transmission capacity useful lifetime was considered to be 20 calendar years. Energy storage useful lifetime was assumed equal to 10 calendar years. The model did not account for degradation of storage in relation to the depth of discharge. Transmission cost c_T and storage cost c_S were adapted for a single year analysis by dividing overall project lifetime costs by 20 years. Useful lifetime for energy storage was assumed to be 10 calendar years, after which the storage system is replaced. This is reflected in the storage cost c_S assumed. No remaining value of energy system assets was considered, although for several components, such as the transmission line, there is significant value remaining after the end of the project lifetime of 20 years. A linear dependence of c_S and c_T per unit of capacity installed was considered in this work. Finally, profit estimation did not account for discounting factors or net present value calculations for future cash flows.

7.5.1 Scenario 1: Varying c_{G_1}

The first scenario shows how the equilibrium results depend on the line investor's generation cost c_{G_1}. Other cost parameters remain fixed $c_{G_2} = 0.30p_G$, $p_T = 0.30p_G$, $p_S = 0.10p_G$, $c_S = 15,000$ (for energy storage a cost of $\$200/\text{kWh}$ of capacity installed was assumed, a useful lifetime of 10 years leading to a cost per MWh installed of £15,000), $p_G = 74.3$ and $c_t = 76,666.67$ ($£230m/(150\text{ MW} \cdot 20\text{ years})$, while c_{G_1} varies from $0.10p_G$ to $0.70p_G$ with a step of $0.02p_G$.

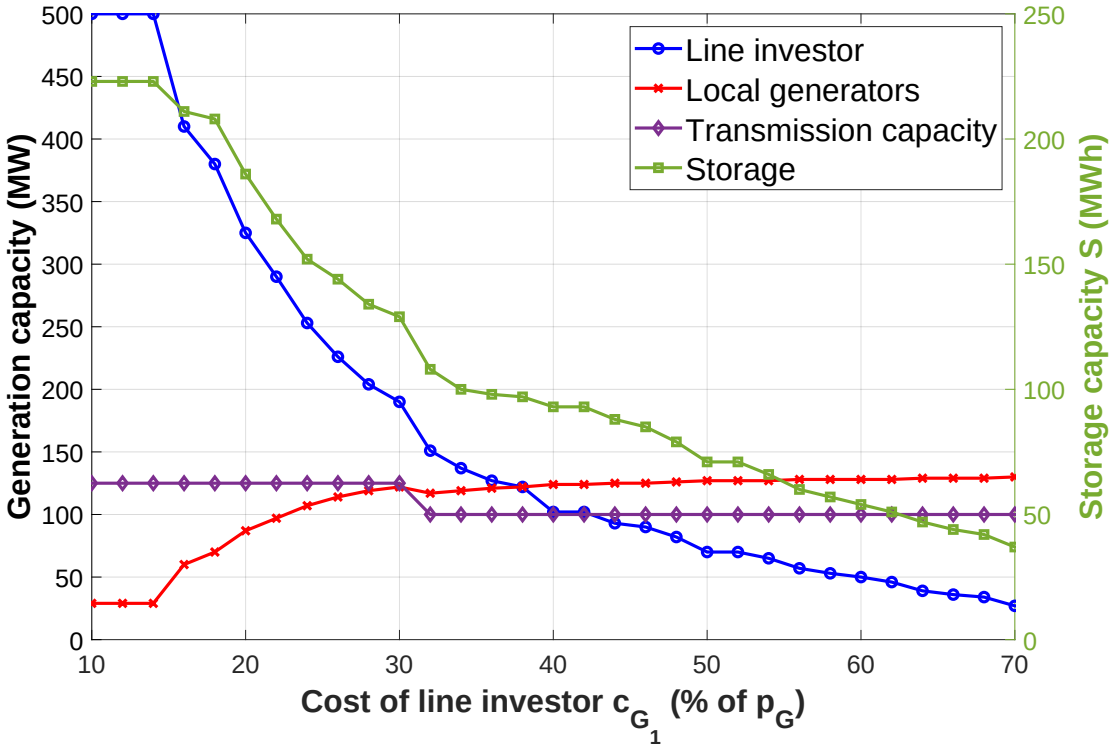

Fig. 7.10 Scenario 1: Generation capacity installed at equilibrium and its dependence on the line investor's generation cost. Storage capacity value is shown in green color and on the right y-axis, while all other variables are shown on the left axis.

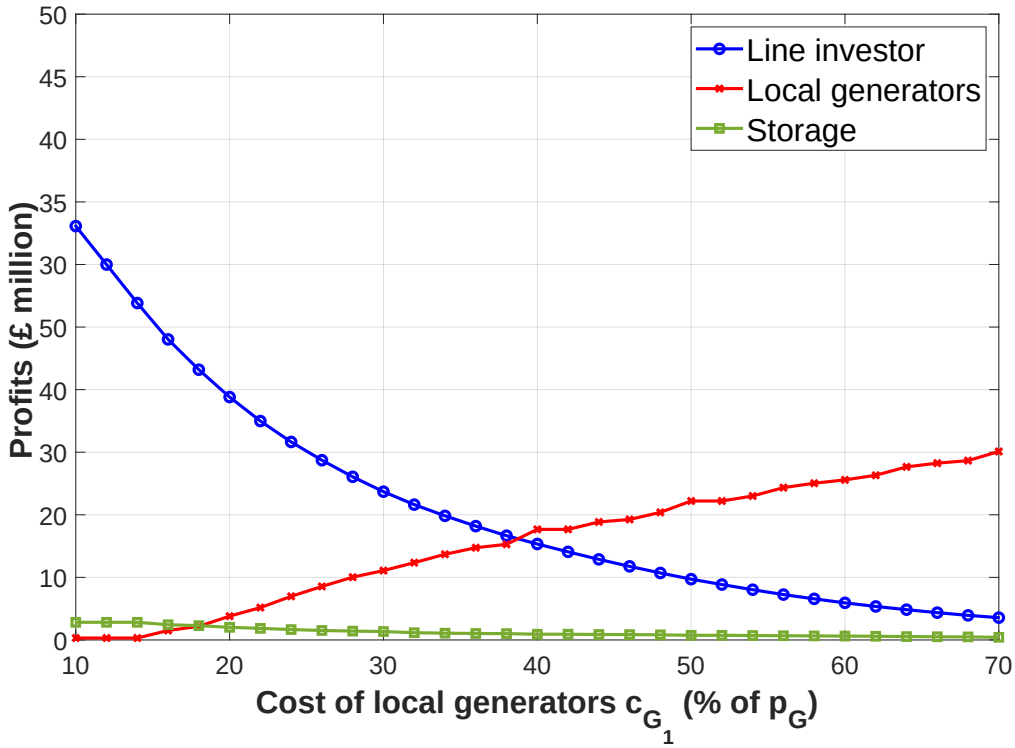

Fig. 7.11 Scenario 1: Profits at equilibrium and their dependence on the line investor's generation cost

Fig. 7.10 reveals the generation capacity installed by the players for varying generation cost of the line investor. Fig. 7.11 shows the profits earned by players at the Stackelberg-Cournot game equilibrium. Transmission capacity, storage capacity and generation capacity installed by the line investor, decreases as c_{G_1} increases with other parameters remaining equal. On the contrary, generation capacity installed by local generators increases as c_{G_1} increases and P_{N_1} decreases. For low leader's generation cost, the line investor installs more generation capacity, leading also to larger profits earned. However, as c_{G_1} increases less capacity is installed by the line investor leading to reduced profits. At $c_{G_1} \simeq 0.38 p_G$, the line investor and local generators install equal RES capacities, with the line investor generating slightly higher profits. Storage capacity decreases as total RES capacity drops, mainly caused by the line investor installing less generation capacity. Storage capacity ranges from 223 MWh to 37 MWh for $c_{G_1} = 0.10 p_G$ and $c_{G_1} = 0.70 p_G$, respectively. The transmission capacity drops from $T = 125$ MW to $T = 100$ MW from $c_{G_1} = 0.30 p_G$ to $c_{G_1} = 0.32 p_G$. In other areas, transmission capacity remains unchanged. Profit functions follow similar trends to the growing or reducing generation capacity installed. Storage player profits are significant lower in magnitude than other players in the game and despite presenting a large range in the rated storage capacity installed. This result is expected as the storage investor is allowed to purchase energy only in the cases of oversupply. Recall here, the storage player is allowed to serve the demand only when this cannot be satisfied by renewable generators. Moreover, storage investor also incurs significant costs, related to the installation of storage capacity itself, but also charges for transmission and energy purchase by renewable generators.

It is also worth exploring here, the difference between the capacities installed at the equilibrium of the game, before and after the introduction of storage. When no storage is present, the game reduces into a Stackelberg game between the line investor and local generators. The behaviour of players in this game was studied extensively in previous chapters of this thesis. Fig. 7.12 shows the generation and transmission capacity installed by the line investor at the equilibrium of the game with and without storage. It is shown (Fig. 7.12) that the line investor can increase the RES capacity installed, while also increasing his profits, as in Fig. 7.14, when storage is introduced. The margin is higher when c_{G_1} is in a lower range. For the line investor, profits are higher due to an increase in the capacity installed, but also because the line investor can generate additional revenue from the storage player by both trading (charged with p_S) and transmission (charged with p_T). Note here, this result is not obvious, as in the case of RES shortage, the storage investor and RES generators compete for serving the demand on equal terms (Pro Rata access rules). This may be a significant factor in the different behaviour observed for local generators. Fig. 7.14 shows a minor reduction in local generators profits, when storage is introduced. A similar minor decrease in capacity is observed in Fig. 7.13. Recall here that local generators can also increase their revenues by trading their energy surplus with the storage system, however they also compete with storage when there is a shortage of supply. The introduction of storage does not bring significant benefits for local generators,

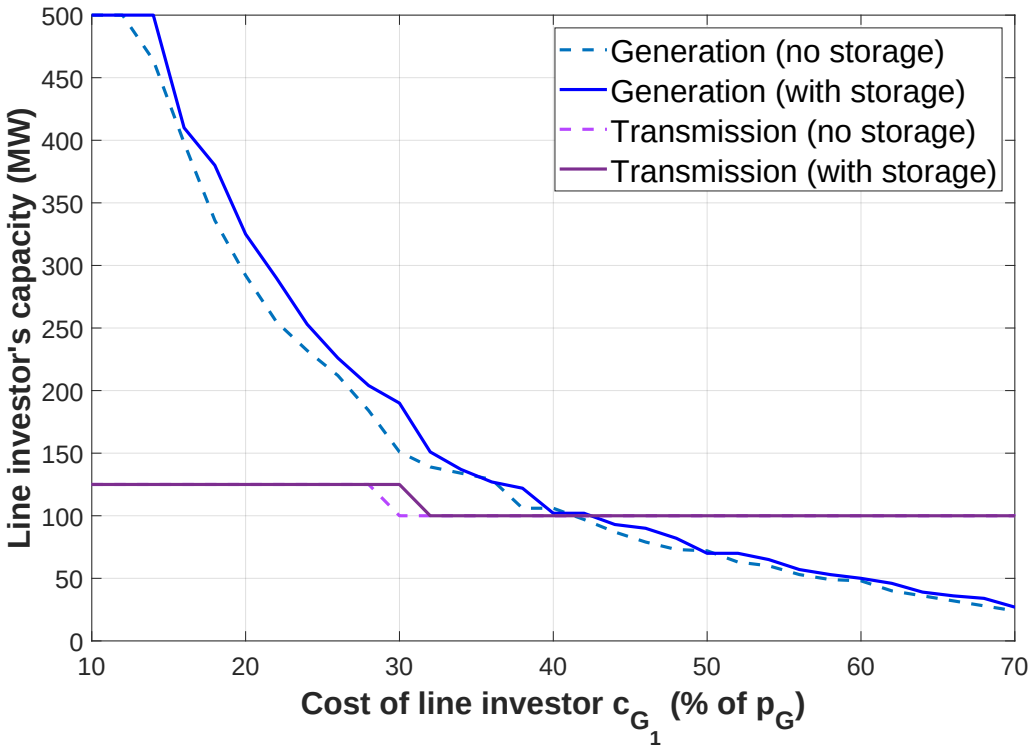

Fig. 7.12 Scenario 1: Line investor's generation and transmission capacity with and without storage

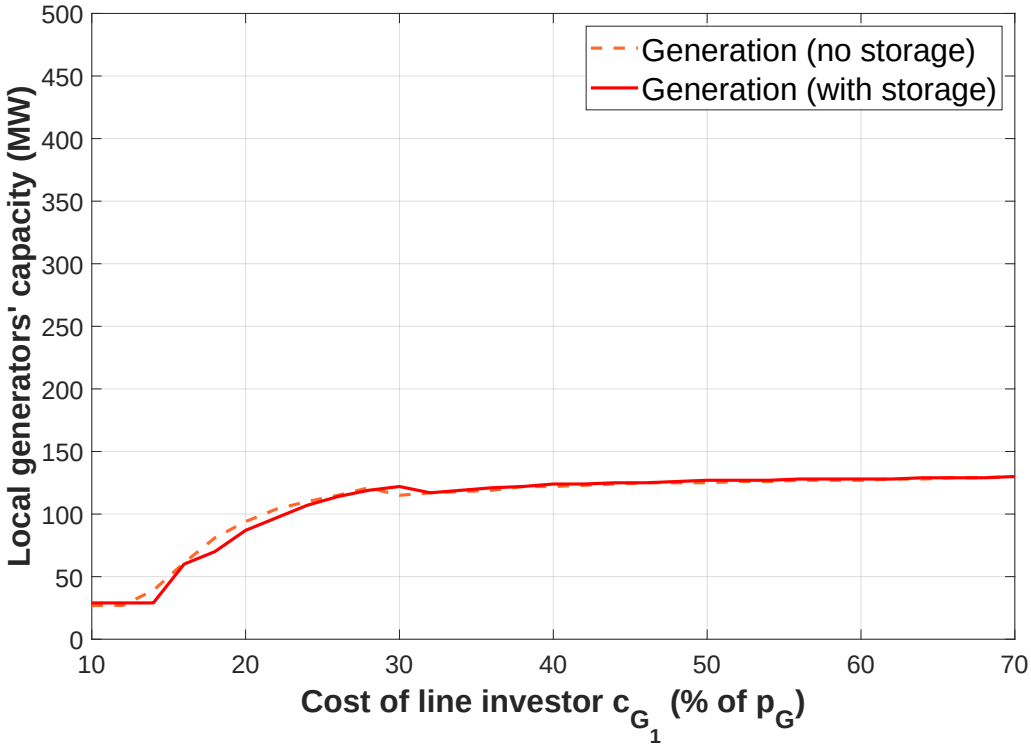

Fig. 7.13 Scenario 1: Local generators generation capacity with and without storage

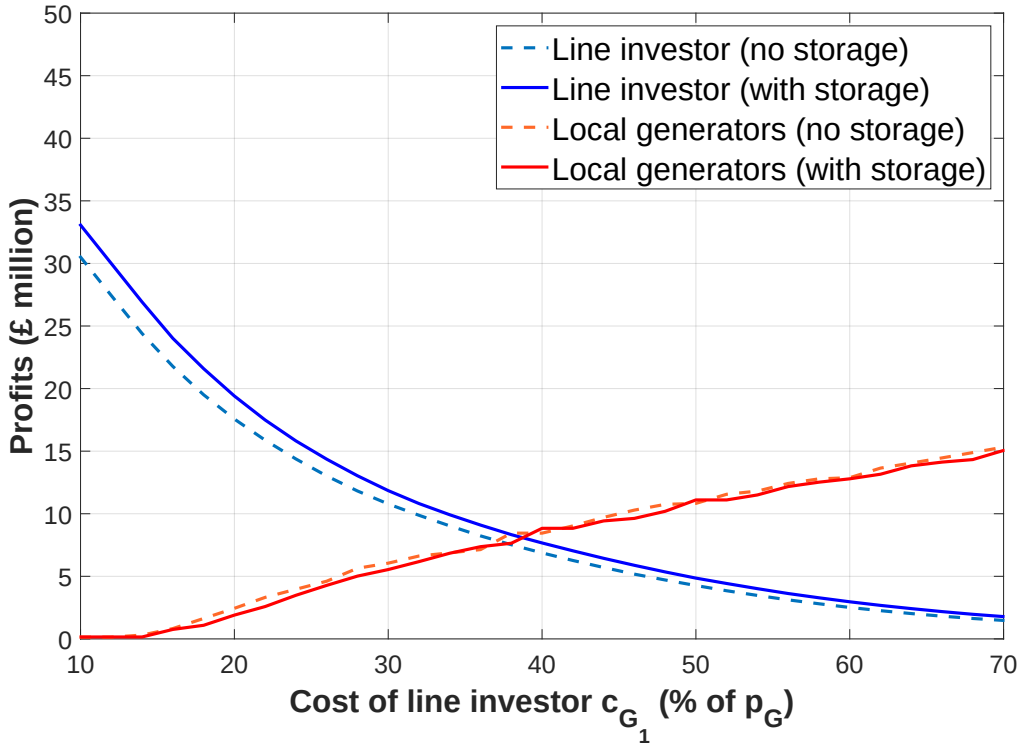

Fig. 7.14 Scenario 1: Profits of line investor and local generators at equilibrium with and without storage

as they are slightly worst off, after storage is introduced in the game. On the contrary, the line investor reaps the rewards of its advantageous market position.

An important aspect to compare is the curtailment imposed to the energy system with and without energy storage. As shown in Fig. 7.15, the curtailment issue is not eliminated. In fact, curtailment happens when storage devices have already reached their maximum storage capacity, therefore excess power generated by RES producers, needs to be curtailed. Low generation costs c_{G_1}, cause a massive deployment in RES capacity installed by the line investor, leading to extremely high curtailment rates reaching approximately 64% of the potential RES capacity. Storage devices, however, managed to reduce total curtailment at a range of 5.6% (117 GWh) to 1.9% (1.1 GWh), as c_{G_1} increases. Fig. 7.16 shows a breakdown of energy curtailed by individual RES investors.

Finally, Fig. 7.17 shows a significant decrease in the demand (local or remote) served by other sources in the energy system. The most significant increase is observed for the remote demand served. Local demand d is significantly lower than remote demand D (about 20% according to model assumptions). Moreover, local investors are not charged for transmission when serving the local demand. Furthermore, local demand is also prioritised over remote demand D due to lower energy losses. All these factors contribute to lower magnitude increase in local demand served rather than in remote demand. Fig. 7.17 also reveals that larger penetration of RES generation is possible with the introduction of energy storage in energy systems.

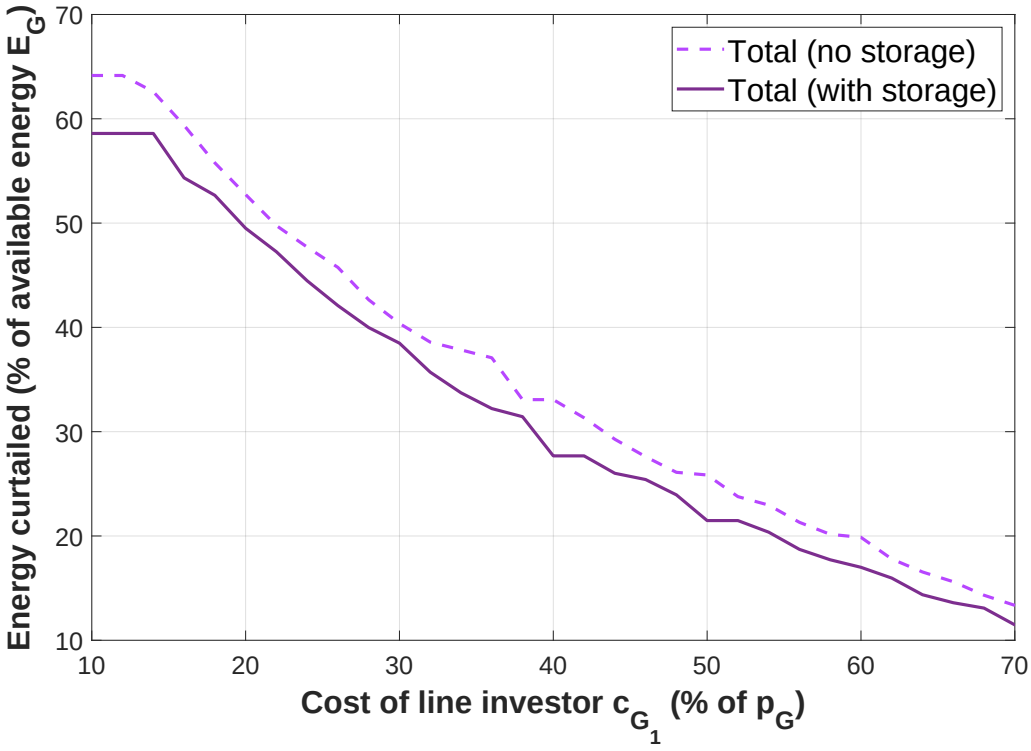

Fig. 7.15 Scenario 1: Total curtailed energy as a percentage of available energy at equilibrium with and without storage

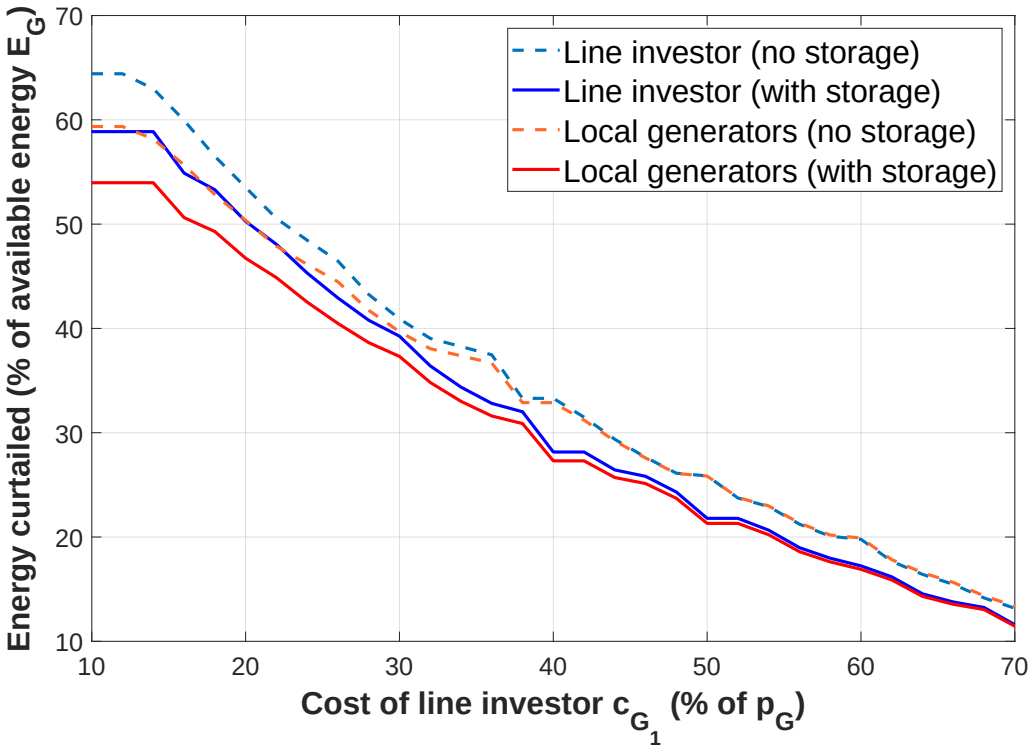

Fig. 7.16 Scenario 1: Curtailed energy as a percentage of available energy at equilibrium with and without storage

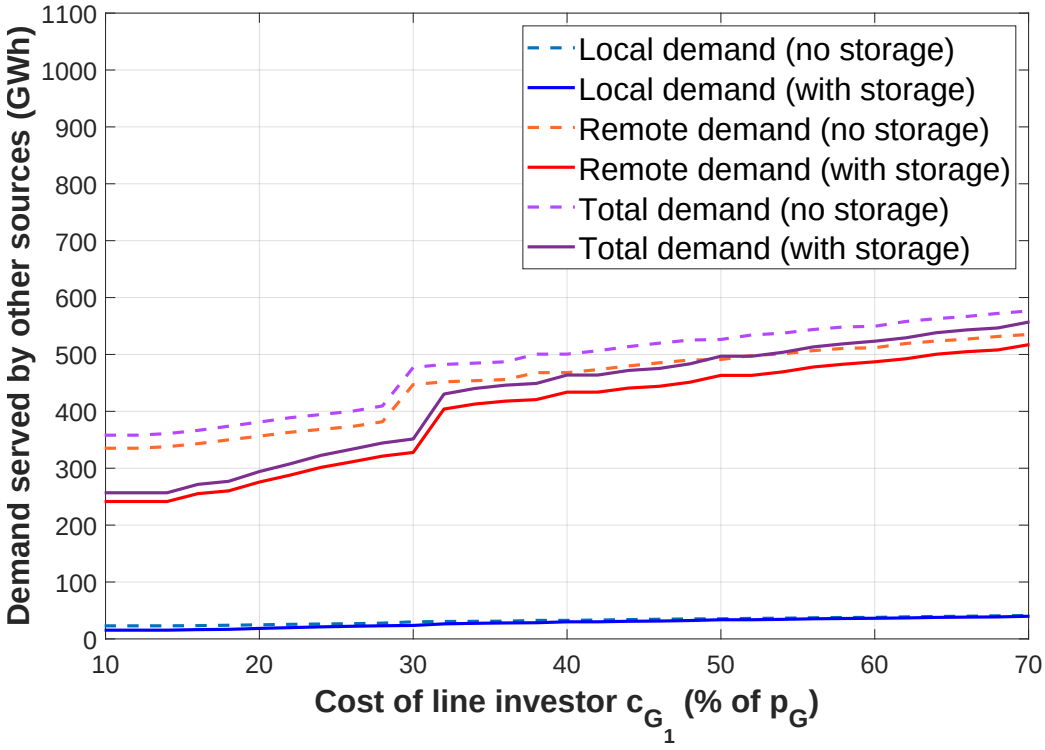

Fig. 7.17 Scenario 1: Demand served by other sources with and without storage

7.5.2 Scenario 2: Varying c_{G_2}

The second scenario shows how the equilibrium results depend on the local generators' generation cost c_{G_2}. Other cost parameters remain fixed $c_{G_1} = 0.30p_G$, $p_T = 0.30p_G$, $p_S = 0.10p_G$, $c_S = £15,000/\text{MWh}$, $p_G = £74.3/\text{MWh}$ and $c_t = £76,666.67/\text{MW}$, while c_{G_2} varies from $0.10p_G$ to $0.70p_G$ with a step of $\delta c_{G_2} = 0.02p_G$.

Fig. 7.18 indicates the generation capacity installed by players for varying generation costs of the local generators. Fig. 7.19 shows the profits at the equilibrium of the game. Transmission and generation capacity installed by the line investor, increases as c_{G_2} increases with other parameters remaining equal. On the contrary, generation capacity installed by local generators decreases as c_{G_2}, as expected, due to higher costs. For lower values of c_{G_2}, local generators install more generation capacity, leading also to larger profits earned. However, as c_{G_2} increases less capacity is installed by local generators, leading to reduced profits. At $c_{G_2} \simeq 0.24p_G$, the line investor and local generators install approximately equal RES capacities, with the line investor generating slightly higher profits. Profits are equalised approximately for $c_{G_2} \simeq 0.22p_G$. Storage capacity decreases as total RES capacity drops, mainly caused by the local generators installing less generation capacity. Storage capacity ranges from 179 MWh to 65 MWh for $c_{G_2} = 0.10p_G$ to $c_{G_2} = 0.70p_G$. The transmission capacity increased from $T = 100$ MW to $T = 150$ MW from $c_{G_2} = 0.26p_G$ to $c_{G_2} = 0.28p_G$. In other areas, transmission capacity remains unchangeable. Profit functions follow similar trends to the growing or reducing generation capacity installed. Storage player profits are significantly lower in magnitude than other players in the game and despite presenting a large range in the rated storage capacity installed.

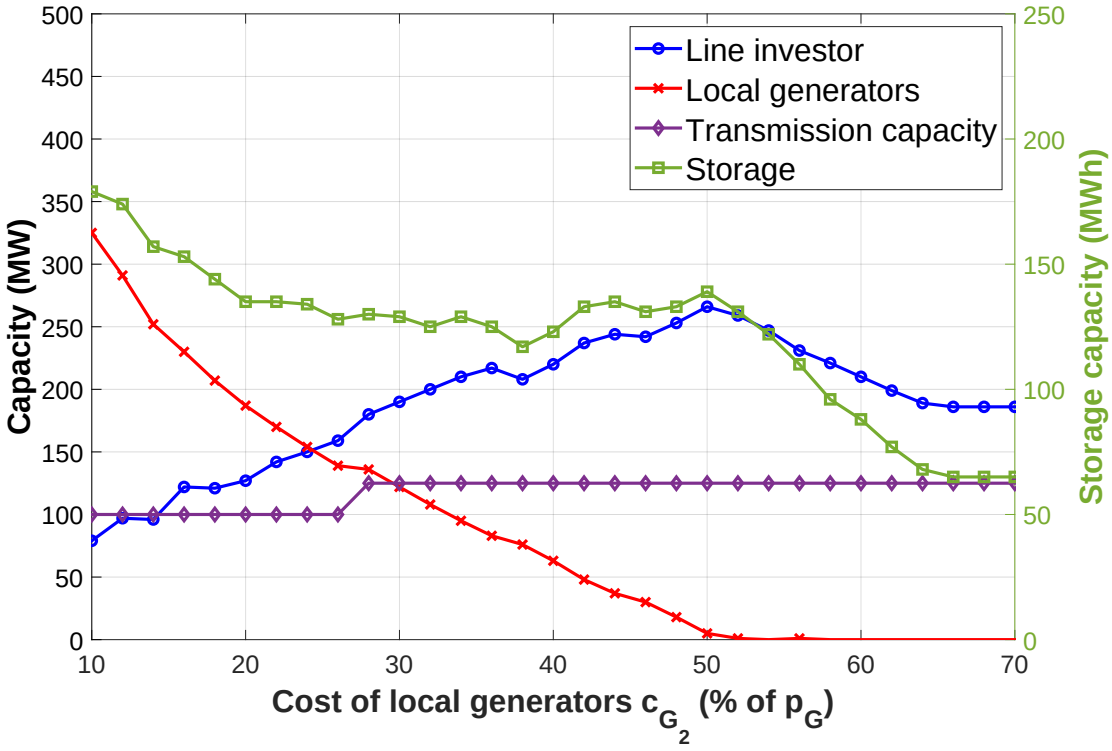

Fig. 7.18 Scenario 2: Generation capacity installed at equilibrium and dependence on the local generators' generation cost. Storage capacity value is shown in green color and on the right y-axis, while all other variables are shown on the left axis.

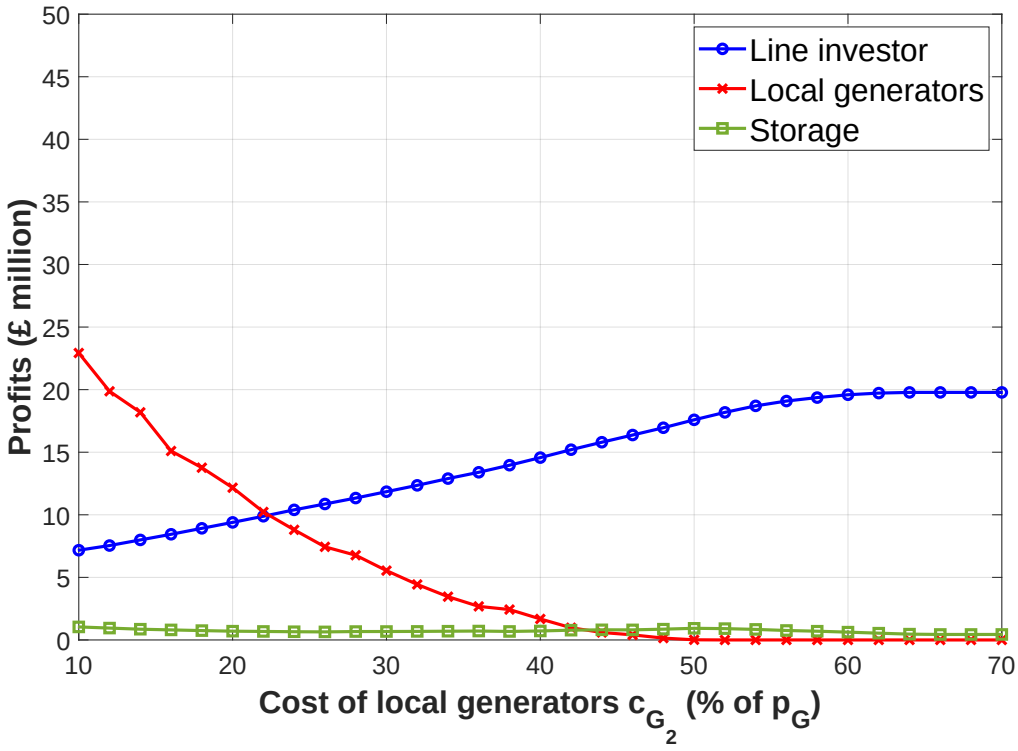

Fig. 7.19 Scenario 2: Profits at equilibrium and dependence on the local generators' generation cost

The storage investor may purchase energy only in the case there is a RES oversupply. Moreover, it is allowed to serve the demand only when this cannot be satisfied by renewable generators. The storage investor also incurs significant costs, related to the installation of storage capacity itself, but also charges for transmission and energy purchase by renewable generators.

Fig. 7.18 shows that for $c_{G_2} \geq 0.50 p_G$ RES capacity investment is not profitable for local generators. An interesting observation is that in the range of $c_{G_2} = 0.50 p_G$ to $c_{G_2} = 0.66 p_G$, while local generators install zero or approximately zero capacity, generation capacity by the line investor and storage capacity gradually decrease until constant values are reached $c_{G_2} \geq 0.66 p_G$. This is due to the method followed for the Stackelberg-Cournot equilibrium estimation. First, the Cournot equilibrium is found for every $\langle P_{N_1}, T \rangle$. Crucially, the Cournot game equilibrium depends on local investors profits Π_2 and Π_3. However, Π_2 directly depends on c_{G_2}. When c_{G_2} increases, Π_2 decreases. This dependence leads to a different estimation of the Cournot game equilibrium with regards to the storage capacity $S^{\dagger}$, as solution points to a different $\langle \Pi_2^{\dagger}, \Pi_3^{\dagger} \rangle$, albeit the generation capacity of local generators is estimated as $P_{N_2}^{\dagger} \simeq 0$, in this value range. Consequently, this also leads to a different estimation of the Stackelberg-Cournot equilibrium, as shown in Fig. 7.18. A careful examination of the equilibrium profit values in the same region shows an increase in the line investor's profit values and a decrease in storage profit values. Line investors profit values increased from £17.59m to £19.78m, while capacity dropped from 266 MW to 189 MW. This corresponds to a 112.5% profit increase and a 30% capacity decrease. Storage profit values decreased from £0.93m to £0.46m (50.5% decrease), while capacity dropped from 139 MWh to 68 MWh (51.1% decrease).

It is also worth exploring here, the difference between the capacities installed at the equilibrium of the game, before and after the introduction of storage. When no storage is present, the game reduces into a Stackelberg game between the line investor and local generators. The behaviour of players in this game was studied extensively in previous chapters of this thesis. Fig. 7.20 shows the generation and transmission capacity installed by the line investor at the equilibrium of the game with and without storage. It is shown in Fig. 7.20 that the line investor can increase the RES capacity installed, while also increasing his profits, as in Fig. 7.22, when storage is introduced. The profit margin increase is more or less equal for all values of c_{G_2}. However, the capacity margin is higher when c_{G_2} is more expensive, as it is cheaper for the line player to invest in RES capacity. For the line investor, profits are higher due to an increase in the capacity installed, but also because the line investor can generate additional revenue from the storage player by both trading (charged with p_S) and transmission (charged with p_T). Note here, this result is not obvious, as in the case of RES shortage, the storage investor and RES generators compete for serving the demand on equal terms (Pro Rata access rules). This may be a significant factor in the different behaviour observed for local generators. Fig. 7.22 shows similar profit values for $c_{G_2} < 0.24 p_G$ and a minor reduction in local generators profits for higher c_{G_2} values, when storage is introduced. Fig. 7.21 shows that profit values are largely affected by generation capacity installed by local generators. For $c_{G_2} < 0.32 p_G$, local generators install more

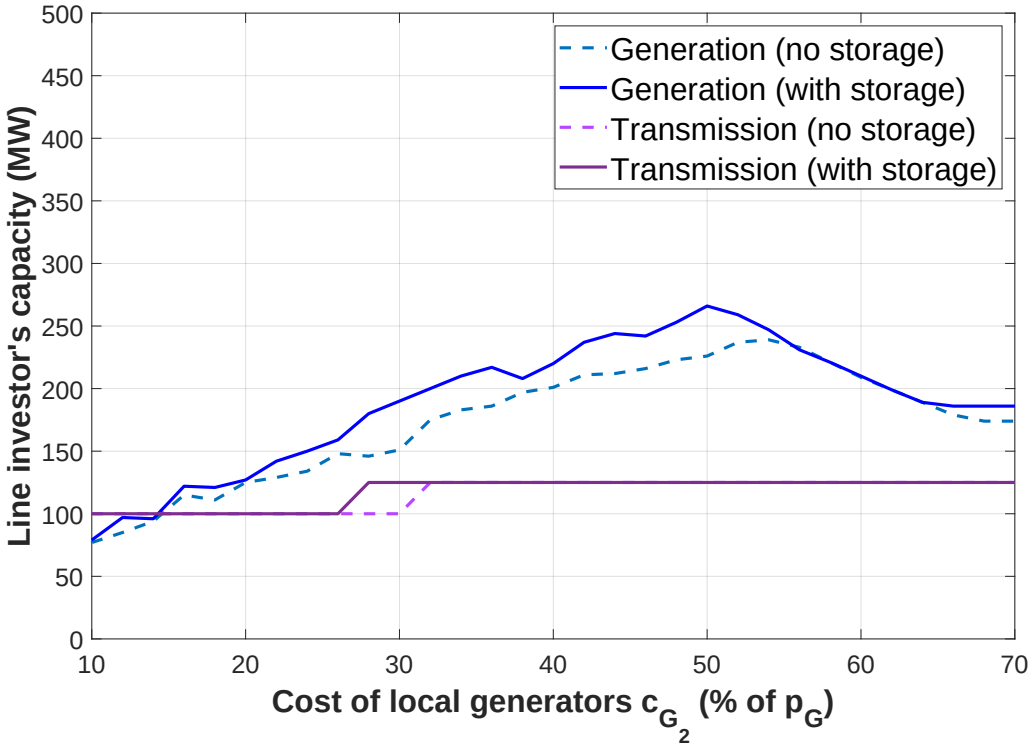

Fig. 7.20 Scenario 2: Line investor's generation and transmission capacity with and without storage

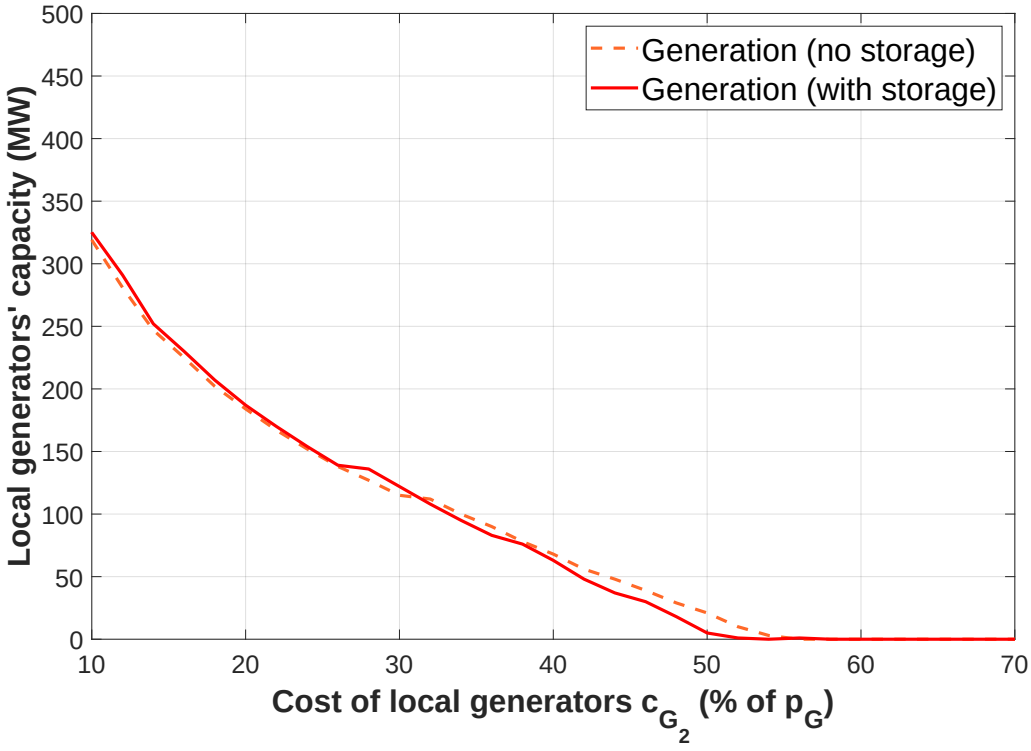

Fig. 7.21 Scenario 2: Local generators generation capacity with and without storage

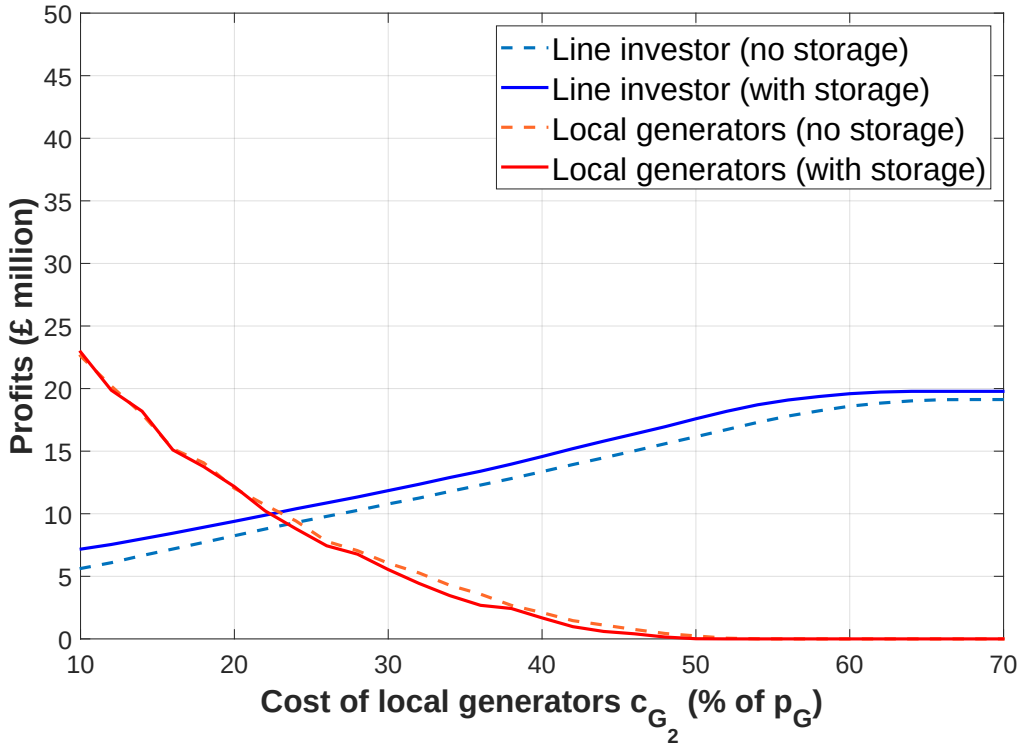

Fig. 7.22 Scenario 2: Profits of line investor and local generators at equilibrium with and without storage

capacity when storage is introduced. Larger c_{G_2} values display a decrease in capacity, as the storage investor competes with local generators for serving the demand. Recall here that local generators can also increase their revenues by trading their energy surplus with the storage system, however, they compete with storage when there is a shortage of supply. The introduction of storage brings higher profits for local generators, only if they have a lower cost of generation than the line investor. When generation costs are more expensive, storage does not bring significant benefits for local generators, as they are worst off. On the contrary, the line investor can increase his profit in all scenarios.

An important aspect to compare is the curtailment imposed to the energy system with and without energy storage. As shown in Fig. 7.15, the issue of curtailment is not eliminated. In fact, curtailment happens when storage devices have already reached their maximum storage capacity, therefore excess power generated by RES producers, needs to be curtailed. Low generation costs c_{G_2}, cause a massive deployment in RES capacity installed by local generators, leading to extremely high curtailment rates reaching approximately 57% of the potential RES capacity. Storage devices, however, managed to reduce total curtailment up to 6.8% (for $c_{G_2} = 0.56 p_G$) and up to 130 GWh ($c_{G_2} = 0.10 p_G$). Fig. 7.24 shows a breakdown of energy curtailed by individual RES investors. When local generators are driven out of the game, RES curtailment is imposed only to the line investor.

Finally, Fig. 7.25 shows how a significant decrease in the demand (local or remote) served by other sources in the energy system. Most significant change is shown in the remote demand served. Local demand d is significantly lower than remote demand D

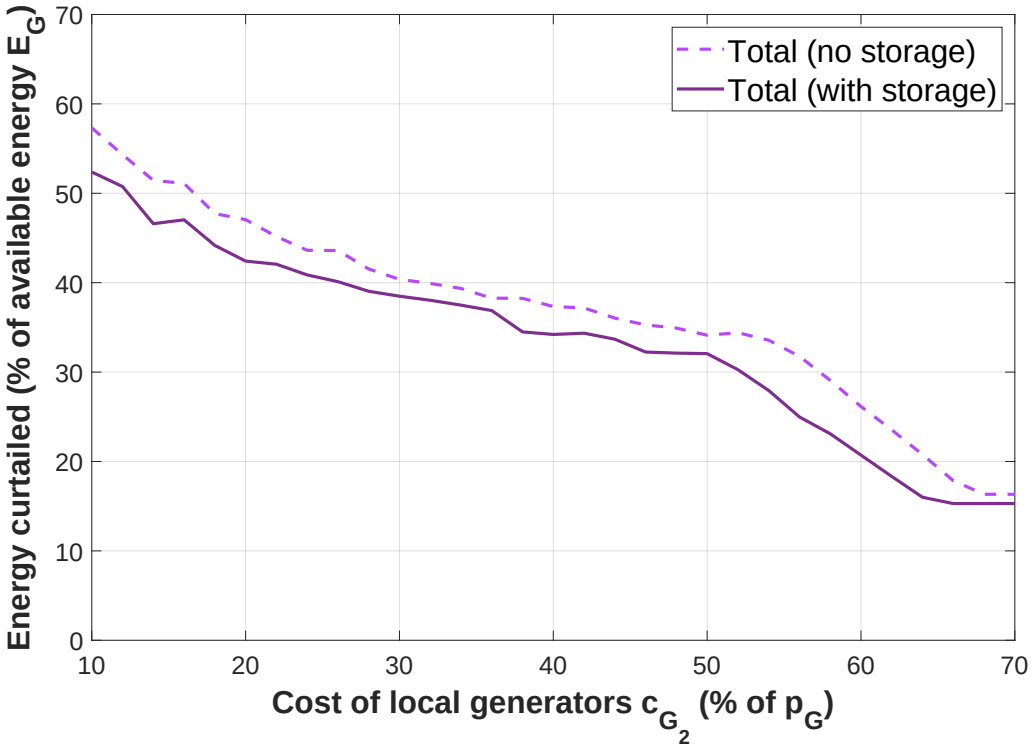

Fig. 7.23 Scenario 2: Total curtailed energy as a percentage of available energy at equilibrium with and without storage

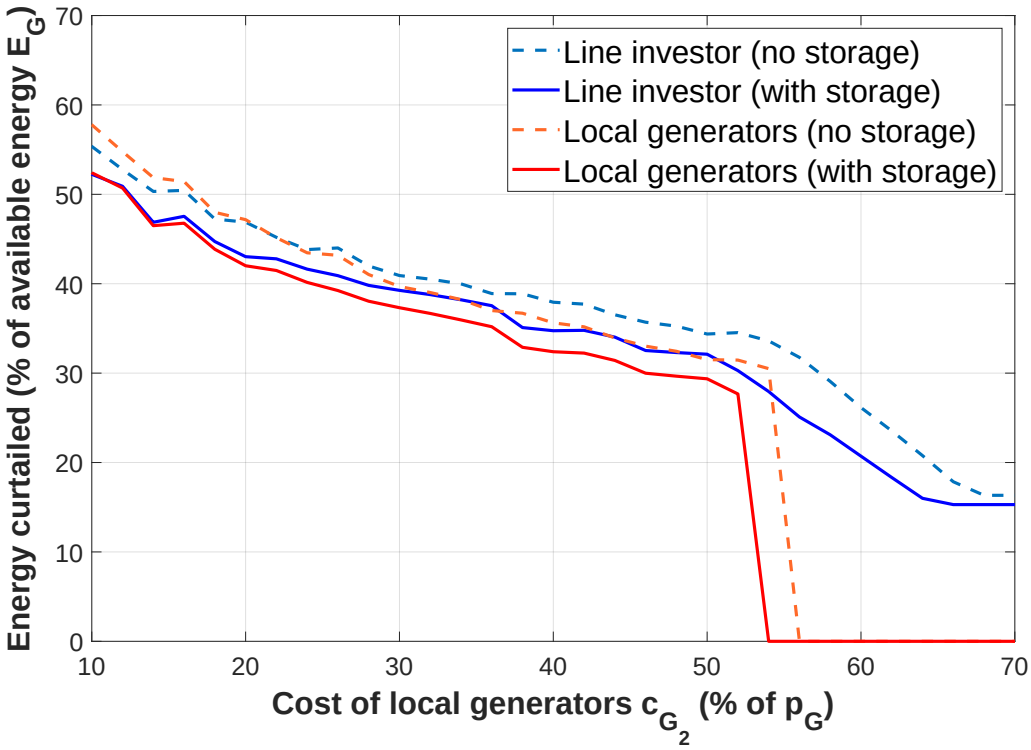

Fig. 7.24 Scenario 2: Curtailed energy as a percentage of available energy at equilibrium with and without storage

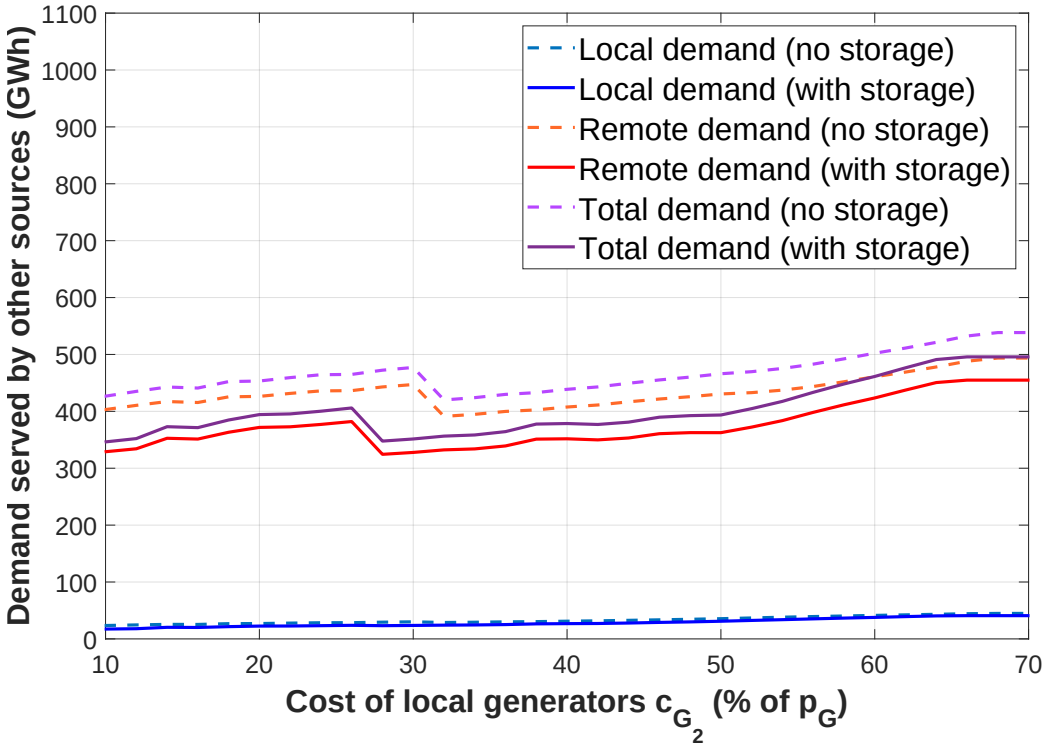

Fig. 7.25 Scenario 2: Demand served by other sources with and without storage

(about 20% according to model assumptions). Moreover, local investors are not charged for transmission when serving the local demand. Furthermore, local demand is also prioritised over remote demand D due to lower energy losses. All these factors contribute to lower magnitude increase in local demand served rather than in remote demand. Fig. 7.25 shows that larger penetration of RES generation is possible with the introduction of energy storage in energy systems.

7.5.3 Scenario 3: Varying p_T

The third scenario shows how the equilibrium results depend on the transmission fee p_T. Other cost parameters remain fixed $c_{G_1} = 0.36p_G$, $c_{G_2} = 0.30p_G$, $p_S = 0.10p_G$, $c_S = £15,000/\text{MWh}$, $p_G = £74.3/\text{MWh}$ and $c_t = £76,666.67/\text{MW}$, while p_T varies from $0.10p_G$ to $0.90p_G$ with a step of $\delta p_T = 0.02p_G$.

Fig. 7.26 shows the generation capacity installed by the players for varying transmission fee p_T and Fig. 7.27 shows the profits at the Stackelberg-Cournot game equilibrium.

As shown in Fig. 7.26, total generation capacity in location B decreases, as p_T increases, due to local generators installing less capacity. The leader's generation capacity is relatively constant with varying p_T, and increases slightly for large values of p_T. On the contrary, the leader responds to the increase of p_T by increasing the transmission capability of the power line installed. Generation capacity installed by local generators decreases with p_T, as expected, due to higher transmission costs and inability to serve remote demand. A transmission fee of $p_T = 0.10p_G$ is sufficient for the line investor to build

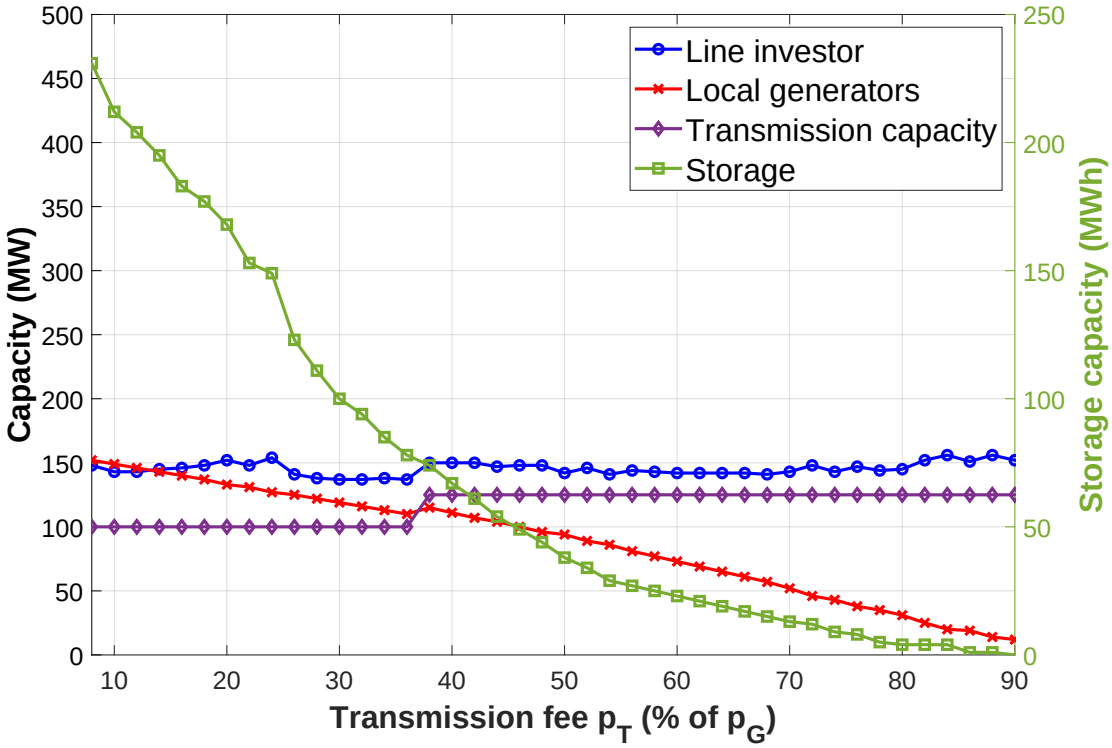

Fig. 7.26 Scenario 3: Generation capacity installed at equilibrium and dependence on the transmission fee. Storage capacity value is shown in green color and on the right y-axis, while all other variables are shown on the left axis.

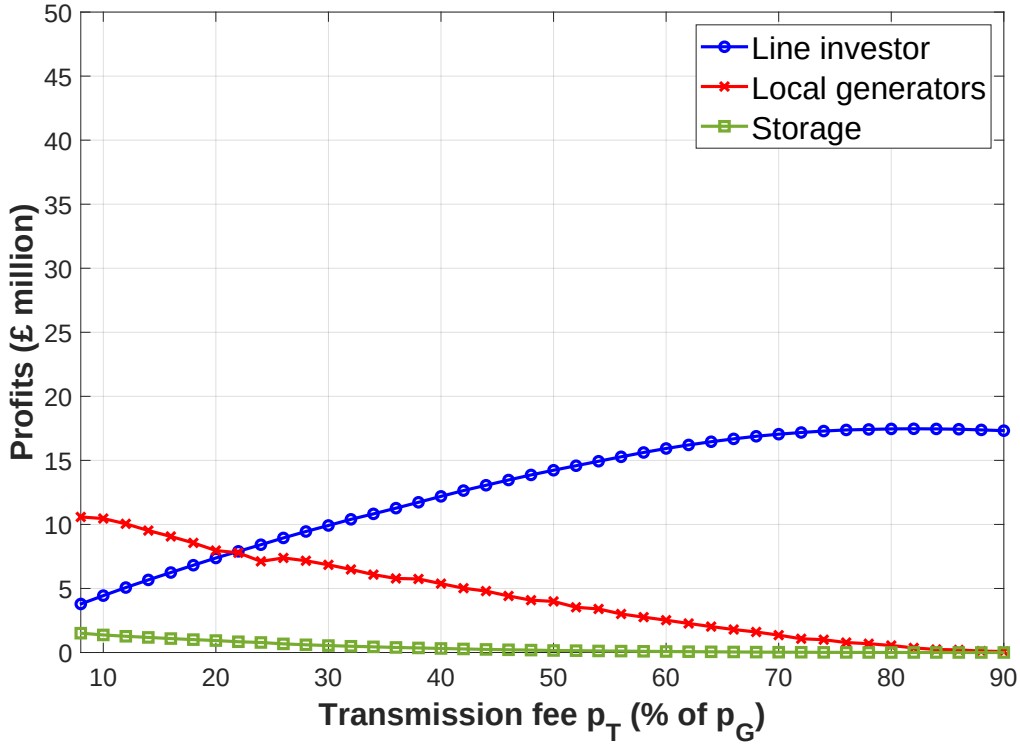

Fig. 7.27 Scenario 3: Profits at equilibrium and dependence on the transmission fee

larger generation capacity than local generators, despite the fact that $c_{G_1} > c_{G_2}$. However, the line investor achieves greater profits than the local investors only for greater values of transmission charges $p_T \geq 0.22 p_G$. Local generators' profits reduce as p_T increases and P_{N_2} decreases. Storage capacity decreases as total RES capacity drops, mainly caused by the local generators installing less generation capacity. Storage capacity ranges from 212 MWh to 0 MWh for $c_{G_2} = 0.10 p_G$ to $c_{G_2} = 0.90 p_G$. The transmission capacity increased from $T = 100$ MW to $T = 150$ MW from $c_{G_2} = 0.36 p_G$ to $c_{G_2} = 0.38 p_G$. In other areas, transmission capacity remains unchangeable. Profit functions follow similar trends to the growing or reducing generation capacity installed. Storage player's profits are significantly lower in magnitude than other players in the game and despite presenting a large range in the rated storage capacity installed. The storage investor may purchase energy only in the case there is a RES oversupply. Moreover, it is allowed to serve the demand only when this cannot be satisfied by renewable generators. The storage investor also incurs significant costs, related to the installation of storage capacity itself, but also charges for transmission and energy purchase by renewable generators.

Fig. 7.27 shows that high transmission fees might negatively impact the uptake of RES generation and storage by local producers. On the other hand, when transmission charges are set low, the line investor can still make a profit, as the transmission line permits him to access the demand at the remote location A. The line investor also generates revenue from serving the local demand and from trading with the storage player. Storage capacity drops as p_T increases in direct correlation with the total generation capacity installed by RES investors. An interesting observation is that the leader reacts to other investors capacity being reduced and higher transmission fees, by first increasing the line's transmission capacity, instead of increasing his RES capacity installed.

It is also worth exploring here, the difference between the capacities installed at the equilibrium of the game, before and after the introduction of storage. When no storage is present, the game reduces into a Stackelberg game between the line investor and local generators. The behaviour of players in this game was studied extensively in previous chapters of this thesis. Fig. 7.28 shows the generation and transmission capacity installed by the line investor at the equilibrium of the game with and without storage. It is shown in Fig. 7.28 that the line investor can increase the RES capacity installed, while also increasing his profits, as in Fig. 7.30, when storage is introduced. The profit margin increase is larger for lower values of p_T. For the line investor, profits are higher due to an increase of the capacity installed, but also because the line investor can generate additional revenue from the storage player by both trading (charged with p_S) and transmission (charged with p_T). Note here, this result is not obvious, as in the case of RES shortage, the storage investor and RES generators compete for serving the demand on equal terms (Pro Rata access rules). This may be a significant factor in the different behaviour observed for local generators. Fig. 7.30 shows similar or minor reduction in local generators profits as p_T increases, when storage is introduced. Fig. 7.29 shows that profit values are largely affected by the minor reduction in generation capacity installed by local generators and higher transmission fees. Local generators are also affected by competition with the storage investor. Recall here

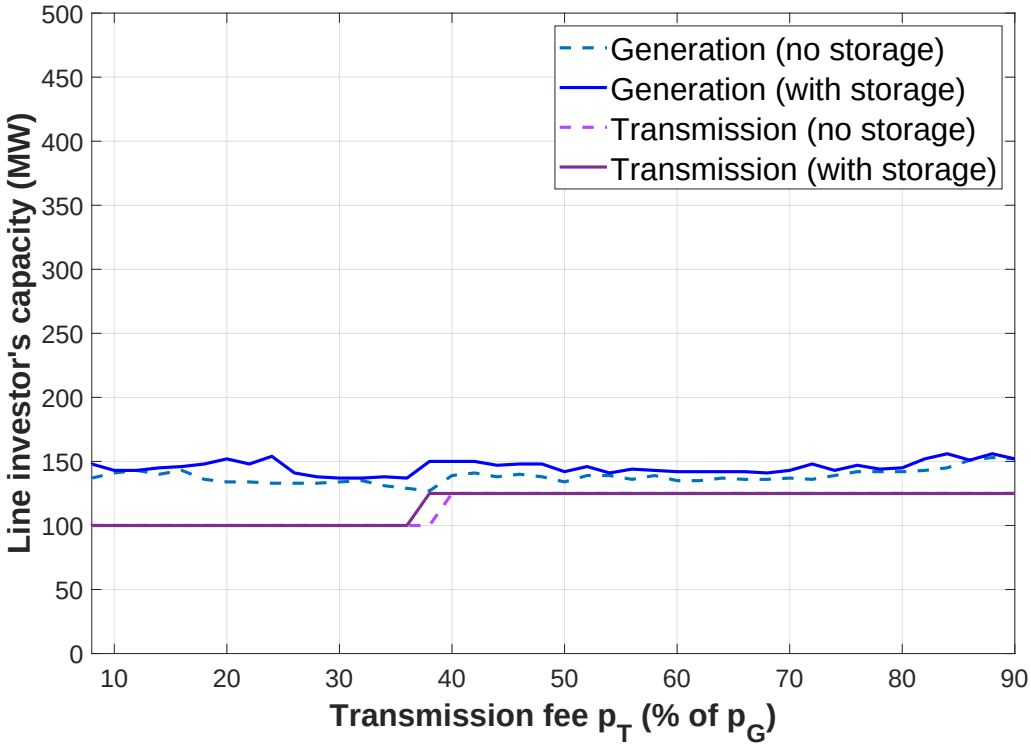

Fig. 7.28 Scenario 3: Line investor's generation and transmission capacity with and without storage

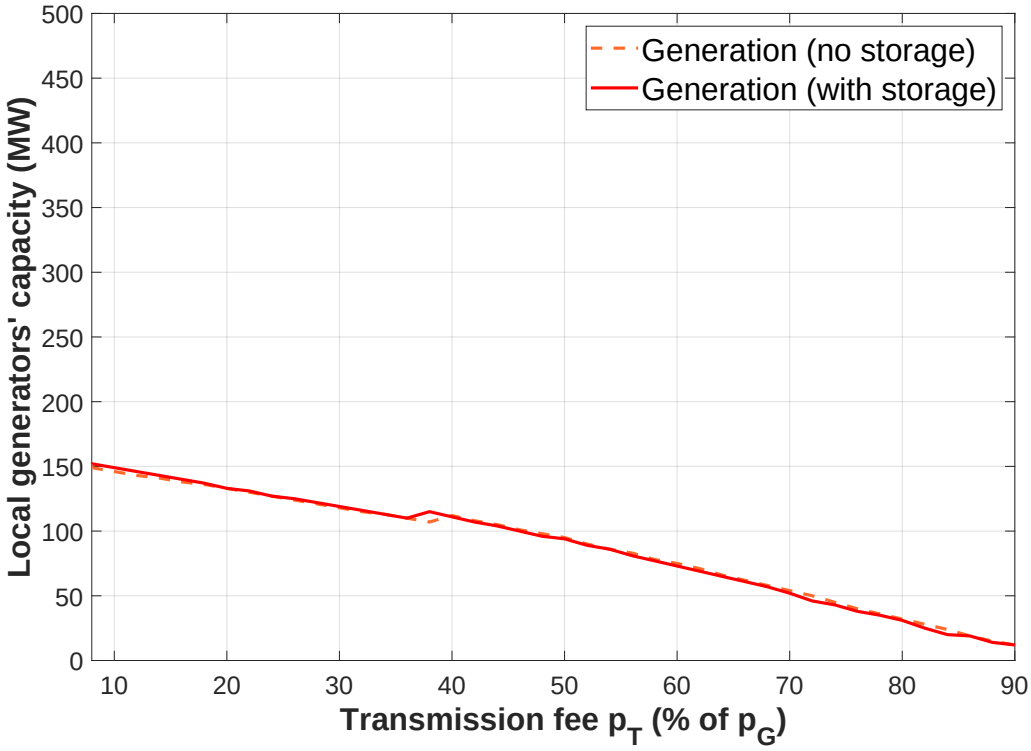

Fig. 7.29 Scenario 3: Local generators generation capacity with and without storage

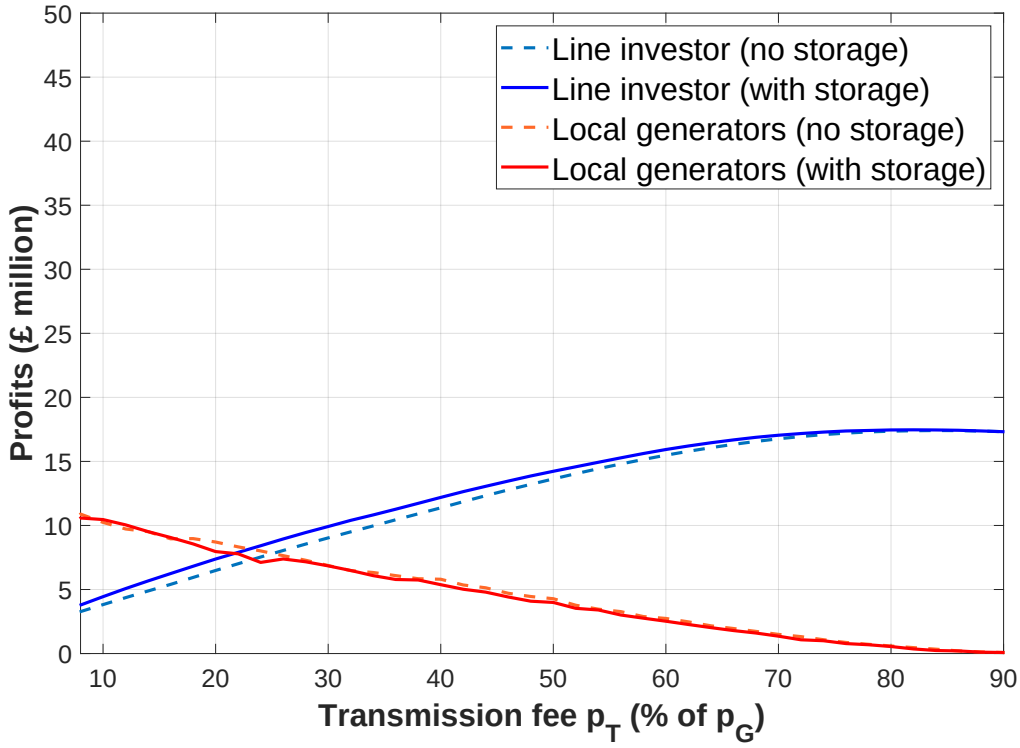

Fig. 7.30 Scenario 3: Profits of line investor and local generators at equilibrium with and without storage

that local generators can also increase their revenues by trading their energy surplus with the storage system, however, they compete with storage when there is a shortage of supply. The introduction of storage brings slightly lower profits for local generators, as they are slightly worst off. On the contrary, the line investor can increase his profit in all the range of the parameter p_T under study.

An important aspect to compare is the curtailment imposed to the energy system with and without energy storage. As shown in Fig. 7.31, the curtailment issue is not eliminated. In fact, curtailment happens when storage devices have already reached their maximum storage capacity, therefore excess power generated by RES producers, needs to be curtailed. Low transmission charges p_T, cause a larger deployment in RES capacity installed, especially by local generators, leading to high curtailment rates reaching approximately 43.8% of the potential RES capacity.

Storage devices, however, managed to reduce total curtailment up to 7% and up to 76 GWh ($p_T = 0.10 p_G$). For very large transmission charges a small increase in curtailment is observed. Fig. 7.32 shows a breakdown of energy curtailed by individual RES investors.

Finally, Fig. 7.33 shows how a significant decrease in the demand (local or remote) served by other sources in the energy system. Most significant increase is shown in the remote demand served. Local demand d is significantly lower than remote demand D (about 20% according to model assumptions). Moreover, local investors are not charged for transmission when serving the local demand. Furthermore, local demand is also prioritised over remote demand D due to lower energy losses. All these factors contribute to lower

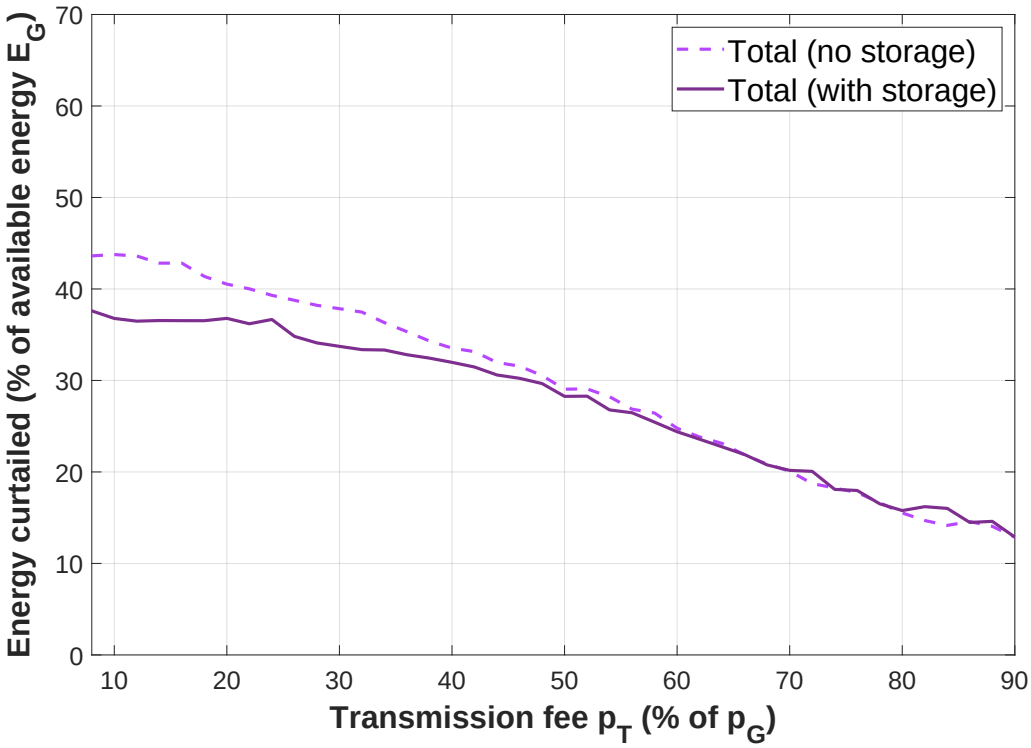

Fig. 7.31 Scenario 3: Total curtailed energy as a percentage of available energy at equilibrium with and without storage

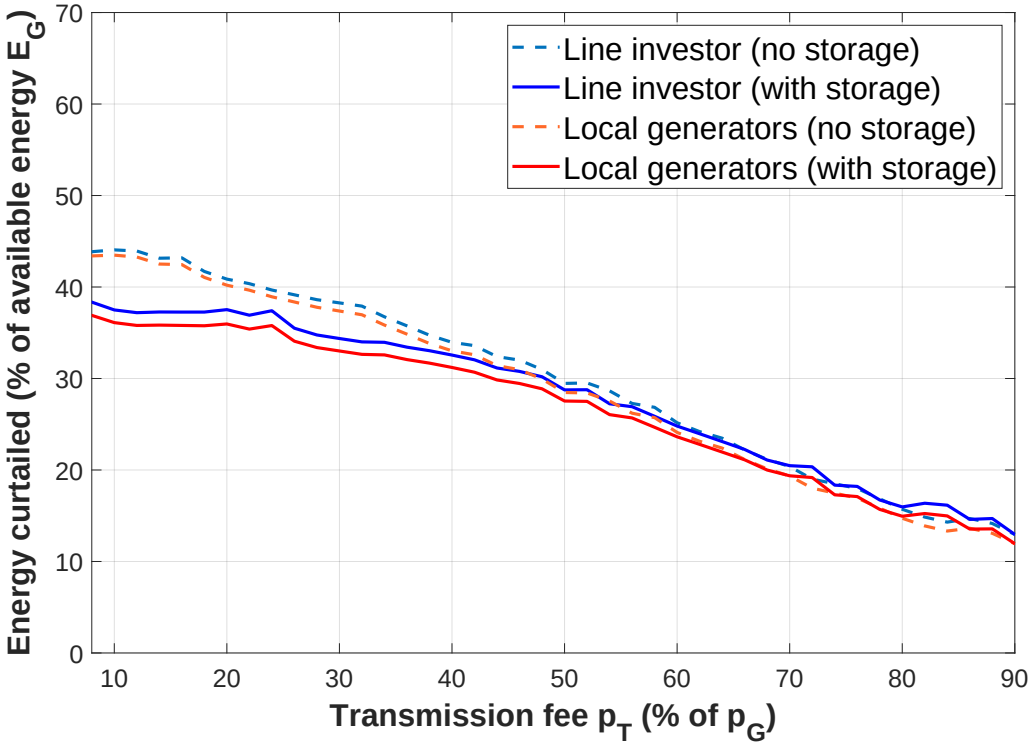

Fig. 7.32 Scenario 3: Curtailed energy as a percentage of available energy at equilibrium with and without storage

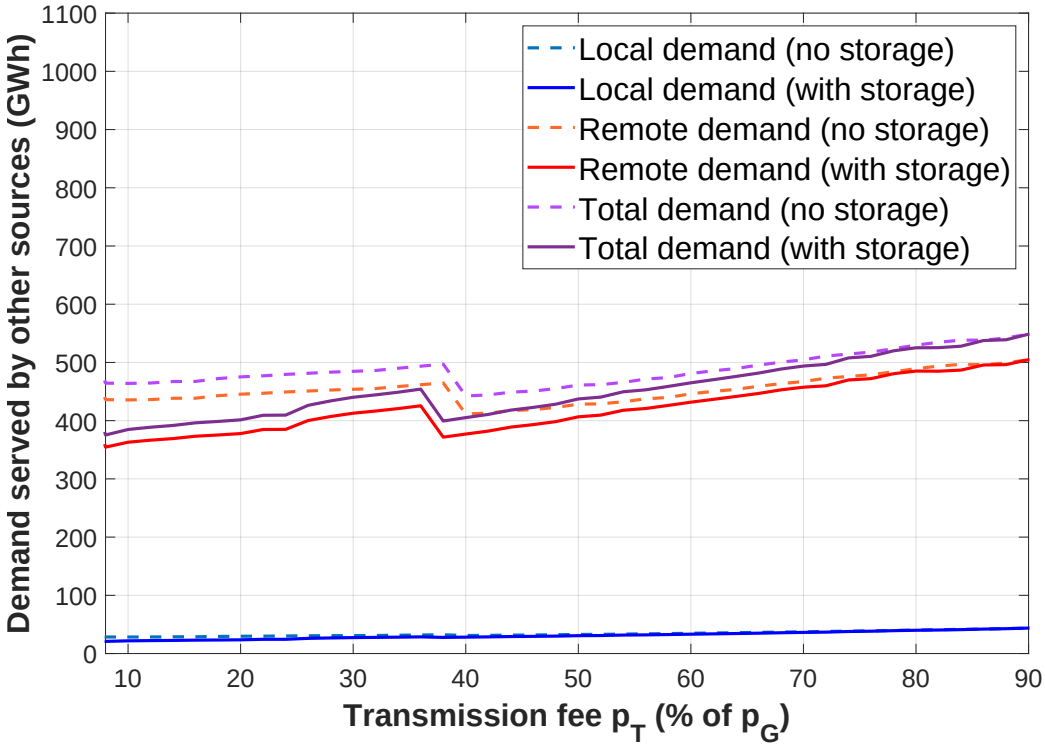

Fig. 7.33 Scenario 3: Demand served by other sources with and without storage

magnitude increase in local demand served rather than in remote demand. Fig. 7.33 shows that larger penetration of RES generation is possible with the introduction of energy storage in energy systems. The decrease in values observed after $p_T \simeq 0.36 p_G$ is caused by an increase in transmission capacity installed by the line investor.

7.5.4 Scenario 4: Varying p_S

The fourth scenario shows how the equilibrium results depend on the transmission fee p_S. Other cost parameters remain fixed $c_{G_1} = 0.36 p_G$, $c_{G_2} = 0.30 p_G$, $p_T = 0.30 p_G$, $c_S = £15,000/\text{MWh}$, $p_G = £74.3/\text{MWh}$ and $c_t = £76,666.67/\text{MW}$, while p_S varies from 0 to p_G with a step of $\delta p_S = 0.02 p_G$.

The capacity results installed by players at the game equilibrium are shown in Fig. 7.34. Storage capacity decreases as the storage fee increases. Recall here that the storage fee p_S represents the cost for purchasing energy from RES investors. Increase of p_S beyond 40% of p_G results in no storage capacity installed, as charges for energy purchased make investing in energy storage not profitable. The storage player purchases only energy that would otherwise have been curtailed, therefore in practice p_S charges can be set quite low. Moreover, the effect of p_S on generation and transmission capacity installed is not significant, with most variables remaining approximately constant.

The profit results are shown in Fig. 7.35. The storage player's profits decrease as p_S increases. Line investors profits decrease slightly as the storage capacity decreases, while local generators capacity shows a slight increase. For the cost parameters assumed in

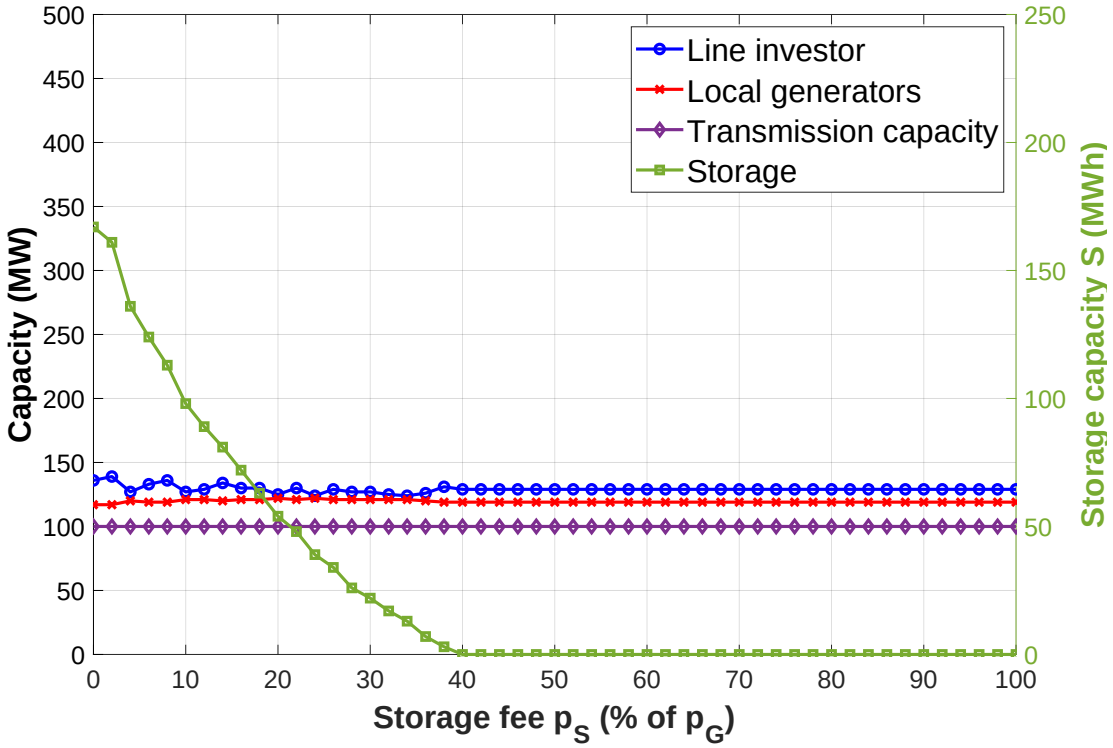

Fig. 7.34 Scenario 4: Generation capacity installed at equilibrium and its dependence on the storage fee. Storage capacity value is shown in green color and on the right y-axis, while all other variables are shown on the left axis.

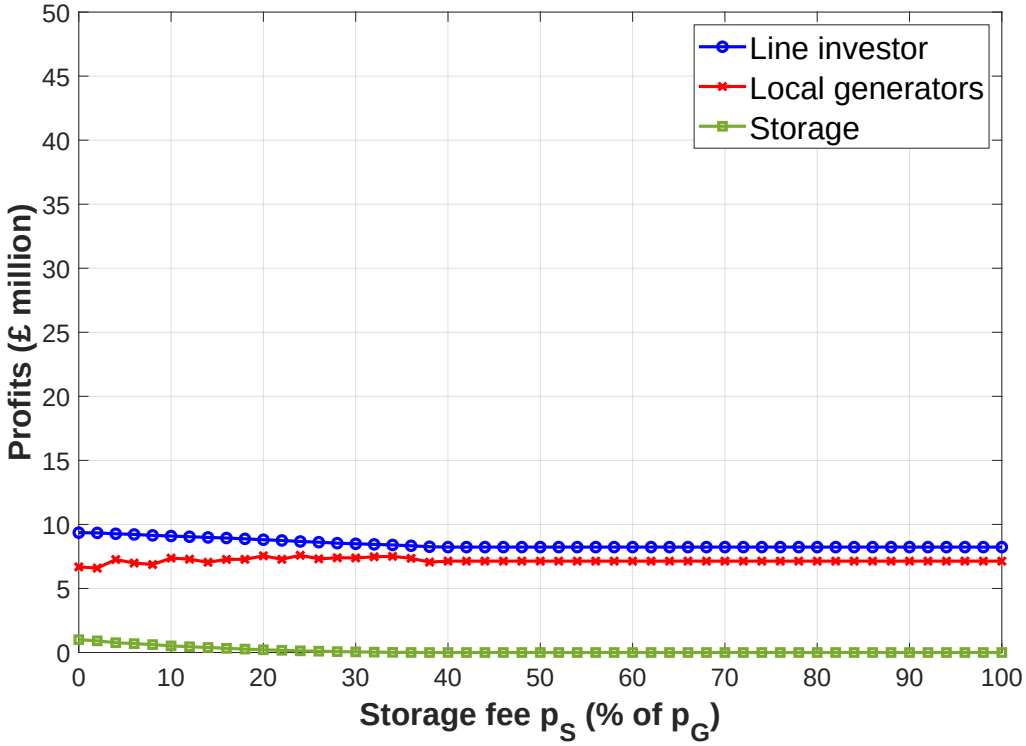

Fig. 7.35 Scenario 4: Profits at equilibrium and their dependence on the storage fee

Scenario 4, when $p_S = 0$ the storage capacity is equal to 167 MWh and generates a profit of $\simeq £1m$. When p_S increases to $0.20p_G$, the storage capacity drops to 54 MWh and profits fall to $£0.212m$. This equals to 68% drop in storage capacity and a 79% drop in the storage player profit.

7.5.5 Scenario 5: Varying c_S

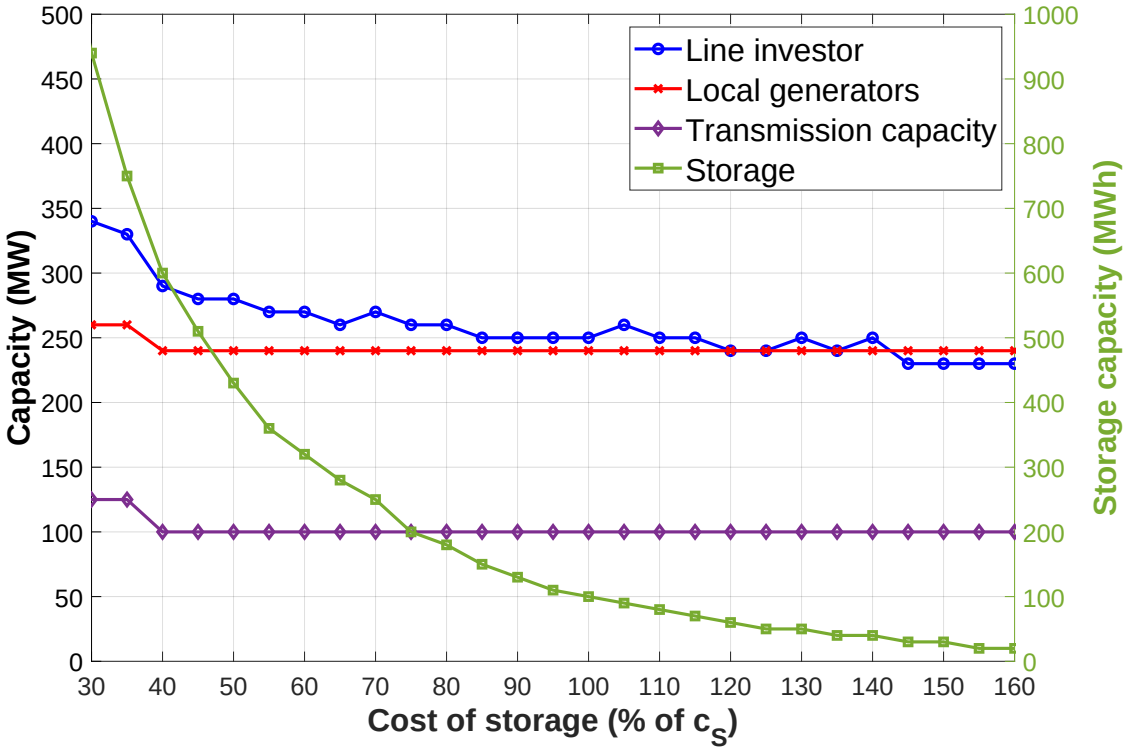

Fig. 7.36 Scenario 5: Generation capacity installed at equilibrium and its dependence on the cost of storage. Storage capacity value is shown in green color and on the right y-axis, while all other variables are shown on the left axis.

The fifth scenario shows how the equilibrium results depend on the cost of storage c_S. Other cost parameters remain fixed $c_{G_1} = 0.36p_G$, $c_{G_2} = 0.30p_G$, $p_T = 0.30p_G$, $p_S = 0.10p_G$, $p_G = £74.3/\text{MWh}$, $c_t = £76,666.67/\text{MW}$ and $c_S = £15,000/\text{MWh}$. The cost of storage in this scenario varies from $0.30c_S$ to $1.60c_S$ with a step of $\delta c_S = 0.05c_S$.

The capacity results installed by players at the game equilibrium are shown in Fig. 7.36. The value of $c_S = 100\%$ represents the current cost of storage. Values lower than 100% represent different levels of cost storage reduction, up to 30% of the current value, while larger values represent potentially higher costs. Figures up to 160% of current costs were examined. Higher costs may also represent other storage technology types that are more expensive. Storage capacity is equal to 100 MWh for current prices and varies from $950 - 10$ MWh as the cost of storage increases. As expected, Fig. 7.36 shows a significant drop in the storage capacity installed at equilibrium, however the reduction is not linear. This result indicates that further reduction in storage costs could lead to massive adoption of storage devices. For very low costs $c_S = 30\% - 35\%$, increased storage capacity leads

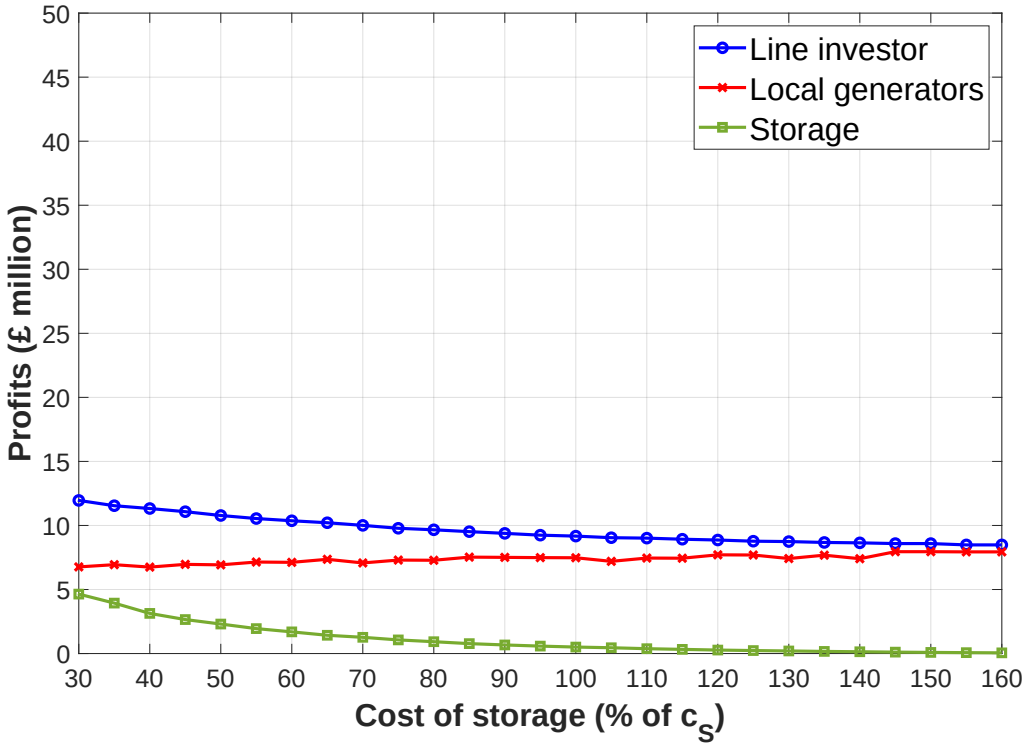

Fig. 7.37 Scenario 5: Profits at equilibrium and its dependence on the cost of storage

to higher generation capacity installed by RES investors and higher transmission capacity. Generation capacity installed by the line investor drops slightly as cost of storage increases, while capacity from local generators and transmission capacity remains largely unaffected. Local generators benefit from less competition when serving the demand as less storage is installed. Recall here that RES investors can generate higher revenues by trading their energy surplus with the storage player, but they also engage in competition when there is RES shortfall. The transmission capacity also appears largely unaffected, however the step size considered for T in the simulations was quite large 25 MW, therefore any trends in the reduction in T may take a smaller step size to show.

Similarly, the results on profits achieved by players at the equilibrium of the game are shown in Fig. 7.37. Storage and line investor's profits decrease as the cost of storage increases. An interesting result shown here is that local generators profits slightly increase, as storage costs increase, despite the fact that the generation capacity remains unaffected. This result is due to the line investor installing less generation capacity, leading to larger participation of local generators in serving the demand.

7.6 Discussion of results

The scenarios presented in Section 7.5 were developed to explore the dynamics of the Stackelberg-Cournot game and its equilibrium properties for a wide range of cost parameters. For each scenario, the value of the tested cost parameter varies, while other financial parameters remain fixed.

Scenarios 1-3 showed that the total generation capacity installed by RES investors decreases, as the tested parameter value increases. RES generation investors, i.e. the line investor and local generators, install less capacity as their individual generation cost increases. Reduction on one type of investor RES capacity benefits their opponents (other RES investor), who may respond by increasing their own generation capacity. For example, results from Scenario 1 show that P_{N_1} decreases with c_{G_1}, while local generators increase P_{N_2}. In a similar fashion, in Scenario 2, local generators decrease P_{N_2} as c_{G_2} increases, while P_{N_1} increases. In Scenario 3, P_{N_1} is relatively constant (it increases slightly for large p_T), while P_{N_2} decreases.

The storage player also invests in smaller storage capacity as the storage fee p_S (Scenario 4) or cost of storage c_S increases (Scenario 5). In scenarios 1-3, storage capacity decreases as RES generation installed by the line investor decreases, leading also to decreasing total RES capacity installed.

Transmission capacity remains largely unchanged, with some step changes presented within the range of the cost parameter tested in each Scenario. In Scenarios 1 and 5, T decreases while lower RES generation capacity is installed by the line investor. In Scenarios 2 and 3, T increases as more RES capacity is installed by the line investor. The transmission capacity does not show significant dependence on the storage fee p_S or the cost of storage c_S.

Profit functions have a similar behaviour to the capacity installed by players. Note here that RES players profits are not equalised when $P_{N_1} = P_{N_2}$, because of transmission charges p_T, but also because of different generation costs and cost for transmission capacity installation c_T. In all tested scenarios, the storage player's profits demonstrate significantly lower values than profits achieved by the line investor or local generators. This outcome is attributable to high installation cost for energy storage investments c_S and the additional tariff charges p_S and p_T. These costs can be substantial and are related to the installation of storage capacity itself, but also charges for transmission and energy purchase by renewable generators. The storage player has limited control over the market as he is allowed to purchase energy only when there is RES oversupply and can participate in serving the demand, only when this cannot be satisfied by renewable generation. On the other hand, energy purchased from RES generators can be charged with low prices of p_S, as it represents energy that would otherwise be curtailed.

In Scenario 3, Fig. 7.27 shows that high transmission fees might negatively impact the uptake of RES generation and storage projects by local investors. Local generators and storage player invest in lower capacity, as their profits diminish by high charges for transmission. On the other hand, when transmission charges are set low, the line investor can still make a profit, as the transmission line permits him to access demand at remote location A. The line investor also generates revenue from serving the local demand and from trading with the storage player. As p_T is set by the system regulator, the method developed here determines a feasible range that allows transmission, generation and storage capacity investments to be profitable.

Scenario 4 studied the effects of the storage p_S on the capacities installed at the game equilibrium. While the effect of p_S on generation and transmission capacities is not significant, with most variables remaining approximately constant, the results showed that an increase of p_S beyond 40% of p_G results in no storage capacity installed, as fees for energy purchased constitute investing in energy storage not profitable. However, the storage player purchases only energy that would otherwise have been curtailed, therefore in practice p_S charges can be set quite low. Suitable values for p_S can be agreed between players under the oversight of the system regulator, so that storage capacity investments are not discouraged.

A significant beneficiary in the energy system when storage is introduced is the line investor. In all scenarios under consideration (Scenarios 1-3), the line investor is able to achieve larger profits, when storage devices are deployed. The line investor is able to do so by increasing the RES capacity installed. Comparison of results with and without energy storage also show that the step change in transmission capacity is achieved for different values of the tested parameter. In Scenario 1, T reduces for $c_{G_1} = 0.30 p_G$ when no storage is deployed, compared to a reduction of $c_{G_1} = 0.32 p_G$ observed after the introduction of energy storage. In Scenario 2, T increases for $c_{G_2} = 0.32 p_G$ and $c_{G_2} = 0.28 p_G$, without and with storage, respectively. In Scenario 3, T increases for $p_T = 0.40 p_G$ and $c_{G_2} = 0.38 p_G$, without and with storage, respectively. For the line investor, profits are higher due to an increase in the capacity installed, but also because the line investor can generate additional revenue from the storage player from engaging in trading (charged with p_S) and transmission (charged with p_T). Note here, this result is not obvious, as in the case of a RES generation shortage, the storage investor and RES generators compete for serving the demand on equal terms (Pro Rata access rules).

On the other hand, in the majority of cases, local generators are slightly worst off when storage is deployed. In Scenarios 1 and 3, local generators deploy slightly less generation capacity when storage is introduced and achieve slightly lower profits. In Scenario 2, local generators achieve similar profit values for low c_{G_2} values and slightly lower profits for larger c_{G_2} values. In Scenario 2, the introduction of storage brings higher profits for local generators, only if they have a lower generation cost than the line investor. When generation costs are higher, storage does not bring significant benefits for local generators, as they are worst off. A significant factor in the different behaviour observed for local generators is the competitive game between local generators and storage. Local generators can generate additional revenue by trading energy surplus with the storage system, however, they also compete with storage when there is a shortage of supply. The outcome of the competitive behaviour is a reduction in profits for local generators. As a result, with regards to profitability, introduction of storage does not bring significant benefits for local generators, as they are slightly worst off, after storage is introduced in the game. On the contrary, the line investor is able to exploit his competitive advantage, as a first mover, to reap the benefits from the introduction of storage. This is a key finding, which is expected by the rules of the game. In real world applications, energy trading might be determined in a level-playing field in energy markets. In addition, the storage investor may achieve

additional revenue streams, by participating in flexibility markets or ancillary services for the grid. Provision of such services can significantly increase profitability and the value added by energy storage into achieving more efficient operation of energy systems.

Despite energy storage entering the market, RES generation curtailment is not eliminated. In the system with energy storage, curtailment takes place when storage devices have already reached their maximum storage capacity, hence, excess power generated by RES producers cannot be absorbed. Complete elimination of RES curtailment would require a massive storage capacity installed that in the current financial situation would not be profitable. Simulation results, however, show significant reduction in the curtailment rates imposed that reach savings up to 7% and 130 TWh.

Comparison between results with and without energy storage showed significant decrease in the demand (local or remote) served by other sources in the energy system, after utilisation of storage. Most significant decrease is shown in the remote demand served. Local demand d is significantly lower than remote demand D (about 20% according to model assumptions), therefore the largest part of d is already served by RES generators before storage is introduced. Local investors are not charged for transmission when serving the local demand and furthermore, local demand is also prioritised over remote demand D, due to lower energy losses. These factors contribute to a lower magnitude change in local demand served rather than in the remote demand served by other sources in the system. Storage introduction causes an increase in the RES capacity installed and reduces the remote energy demand served by other sources in the grid. As a consequence, results show that energy storage deployments may achieve larger penetration of RES generation in energy systems.

A sensitivity analysis was performed by investigating the cost of storage c_S in Scenario 5. Results showed a significant drop in the storage capacity installed at the equilibrium of the game, as c_S increases, however the reduction is not linear. This indicates that large reduction in storage costs, at the range of $c_S = 30\% - 35\%$ of current prices or below, could lead to massive adoption of storage devices. Large storage capacity leads to higher generation capacity installed by RES investors and higher transmission capacity. Generation capacity installed by the line investor drops slightly as cost of storage increases, while capacity from local generators and transmission capacity remains largely unaffected.

A general observation is that results from tested scenarios may fluctuate and may not be monotonic. The main reason for the behaviour observed is the empirical approach on the Stackelberg-Cournot game estimation that is based on simulation and data analysis. Traditional game-theoretic approaches employ purely theoretical studies that assume mathematical functions with properties that allow for analytical estimation of the game equilibrium. Moreover, as shown in Section 7.4.1, granularity assumed in the search space of strategy actions, dictated at a significant extent by computational limitations, combined with non-linearities introduced by storage, lead in several cases in multiple equilibria or intersection solutions that are positioned in-between actions in the discrete search space. In these cases, the equilibrium solution was approximated either by the average or the

intersection of the line segments formed by the nearest available results, respectively. The approximation process therefore may contribute to the fluctuation of the final result.

7.7 Concluding remarks

In summary, the work in Chapter 7 presented a game-theoretic approach that can model new low-carbon capacity investments, such as RES generation capacity, energy storage and network expansion projects, undertaken by private investors, who are self-interested and aim to maximise their profits. Curtailment and line access rules play a key role in the strategic game formed, the equilibrium of which can be used to determine optimal generation, transmission and storage capacity installed in such settings and their associated profits. Low-carbon technology investors form a bilevel Stackelberg-Cournot game between the leader (line investor) and multiple followers (local generators and storage investor). Followers' competitive behaviour is studied as a Cournot game. Optimal generation, transmission and storage capacities installed at the equilibrium of the game are estimated by backward induction. The simulation analysis and empirical approach for equilibrium estimation studied the dynamics of the game for a range of cost parameters that can help investors, network operators and regulators evaluate suitable tariff prices for transmission or storage, that allow low-carbon investments to be profitable. The results show that low charges for storage and transmission are able to achieve profitable investments. Most crucially, this work shows that a profitable business model is possible for energy storage investments that make use of curtailed energy from RES generation installed. It would be possible for the storage player to negotiate a low storage fee that would allow energy purchase from RES generators in a favourable price. Typical settings where this model can be applied in practice include numerous locations where demand and generation are not co-located leading to large curtailment rates.

Moreover, the results showed that energy storage can increase the total RES generation capacity built at a particular location. Leader's profits and RES generation capacity increase in all scenarios studied in this work. In fact, the analysis results show that the line investor is able to exploit his competitive advantage, as a first mover, to reap the benefits from the introduction of storage. Local generators on the other hand, are slightly worse off when storage is deployed. Local generators deploy slightly less generation capacity when storage is introduced and achieve slightly lower profits, in the majority of cases. They are able to generate larger profits only if they have a lower cost of generation than the line investor. While curtailment is not eliminated, energy storage can significantly reduce imposed curtailment up to a 7% factor. Energy storage causes an increase in the RES capacity installed and reduces the total energy demand served by other sources in the system. As a result, it is shown that energy storage deployments may achieve larger penetration of RES generation in energy systems. Finally, a sensitivity analysis on the cost of storage, indicated that large reduction in storage costs, could lead to massive adoption of storage devices.

Several extensions of the work presented in Chapter 7 are considered for future work. The current approach did not account for lifetime degradation of battery storage with usage or the development of a battery control energy management system that aims to optimally control battery operation and preserve degradation. Another extension would be repeating the analysis for multiple storage types, in addition to Lithium-ion batteries, used in the current work. Different energy storage types and costs consideration is key to identify the most promising technologies for similar applications. Consideration of different configurations in storage ownership could significantly alter the results. For example, RES investors could decide to invest in their own storage capacity or they can jointly invest in a common storage system. Fair allocation of profits generated by co-owned storage system is of interest especially as RES generators may have invested in dissimilar generation capacities. Different configurations would lead to significant changes in the strategic games formed between low-carbon investors. Finally, the game could be expanded to consider for numerous local investors, each modelled as an individual agent. This would lead to an interesting formulation of the game and a model of distributed storage.

Chapter 8

Conclusions

Research work in this thesis studied the effects of curtailment and line access rules to strategic decision-making of privately developed generation, transmission and energy storage infrastructure. Procedures on how renewable generators get grid access and how curtailment is applied, are key factors that determine, to a significant extent, the interplay between investors and their decisions on capacity investments. This dissertation investigated the effect of curtailment strategies and flexible interruptible connections, imposed to variable and intermittent renewable generators, on the viability of RES investment projects. Critical features and characteristics of curtailment rules, such as fairness, were discussed along with their effect on existing and future volumes of renewable energy generation capacity, installed and connected to electricity grids.

A game-theoretic framework was produced to address challenges caused by excess renewable generation at constrained grid areas with notable curtailment. Settings where one private investor develops the required infrastructure to access the grid and multiple low-carbon technology projects (such as wind generation and energy storage) can use this infrastructure against the payment of a transmission fee, were considered in this thesis. Stackelberg and Cournot game formulations were utilised to model private low-carbon technology investors, as self-interested and profit-maximising entities that act autonomously in order to achieve their own local objective. Strategy actions of players on the optimal capacity installed are interdependent on strategies adopted by opponents. Theoretical formulations of the strategic games were produced conjointly with practical applications of the theoretical models to relevant case studies. Empirical solution concepts and algorithmic approaches were developed for game equilibrium estimation of optimal capacity decisions for a wide range of cost parameters. The solutions proposed rely on detailed simulation analysis for players' payoff estimation, as opposed to smooth mathematical functions. Similar approaches can be used in other game-theoretic models in the energy sector allowing for more accurate enumeration of the players' action sets and payoff functions, hence leading to more accurate estimation of the game equilibrium. Similar market frameworks can model private network infrastructure investments and help network operators to bridge the knowledge gap about setting the optimal curtailment rule

and deduce transmission charges and tariff prices for privately developed energy system assets and infrastructure.

8.1 Summary of research work

Proliferation of RES generation and deregulation of the energy markets pose new challenges to the ever changing energy landscape. Generating assets and energy system infrastructure are increasingly decentralised and owned by independent agents, who act with the aim of satisfying their own private objectives. In this light, game-theoretic modelling and multi-agent techniques are required to model agent behaviours and their interactions. One emerging issue is the unprecedented growth in renewable generation curtailment. Methods to tackle curtailment include operational techniques, such as smart interruptible renewable connections and curtailment strategies, network expansion, energy storage and the development of local energy marketplaces that aim to match renewable supply to local demand. A literature survey on the techniques applied to minimise curtailment was presented in this thesis. The innovative technology of blockchain or distributed ledgers is recently being reported as a potential enabler of smart local energy marketplaces, hence, a detailed literature review on the potential of the technology was also part of this research work.

The first part of the research work undertaken studied the impact of curtailment rules applied in several countries, including the UK, on the economic performance of renewable generators and the aggregate generation capacity investment at a certain location. Three widely used curtailment rules were considered, LIFO, Pro Rata and Rota. Their effect on the capacity factor of wind generators was also estimated. Upper bounds of tolerable curtailment at a given location were assessed and the effects of renewable resource spatial correlation on the resulting curtailment. The analysis performed highlighted the importance of fair allocation of curtailment among generators. In fact, network operators face a significant knowledge gap about how to implement curtailment rules that achieve desired operational objectives, but at the same time minimise disruption and economic losses for renewable generators. In this context, this thesis showed that equal allocation of imposed curtailment resulted in maximisation of the renewable generation capacity installed at a certain area. A new curtailment rule was proposed, called FRR, that abides by this criteria and ensures equal share of curtailment among generators of unequal rated capacity.

A long-term solution to dealing with curtailment is network expansion. Investment in additional grid capacity, however, is costly, therefore, from a public policy viewpoint, privately developed network infrastructure is highly desirable. A key knowledge gap faced by network operators and regulators is how to incentivise privately developed network upgrades projects, that could prove beneficial, especially in cases where several distributed generators can use the same power lines against the payment of a transmission fee (‘common access’ line rule). Line access rules and curtailment play a crucial role in network capacity investments. To study this, a two-node transmission model was considered and two agent types, a line investor, who builds a transmission line and RES

generation, and a second agent representing local RES generators. Both agents access demand via the same transmission line. This formulation leads to a leader-follower Stackelberg game with the line investor having the 'first mover advantage' and local generators acting after observing the leader's actions. Moreover, two agent settings were assumed in this work, myopic and strategic agents, who are able to foresight and forecast opponents' strategic moves. In the first case, a relation that makes investments profitable was established between the curtailment rate and transmission capacity installed. In the second case, decisions on optimal (and interdependent) renewable capacities built by investors were determined in the equilibrium of the game.

Strategic behaviour of agents was first examined for a simple model and assumptions based on average values of RES production and demand over a larger time horizon. This achieved a closed-form, analytical solution of the game equilibrium and an investigation of equilibrium properties for a wide range of cost parameters.

Subsequently, a refined model was developed with the ability to capture stochastic RES production and variability of energy demand. A theoretical formulation of the problem was presented along with an empirical algorithmic approach for game equilibrium estimation that utilised large datasets of wind speed and demand data. The proposed method for equilibrium assessment represents a general framework that is applicable to locations where there is excess of renewable generation capacity, and where sufficient data is available.

Effectively however, limited data may be available or data may be erroneous and experience significant gaps. To deal with this issue, a MCMC method for generating time series data was developed, based on Gibbs sampling. The technique allowed for exploration of the solution space for future scenarios of generation and demand by repetition of the simulation analysis with different time series data. The process is of great importance for reducing uncertainties regarding decisions taken by investors on optimal generation capacities to be installed.

The last part of this work was devoted to the study of energy storage that could reduce curtailment or defer network upgrades. An extension of the game-theoretic model was considered consisting of a line investor, local generators and a third independent storage player, who can absorb part of the renewable production, that would otherwise have been curtailed. Optimal transmission, generation and storage capacity decisions were determined by the computation of the Stackelberg-Cournot game equilibrium formed between the line investor (leader) and local investors of generation and storage (followers). The equilibrium properties were studied for different scenarios and financial parameters. A comparison of the energy system before and after the introduction of energy storage revealed the value added by storage devices for achieving reduction of curtailment and further integration of renewables.

All models proposed in this thesis were validated and applied to a practical setting of a grid reinforcement project, in the UK, and a large dataset of wind speed measurements and demand. Algorithmic approaches based on large dataset analysis were developed for the assessment of the equilibria formed and determination of optimal decisions. The game-theoretic modelling solutions proposed in this thesis rely on direct enumeration of

the players' utility functions (payoffs) from simulation analysis and energy system control algorithms, as opposed to smooth mathematical functions. Similar approaches can be used in other game-theoretic models in the energy sector allowing for more accurate estimation of the game equilibrium.

Overall, this thesis studied the interplay among self-interested and independent low-carbon investors, at areas of excess renewable capacity with network constraints and high curtailment. The work proposed mechanisms for setting suitable charges for transmission and trading that ensure the transmission line gets built, but also investors from the local community can benefit from investing in renewable energy and energy storage. In summary, the results of this work showed how game-theoretic modelling frameworks can help network operators to bridge the knowledge gap about setting optimal curtailment rules and determining appropriate tariffs for privately developed energy system infrastructure.

The following section digs deeper into the novelty and contributions of the work presented in this thesis and the main conclusions reached by the analysis and model development.

8.2 Research contributions revisited and main conclusions

As stated in Section 1.2 of the Introduction of this thesis, the broader objective of the work was *to explore how game-theoretic and artificial intelligence techniques can address challenges caused by excess renewable generation at areas of the grid with network constraints and significant volumes of curtailment.* Methodologies and model formulations produced in this work are relevant to the fields of smart energy systems, energy economics, game theory, artificial intelligence and multi-agent systems. Main research contributions, model outputs and conclusions of this work can be summarised below:

- **Comprehensive review of the topic of renewable curtailment**:

  First of all, this thesis provided a detailed analysis, description and comparison of curtailment rules and practices applied by network operators for curtailment allocation in ANM schemes. The literature survey revealed that curtailment rules may significantly impact the profitability of existing renewable generators and future RES development. Theoretical assessments to evaluate curtailment rules were found in the literature, however, effects of curtailment rules in RES capacity investments, but also in transmission capacity were not formalised and required further investigation. This knowledge gap was addressed in this work by the provision of a principled study of curtailment rules and their impact on renewable and transmission capacity.

  Second, the thesis provided a state-of-the-art analysis on game-theoretic and economic models that are suitable for analysing market behaviour and strategic decision-making of investors in settings where renewable curtailment plays a significant role. Literature review on game-theoretic modelling for network upgrades and generation capacity investments shows a shortfall in works that jointly consider transmission and generation expansion, while also considering curtailment and line access rules.

Research works have studied transmission constraints and congestion, however to the best of our knowledge, the current work was one of the first to study the effect of commercial agreements, curtailment and line access rules, in settings of private grid reinforcement.

Finally, potential solutions to dealing with the issue of curtailment were also investigated in the literature survey of this work, including energy storage and novel technologies such as blockchain technologies.

Blockchains offer a novel way and promise secure, tamper-proof and transparent transactional or data exchanges in energy systems, including decentralised P2P energy networks. The systematic review on blockchain technologies revealed a wide range of potential applications in the energy sector, including facilitating smart grid applications and local energy markets. In relation to the topic of this thesis, i.e. the topic of curtailment and privately developed energy system assets and infrastructure, the literature review revealed several key advantages. First, when combined with smart metering infrastructure, blockchain technologies can be used to record traceability of energy flows and verify proof of origin for energy produced and consumed in energy systems. Second, in combination with smart contracts, blockchains can be used to impose curtailment rules or develop new business models for contractual arrangements between private investors, such as enforcing the rules for 'common access' grid infrastructure. Third, blockchains promise automated market platforms that could facilitate the adoption of local energy marketplaces by enabling consumers to take an active role in energy systems and change their behaviour towards energy usage. Smart local energy marketplaces may lead to better matching of locally produced renewable supply to local demand, hence may also reduce curtailment and network congestion. Finally, blockchain technologies may increase or facilitate regulatory compliance due to tamper-proof and transparent record keeping. Our literature survey was one of the first academic-led, peer-reviewed studies on blockchains and revealed a good potential, however it also found that the technology needs to mature and overcome several technical challenges that inhibit further adoption and deployment. Research efforts on technology improvements, such as scalability, sustainability and speed of transactions, are ongoing. Other challenges come from the legal and regulatory sphere and need to be addressed for mainstream adoption.

- **Effects of curtailment rules to existing and future renewable generation**

  A principled study on different curtailment strategies and their underlying properties was undertaken in this work. Network operators face a significant knowledge gap about how to implement curtailment rules that achieve desired operational objectives, but at the same time minimise disruption and economic losses for renewable generators. The effects of curtailment rules on the RES capacity installed at a particular location were studied and formalised. The results revealed that the capacity installed and profitability of different generators can differ widely under different curtailment models. Work focused on three widely used curtailment rules, LIFO,

Rota and Pro Rata. A simulation analysis for wind generation showed how these rules affect the capacity factor of RES generators in our study. Results revealed that LIFO favours early connections, since the CF of the last generator was substantially reduced. Rota might disfavour smaller size generators. Pro Rata achieved equal sharing of curtailment and similar reduction of CF across all generators. However, it required simultaneous intervention to all generators participating in the scheme. A new rule was proposed in this study (FRR), which equally allocates curtailment to generators according to their actual production, while also achieving minimal disruption. Reduced disruption was shown in the simulation results by the average number of curtailment events per generator.

This work also studied the effect of *spatial wind speed correlation* to the resulting curtailment and lost generator revenues. It was found that CF reduction is closely linked to higher correlation. This highlights the importance of geographical dispersion of RES resources, when possible, to minimise curtailment.

Next, the work focused on the long-term effects of curtailment on decisions about future investments in RES capacity. A Cournot game approach was used to determine the feasible level of RES capacity that can be built at a single location with network constraints. An upper bound of tolerable curtailment was estimated in relation to the curtailment rate at location. More specifically, it was shown that a RES project is profitable, if the curtailment rate is smaller than a threshold that depends on the economic parameters of the investment and more specifically on the ratio of the generation cost to the selling tariff price. If marginal costs of generation at a single location are equal, this threshold is the same for all generators and can characterise a particular location.

Moreover, under perfect competition analysis assumptions, it was proved that fair curtailment rules such as Pro Rata and FRR can be selected by network operators and regulators in order to maximise the generation capacity built at a single location. The generation capacity is maximised when generators are curtailed at their maximum acceptable curtailment rate. This conclusion highlights the importance of fairness when allocating curtailment. In real-world applications however, marginal costs of generators may not be known, therefore a promising approach would be the establishment of a market for curtailment and required flexibility. This would allow curtailment allocation according to the real cost of curtailment for each generator.

- **Impact of curtailment and line access rules to network upgrade expansion**

  An interesting problem studied was the effect of curtailment and line access rules to new transmission capacity. Network upgrades investments were performed by private investors. The research work developed appropriate modelling techniques that capture the strategic decision-making and interdependencies between low-carbon energy investors, modelled as self-interested agents and profit maximising agents. Two agent settings were explored, myopic and strategic agents.

The behaviour of myopic agents was examined in areas experiencing high curtailment rates. The model results showed that the transmission line investment is viable if and only if the curtailment rate (prior to the construction of the line) is higher than a threshold τ_T. Model results also showed that local generators would be willing to accept high transmission charges, which theoretically converge to the energy selling price, as long as they are able to trade even an infinitesimally larger energy that would otherwise have been curtailed and marginally increase their profits. Arguably, however, in real-world situations, such rates may not be acceptable.

The analysis for strategic agents was analysed for two cases of curtailment rules, LIFO and Pro Rata/FRR. For the latter case, the work showed that grid capacity can be built under a 'common access principle', where a private investor is granted a license to build the line, subjected to the condition he grants network access to other competing generators, who pay a transmission fee for the energy transported through the line.

A theoretical formulation of a simple model based on average values of renewable production and demand was studied, and an analytical solution provided for the optimal generation capacities were found at the equilibrium of the Stackelberg game.

Afterwards, the model was expanded in order to have the ability to capture stochasticity in renewable production and variability of demand. A theoretical analysis of the game was presented along with an algorithmic estimation of the equilibrium by utilisation of empirical game theory and large datasets of production/demand data from a real network upgrade project in the UK. The algorithmic approach developed for equilibrium estimation represents a general game-theoretic framework that can be applied in areas where supply and demand are not co-located and sufficient data is available. Moreover, the formulation used energy system control algorithms and simulation analysis to enumerate the players' utility functions, which were then used to inform the equilibrium estimation. Similar solution concepts can be used in other energy-related settings with game-theoretic formulations for payoff and equilibrium estimation. Equilibrium properties and evolution of the Stackelberg game were studied for a wide range of cost parameters, including dependence on agent cost of generation and transmission fee. Results identified a feasible range for transmission charges that allows both transmission and generation capacity investments to be profitable.

As a result, this work developed a game-theoretic model that enabled network operators to bridge the knowledge gap of incentivising privately developed grid infrastructure, especially in settings where multiple generators can share access through the same transmission line, and determining suitable transmission charges. Shared-capacity line models can also be used in privately developed grid infrastructure settings. In real-world settings, the line investor would be inclined to share grid access if there is spare capacity or RES resources are not correlated, and would prefer a LIFO type of rule. Limitations on such schemes are associated with increased

capital costs and risks. Investments on larger capacity lines, in expectation that other generators might connect and use the line, are very expensive and hold huge risks. Finally, regulatory challenges may inhibit such schemes.

- **Technique for data generation and multiple simulation of future events**

  Practical applications and algorithmic approaches developed for the estimation of the Stackelberg game equilibrium rely on the availability of large datasets and followed a single-shot approach. However, in real-world settings, only limited data may be available or data may experience significant gaps. This work showed that significant improvement on these issues is possible. A Gibbs sampler was used to generate observations from historic resource and demand data in order to simulate multiple future scenarios. Generated data display correlation in the same fashion as real data available. This allowed for multiple iterations of the simulation analysis with different time series data, on the principles of Markov Chain Monte Carlo (MCMC) analysis, that allowed the exploration of the solution space for multiple future scenarios, leading to a reduction of uncertainties when considering future renewable generation capacity decisions. A significant limitation of the method is that adequate historic data are required for the sampling procedure to be reliable.

- **Value of energy storage in network expansion with renewable generation**

  Evaluation of energy storage was accomplished by the extension of the work to a three-player game, consisting of a line investor, local generators and a third independent storage player, who can purchase energy from renewable generators that would otherwise have been curtailed. The model can estimate optimal capacity decisions on transmission, generation and storage, based on a Stackelberg-Cournot game analysis. The line investor is the leader of the game, whose decision variables are the transmission capacity of the line and RES generation capacity to be installed. Local investors, i.e. local generators and storage investor, represent the followers. Followers optimal generation and storage capacities are determined at a Cournot game equilibrium. A simulation analysis and empirical algorithmic approach for equilibrium estimation was developed. The evolution of the Stackelberg-Cournot game equilibrium was studied for a range of cost parameters. Model outputs showed that investors, network operators and regulators can use game-theoretic formulations to deduce suitable tariff prices for transmission or storage, that allow low-carbon investments to be profitable.

  Model results showed that low charges for storage and transmission are able to achieve profitable investments. Most crucially, this work showed that a profitable business model is possible for energy storage investments that make use of curtailed energy from RES generation installed, although profits for storage are much lower than other investors. Moreover, it would be possible for the storage player to negotiate a low storage fee that would allow energy purchase from RES generators in a favourable price.

The main findings of the work revealed that energy storage increases the total RES generation capacity built at a particular location. Comparative results with and without storage showed that a beneficiary is the line investor, who is able to exploit his competitive advantage and raise profits in all scenarios under consideration, when storage is introduced to the game. Local generators on the other hand, are slightly worse off when storage is deployed. They deploy slightly less generation capacity when storage is introduced and achieve slightly lower profits, in the majority of cases. Local generators are able to generate larger profits only if they have a lower cost of generation than the line investor.

Moreover, model results showed that energy storage can significantly reduce imposed curtailment up to a 7% factor and may reduce the total energy demand served by other sources in the system. Hence, energy storage deployments may achieve larger penetration of RES generation in energy systems. Finally, a sensitivity analysis on the cost of storage, indicated that large reduction in storage costs, could lead to massive adoption of storage devices coupled with larger RES generation capacity installed.

- **Application of models and algorithmic approaches for equilibrium estimation in practical settings**

  All models and solution concepts of the strategic games formed between low-carbon investors in this thesis, were experimentally validated by a practical application based on realistic assumptions from the Kintyre-Hunterston grid reinforcement project, in the western coast of Scotland. Large datasets of renewable resources and electricity demand were utilised for this purpose reaching 17 years of hourly data. The direct use of data for equilibrium estimation, distinguishes this work from other works in the literature, which usually assume that profits or costs are represented bysmooth mathematical functions of special form and follow a theoretical analysis of game-theoretic approach. As opposed to the theoretical approach, we followed an alternative formulation that used energy system control algorithms and simulation analysis payoff estimation. Similar solution concepts can be used in renewable energy settings with game-theoretic modelling to allow for accurate game equilibrium estimation. Moreover, it is worth noting that, while the numerical application is specific to the UK case, the analysis and equilibrium results are general, and the underlying problem of renewable generation and demand not being co-located occurs in many other places around the globe, facing similar challenges. Therefore, results from this work can easily be replicated to model other case studies.

8.3 Future work

The following directions are appraised for future work consideration with regards to the work presented in this thesis:

- **Model extension for multiple players**

  One of the assumptions followed in this thesis is that local generators and their behaviour are represented as a single player in the game. However, local generators may act autonomously and may even experience different costs. Relaxation of the single player assumption leads to a more complex game formulation, i.e. to a leader-multifollower Stackelberg game between the line investor and multiple local generators. In this case, local generators would share the available generation capacity by playing a Cournot game between each other. The approach for the strategy followed by the line investor would be similar to the approach taken in this thesis (e.g. Chapter 7 analysis), i.e. the line investor needs to estimate the Cournot equilibrium reached between local players for each strategy of the line investor. For a given line investor's strategy, each player belonging to the class of local generators would need to determine their best response to every possible strategy followed by their opponents. An estimation of each opponent strategy would not be required, on the contrary only aggregate opponents' strategies need to be accounted for. The Cournot equilibrium would be found by the intersection of local generators' best response curves. Pragmatic estimation of the equilibrium by an empirical and algorithmic approach such as the one developed in this thesis would be challenging due to issues expected by limitation in computational resources and data granularity. To overcome such issues, a new approach for the equilibrium estimation might prove useful, such as by formulating the problem and solving it with a dynamic programming or genetic optimisation algorithm. Moreover, an interesting case study would be to follow a similar relaxation approach for the storage investor. This would lead towards a model of distributed storage (such as home battery systems or EVs) and an interesting formulation of the strategic game.

- **Model extension for multiple locations**

  The models produced in this thesis considered a two-node location. An interesting extension of the work would be to consider multiple locations for RES generation or storage, which could also lead to multiple leaders installing transmission capacity lines and multiple followers. In similar settings, a computationally tractable algorithmic approach is highly relevant due to the increased complexity of the distributed model. Moreover, transmission losses need to be accounted for. A comparison between complex and distributed model formulations to traditional approaches where network expansion is performed by the system operator would be extremely useful in order to evaluate decentralised versus centralised decision-making processes.

- **Consideration of transmission losses, real-time constraints and power flows**

  Future directions of this work need to account for power losses during transmission, so far considered negligible, and enhanced estimation of curtailment events caused by technical constraints and power flows of the energy system under study. Current work followed a techno-economic approach and used energy calculations for the

estimation of energy flows and equilibrium properties. Note here that a more realistic approach for network constraints estimation and imposed curtailment would require simulation analysis on a much smaller time scale than the hourly analysis assumed so far, to be able to capture technical constraints caused by RES volatility and demand.

- **Exploration of different renewable and storage technology types**

  An interesting future extension of the work, would be the study of different types of RES technology for more realistic estimation of curtailment. Current work focused on wind generation, as it represents the dominant RES technology in terms of market share and capacity installed in the UK. However, combination of different RES technologies and diversification of resources could minimise imposed curtailment.

  In addition, it would be of high importance, to repeat the analysis of the three-player Stackelberg-Cournot game for multiple storage technology types. Different storage technologies and different cost consideration are key factors in identifying the most promising type for applications that aim to reduce curtailment. Moreover, consideration of alternative configurations in storage ownership could significantly alter the results. For example, RES investors could decide to invest in their own storage capacity or they can jointly invest in a common storage system. In the latter case, fair allocation of profits generated by the co-owned storage system becomes of interest, especially as RES generators may have invested in dissimilar generation capacities. Fair profit allocation could be achieved by cooperative game-theoretic solution concepts, such as the Shapley value. Different configurations could lead to significant changes in the strategic game formed between low-carbon technology investors.

- **Refinement of financial assumptions and life-cycle cost of storage**

  Research work presented in this thesis could be improved by further refinement of the financial and cost assumptions and by integrating a realistic model that estimates the life-cycle cost of storage. Depreciation of future cash flows was not considered in this thesis. Moreover, per unit costs of generation, transmission and storage were considered constant and independent from the size of capacity installed. However, in realistic settings, building a larger storage system or RES capacity might have a lower cost per capacity installed, when compared to smaller-scale systems. In addition, the energy selling price in this thesis was considered constant in order to simplify the interpretation of results. A future direction of the work, however, could utilise real data from the wholesale energy market that would lead to varying tariff prices, changing with the shape of the electricity demand. Finally, current approach did not account for lifetime degradation of battery storage with usage or the development of a battery control energy management system that aimed to optimally control battery operation and preserve storage capacity and useful lifetime. Future work will develop methods to accurately estimate a cost per cycle (or partial

cycle) of the storage system based on DOD-useful cycles curve and degradation for different SOCs.

- **Creation of curtailment market**

  Efficient allocation of curtailment could be achieved by the creation of a curtailment market and flexibility services, where generators submit offers and bids for curtailment. This would allow curtailment allocation according to the real cost of individual generators, as lower-cost generators should be able to tolerate larger quantities of curtailment. In this vein, a research question of interest would be to design suitable market rules that encourage generators to report their true costs and avoid collusion and market manipulation. Generally speaking, market solutions may be preferred by regulators and are compliant with continuous trend towards deregulation of electricity markets. Hence, it would be very valuable to consider such market models in future work.

- **Blockchain-enabled management of curtailment**

  Finally, future work will investigate using blockchain technologies and transactive energy systems to track renewable curtailment arrangements. In combination with smart contracts, blockchain technologies could be used to enforce renewable curtailment rules or to enable novel contractual arrangements between private investors with shared access to energy system infrastructure. For example, blockchain technology could track use of shared transmission lines or storage devices in a local energy community. Future work will also focus on technical requirements such as scalability or speed of transactions that are required to achieve efficient operation in decentralised energy systems.

8.4 Concluding remarks

Overall, this thesis presented a framework on the study of low-carbon capacity investment and the interplay between self-interested, independent and profit-maximising agents, at areas of excess renewable capacity, with network constraints and high curtailment rates. The work proposed a game-theoretic framework for setting charges and trade tariff fees that ensure the transmission line gets built, while investors from the local community also benefit from investing in renewable energy and energy storage. Overall, the results of this work show how game-theoretic techniques can help network operators to bridge the knowledge gap about setting optimal curtailment rules and determining appropriate market models for privately developed network infrastructure.

References

[1] Aguado, J., de la Torre, S., and Triviño, A. (2017). Battery energy storage systems in transmission network expansion planning. *Electric Power Systems Research*, 145:63–72.

[2] Akasiadis, C. and Chalkiadakis, G. (2016). Decentralized large-scale electricity consumption shifting by prosumer cooperatives. In Kaminka, G. A., Fox, M., and P, B., editors, *ECAI 2016: 22nd European Conference on Artificial Intelligence*, pages 175–83.

[3] Akbari, T., Rahimikian, A., and Kazemi, A. (2011). A multi-stage stochastic transmission expansion planning method. *Energy Conversion and Management*, 52(8-9):2844–2853.

[4] Akhil, A. A., Huff, G., Currier, A. B., Kaun, B. C., Rastler, D. M., Chen, S. B., Cotter, A. L., Bradshaw, D. T., and Gauntlett, W. D. (2013). *DOE/EPRI 2013 electricity storage handbook in collaboration with NRECA*. Sandia National Laboratories Albuquerque, NM.

[5] Al Kawasmi, E., Arnautovic, E., and Svetinovic, D. (2015). Bitcoin-based decentralized carbon emissions trading infrastructure model. *Systems Engineering*, 18(2):115–30.

[6] Anaya, K. L. and Pollitt, M. G. (2014). Experience with smarter commercial arrangements for distributed wind generation. *Energy Policy*, 71:52–62.

[7] Anaya, K. L. and Pollitt, M. G. (2015). Options for allocating and releasing distribution system capacity: Deciding between interruptible connections and firm DG connections. *Applied Energy*, 144:96–105.

[8] Andoni, M. and Robu, V. (2016). *Using Stackelberg Games to Model Electric Power Grid Investments in Renewable Energy Settings*, volume 10002, pages 127–146. Springer, Cham.

[9] Andoni, M., Robu, V., and Flynn, D. (2017a). Blockchains: Crypto-control your own energy supply. *Nature*, 548(7666):158.

[10] Andoni, M., Robu, V., Flynn, D., Abram, S., Geach, D., Jenkins, D., McCallum, P., and Peacock, A. (2019). Blockchain technology in the energy sector: A systematic review of challenges and opportunities. *Renewable and Sustainable Energy Reviews*, 100:143–174.

[11] Andoni, M., Robu, V., Flynn, D., and Früh, W.-G. (2018). Gibbs sampling for game-theoretic modeling of private network upgrades with distributed generation. In *2018 IEEE PES Innovative Smart Grid Technologies Conference Europe (ISGT-Europe)*, pages 1–6. IEEE.

[12] Andoni, M., Robu, V., and Früh, W.-G. (2016). Game-theoretic modeling of curtailment rules and their effect on transmission line investments. In *IEEE PES Innovative Smart Grid Technologies Europe 2016*, Ljubljana. IEEE PES.

[13] Andoni, M., Robu, V., Früh, W.-G., and Flynn, D. (2017b). Game-theoretic modeling of curtailment rules and network investments with distributed generation. *Applied Energy*, 201:174–187.

[14] Andoni, M., Tang, W., Robu, V., and Flynn, D. (2017c). Data analysis of battery storage systems. *CIRED-Open Access Proceedings Journal*, 2017(1):96–99.

[15] Arabali, A., Ghofrani, M., Etezadi-Amoli, M., Fadali, M. S., and Moeini-Aghtaie, M. (2014). A multi-objective transmission expansion planning framework in deregulated power systems with wind generation. *IEEE Transactions on Power Systems*, 29(6):3003–3011.

[16] Armbrust, M., Fox, A., Griffith, R., Joseph, A. D., Katz, R., Konwinski, A., et al. (2010). A view of cloud computing. *Communications of the ACM*, 53(4):50–8.

[17] Asimakopoulou, G. E., Dimeas, A. L., and Hatziargyriou, N. D. (2013). Leader-follower strategies for energy management of multi-microgrids. *IEEE Transactions on Smart Grid*, 4(4):1909–1916.

[18] Back, A., Corallo, M., Dashjr, L., Friedenbach, M., Maxwell, G., Miller, A., et al. (2014). Enabling blockchain innovations with pegged sidechains. http://www.opensciencereview.com/papers/123/enablingblockchain-innovations-with-pegged-sidechains. [Accessed 15 May 2017].

[19] Baliga, A. (2017). Understanding blockchain consensus models. https://pdfs.semanticscholar.org/da8a/37b10bc1521a4d3de925d7ebc44bb606d740.pdf. [Accessed 29 Jun. 2017].

[20] Baringa Partners, U. (2012). Flexible plug and play principles of access report. Technical report, Baringa, UK Power Networks.

[21] Baringo, L. and Conejo, A. J. (2012). Transmission and wind power investment. *Power Systems, IEEE Transactions on*, 27(2):885–893.

[22] Behl, M., Smarra, F., and Mangharam, R. (2016). DR-Advisor: A data-driven demand response recommender system. *Applied Energy*, 170:30–46.

[23] Bell, K., Green, R., Kockar, I., Ault, G., and McDonald, J. (2011). Academic review of transmission charging arrangements. *A Report Produced for the Gas and Electricity Markets Authority*.

[24] Bell, M. C. (2013). Renewable energy and network sharing capacity: How do variations in wind, wave and tidal energy resources determine need for grid capacity? Technical report, Institute of Petroleum Engineering, Heriot-Watt University.

[25] Bennett, C. J., Stewart, R. A., and Lu, J. W. (2015). Development of a three-phase battery energy storage scheduling and operation system for low voltage distribution networks. *Applied Energy*, 146:122–134.

[26] Bentke, J. (2018). On-Chain vs Off-Chain. https://energyweb.atlassian.net/wiki/spaces/EWF/pages/17760291/On-Chain+vs+Off-Chain. [accessed 8 Jun. 2018].

[27] Berka, A. L. and Creamer, E. (2017). Taking stock of the local impacts of community owned renewable energy: A review and research agenda. *Renewable and Sustainable Energy Reviews*, 82(Part 3):3400–19.

[28] Blanco, H. and Faaij, A. (2018). A review at the role of storage in energy systems with a focus on power to gas and long-term storage. *Renewable and Sustainable Energy Reviews*, 81:1049–1086.

[29] Block, C., Neumann, D., and Weinhardt, C. (2008). A market mechanism for energy allocation in micro-CHP grids. In *Proceedings of the 41st Annual Hawaii International Conference on System Sciences (HICSS 2008)*, page 172. IEEE.

[30] Block, C. A., Collins, J., Ketter, W., and Weinhardt, C. (2009). A multi-agent energy trading competition. www.erim.eur.nl. [Accessed 22 Nov. 2017].

[31] BloombergNEF (2019). A Behind the Scenes Take on Lithium-ion Battery Prices. https://about.bnef.com/blog/behind-scenes-take-lithium-ion-battery-prices/. [Accessed 14 Aug. 2019].

[32] Bronski, P., Creyts, J., Crowdis, M., Doig, S., Glassmire, J., Guccione, L., et al. (2015). The economics of load defection: How grid-connected solar-plus-battery systems will compete with traditional electric service-Why it matters, and possible paths forward. https://www.rmi.org/wp-content/uploads/2017/04/2015-05_RMI-TheEconomicsOfLoadDefection-FullReport-1.pdf. [Accessed 20 Nov. 2017].

[33] Brouwer, A. S., Van Den Broek, M., Seebregts, A., and Faaij, A. (2014). Impacts of large-scale intermittent renewable energy sources on electricity systems, and how these can be modeled. *Renewable and Sustainable Energy Reviews*, 33:443–466.

[34] Burger, C., Kuhlmann, A., Richard, P., and Weinmann, J. (2016). Blockchain in the energy transition a survey among decision-makers in the German energy industry. Technical report, German Energy Agency. [Accessed 15 May 2017].

[35] Business Electricity Prices (2017). A guide to wholesale electricity pricing. Technical report. [Accessed 30 Jun. 2017].

[36] Bustos, C., Sauma, E., de la Torre, S., Aguado, J. A., Contreras, J., and Pozo, D. (2017). Energy storage and transmission expansion planning: substitutes or complements? *IET Generation, Transmission & Distribution*, 12(8):1738–1746.

[37] California Independent System Operator (CAISO) (2016). What the duck curve tells us about managing a green grid. https://www.caiso.com/Documents/FlexibleResourcesHelpRenewables_FastFacts.pdf. [Accessed 20 Jul. 2019].

[38] Castillo-Cagigal, M., Matallanas, E., Caamaño-Martín, E., and Martín, Á. (2018). Swarmgrid: Demand-side management with distributed energy resources based on multifrequency agent coordination. *Energies*, 11(9):2476.

[39] Castor, A. (2017). A (short) guide to blockchain consensus protocols. https://www.coindesk.com/short-guide-blockchain-consensus-protocols/. [Accessed 11 Nov. 2017].

[40] Centrica (2019). Cornwall local energy market. https://www.centrica.com/innovation/cornwall-local-energy-market. [Accessed 01 Aug. 2019].

[41] Chalkiadakis, G., Elkind, E., and Wooldridge, M. (2011). Computational aspects of cooperative game theory. *Synthesis Lectures on Artificial Intelligence and Machine Learning*, 5(6):1–168.

[42] Chamorro, J. M., Abadie, L. M., de Neufville, R., and Ilić, M. (2012). Market-based valuation of transmission network expansion. A heuristic application in GB. *Energy*, 44(1):302–320.

[43] Chapter 27 (2008). Climate change act 2008. http://www.legislation.gov.uk/ukpga/2008/27/contents. [Accessed 04 Apr. 2016].

[44] Chen, C. and Pecht, M. (2012). Prognostics of lithium-ion batteries using model-based and data-driven methods. In *Proceedings of the IEEE 2012 Prognostics and System Health Management Conference (PHM-2012 Beijing)*, pages 1–6. IEEE.

[45] Committee on Climate Change (2015). Road transport. https://www.theccc.org.uk/charts-data/ukemissions-by-sector/transport/. [Accessed 22 Apr. 2015].

[46] Competition and Markets Authority (2016). Energy market investigation summary of final report. Technical report, Competition and Markets Authority. [Accessed 15 May 2017].

[47] Cournot, A. A. (1897). *Researches into the Mathematical Principles of the Theory of Wealth*. Macmillan.

[48] Cox, J. (2009). Impact of intermittency: How wind variability could change-the shape of the British and Irish electricity markets, Poyry Energy. Technical report, Oxford Technical Report.

[49] Currie, R., O'Neill, B., Foote, C., Gooding, A., Ferris, R., and Douglas, J. (2011). Commercial arrangements to facilitate active network management. In *CIRED 21st International Conference on Electricity Distribution*.

[50] D'Aprile Paolo and Newman John and Pinner Dickon (2016). The new economics of energy storage. https://www.mckinsey.com/business-functions/sustainability/our-insights/the-new-economics-of-energy-storage. [Accessed 14 Aug. 2019].

[51] Day, C. J., Hobbs, B. F., and Pang, J.-S. (2002). Oligopolistic competition in power networks: a conjectured supply function approach. *IEEE Transactions on Power Systems*, 17(3):597–607.

[52] DECC (2015a). 2010 to 2015 government policy: low carbon technologies. https://www.gov.uk/government/publications/2010-to-2015-government-policy-low-carbon-technologies/2010-to-2015-government-policy-low-carbon-technologies#appendix-5-the-renewables-obligation-ro. [Accessed 25 Jul. 2015].

[53] DECC (2015b). Electricity market reform: Contracts for difference. https://www.gov.uk/government/collections/electricity-market-reform-contracts-for-difference. [Accessed 25 Jul. 2015].

[54] Deetman, S. (2016). Bitcoin could consume as much electricity as Denmark by 2020. https://motherboard.vice.com/en_us/article/aek3za/bitcoin-could-consume-as-much-electricity-as-denmark-by-2020. [Accessed 19 Jul. 2017].

[55] Denholm, P., Ela, E., Kirby, B., and Milligan, M. (2010). Role of energy storage with renewable electricity generation. Technical report, National Renewable Energy Lab.(NREL), Golden, CO (United States).

[56] Department for Business, Energy & Industrial Strategy (2016). Electricity generation costs. Technical report.

[57] Department for Business, Energy & Industrial Strategy (BEIS) (2018). DIGEST of United Kingdom energy statistics 2018 Chapter 6 Renewable sources of energy. https://assets.publishing.service.gov.uk/government/uploads/system/uploads/attachment_data/file/736148/DUKES_2018.pdf. [Accessed 26 May 2019].

[58] Diffie, W. and Hellman, M. (1976). New directions in cryptography. *IEEE Transactions on Information Theory*, 22(6):644–54.

[59] Dimeas, A. L. and Hatziargyriou, N. D. (2005). Operation of a multiagent system for microgrid control. *IEEE Transactions on Power Systems*, 20(3):1447–55.

[60] DOE (2012). Smart Grid System Report: Report to Congress in U.S. Department of Energy, Washington DC. Technical report.

[61] Edwards, P. J. and Hurst, R. B. (2001). Level-crossing statistics of the horizontal wind speed in the planetary surface boundary layer. *Chaos: An Interdisciplinary Journal of Nonlinear Science*, 11(3):611–618.

[62] EirGrid, S. (2011). Ensuring a secure, reliable and efficient power system in a changing environment. *EIRGRID, SONI Report June*.

[63] Ekins, P. (2014). Replacing the internal combustion engine: Why the future is electric. http://www.huffingtonpost.co.uk/intelligence-squared/replacing-the-internal-combustion-engine-why-the-future-is-electric_b_5018669.html. [Accessed 04 Apr. 2016].

[64] Energy Union Package (2015). A framework strategy for a resilient energy union with a forward-looking climate change policy. https://eur-lex.europa.eu/legal-content/en/TXT/?uri=COM%3A2015%3A80%3AFIN. [Accessed 30 Jun. 2017].

[65] Energy Web Foundation (2017). Energy web foundation. http://energyweb.org/. [Accessed 24 Nov. 2017].

[66] Engerati (2017). Blockchain Europe: Utilities pilot peer-to-peer energy trading. https://www.engerati.com/article/blockchain-europe-utilities-pilot-peer-peer-energy-trading. [Accessed 22 Nov. 2017].

[67] Environmental and Energy Study Institute (2019). Factsheet Energy Storage. Technical report, Environmental and Energy Study Institute.

[68] Estopier, A. L., Eyre, E. C., Georgiopoulos, S., and Marantes, C. (2013). Flexible plug and play low carbon networks: Commercial solutions for active network management.

[69] Ethereum Wiki (2017). Proof of stake FAQ. https://github.com/ethereum/wiki/wiki/Proof-of-Stake-FAQ). [Accessed 24 Oct. 2017].

[70] Ethereum Wiki (2018). On sharding blockchains. https://github.com/ethereum/wiki/wiki/Sharding-FAQ. [Accessed 8 Jun. 2018].

[71] Eurelectric (2017). Eurelectric launches expert discussion platform on blockchain. http://www.eurelectric.org/news/2017/eurelectric-launches-expert-discussion-platform-on-blockchain/. [Accessed 24 Nov. 2017].

[72] European Commission (2006). European SmartGrids Technology Platform: Vision and strategy for Europe's electricity networks of the future. Technical report, European Commission. [Accessed 20 Nov. 2017].

[73] European Commission (2015). Paris agreement. http://ec.europa.eu/clima/policies/international/negotiations/paris/index_en.htm. [Accessed 20 Apr. 2020].

[74] European Commission (2018). 2030 climate and energy framework. https://ec.europa.eu/clima/policies/strategies/2030_en. [Accessed 25 Apr. 2019].

[75] Eyal, I. and Sirer, E. G. (2014). Majority is not enough: Bitcoin mining is vulnerable.

[76] Fabbri, A., Roman, T. G. S., Abbad, J. R., and Quezada, V. M. (2005). Assessment of the cost associated with wind generation prediction errors in a liberalized electricity market. *IEEE Transactions on Power Systems*, 20(3):1440–1446.

[77] Fang, R. and David, A. (1999). Transmission congestion management in an electricity market. *IEEE Transactions on Power Systems*, 14(3):877–883.

[78] Feehally, T., Forsyth, A., Todd, R., Foster, M., Gladwin, D., Stone, D., and Strickland, D. (2016). Battery energy storage systems for the electricity grid: Uk research facilities. In *8th IET International Conference on Power Electronics, Machines and Drives (PEMD 2016)*, pages 1–6. IET.

[79] Ferreira, H. L., Garde, R., Fulli, G., Kling, W., and Lopes, J. P. (2013). Characterisation of electrical energy storage technologies. *Energy*, 53:288–298.

[80] Fini, A. S., Moghaddam, M. P., and Sheikh-El-Eslami, M. (2013). An investigation on the impacts of regulatory support schemes on distributed energy resource expansion planning. *Renewable energy*, 53:339–349.

[81] Foroud, A. A., Abdoos, A. A., Keypour, R., and Amirahmadi, M. (2010). A multi-objective framework for dynamic transmission expansion planning in competitive electricity market. *International Journal of Electrical Power & Energy Systems*, 32(8):861–872.

[82] Fox, C. and Parker, A. (2014). Convergence in variance of Chebyshev accelerated Gibbs samplers. *SIAM Journal on Scientific Computing*, 36(1):A124–A147.

[83] Froystad, P. and Holm, J. (2016). Blockchain: powering the internet of value (White paper). https://www.evry.com/globalassets/insight/bank2020/bank-2020---blockchain-powering-the-internet-of-value---whitepaper.pdf. [Accessed 18 Jun. 2017].

[84] Früh, W.-G. (2015). From local wind energy resource to national wind power production. *AIMS Energy*, 3(1):101–120.

[85] Gartner (2017). Gartner identifies three megatrends that will drive digital business into the next decade. Technical report. [Accessed 5 Jun. 2018].

[86] Georgiopoulos, Sotiris (2014). Flexible Plug and Play. https://innovation.ukpowernetworks.co.uk/wp-content/uploads/2019/05/Flexible-Plug-and-Play.pdf. [Accessed 04 Mar. 2015].

[87] Geyer, C. J. (1992). Practical Markov chain Monte Carlo. *Statistical science*, pages 473–483.

[88] Gill, S., Plecas, M., and Kockar, I. (2014). Coupling demand and distributed generation to accelerate renewable connections: Options for the accelerating renewable connections project.

[89] Greenspan, G. (2015). Ending the Bitcoin vs Blockchain debate. http://www.multichain.com/blog/2015/07/bitcoin-vs-blockchain-debate. [Accessed 25 Jul. 2017].

[90] Grewal-Carr, V. and Marshall, S. (2016). Blockchain enigma paradox opportunity. Technical report, Deloitte. [Accessed 15 May 2017].

[91] Gross, R. (2006). *The Costs and Impacts of Intermittency: An assessment of the evidence on the costs and impacts of intermittent generation on the British electricity network*. UK Energy Research Centre.

[92] Gu, C., Yan, X., Yan, Z., and Li, F. (2017). Dynamic pricing for responsive demand to increase distribution network efficiency. *Applied Energy*, 205:236–243.

[93] Guo, Y. and Liang, C. (2016). Blockchain application and outlook in the banking industry. *Journal of Financial Innovation*, 2(1):24.

[94] Gupta, A., Mukherjee, B., and Upadhyay, S. K. (2008). Weibull extension model: A Bayes study using Markov chain Monte Carlo simulation. *Reliability Engineering & System Safety*, 93(10):1434–1443.

[95] Gupta, N., Shekhar, R., and Kalra, P. K. (2014). Computationally efficient composite transmission expansion planning: A pareto optimal approach for techno-economic solution. *International Journal of Electrical Power & Energy Systems*, 63:917–926.

[96] Han, X., Ji, T., Zhao, Z., and Zhang, H. (2015). Economic evaluation of batteries planning in energy storage power stations for load shifting. *Renewable Energy*, 78:643–647.

[97] Hatziargyriou, N., editor (2014). *Microgrids: architectures and control*. Wiley Online Library.

[98] Heptonstall, P., Gross, R., and Steiner, F. (2017). The costs and impacts of intermittency – 2016 update. http://www.ukerc.ac.uk/publications/the-costs-and-impacts-of-intermittency-2016-update.html. [Accessed 03 Jun. 2019].

[99] Heptonstall P and Gross R (2017). The costs and impacts of intermittency – 2016 update. http://www.ukerc.ac.uk/publications/the-costs-and-impacts-of-intermittency-2016-update.html. [Accessed 18 Oct. 2018].

[100] HM Government (2009). The UK low-carbon transition plan: National strategy for climate and energy. Technical report, HM Government).

[101] HM Government (2015). Cutting the cost of keeping warm – a fuel poverty strategy for England. Technical report, HM Government. [Accessed 20 Nov. 2017].

[102] Hobbs, B. F. (1995). Optimization methods for electric utility resource planning. *European Journal of Operational Research*, 83(1):1–20.

[103] Holttinen, H., Meibom, P., Orths, A., Lange, B., O'Malley, M., Tande, J. O., Estanqueiro, A., Gomez, E., Söder, L., Strbac, G., et al. (2011). Impacts of large amounts of wind power on design and operation of power systems, results of IEA collaboration. *Wind Energy*, 14(2):179–192.

[104] Huppmann, D. and Jonas, E. (2015). National-strategic investment in european power transmission capacity. *European Journal of Operational Research*, 247(1):191–203.

[105] Hyperledger (2016). Hyperledger architecture, volume 1: Introduction to hyperledger business blockchain design philosophy and consensus. https://www.hyperledger.org/wp-content/uploads/2017/08/Hyperledger_Arch_WG_Paper_1_Consensus.pdf. [Accessed 20 Nov. 2017].

[106] Idlbi, B., von Appen, J., Kneiske, T., and Braun, M. (2016). Cost-benefit analysis of battery storage system for voltage compliance in distribution grids with high distributed generation. *Energy Procedia*, 99:215–228.

[107] IEA Wind Task Force 25 (2014). Design and operation of power systems with large amounts of wind power. http://www.ieawind.org/task_25/PDF/factSheets/FactSheet_1_121014.pdf. [Accessed 07 Mar. 2015].

[108] IEEE Smart Grid (2019). Smart Grid concept. https://innovationatwork.ieee.org/the-smart-grid-could-hold-the-keys-to-electric-vehicles/bigstock-127573223/. [Accessed 20 Jul. 2019].

[109] Imbault, F., Swiatek, M., De Beaufort, R., and Plana, R. (2017). The green blockchain: Managing decentralized energy production and consumption. In *2017 IEEE International Conference on Environment and Electrical Engineering and 2017 IEEE Industrial and Commercial Power Systems Europe (EEEIC/I&CPS Europe)*, pages 1–5. IEEE.

[110] Indigo Advisory Group (2017). Blockchain in energy and utilities use cases, vendor activity, market analysis. https://www.indigoadvisorygroup.com/blockchain. [Accessed 2 Nov. 2017].

[111] International Energy Agency (2017). EV3030 Campaign. https://www.iea.org/media/topics/transport/3030CampaignDocumentFinal.pdf. [Accessed 01 Sep. 2019].

[112] International Renewable Energy Agency (IRENA) (2017). Electricity storage and renewables: Costs and markets to 2030. https://www.irena.org/-/media/Files/IRENA/Agency/Publication/2017/Oct/IRENA_Electricity_Storage_Costs_2017.pdf. [Accessed 02 Aug. 2019].

[113] International Renewable Energy Agency (IRENA) (2018). Renewable Energy Statistics 2018. https://www.irena.org/publications/2018/Jul/Renewable-Energy-Statistics-2018. [Accessed 25 Apr 2019].

[114] IPCC (2018). Global warming of 1.5°c. an ipcc special report on the impacts of global warming of 1.5°c above pre-industrial levels and related global greenhouse gas emission pathways, in the context of strengthening the global response to the threat of climate change, sustainable development, and efforts to eradicate poverty.

[115] J, C., G, G., M, A. J., and I, M. J. (2009). An incentive-based mechanism for transmission asset investment. *Decision Support Systems*, 47(1):22–31.

[116] Joos, M. and Staffell, I. (2018). Short-term integration costs of variable renewable energy: Wind curtailment and balancing in britain and germany. *Renewable and Sustainable Energy Reviews*, 86:45–65.

[117] Jorgensen, J., Mai, T., and Brinkman, G. (2017). Reducing wind curtailment through transmission expansion in a wind vision future. Technical report, National Renewable Energy Lab.(NREL), Golden, CO (United States).

[118] Joskow, P. and Tirole, J. (2005). Merchant transmission investment. *The Journal of Industrial Economics*, 53(2):233–264.

[119] Joskow, P. L. and Tirole, J. (2000). Transmission rights and market power on electric power networks. *The Rand Journal of Economics*, pages 450–487.

[120] Jülch, V. (2016). Comparison of electricity storage options using levelized cost of storage (lcos) method. *Applied energy*, 183:1594–1606.

[121] Kagiannas, A. G., Askounis, D. T., and Psarras, J. (2004). Power generation planning: a survey from monopoly to competition. *International journal of electrical power & energy systems*, 26(6):413–421.

[122] Kamalinia, S., Shahidehpour, M., and Wu, L. (2014). Sustainable resource planning in energy markets. *Applied Energy*, 133:112–120.

[123] Kamel, R. M., Chaouachi, A., and Nagasaka, K. (2010). Carbon emissions reduction and power losses saving besides voltage profiles improvement using microgrids. *Low Carbon Economy*, 1(1):1.

[124] Kane, L. and Ault, G. (2014). A review and analysis of renewable energy curtailment schemes and principles of access: Transitioning towards business as usual. *Energy Policy*, 72:67–77.

[125] Kane, L., Ault, G., and Gill, S. (2013). An assessment of principles of access for wind generation curtailment in active network management schemes. In *CIRED 2013, 22nd International Conference on Electricity Distribution*.

[126] Kane, L. and Ault, G. W. (2015). Evaluation of wind power curtailment in active network management schemes. *IEEE Transactions on Power Systems*, 30(2):672–679.

[127] Katiraei, F. and Iravani, M. R. (2006). Power management strategies for a microgrid with multiple distributed generation units. *IEEE Transactions on Power Systems*, 21(4):1821–31.

[128] Kayser-Bril, C., Liotard, C., Maïzi, N., and Mazauric, V. (2008). Power grids on islands: from dependency to sustainability? In *Energy 2030 Conference, 2008. ENERGY 2008. IEEE*, pages 1–7. IEEE.

[129] Ketter, W., Collins, J., and Reddy, P. (1981). Power TAC: A competitive economic simulation of the smart grid. *Energy Economics*, 39:262–270.

[130] Konashevych, O. (2016). Advantages and current issues of blockchain use in microgrids. Technical report. [Accessed 18 Jun. 2017].

[131] Kota, R., Chalkiadakis, G., Robu, V., Rogers, A., and Jennings, N. R. (2012). Cooperatives for demand side management. In *The Seventh Conference on Prestigious Applications of Intelligent Systems*, pages 969–974. PAIS @ ECAI.

[132] Kristiansen, T. and Rosellon, J. (2010). Merchant electricity transmission expansion: A European case study. *Energy*, 35(10):4107–4115.

[133] Kubik, M., Coker, P., and Hunt, C. (2012). The role of conventional generation in managing variability. *Energy Policy*, 50:253–261.

[134] Lamparter, S., Becher, S., and Fischer, J.-G. (2010). An agent-based market platform for smart grids. In *Proceedings of the 9th international conference on autonomous agents and multiagent systems: industry track*, pages 1689–96. IFAAMAS.

[135] Lamport, L., Shostak, R., and Pease, M. (1982). The Byzantine generals problem. *ACM Transactions on Programming Languages and Systems (TOPLAS)*, 4(3):382–401.

[136] Lashof, D. A. and Ahuja, D. R. (1990). Relative contributions of greenhouse gas emissions to global warming. *Nature*, 344(6266):529.

[137] Lasseter, R. H. and Paigi, P. (2004). Microgrid: A conceptual solution. In *IEEE 35th Annual IEEE Power Electronics Specialists Conference*, volume 6, pages 4285–90. IEEE.

[138] Lazard (2018). Lazard's levelized cost of storage analysis - version 4.0. https://www.lazard.com/media/450774/lazards-levelized-cost-of-storage-version-40-vfinal.pdf. [Accessed 02 Aug. 2019].

[139] Lee, J., Guo, J., Choi, J. K., and Zukerman, M. (2015). Distributed energy trading in microgrids: A game-theoretic model and its equilibrium analysis. *IEEE Transactions on Industrial Electronics*, 62(6):3524–3533.

[140] Lee, W-J., Andoni, M., Bani-Ahmed, S., Flynn, D., Hartmann, B., Majd, A., Rostami, M., et al. (2018). IEEE Smart Grid: Battery storage White paper # 1. http://resourcecenter.smartgrid.ieee.org/sg/product/publications/SGWP0005. [Accessed 20 Apr. 2019].

[141] Li, N., Chen, L., and Dahleh, M. (2015). Demand response using linear supply function bidding. *IEEE Transactions on Smart Grid*, 6(4):1827–1838.

[142] Li, Y. and Conitzer, V. (2013). Game-theoretic question selection for tests. In *Twenty-Third International Joint Conference on Artificial Intelligence*.

[143] Liew, S. N., Beddoes, A., and Strbac, G. (2002). Ancillary services market opportunities in active distribution networks. In *International symposium on distributed generation: power system and market aspects*, pages 1V–11.

[144] Locatelli, G., Palerma, E., and Mancini, M. (2015). Assessing the economics of large energy storage plants with an optimisation methodology. *Energy*, 83:15–28.

[145] Lomas, N. (2015). Everledger is using blockchain to combat fraud, starting with diamonds. Technical report. [Accessed 29 Jun. 2017].

[146] Lu, Q., Lü, S., and Leng, Y. (2019). A Nash-Stackelberg game approach in regional energy market considering users' integrated demand response. *Energy*, 175:456–470.

[147] Luo, G.-l., Li, Y.-l., Tang, W.-j., and Wei, X. (2016). Wind curtailment of china wind power operation: evolution, causes and solutions. *Renewable and Sustainable Energy Reviews*, 53:1190–1201.

[148] Luo, X., Wang, J., Dooner, M., and Clarke, J. (2015). Overview of current development in electrical energy storage technologies and the application potential in power system operation. *Applied energy*, 137:511–536.

[149] Ma, H., Parkes, D. C., and Robu, V. (2017). Generalizing demand response through reward bidding. In *Proceedings of the 16th Conference on Autonomous Agents and MultiAgent Systems*, pages 60–68. International Foundation for Autonomous Agents and Multiagent Systems.

[150] Ma, H., Robu, V. P., Li, N., and Parkes, D. C. (2016). Incentivizing reliability in demand-side response. In *Proceedings of 25th International Joint Conference On Artificial Intelligence, IJCAI*, pages 352–358.

[151] MacDonald, R., Ault, G., and Currie, R. (2008). Deployment of active network management technologies in the uk and their impact on the planning and design of distribution networks.

[152] Marnay, C., Chatzivasileiadis, S., Abbey, C., Iravani, R., Joos, G., Lombardi, P., et al. (2015). Microgrid evolution roadmap. In *2015 International Symposium on Smart Electric Distribution Systems and Technologies (EDST)*, pages 139–44. IEEE.

[153] Martin, W. (2017). The electricity required for a single bitcoin trade could power a house for a whole month. http://uk.businessinsider.com/electricity-required-for-single-bitcoin-trade-could-power-a-house-for-a-month-2017-10?r=US&IR=T. [Accessed 20 Nov. 2017].

[154] Matamoros, J., Gregoratti, D., and Dohler, M. (2012). Microgrids energy trading in islanding mode. In *2012 IEEE Third International Conference on Smart Grid Communications (SmartGridComm)*, pages 49–54. IEEE.

[155] Mattila, J. (2016). The blockchain phenomenon-the disruptive potential of distributed consensus architectures. Technical report, The Research Institute of the Finnish Economy. [Accessed 15 May 2017].

[156] Mattila, J., Seppälä, T., Naucler, C., Stahl, R., Tikkanen, M., Bådenlid, A., et al. (2016). Industrial blockchain platforms: An exercise in use case development in the energy industry. Technical report, The Research Institute of the Finnish Economy. [Accessed 5 Jun. 2017].

[157] Maurovich-Horvat, L., Boomsma, T. K., and Siddiqui, A. S. (2015). Transmission and wind investment in a deregulated electricity industry. *IEEE Transactions on Power Systems*, 30(3):1633–1643.

[158] McCallum, P., Jenkins, D. P., Peacock, A. D., Patidar, S., Andoni, M., Flynn, D., and Robu, V. (2019). A multi-sectoral approach to modelling community energy demand of the built environment. *Energy Policy*, 132:865–875.

[159] McCallum, P., Patidar, S., Jenkins, D., Peacock, A., Robu, V., Andoni, M., and Flynn, D. (2018). The use of demand modelling for community energy analysis. In *2018 IEEE International Symposium on Circuits and Systems (ISCAS)*, pages 1–5. IEEE.

[160] McGarvey, J. (2006). Transmission investment: a primer. *The Electricity Journal*, 19(8):71–82.

[161] Mehr, T. H., Masoum, M. A., and Jabalameli, N. (2013). Grid-connected lithium-ion battery energy storage system for load leveling and peak shaving. In *2013 Australasian Universities Power Engineering Conference (AUPEC)*, pages 1–6. IEEE.

[162] Mengelkamp, E., Gärttner, J., Rock, K., Kessler, S., Orsini, L., and Weinhardt, C. (2018). Designing microgrid energy markets A case study: The Brooklyn Microgrid. *Applied Energy*, 210:870–80.

[163] Merz, S. K. (2008). *Growth scenarios for UK renewables generation and implications for future developments and operation of electricity networks*. BERR.

[164] Met Office NCAS British Atmospheric Data Centre (2016). MIDAS: UK Mean Wind Data. http://catalogue.ceda.ac.uk/uuid/a1f65a362c26c9fa667d98c431a1ad38. Accessed: 2016-03-01.

[165] Michiorri, A., Currie, R., Taylor, P., Watson, F., and Macleman, D. (2011). Dynamic line ratings deployment on the Orkney Smart Grid. In *CIRED*.

[166] Mihaylov, M., Jurado, S., Avellana, N., Razo-Zapata, I., Van Moffaert, K., Arco, L., et al. (2015). Scanergy: a scalable and modular system for energy trading between prosumers. In *Proceedings of the 2015 International Conference on Autonomous Agents and Multiagent Systems*, pages 1917–18. IFAAMAS.

[167] Mihaylov, M., Jurado, S., Avellana, N., Van Moffaert, K., de Abril, I. M., and Nowe, A. (2014). Nrgcoin: Virtual currency for trading of renewable energy in smart grids. In *Proceedings of 11th International Conference on the European Energy Market (EEM)*, pages 1–6. IEEE.

[168] Min, C., Kim, M., Park, J., and Yoon, Y. (2013). Game-theory-based generation maintenance scheduling in electricity markets. *Energy*, 55:310–318.

[169] Motamedi, A., Zareipour, H., Buygi, M. O., and Rosehart, W. D. (2010). A transmission planning framework considering future generation expansions in electricity markets. *IEEE Transactions on Power Systems*, 25(4):1987–1995.

[170] Muftic, S. (2016). Overview and analysis of the concept and applications of virtual currencies. http://publications.jrc.ec.europa.eu/repository/bitstream/JRC105207/lbna28386enn.pdf. [Accessed 18 Jun. 2017].

[171] Muhssin, M. T., Cipcigan, L. M., Sami, S. S., and Obaid, Z. A. (2018). Potential of demand side response aggregation for the stabilization of the grids frequency. *Applied energy*, 220:643–656.

[172] Mustafa, M. A., Cleemput, S., and Abidin, A. (2016). A local electricity trading market: Security analysis. In *IEEE PES Innovative Smart Grid Technologies Conference Europe (ISGT-Europe)*, pages 1–6. IEEE.

[173] Mylrea, M. and Gourisetti, S. N. G. (2017a). Blockchain for smart grid resilience: Exchanging distributed energy at speed, scale and security. In *Resilience Week (RWS) 2017*, pages 18–23. IEEE.

[174] Mylrea, M. and Gourisetti, S. N. G. (2017b). Cybersecurity and optimization in smart "autonomous" buildings. In *Autonomy and Artificial Intelligence: A Threat or Savior?*, pages 263–294. Springer.

[175] Nosratabadi, S. M., Hooshmand, R.-A., and Gholipour, E. (2017). A comprehensive review on microgrid and virtual power plant concepts employed for distributed energy resources scheduling in power systems. *Renewable and Sustainable Energy Reviews*, 67:341–63.

[176] Nourai, A., Kogan, V., and Schafer, C. M. (2008). Load leveling reduces t&d line losses. *IEEE Transactions on Power Delivery*, 23(4):2168–2173.

[177] Nuhic, A., Terzimehic, T., Soczka-Guth, T., Buchholz, M., and Dietmayer, K. (2013). Health diagnosis and remaining useful life prognostics of lithium-ion batteries using data-driven methods. *Journal of Power Sources*, 239:680–688.

[178] Office of Gas and Electricity Markets (Ofgem) (2017). Consumer empowerment and protection. Technical report. [Accessed 6 Dec. 2017].

[179] Office of Gas and Electricity Markets (Ofgem) (2017). Transition to smart meters. https://www.ofgem.gov.uk/gas/retail-market/metering/transition-smart-meters. [Accessed 6 Dec. 2017].

[180] OFGEM (2015a). Feed-in tariff (fit) scheme. https://www.ofgem.gov.uk/environmental-programmes/feed-tariff-fit-scheme. [Accessed 25 Jul. 2015].

[181] OFGEM (2015b). Low Carbon Networks Fund. https://www.ofgem.gov.uk/electricity/distribution-networks/network-innovation/low-carbon-networks-fund. [Accessed 04 Apr. 2015].

[182] OFGEM (2015c). Renewables Obligation (RO). https://www.ofgem.gov.uk/environmental-programmes/renewables-obligation-ro. [Accessed 04 Apr. 2015].

[183] Ofgem (2018). Electricity Network Access and Forward-Looking Charging Review - Significant Code Review launch statement and decision on the wider review. https://www.ofgem.gov.uk/system/files/docs/2018/12/scr_launch_statement.pdf. [Accessed 01 Aug. 2019].

[184] Orkney Islands Council (2010). Orkney's Fuel Poverty Strategy 2017-2022. http://www.orkney.gov.uk/Files/Housing/Housing%20Options/Housing%20Strategy/Fuel_Poverty_Strategy.pdf. [Accessed 03 Jun. 2019].

[185] Orkney Islands Council (2019). 28.5m ReFLEX Orkney project to create a 'smart energy island'. https://www.orkney.gov.uk/OIC-News/285m-ReFLEX-Orkney-project-to-create-a-smart-energy-island.htm. [Accessed 01 Sep. 2019].

[186] Ortega, M. P. R., Perez-Arriaga, J. I., Abbad, J. R., and Gonzalez, J. P. (2008). Distribution network tariffs: A closed question? *Energy Policy*, 36(5):1712–1725.

[187] Palizban, O., Kauhaniemi, K., and Guerrero, J. M. (2014). Microgrids in active network management Part I: Hierarchical control, energy storage, virtual power plants, and market participation. *Renewable and Sustainable Energy Reviews*, 36:428–39.

[188] Palsson, M. P., Toftevaag, T., Uhlen, K., and Tande, J. O. G. (2002). Large-scale wind power integration and voltage stability limits in regional networks. In *Power Engineering Society Summer Meeting, 2002 IEEE*, volume 2, pages 762–769. IEEE.

[189] Papaefthymiou, G. and Klockl, B. (2008). MCMC for wind power simulation. *IEEE Trans. on Energy Conversion*, 23(1):234–240.

[190] Park, C. and Yong, T. (2017). Comparative review and discussion on P2P electricity trading. *Energy Procedia*, 128:3–9.

[191] Paruchuri, P., Pearce, J. P., Marecki, J., Tambe, M., Ordonez, F., and Kraus, S. (2008). Efficient algorithms to solve bayesian stackelberg games for security applications. In *AAAI*, pages 1559–1562.

[192] Pearre, N. S. and Swan, L. G. (2015). Technoeconomic feasibility of grid storage: Mapping electrical services and energy storage technologies. *Applied Energy*, 137:501–510.

[193] Perrault, A. and Boutilier, C. (2014). Efficient coordinated power distribution on private infrastructure. In *Proceedings of the 2014 International Conference on Autonomous Agents and Multi-agent Systems*, pages 805–812. International Foundation for Autonomous Agents and Multiagent Systems.

[194] Perrault, A. and Boutilier, C. (2015). Approximately stable pricing for coordinated purchasing of electricity. In *IJCAI*, pages 2624–2631.

[195] Pilkington, M. (2015). Blockchain technology: principles and applications. https://ssrn.com/abstract=2662660. [Accessed 18 Jun. 2017].

[196] Pinson, P., Baroche, T., Moret, F., Sousa, T., Sorin, E., and You, S. (2018). The emergence of consumer-centric electricity markets. Technical report. [Accessed 31 Jan. 2018].

[197] Poon, J. and Dryja, T. (2016). The Bitcoin Lightning Network: Scalable off-chain instant payments. https://lightning.network/lightning-network-paper.pdf. [Accessed 29 Aug. 2018].

[198] Prete, C. L. and Hobbs, B. F. (2016). A cooperative game theoretic analysis of incentives for microgrids in regulated electricity markets. *Applied Energy*, 169:524–541.

[199] Puga, J. N. (2010). The importance of combined cycle generating plants in integrating large levels of wind power generation. *The Electricity Journal*, 23(7):33–44.

[200] Pullum, L. L., Jindal, A., Roopaei, M., Diggewadi, A., Andoni, M., Zobaa, A., et al. (2018). IEEE Smart Grid: Big Data Analytics in the Smart Grid: Big Data Analytics, Machine Learning and Artificial Intelligence in the Smart Grid: Introduction, Benefits, Challenges and Issues. http://resourcecenter.smartgrid.ieee.org/sg/product/publications/SGWP0003. [Accessed 20 Apr. 2019].

[201] PwC global power & utilities (2016). Blockchain - an opportunity for energy producers and consumers? Technical report, PricewaterhouseCoopers. [Accessed 22 Nov. 2017].

[202] Ramchurn, S., Vytelingum, P., Rogers, A., and Jennings, N. R. (2012). Putting the 'smarts' into the smart grid: A grand challenge for artificial intelligence. *Communications of the ACM*, 55(4):86–97.

[203] Rao, A. G., van den Oudenalder, F., and Klein, S. (2019). Natural gas displacement by wind curtailment utilization in combined-cycle power plants. *Energy*, 168:477–491.

[204] Rastler, D. (2010). *Electricity energy storage technology options: a white paper primer on applications, costs and benefits*. Electric Power Research Institute.

[205] Reihani, E., Sepasi, S., Roose, L. R., and Matsuura, M. (2016). Energy management at the distribution grid using a battery energy storage system (bess). *International Journal of Electrical Power & Energy Systems*, 77:337–344.

[206] REN21: Renewable Energy Policy Network for the 21st Century (2018). Advancing the global renewable energy transition. http://www.ren21.net/wp-content/uploads/2018/06/GSR_2018_Highlights_final.pdf. [Accessed 26 May 2019].

[207] Renewable UK (2019). Energy storage capacity set to soar, 300 UK-based companies involved in new sector. https://www.renewableuk.com/news/425522/Energy-storage-capacity-set-to-soar-300-UK-based-companies-involved-in-new-sector.htm. [Accessed 14 Aug. 2019].

[208] RenewableUK (2015a). UK Marine Energy Database (UKMED). https://maps.espatial.com/maps/pages/map.jsp?geoMapId=19671&TENANT_ID=115744. [Accessed 15 Mar. 2015].

[209] RenewableUK (2015b). UK Wind Energy Database (UKWED). http://www.renewableuk.com/en/renewable-energy/wind-energy/uk-wind-energy-database/index.cfm. [Accessed 15 Mar. 2015].

[210] Robu, V., Chalkiadakis, G., Kota, R., Rogers, A., and Jennings, N. R. (2016). Rewarding cooperative virtual power plant formation using scoring rules. *Energy*, 117, Part 1:19–28.

[211] Robu, V., Kota, R., Chalkiadakis, G., Rogers, A., and Jennings, N. R. (2012). Cooperative virtual power plant formation using scoring rules. In *Proceedings of the 11th International Conference on Autonomous Agents and Multiagent Systems*, pages 1165–1166. International Foundation for Autonomous Agents and Multiagent Systems.

[212] Robu, V., Vinyals, M., Rogers, A., and Jennings, N. R. (2014). Efficient buyer groups for prediction-of-use electricity tariffs. In *Twenty-Eighth Conference on Artificial Intelligence*, pages 451–457, Quebec. AAAI.

[213] Rogers, J., Fink, S., and Porter, K. (2010). Examples of wind energy curtailment practices. *NREL, Subcontract Report NREL/SR-550*, 48737.

[214] Roth, A. E. (1988). *The Shapley value: essays in honor of Lloyd S. Shapley*. Cambridge University Press.

[215] Ruiz, C., Conejo, A. J., Fuller, J. D., Gabriel, S. A., and Hobbs, B. F. (2014). A tutorial review of complementarity models for decision-making in energy markets. *EURO Journal on Decision Processes*, 2(1-2):91–120.

[216] S. Fink and C. Mudd and K. Porter and B. Morgenstern (2009). Wind energy curtailment case studies. Technical report.

[217] Saad, W., Han, Z., and Poor, H. V. (2011). Coalitional game theory for cooperative micro-grid distribution networks. In *2011 IEEE International Conference on Communications Workshops (ICC)*, pages 1–5. IEEE.

[218] Saguan, M. and Meeus, L. (2014). Impact of the regulatory framework for transmission investments on the cost of renewable energy in the EU. *Energy Economics*, 43:185–194.

[219] Sanders, D and Hart, A and Ravishankar, M and Brunert, J and Strbac, G and Aunedi, M and others (2016). An analysis of electricity system flexibility for Great Britain. https://assets.publishing.service.gov.uk/government/uploads/system/uploads/attachment_data/file/568982/An_analysis_of_electricity_flexibility_for_Great_Britain.pdf. [Accessed 01 Jul. 2019].

[220] Sandia National Laboratories (2019). DOE Global energy storage database. https://www.energystorageexchange.org/. [Accessed 14 Aug. 2019].

[221] Sauma, E. E. and Oren, S. S. (2006). Proactive planning and valuation of transmission investments in restructured electricity markets. *Journal of Regulatory Economics*, 30(3):261–290.

[222] Sauma, E. E. and Oren, S. S. (2007). Economic criteria for planning transmission investment in restructured electricity markets. *IEEE Transactions on Power Systems*, 22(4):1394–1405.

[223] Schweppe, F. C., Caramanis, M. C., Tabors, R. D., and Bohn, R. E. (2013). *Spot pricing of electricity*. Springer Science & Business Media.

[224] Scottish and Southern Energy Power Distribution (2012). London may 2012 - britains first smart grid overview - orkney smart grid. https://www.ssepd.co.uk/WorkArea/DownloadAsset.aspx?id=2528. [Accessed 15 Mar. 2015].

[225] Scottish and Southern Energy Power Distribution (2014). Northern Isles New Energy Solutions (NINES. https://www.ssepd.co.uk/NINES/. [Accessed 04 Mar. 2015].

[226] Scottish Power Transmission (2019). Western link Project. http://www.westernhvdclink.co.uk/. [Accessed 23 Jul. 2019].

[227] Seppälä, J. (2016). The role of trust in understanding the effects of blockchain on business models. https://aaltodoc.aalto.fi/handle/123456789/23302. [Accessed 11 Jun. 2017].

[228] Shrestha, G. B. and Fonseka, P. A. J. (2004). Congestion-driven transmission expansion in competitive power markets. *IEEE Transactions on Power Systems*, 19(3):1658–1665.

[229] Si, X.-S., Wang, W., Hu, C.-H., and Zhou, D.-H. (2011). Remaining useful life estimation–a review on the statistical data driven approaches. *European Journal of Operational Research*, 213(1):1–14.

[230] Singh, H., Hao, S., and Papalexopoulos, A. (1998). Transmission congestion management in competitive electricity markets. *IEEE Transactions on Power Systems*, 13(2):672–680.

[231] Skarvelis-Kazakos, S., Rikos, E., Kolentini, E., Cipcigan, L. M., and Jenkins, N. (2013). Implementing agent-based emissions trading for controlling virtual power plant emissions. *Electric Power Systems Research*, 102:1–7.

[232] SKM (2004). Technical evaluation of transmission network reinforcement expenditure proposals by licensees in great britain - draft report, Sinclair Knight Merz. Technical report.

[233] Sonder, H. B., Cipcigan, L., and Loo, C. U. (2019). Using electric vehicles and demand side response to unlock distribution network flexibility. In *2019 IEEE Milan PowerTech*, pages 1–6. IEEE.

[234] Soroudi, A. and Ehsan, M. (2010). A distribution network expansion planning model considering distributed generation options and techo-economical issues. *Energy*, 35(8):3364–3374.

[235] SSE (2015a). Kintyre-hunterstone. https://www.ssepd.co.uk/KintyreHunterston. [Accessed 01 Aug. 2015].

[236] SSE (2015b). NINES. http://www.ninessmartgrid.co.uk/wp-content/uploads/2013/11/Shetland-Active-Network-Management-System_Use-Cases_Sep20121-v-0.1.pdf. [Accessed 20 Aug. 2015].

[237] Stadler, M., Cardoso, G., Mashayekh, S., Forget, T., DeForest, N., Agarwal, A., and Schönbein, A. (2016). Value streams in microgrids: A literature review. *Applied Energy*, 162:980–9.

[238] Su, W. and Huang, A. Q. (2014). A game theoretic framework for a next-generation retail electricity market with high penetration of distributed residential electricity suppliers. *Applied Energy*, 119:341–350.

[239] Swan, M. (2015). *Blockchain: Blueprint for a new economy*. O'Reilly Media Inc.

[240] Swanson, T. (2015). Consensus-as-a-service: a brief report on the emergence of permissioned, distributed ledger systems. http://www.ofnumbers.com/wp-content/uploads/2015/04/Permissioned-distributed-ledgers.pdf. [Accessed 21 Jul. 2017].

[241] Tang, W., Andoni, M., Robu, V., and Flynn, D. (2018). Accurately forecasting the health of energy system assets. In *2018 IEEE International Symposium on Circuits and Systems (ISCAS)*, pages 1–5. IEEE.

[242] Tapscott, D. and Tapscott, A. (2016). *Blockchain Revolution: How the technology behind Bitcoin is changing money, business, and the world*. Penguin. [Accessed 20 Nov. 2017].

[243] Tendermint (2017). Tendermint. https://tendermint.readthedocs.io/en/master/. [Accessed 1 Feb. 2018].

[244] Ton, D. T. and Smith, M. A. (2012). The US Department of Energy's microgrid initiative. *The Electricity Journal*, 25(8):84–94.

[245] Tuller, S. E. and Brett, A. C. (1984). The characteristics of wind velocity that favor the fitting of a Weibull distribution in wind speed analysis. *Journal of Climate and Applied Meteorology*, 23(1):124–134.

[246] Uddin, M., Romlie, M. F., Abdullah, M. F., Halim, S. A., Kwang, T. C., et al. (2017). A review on peak load shaving strategies. *Renewable and Sustainable Energy Reviews*, 82(Part 3):3323–32.

[247] U.S. Department of Energy (2003). 'Grid 2030' A national vision for electricity's second 100 years. Technical report.

[248] US Department of Energy (2009). Smart grid system report. Technical report, US Department of Energy. [Accessed 20 Nov. 2017].

[249] van der Weijde, A. H. and Hobbs, B. F. (2012). The economics of planning electricity transmission to accommodate renewables: Using two-stage optimisation to evaluate flexibility and the cost of disregarding uncertainty. *Energy Economics*, 34(6):2089–2101.

[250] Vargas, L. S., Bustos-Turu, G., and Larraín, F. (2014). Wind power curtailment and energy storage in transmission congestion management considering power plants ramp rates. *IEEE Transactions on Power Systems*, 30(5):2498–2506.

[251] Vasirani, M., Kota, R., Cavalcante, R. L. G., Ossowski, S., and Jennings, N. R. (2013). An agent-based approach to virtual power plants of wind power generators and electric vehicles. *IEEE Transactions on Smart Grid*, 4(3):1314–1322.

[252] von Stackelberg, H. (2010). *Market structure and equilibrium*. Springer Science & Business Media.

[253] von Wirth, T., Gislason, L., and Seidl, R. (2017). Distributed energy systems on a neighborhood scale: Reviewing drivers of and barriers to social acceptance. *Renewable and Sustainable Energy Reviews*, 82(Part 3):2618–28.

[254] Vukolic, M. (2015). The quest for scalable blockchain fabric: Proof-of-work vs. BFT replication. In *International Workshop on Open Problems in Network Security*, pages 112–25. Springer.

[255] Vytelingum, P., Ramchurn, S. D., Voice, T. D., Rogers, A., and Jennings, N. R. (2010). Trading agents for the smart electricity grid. In *Proceedings of the 9th International Conference on Autonomous Agents and Multiagent Systems*, pages 897–904. IFAAMAS.

[256] Wade, N. S., Taylor, P., Lang, P., and Jones, P. (2010). Evaluating the benefits of an electrical energy storage system in a future smart grid. *Energy policy*, 38(11):7180–7188.

[257] Walport, M. (2016). Distributed ledger technology: beyond blockchain. Technical report, UK Government Office for Science. [Accessed 5 Jun. 2017].

[258] Ward, J., Pooley, M., and Owen, G. (2012). GB electricity demand-realising the resource: What demand-side services can provide value to the electricity sector. In *Sustainability First*, London.

[259] Watson, S. J., Kritharas, P., and Hodgson, G. J. (2011). Impact of beta-distributed wind power on economic load dispatch. *Electric Power Components and Systems*, 39(8):768–779.

[260] Watson, S. J., Kritharas, P., and Hodgson, G. J. (2015). Wind speed variability across the UK between 1957 and 2011. *Wind Energy*, 18(1):21–42.

[261] Wei, F., Jing, Z., Wu, P. Z., and Wu, Q. (2017). A Stackelberg game approach for multiple energies trading in integrated energy systems. *Applied Energy*, 200:315–329.

[262] Western Power Distribution (2020). Alternative connections. https://www.westernpower.co.uk/connections-landing/connection-offers-and-agreements/alternative-connections. [Accessed 23 Jan. 2020].

[263] Wood Mackenzie Power & Renewables/Energy Storage Association (2019). U.S. energy storage monitor Q2 2019 executive summary . Technical report, Wood Mackenzie Power & Renewables/Energy Storage Association.

[264] Wu, Q., Ren, H., Gao, W., Ren, J., and Lao, C. (2016). Profit allocation analysis among the distributed energy network participants based on game-theory. *Energy*, 118:783–794.

[265] Wu, T., Ai, X., Lin, W., Wen, J., and Weihua, L. (2012). Markov chain Monte Carlo method for the modeling of wind power time series. In *2012 IEEE PES ISGT Asia*, pages 1–6. IEEE.

[266] Xethalis, G., Moriarty, K., Claassen, R., and Levy, J. (2016). An introduction to Bitcoin and blockchain technology. https://files.arnoldporter.com//docs/IntrotoBitcoinandBlockchainTechnology.pdf. [Accessed 5 Jun. 2017].

[267] Xu, Y., Li, N., and Low, S. H. (2015). Demand response with capacity constrained supply function bidding. *IEEE Transactions on Power Systems*, PP(99):1–18.

[268] Xydas, E., Marmaras, C., and Cipcigan, L. M. (2016). A multi-agent based scheduling algorithm for adaptive electric vehicles charging. *Applied energy*, 177:354–365.

[269] Zakeri, B. and Syri, S. (2015). Electrical energy storage systems: A comparative life cycle cost analysis. *Renewable and sustainable energy reviews*, 42:569–596.

[270] Zeng, B., Wen, J., Shi, J., Zhang, J., and Zhang, Y. (2016). A multi-level approach to active distribution system planning for efficient renewable energy harvesting in a deregulated environment. *Energy*, 96:614–624.

[271] Zhang, N., Yan, Y., and Su, W. (2015). A game-theoretic economic operation of residential distribution system with high participation of distributed electricity prosumers. *Applied Energy*, 154:471–479.

[272] Zhao, J., Wang, C., Zhao, B., Lin, F., Zhou, Q., and Wang, Y. (2014). A review of active management for distribution networks: Current status and future development trends. *Electric Power Components and Systems*, 42(3-4):280–293.

[273] Zheng, R., Xu, Y., Chakraborty, N., and Sycara, K. (2015). A crowdfunding model for green energy investment. In *24th Int. Joint Conference on Artificial Intelligence*, pages 2669–2675, Buenos Aires. IJCAI.

[274] Zheng, Z., Xie, S., Dai, H.-N., and Wang, H. (2017). Blockchain challenges and opportunities: A survey. https://www.henrylab.net/wp-content/uploads/2017/10/blockchain.pdf. [Accessed 5 Jun. 2018].

[275] Zhou, S. and Brown, M. A. (2017). Smart meter deployment in Europe: A comparative case study on the impacts of national policy schemes. *J Clean Produc*, pages 22–32.

[276] Zhu, L., Zhang, Q., Lu, H., Li, H., Li, Y., McLellan, B., and Pan, X. (2017). Study on crowdfunding's promoting effect on the expansion of electric vehicle charging piles based on game theory analysis. *Applied Energy*, 196:238–248.

[277] Ziegler, M. S., Mueller, J. M., Pereira, G. D., Song, J., Ferrara, M., Chiang, Y.-M., and Trancik, J. E. (2019). Storage requirements and costs of shaping renewable energy toward grid decarbonization. *Joule*.

Appendix A

The Appendix provides additional information and sample codes for the simulation analysis of the research work presented in this thesis.

A.1 Simulation analysis presented in Chapter 3

Listing A.1 Sample code for simulation analysis in Section 3.2.3: CF of wind generators, fairness and correlation effects under different curtailment schemes

```
%With Pearson correlation
%U = wblrnd(A,B)generates random numbers for the Weibull distribution
    with scale parameter, A and shape parameter, B.
URef = wblrnd(9,1.8,[1,8760]);
U1r = URef;
U2r = wblrnd(9,1.8,[1,8760]);
U3r = wblrnd(9,1.8,[1,8760]);
%Power curve Enercon E44
Uw=[1:25];
P=[0,0,4,20,50,96,156,238,340,466,600,710,790,850,880,905,910,..];
P_nom=910;
P_pu=P/910;
%Power Curve fit in the region [U_cut_in - U_nom] as polynomial
U_fit=[3:16];
P_fit=[4,20,50,96,156,238,340,466,600,710,790,850,880,905];
p1 = 0.01877; %polynomial coefficients
p2 = -0.9387;
p3 = 16.68;
p4 = -125;
p5 = 436.3;
p6 = -563.2;
%Nominal Capacities of wind turbines
Pn1=7;
Pn2=2;
Pn3=3;
```

```
%Intialisations
index=0;% index for each r=Pearson correlation factor
%Help Array H_A – order of curtailment for Rota
H_A1(1:26280)=0;
for n=1:1:26280
    if mod(n,3)==1
        H_A1(n)=1;
    end
end
H_A2(1:26280)=0;
for n=1:1:26280
    if mod(n,3)==2
        H_A2(n)=1;
    end
end
H_A3(1:26280)=0;
for n=1:1:26280
    if mod(n,3)==0
        H_A3(n)=1;
    end
end

%Help Array H_Ar – order of curtailment for FRR
H_Ar1(1:26280)=0;
for n=1:1:26280
    if mod(n,3)==1
        H_Ar1(n)=Pn1;
    end
end
H_Ar2(1:26280)=0;
for n=1:1:26280
    if mod(n,3)==2
        H_Ar2(n)=Pn2;
    end
end
H_Ar3(1:26280)=0;
for n=1:1:26280
    if mod(n,3)==0
        H_Ar3(n)=Pn3;
    end
end

```

```
for r=0:0.05:1 %r=Pearson correlation factor
    index=index+1;
    R(index)=r;
    %cr calculate such as in Wolf's paper
    cr=1/pi*acos(1-2*r);
    %Generate wind speeds data series with different correlations
    U1=cr*URef+(1-cr)*U1r;
    U2=cr*URef+(1-cr)*U2r;
    U3=cr*URef+(1-cr)*U3r;
    %Inintialisation for Pout=Power output per unit
    Pout1(1:8760)=-1;
    Pout2=Pout1;
    Pout3=Pout1;
    Pout1 = powerGen(U1, p1, p2, p3, p4, p5, p6, P_nom);
    Pout2 = powerGen(U2, p1, p2, p3, p4, p5, p6, P_nom);
    Pout3 = powerGen(U3, p1, p2, p3, p4, p5, p6, P_nom);
    %Power that can be generated (no curtailment)
    Pg1=Pn1*Pout1;
    Pg2=Pn2*Pout2;
    Pg3=Pn3*Pout3;
    %Sum
    S_Pg=Pg1+Pg2+Pg3;
    %Demand
    P_d=6;
    %Residual demand
    RD=S_Pg-P_d;
    %Capacity factor no curtailment
    CFg1(index)=sum(Pg1)/(8760*Pn1);
    CFg2(index)=sum(Pg2)/(8760*Pn2);
    CFg3(index)=sum(Pg3)/(8760*Pn3);
    %Initialisations
    cur_yes=0;%number of curtailment events
    cur_no=0;
    PG=[Pg1;Pg2;Pg3];%Power without curtailment
    PG_rota=PG;
    P_rota=PG*0;
    P_frr=PG;
    Pc=Pg1*0;%Counts total curtialment

    pc_lifo=0;%power curtailed for LIFO at each time step
    P_lifo=PG;%Power generated with LIFO scheme
```

```
    c_lifo=[0,0,0];%number of curtailment events for LIFO, for each
       generator
    Clifo=Pg1*0;%sum of power curtailed Clifo(i) at LIFO at each time
        step

    pc_pr=0;%power curtailed for Pro rata at each time step
    P_pr=PG;%Power generated with Pro rata scheme
    c_pr=[0,0,0];%number of curtailment events for Pro rata, for each
        generator
    Cpr=Pg1*0;%sum of power curtailed Cpr(i) at Pro rata at each time
        step

    pc_rota=0;%power curtailed for Rota at each time step
    P_rota=PG;%Power generated with Rota scheme
    c_rota=[0,0,0];%number of curtailment events for Rota, for each
       generator
    Crota=Pg1*0;%sum of power curtailed Crota(i) at Rota at each time
        step
    H_A=[H_A1;H_A2;H_A3];
    ignH_A=H_A;
    uplim=0;

    pc_frr=0;%power curtailed for FRR at each time step
    P_frr=PG;%Power generated with FRR scheme
    c_frr=[0,0,0];%number of curtailment events for FRR, for each
       generator
    Cfrr=Pg1*0;%sum of power curtailed Cfrr(i) at FRR at each time
       step
    H_Ar=[H_Ar1;H_Ar2;H_Ar3];
    ignH_Ar=H_Ar;
    uplimit=0;

    for i=1:1:8760
        if RD(i)>0
            cur_yes=cur_yes+1;
            Pc(i)=RD(i);
            %LIFO
            pc_lifo=RD(i);%power to be curtailed
            if pc_lifo<=PG(3,i)
                P_lifo(3,i)=PG(3,i)-pc_lifo;
                c_lifo(3)=c_lifo(3)+1;
                Clifo(i)=Clifo(i)+pc_lifo;
```

```
142             else
143                 pc_lifo=pc_lifo-PG(3,i);
144                 P_lifo(3,i)=0;
145                 c_lifo(3)=c_lifo(3)+1;
146                 Clifo(i)=Clifo(i)+PG(3,i);
147                 if pc_lifo<=PG(2,i)
148                     P_lifo(2,i)=PG(2,i)-pc_lifo;
149                     c_lifo(2)=c_lifo(2)+1;
150                     Clifo(i)=Clifo(i)+pc_lifo;
151                 else
152                     pc_lifo=pc_lifo-PG(2,i);
153                     Clifo(i)=Clifo(i)+PG(2,i);
154                     P_lifo(2,i)=0;
155                     c_lifo(2)=c_lifo(2)+1;
156                     P_lifo(1,i)=PG(1,i)-pc_lifo;
157                     c_lifo(1)=c_lifo(1)+1;
158                     Clifo(i)=Clifo(i)+pc_lifo;
159                 end
160             end
161             %Pro Rata
162             pc_pr=RD(i);
163             P_pr(1,i)=PG(1,i)-pc_pr*PG(1,i)/S_Pg(i);
164             if PG(1,i)>0
165                 c_pr(1)=c_pr(1)+1;
166             end
167             Cpr(i)=Cpr(i)+ pc_pr*PG(1,i)/S_Pg(i);
168             P_pr(2,i)=PG(2,i)-pc_pr*PG(2,i)/S_Pg(i);
169             if PG(2,i)>0
170                 c_pr(2)=c_pr(2)+1;
171             end
172             Cpr(i)=Cpr(i)+ pc_pr*PG(2,i)/S_Pg(i);
173             P_pr(3,i)=PG(3,i)-pc_pr*PG(3,i)/S_Pg(i);
174             if PG(3,i)>0
175                 c_pr(3)=c_pr(3)+1;
176             end
177             Cpr(i)=Cpr(i)+ pc_pr*PG(3,i)/S_Pg(i);
178             %Rota
179             pc_rota=RD(i);
180             ignH_A=H_A;
181             while pc_rota~=0
182                 [rrow,ccol]=find_turn(ignH_A);
183                 %uplimit
```

```
            if P_rota(rrow,i)>0
                uplim=P_rota(rrow,i);
            else
                uplim=0;
            end
            %remove right amount
            if pc_rota<=uplim
                P_rota(rrow,i)=P_rota(rrow,i)-pc_rota;
                c_rota(rrow)=c_rota(rrow)+1;
                Crota(i)=Crota(i)+pc_rota;
                H_A(rrow,ccol)=0;
                ignH_A(rrow,ccol)=0;
                pc_rota=0;
            else
                P_rota(rrow,i)=P_rota(rrow,i)-uplim;
                if uplim~=0
                    c_rota(rrow)=c_rota(rrow)+1;
                    Crota(i)=Crota(i)+uplim;
                end
                H_A(rrow,ccol)=0;
                ignH_A(rrow,ccol)=0;
                pc_rota=pc_rota-uplim;
            end
        end
        %FRR
        pc_frr=RD(i);
        ignH_Ar=H_Ar;
        while pc_frr~=0
            [W,row,col]=find_left(ignH_Ar);
            %uplimit
            if P_frr(row,i)<W
                uplimit=P_frr(row,i);
            else
                uplimit=W;
            end
            %remove right amount
            if pc_frr<=uplimit
                P_frr(row,i)=P_frr(row,i)-pc_frr;
                c_frr(row)=c_frr(row)+1;
                Cfrr(i)=Cfrr(i)+pc_frr;
                H_Ar(row,col)=H_Ar(row,col)-pc_frr;
                ignH_Ar(row,col)=0;
```

```
                    pc_frr=0;
                else
                    P_frr(row,i)=P_frr(row,i)-uplimit;
                    if uplimit~=0
                        c_frr(row)=c_frr(row)+1;
                        Cfrr(i)=Cfrr(i)+uplimit;
                    end
                    H_Ar(row,col)=H_Ar(row,col)-uplimit;
                    ignH_Ar(row,col)=0;
                    pc_frr=pc_frr-uplimit;
                end
            end
        else
            cur_no=cur_no+1;
        end
    end
    %Total number of curtailment
    Tcur_yes(index)=cur_yes;
    Tcur_no(index)=cur_no;
    %Total curtailed power and comparison with curtailment schemes
    TC(index)=sum(Pc);
    TClifo(index)=sum(Clifo);
    TCpr(index)=sum(Cpr);
    TCrota(index)=sum(Crota);
    TCfrr(index)=sum(Cfrr);
    %Capacity factor with curtailment
    CF1_lifo(index)=sum(P_lifo(1,:))/(8760*Pn1);
    CF2_lifo(index)=sum(P_lifo(2,:))/(8760*Pn2);
    CF3_lifo(index)=sum(P_lifo(3,:))/(8760*Pn3);
    CF1_pr(index)=sum(P_pr(1,:))/(8760*Pn1);
    CF2_pr(index)=sum(P_pr(2,:))/(8760*Pn2);
    CF3_pr(index)=sum(P_pr(3,:))/(8760*Pn3);
    CF1_rota(index)=sum(P_rota(1,:))/(8760*Pn1);
    CF2_rota(index)=sum(P_rota(2,:))/(8760*Pn2);
    CF3_rota(index)=sum(P_rota(3,:))/(8760*Pn3);
    CF1_frr(index)=sum(P_frr(1,:))/(8760*Pn1);
    CF2_frr(index)=sum(P_frr(2,:))/(8760*Pn2);
    CF3_frr(index)=sum(P_frr(3,:))/(8760*Pn3);
    %Count curtailment events for each generator
    count1_lifo(index)=c_lifo(1);
    count2_lifo(index)=c_lifo(2);
    count3_lifo(index)=c_lifo(3);
```

```
    count1_pr(index)=c_pr(1);
    count2_pr(index)=c_pr(2);
    count3_pr(index)=c_pr(3);
    count1_rota(index)=c_rota(1);
    count2_rota(index)=c_rota(2);
    count3_rota(index)=c_rota(3);
    count1_frr(index)=c_frr(1);
    count2_frr(index)=c_frr(2);
    count3_frr(index)=c_frr(3);
end
```

Listing A.2 Sample code for simulation analysis in Section 3.2.3 and function powerGen: Polynominal fit for wind power output

```
function [Pout] = powerGen(U, p1, p2, p3, p4, p5, p6, P_nom)
    for i=1:1:size(U,2)
        if (U(i)>=3) && (U(i)<=16)
            Pout(i)= (p1*U1(i)^5 + p2*U1(i)^4 + p3*U1(i)^3 + p4*U1(i)
               ^2 + p5*U1(i) + p6)/P_nom;
            if Pout(i)<0
                Pout(i)=0;
            end
        elseif (U(i)>16) && (U(i)<=25)
            Pout(i)=1;
        else
            Pout(i)=0;
        end
    end
end
```

Table A.1 First 20 random samples of wind speed from Weibull distribution

Sample	Ur1	Ur2	Ur3
1	3.73	12.83	8.48
2	2.49	7.16	2.6
3	13.46	8.33	8.36
4	2.37	6.27	5.3
5	5.83	10.34	17.55
6	14.39	6.28	12.19
7	10.32	6.36	14.52
8	6.8	13.62	13.51
9	1.58	15.12	11.96
10	1.41	17.88	7.75
11	12.66	12.41	12.33
12	1.28	7.06	7.1
13	1.58	3.39	5.35
14	7.52	9.88	3.03
15	3.91	11.91	4.42
16	13.05	15.73	0.9
17	8.29	1.81	11.34
18	2.33	10.88	12.3
19	4.01	5.91	2.22
20	1.53	11.59	2.59

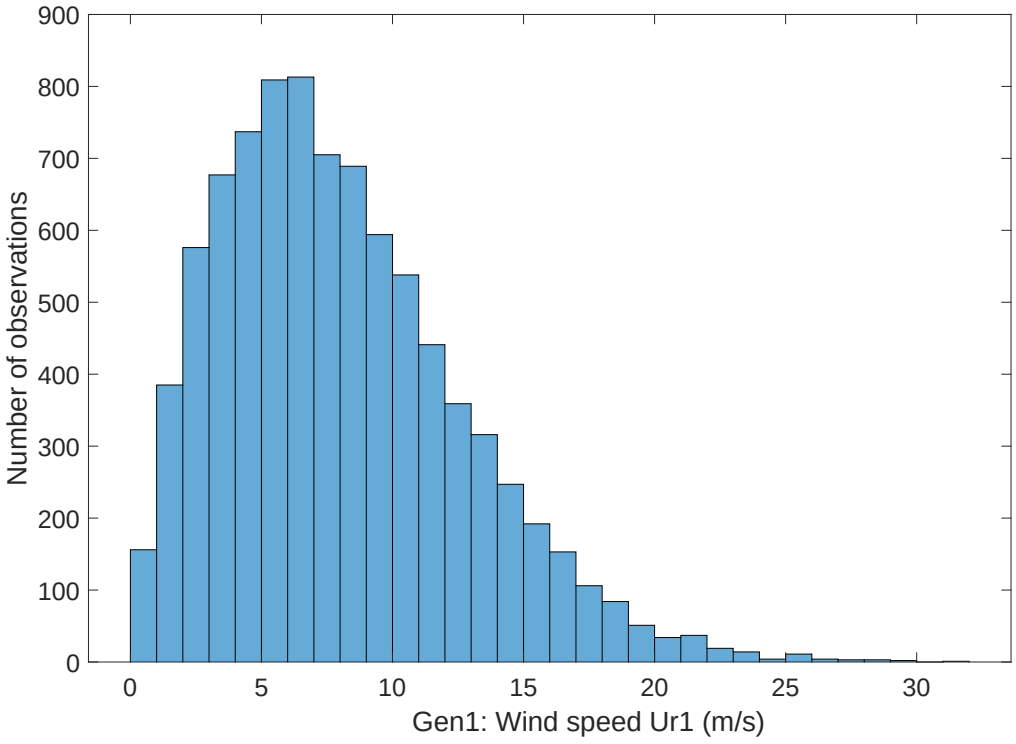

Fig. A.1 Histogram for wind speed Ur1

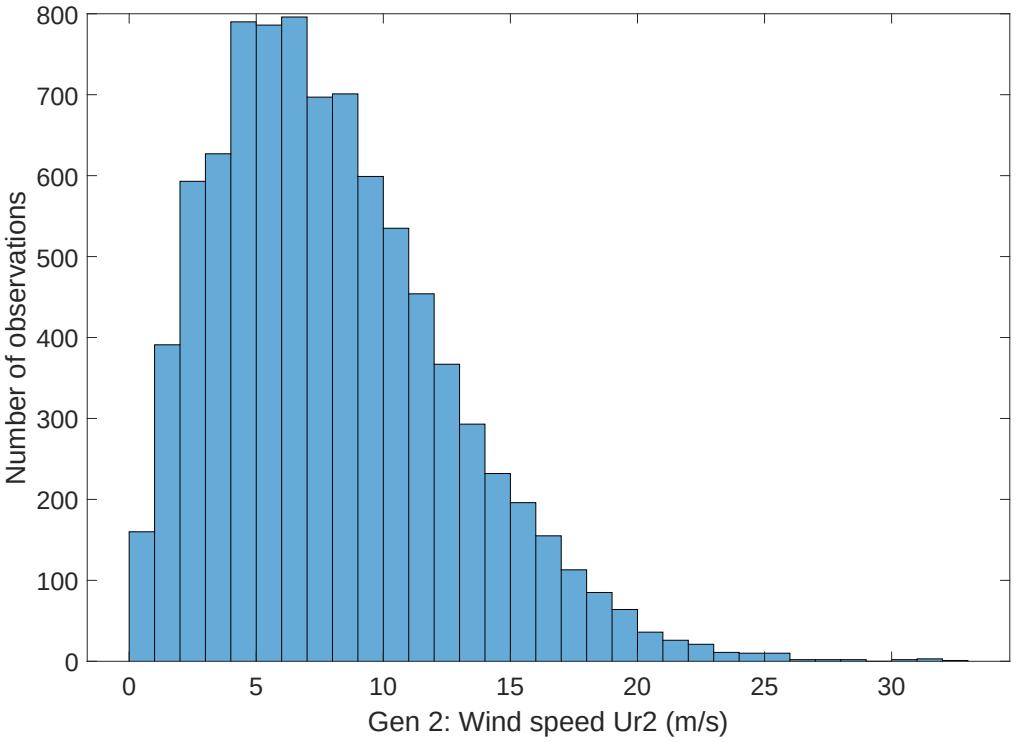

Fig. A.2 Histogram for wind speed Ur2

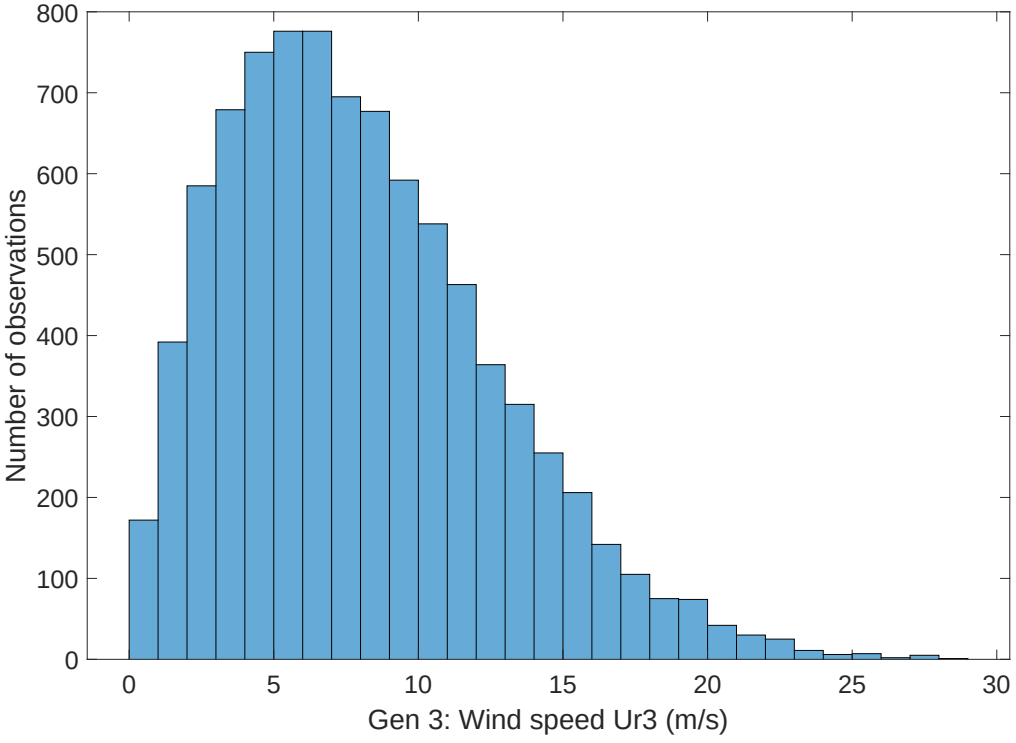

Fig. A.3 Histogram for wind speed Ur3

Calculated power curve

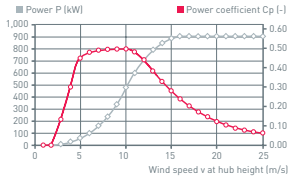

Wind (m/s)	Power P (kW)	Power-coefficient Cp (-)
1	0.0	0.00
2	0.0	0.00
3	4.0	0.16
4	20.0	0.34
5	50.0	0.43
6	96.0	0.48
7	156.0	0.49
8	238.0	0.50
9	340.0	0.50
10	466.0	0.50
11	600.0	0.48
12	710.0	0.44
13	790.0	0.39
14	850.0	0.33
15	880.0	0.28
16	905.0	0.24
17	910.0	0.20
18	910.0	0.17
19	910.0	0.14
20	910.0	0.12
21	910.0	0.11
22	910.0	0.09
23	910.0	0.08
24	910.0	0.07
25	910.0	0.06

ρ = 1.225 kg/m³

Technical specifications E-44

Rated power:	**900 kW**
Rotor diameter:	**44 m**
Hub height in meter:	**45 / 55**
Wind zone (DIBt):	**-**
Wind class (IEC):	**IEC/EN IA**
WEC concept:	Gearless, variable speed, single blade adjustment
Rotor	
Type:	Upwind rotor with active pitch control
Rotational direction:	Clockwise
No. of blades:	3
Swept area:	1,521 m²
Blade material:	GRP (epoxy resin); Built-in lightning protection
Rotational speed:	Variable, 16 - 34.5 rpm
Pitch control:	ENERCON single blade pitch system; one independent pitch system per rotor blade with allocated emergency supply
Drive train with generator	
Main bearing:	Twin tapered roller bearing
Generator:	ENERCON direct-drive annular generator
Grid feed:	ENERCON inverter
Brake systems:	– 3 independent pitch control systems with emergency power supply – Rotor brake – Rotor lock
Yaw system:	Active via yaw gear, load-dependent damping
Cut-out wind speed:	28 - 34 m/s (with ENERCON storm control*)
Remote monitoring:	ENERCON SCADA

* For more information on the ENERCON storm control feature, please see the last page.

E-44
900 kW

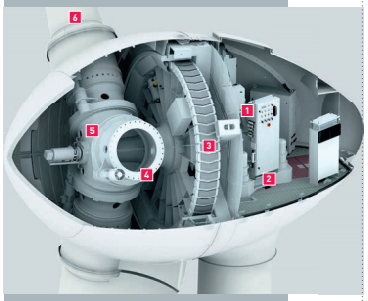

1 Main carrier
2 Yaw drive
3 Annular generator
4 Blade adapter
5 Rotor hub
6 Rotor blade

Fig. A.4 Power curve for Enercon E-44 wind turbine of 910 kW nominal capacity

A.2 Simulation analysis presented in Chapter 4

Listing A.3 Sample code for simulation analysis in Section 4.4.1: Effects of line investor's generation cost c_{G_1}

```
%% Scenario 1: Varying line investor's generation cost c_g1 (all other parameters remain fixed)
p_g=74.3; %Generation tariff price
c_g2=0.30*p_g; %Cost of generation for local generators
%Curtailment condition p_g-p_t>2*c_g1
x_curt=(p_g-2*c_g1)/p_g %Proposed percentage of p_t for curtailment smaller than
x=0.26; %x<=x_curt
p_t=x*p_g; %Transmission fee
% Specify net energy demand at location A in MWh for project lifetime (150MW*35%*8760h*20years)
E_d=150*0.35*8760*20;
c_g1=linspace(p_g/8,p_g*0.50); %Line investor's generation cost
% Energy production
E_g1_max=[(p_g-p_t)*c_g2*E_d]./[4*(c_g1).^2]; %Line investor
E_g2_max=[(p_g-p_t)*(2*c_g1-c_g2)*E_d]./[4*(c_g1).^2]; %Local generators
figure
plot(c_g1,E_g1_max,c_g1,E_g2_max,c_g1,E_g1_max+E_g2_max);

C_t=230*10^6; %Cost of transmission line
% Profits
P_1m=[[(p_g-p_t)*c_g2*E_d]./(4*c_g1)+p_t*E_d-C_t]/10^6; %Line investor
P_2m=[[[(2*c_g1-c_g2).^2]*(p_g-p_t)*E_d]./[4*(c_g1).^2]]/10^6; %Local generators
figure
plot(c_g1,P_1m,c_g1,P_2m,c_g1,P_1m+P_2m);
```

Listing A.4 Sample code for simulation analysis in Section 4.4.1: Effects of local generators' generation cost c_{G_2}

```
%% Scenario 2: Varying local generators' cost c_g2 (all other parameters remain fixed)
p_g=74.3; %Generation tariff price
c_g1=p_g*0.3; %Cost of generation for leader (1) is as a fraction of p_g
%Curtailment condition p_g-p_t>2*c_g1
```

```
x_curt=(p_g-2*c_g1)/p_g; %Proposed percentage of p_t for curtailment
    smaller than
x=0.26; %x<=x_curt
p_t=x*p_g; % Transmission fee
% Specify net energy demand at location A in MWh for project lifetime
    (150MW*35%*8760h*20years)
E_d=150*0.35*8760*20;
c_g2=linspace(0.0*c_g1,p_g); %Local generators' generation cost
% Energy production
E_g1_max=[(p_g-p_t)*c_g2*E_d]/[4*(c_g1)^2]; %Line investor
E_g2_max=[(p_g-p_t)*(2*c_g1-c_g2)*E_d]/[4*(c_g1)^2]; %Local
    generators
figure
plot(c_g2,E_g1_max,c_g2,E_g2_max,c_g2,E_g1_max+E_g2_max)

C_t=230*10^6; %Cost of transmission line
% Profits
P_1m=[[(p_g-p_t)*c_g2*E_d]/(4*c_g1)+p_t*E_d-C_t]/10^6; %Line investor
P_2m=[[[(2*c_g1-c_g2).^2]*(p_g-p_t)*E_d]/[4*(c_g1)^2]]/10^6; %Local
    generators
figure
plot(c_g2,P_1m,c_g2,P_2m,c_g2,P_1m+P_2m);
```

Listing A.5 Sample code for simulation analysis in Section 4.4.1: Effects of transmission fee p_T for $c_{G_1} > c_{G_2}$

```
%% Scenario 3a: Varying transmission fee p_t and c_g1>c_g2 (all other
    parameters remain fixed)
p_g=74.3; %Generation tariff price
c_g1=p_g*0.26; % Line investor's generation cost
c_g2=0.20*p_g; % Local generators' generation cost
p_t=linspace(0,p_g); %Transmission fee
% Specify net energy demand at location A in MWh for project lifetime
    (150MW*35%*8760h*20years)
E_d=150*0.35*8760*20;
% Energy production
E_g1_max=[(p_g-p_t)*c_g2*E_d]./[4*(c_g1).^2]; %Line investor
E_g2_max=[(p_g-p_t)*(2*c_g1-c_g2)*E_d]./[4*(c_g1).^2]; %Local
    generators
figure
plot(p_t,E_g1_max,p_t,E_g2_max,p_t,E_g1_max+E_g2_max);

C_t=230*10^6; %Cost of transmission line
```

```
% Profits
P_1m=[[(p_g-p_t)*c_g2*E_d]./(4*c_g1)+p_t*E_d-C_t]/10^6; %Line
    investor
P_2m=[[[(2*c_g1-c_g2).^2]*(p_g-p_t)*E_d]./[4*(c_g1).^2]]/10^6; %Local
    generators
figure
plot(p_t,P_1m,p_t,P_2m,p_t,P_1m+P_2m);
```

Listing A.6 Sample code for simulation analysis in Section 4.4.1: Effects of transmission fee p_T for $c_{G_1} < c_{G_2}$

```
%% Scenario 3b: Varying transmission fee p_t and c_g1<c_g2 (all other
    parameters remain fixed)
p_g=74.3; %Generation tariff price
c_g1=p_g*0.20; % Line investor's generation cost
c_g2=0.26*p_g; % Local generators' generation cost
p_t=linspace(0,p_g); %Transmission fee
% Specify net energy demand at location A in MWh for project lifetime
    (150MW*35%*8760h*20years)
E_d=150*0.35*8760*20;
% Energy production
E_g1_max=[(p_g-p_t)*c_g2*E_d]./[4*(c_g1).^2]; %Line investor
E_g2_max=[(p_g-p_t)*(2*c_g1-c_g2)*E_d]./[4*(c_g1).^2]; %Local
    generators
figure
plot(p_t,E_g1_max,p_t,E_g2_max,p_t,E_g1_max+E_g2_max);

C_t=230*10^6; %Cost of transmission line
% Profits
P_1m=[[(p_g-p_t)*c_g2*E_d]./(4*c_g1)+p_t*E_d-C_t]/10^6; %Line
    investor
P_2m=[[[(2*c_g1-c_g2).^2]*(p_g-p_t)*E_d]./[4*(c_g1).^2]]/10^6; %Local
    generators
figure
plot(p_t,P_1m,p_t,P_2m,p_t,P_1m+P_2m);
```

ofgem e-serve
Making a positive difference for energy consumers

Feed-in Tariff Generation & Export Payment Rate Table for Non-Photovoltaic Installations

All tariffs have been adjusted by the annual Retail Price Index rate (as at December 2015) of 1.2 percent, and are displayed in pence per kilowatt hour at 2016/17 values.

Anaerobic Digestion

Description	Period in which Tariff Date falls	Tariff (p/kWh)
Anaerobic digestion with total installed capacity of 250kW or less	1 April 2010 to 29 September 2011	13.82
	30 September 2011 to 31 March 2014	16.01
	1 April 2014 to 30 September 2014	12.81
	1 October 2014 to 31 March 2015	11.53
	1 April 2015 to 30 September 2015	10.25
	1 October 2015 to 15 January 2016	9.23
Anaerobic digestion with total installed capacity greater than 250kW but not exceeding 500kW	1 April 2010 to 29 September 2011	13.82
	30 September 2011 to 31 March 2014	14.81
	1 April 2014 to 30 September 2014	11.84
	1 October 2014 to 31 March 2015	10.67
	1 April 2015 to 30 September 2015	9.47
	1 October 2015 to 15 January 2016	8.52
Anaerobic digestion with total installed capacity greater than 500kW	1 April 2010 to 30 November 2012	10.79
	1 December 2012 to 31 March 2014	9.76
	1 April 2014 to 30 September 2014	9.76
	1 October 2014 to 31 March 2015	9.27
	1 April 2015 to 30 September 2015	8.78
	1 October 2015 to 15 January 2016	8.78

Hydro

Description	Period in which Tariff Date falls	Tariff (p/kWh)
Hydro generating station with total installed capacity of 15kW or less	1 April 2010 to 30 November 2012	23.84
	1 December 2012 to 31 March 2014	22.86
	1 April 2014 to 30 September 2014	21.72
	1 October 2014 to 31 March 2015	19.54
	1 April 2015 to 30 September 2015	17.38
	1 October 2015 to 15 January 2016	15.64
Hydro generating station with total installed capacity greater than 15kW but not exceeding 100kW	1 April 2010 to 31 March 2014	21.34
	1 April 2014 to 30 September 2014	20.28
	1 October 2014 to 31 March 2015	18.25
	1 April 2015 to 30 September 2015	16.22
	1 October 2015 to 15 January 2016	14.60
Hydro generating station with total installed capacity greater than 100kW but not exceeding 500kW	1 April 2010 to 14 March 2013	13.19
	15 March 2013 to 31 March 2014	16.87
	1 April 2014 to 30 September 2014	16.03
	1 October 2014 to 31 March 2015	14.42
	1 April 2015 to 30 September 2015	12.82

	1 October 2015 to 15 January 2016	11.54
Hydro generating station with total installed capacity greater than 500kW but not exceeding 2MW	1 April 2010 to 31 March 2014	13.19
	1 April 2014 to 30 September 2014	12.52
	1 October 2014 to 31 March 2015	11.27
	1 April 2015 to 30 September 2015	10.02
	1 October 2015 to 15 January 2016	9.02
Hydro generating station with total installed capacity greater than 2MW	1 April 2010 to 30 November 2012	5.33
	1 December 2012 to 31 March 2013	4.88
	1 April 2013 to 31 March 2014	3.41
	1 April 2014 to 30 September 2014	3.41
	1 October 2014 to 31 March 2015	3.08
	1 April 2015 to 30 September 2015	2.73
	1 October 2015 to 15 January 2016	2.46

Wind

Description	**Period in which Tariff Date falls**	**Tariff (p/kWh)**
Wind with total installed capacity of 1.5kW or less	1 April 2010 to 31 March 2012	41.25
	1 April 2012 to 30 November 2012	38.98
	1 December 2012 to 31 March 2014	22.86
	1 April 2014 to 30 September 2014	18.28
	1 October 2014 to 31 March 2015	16.46
	1 April 2015 to 30 September 2015	14.62
	1 October 2015 to 15 January 2016	13.89
Wind with total installed capacity greater than 1.5kW but not exceeding 15kW	1 April 2010 to 31 March 2012	31.91
	1 April 2012 to 30 November 2012	30.48
	1 December 2012 to 31 March 2014	22.86
	1 April 2014 to 30 September 2014	18.28
	1 October 2014 to 31 March 2015	16.46
	1 April 2015 to 30 September 2015	14.62
	1 October 2015 to 15 January 2016	13.89
Wind with total installed capacity greater than 15kW but not exceeding 100kW	1 April 2010 to 31 March 2012	28.85
	1 April 2012 to 30 November 2012	27.66
	1 December 2012 to 31 March 2014	22.86
	1 April 2014 to 30 September 2014	18.28
	1 October 2014 to 31 March 2015	16.46
	1 April 2015 to 30 September 2015	14.62
	1 October 2015 to 15 January 2016	13.89
Wind with total installed capacity greater than 100kW but not exceeding 500kW	1 April 2010 to 30 November 2012	22.43
	1 December 2012 to 31 March 2014	19.06
	1 April 2014 to 30 September 2014	15.24
	1 October 2014 to 31 March 2015	13.71
	1 April 2015 to 30 September 2015	12.19
	1 October 2015 to 15 January 2016	10.98
Wind with total installed capacity greater than 500kW but not exceeding 1.5MW	1 April 2010 to 30 November 2012	11.32
	1 December 2012 to 31 March 2014	10.33
	1 April 2014 to 30 September 2014	8.27
	1 October 2014 to 31 March 2015	7.45
	1 April 2015 to 30 September 2015	6.62

	1 October 2015 to 15 January 2016	5.96
Wind with total installed capacity greater than 1.5MW	1 April 2010 to 30 November 2012	5.33
	1 December 2012 to 31 March 2013	4.88
	1 April 2013 to 31 March 2014	4.38
	1 April 2014 to 30 September 2014	3.50
	1 October 2014 to 31 March 2015	3.16
	1 April 2015 to 30 September 2015	2.80
	1 October 2015 to 15 January 2016	2.52

Combined Heat and Power (CHP)

Description	**Period in which Tariff Date falls**	**Tariff (p/kWh)**
Combined Heat and Power with total installed electrical capacity of 2kW or less (tariff only available for 30,000 units)	1 April 2010 to 14 March 2013	11.98
	15 March 2013 to 15 January 2016	13.61

Renewables Obligation Order Migrated Installations

Description	**Period in which Tariff Date falls**	**Tariff (p/kWh)**
Eligible Installations with a declared net capacity of 50kW or less Commissioned on or before 14 July 2009 and accredited under the ROO on or before 31 March 2010	1 April 2010 to 31 March 2014	10.79

Export Tariffs

Description	**Period in which Tariff Date falls**	**Tariff (p/kWh)**
All Eligible Installations	1 April 2010 to 30 November 2012	3.48
	on or after 1 December 2012	4.91

Note: FIT Payment rates for installations have been determined by the Gas and Electricity Markets Authority (Ofgem) under Article 13 of the Feed-in Tariffs Order 2012, in accordance with Annexes 2-4 to the Standard Licence Conditions.

All tariff rates are specified as pence per kilowatt hour at 2016/17 values.

Date of publication: 01 February 2016

A.3 Simulation analysis presented in Chapter 5

Wind speed data were imported from the UK MIDAS dataset Met Office. Two weather stations were identified in the region of interest. Weather station with ID 908 located in the Kintyre peninsula and weather station with ID 23417 located in Islay. Distance between the weather stations is 44 km. Available data for ID 908 start from January 1969 until December 2015 and consist of hourly data. Weather ID 23417 available data from January 1999 until December 2015. Common data available from 1999 to 2015 used for analysis. Raw data sample were provided in csv file format.

ob_end_time	id_type	id	ob_hour_count	met_domain_name	version_num	src_id	rec_st_ind	mean_wind_dir	mean_wind_speed	max_gust_dir	max_gust_speed	max_gust_ctime	mean_wind_dir_q	mean_wind_speed_q
01/01/1969 01:00	WIND	604001	1	HWND6910	1	908	1001	300	15				9	9
01/01/1969 02:00	WIND	604001	1	HWND6910	1	908	1001	300	15				9	9
01/01/1969 03:00	WIND	604001	1	HWND6910	1	908	1001	290	15				9	9
01/01/1969 04:00	WIND	604001	1	HWND6910	1	908	1001	280	16				9	9
01/01/1969 05:00	WIND	604001	1	HWND6910	1	908	1001	290	20				9	9
01/01/1969 06:00	WIND	604001	1	HWND6910	1	908	1001	290	18				9	9
01/01/1969 07:00	WIND	604001	1	HWND6910	1	908	1001	280	20				9	9
01/01/1969 08:00	WIND	604001	1	HWND6910	1	908	1001	280	19				9	9
01/01/1969 09:00	WIND	604001	1	HWND6910	1	908	1001	280	22				9	9
01/01/1969 10:00	WIND	604001	1	HWND6910	1	908	1001	270	19				9	9
01/01/1969 11:00	WIND	604001	1	HWND6910	1	908	1001	270	17				9	9
01/01/1969 12:00	WIND	604001	1	HWND6910	1	908	1001	270	15				9	9
01/01/1969 13:00	WIND	604001	1	HWND6910	1	908	1001	270	18				9	9
01/01/1969 14:00	WIND	604001	1	HWND6910	1	908	1001	290	20				9	9
01/01/1969 15:00	WIND	604001	1	HWND6910	1	908	1001	280	20				9	9
01/01/1969 16:00	WIND	604001	1	HWND6910	1	908	1001	290	21				9	9
01/01/1969 17:00	WIND	604001	1	HWND6910	1	908	1001	290	21				9	9
01/01/1969 18:00	WIND	604001	1	HWND6910	1	908	1001	300	18				9	9
01/01/1969 19:00	WIND	604001	1	HWND6910	1	908	1001	300	18				9	9
01/01/1969 20:00	WIND	604001	1	HWND6910	1	908	1001	290	19				9	9

Fig. A.5 First 20 wind speed data points provided my the MIDAS dataset

Listing A.7 Sample code for wind speed data import in Section 5.3.1: Data import for weather station with ID 908

```
%% Import data weather station ID 908 – Clean data
numfiles = 47; %years data is available
temp_data = cell(1, numfiles);
mydata1=cell(1,numfiles);%data without NaN
mydata2=cell(1,numfiles);%full data NaN included
%% Set start date amd end date of first year
start_t1='01-Jan-1969 00:00:00';%1969
start_t1=datetime(start_t1);
end_t2='31-Dec-1969 23:00:00';
end_t2=datetime(end_t2);
%%  Import files
for k = 1:numfiles
    myfilename = sprintf('file%d.csv', k);
    temp_data{k} = importfile(myfilename, 1, 20000);
end
%% Clean data
for k=1:numfiles
    %% Assign data to different variable
    T=temp_data{k};
    T(1,:)=[];
    %% Find empty data and erase them
```

```
toDelete=find(isnan(T.mean_wind_speed));
T(toDelete,:)=[];
%% Find exact duplicates and erase them
count_dupl=size(T)-size(unique(T));
T=unique(T);
%% Find double entries for same point in time
%Store time vector as mumerical data
A=datenum(T.ob_end_time);
[n,bin]=histc(A,unique(A));
multiple=find(n>1);
i_dupl=find(ismember(bin, multiple));%index of rows that are
   duplicate
%% Delete duplicate entries with version_num=0
if not(isempty(i_dupl))
    toKeep=find(ismember(i_dupl,find(T.version_num==1)));%rows
       that have version=1 and must be kept although duplicates
    toDelete=i_dupl;
    toDelete(toKeep,:)=[];
    T(toDelete,:)=[];
end
%% Delete any remaining version_number=0
toDelete=find(T.version_num==0);
T(toDelete,:)=[];
%% Find double entries for same point in time
%Reset variables
A=[];
n=[];
bin=[];
i_dupl=[];
multiple=[];
toKeep=[];
toDelete=[];
count_dupl=[];
%Store time vector as mumerical data
A=datenum(T.ob_end_time);
[n,bin]=histc(A,unique(A));
multiple=find(n>1);
i_dupl=find(ismember(bin, multiple));%index of rows that are
   duplicate
%% Delete duplicate entries with lower midas_stmp_etime
if not(isempty(i_dupl))
    i_dupl_two=reshape(i_dupl,2,[]);
```

```
        [max,indec]=max(T.midas_stmp_etime(i_dupl_two));%indec stores
            the row indices of max in each column
        i_dupl_two=i_dupl_two(indec,:);
        i_dupl_two=i_dupl_two(1,:)';
        toKeep=find(ismember(i_dupl, i_dupl_two));
        toDelete=i_dupl;
        toDelete(toKeep,:)=[];
        T(toDelete,:)=[];
    end
    %% Keep only relevant data
    D=table(T.ob_end_time,T.mean_wind_speed,'VariableNames',{'
        ob_end_time' 'mean_wind_speed'});
    mydata1{k}=D; %data including NaN values
    %% Identify missing data
    %Entries I should have
    A=[];
    A=D.ob_end_time;
    A=datenum(A);

    Aref=start_t1:hours(1):end_t2;
    A_dt=Aref';%copy in datetime format
    Aref=datenum(Aref');
    C=setxor(A,Aref);%setxor(A,B) returns the data of A and B that
        are not in their intersection
    C(:,2)=nan;
    A(:,2)=D.mean_wind_speed;
    A=cat(1,A,C);
    [Y,I]=sort(A(:,1));
    B=A(I,:);%use the column indices from sort() to sort all columns
        of A.
    Data=table(A_dt,B(:,2),'VariableNames',{'ob_end_time' '
        mean_wind_speed'});
    mydata2{k}=Data;
    %% Clear all variables except what we need for next iteration
    clearvars -except mydata1 mydata2 numfiles temp_data start_t1
        end_t2
    %% Go to next year
    start_t1=start_t1+calyears(1);
    end_t2=end_t2+calyears(1);
end
%% Data interpolation for gaps smaller or equal to 6 hr
small_gap=6;%define here desired gap
```

```
data_interp=cell(1,numfiles);
count_non_sub=0;
for i=1:numfiles
    %remove nans for interpolation first
    mydata=mydata2{1,i}.mean_wind_speed;
    x=1:length(mydata2{1,i}.mean_wind_speed);
    y=mydata(~isnan(mydata));
    x=x(~isnan(mydata));
    x=x';
    xq=ind_int{1,i};
    vq1=round(interp1(x,y,xq,'linear'));%round to nearest knot
    %plug in data to variable
    mydata(xq)=vq1;
    mytime=mydata2{1,i}.ob_end_time;
    D=table(mytime,mydata,'VariableNames',{'ob_end_time' '
       mean_wind_speed'});
    data_interp{1,i}=D;
end
save('qual_data_908.mat','data_interp');
```

Listing A.8 Sample code for wind speed data analysis in Section 5.3.1: Data analysis and quality check for weather station with ID 908

```
%% Load data
load qual_data_908;%908
%% Collect data from 1999-2015
data20=[];
for k=31:47 %12-31
    data20=cat(1,data20,data_interp{1,k});%put data in one table
end
%% Store data according to time and season
%Hourly data
data_hr=cell(1,24);
for i=1:24
    toKeep=find(data20.ob_end_time.Hour==(i-1));
    data_hr{1,i}=data20(toKeep,:);
end
%Data by season
data_season=cell(1,4);
%Spring
toKeep=[];
toKeep=find((data20.ob_end_time.Month==3)|(data20.ob_end_time.Month
   ==4)|(data20.ob_end_time.Month==5));
```

```
data_season{1,1}=data20(toKeep,:);
%Summer
toKeep=[];
toKeep=find((data20.ob_end_time.Month==6)|(data20.ob_end_time.Month
   ==7)|(data20.ob_end_time.Month==8));
data_season{1,2}=data20(toKeep,:);
%Autumn
toKeep=[];
toKeep=find((data20.ob_end_time.Month==9)|(data20.ob_end_time.Month
   ==10)|(data20.ob_end_time.Month==11));
data_season{1,3}=data20(toKeep,:);
%Winter
toKeep=[];
toKeep=find((data20.ob_end_time.Month==12)|(data20.ob_end_time.Month
   ==1)|(data20.ob_end_time.Month==2));
data_season{1,4}=data20(toKeep,:);
data908=cell(24,4);
for j=1:4
    for i=1:24
        toKeep=[];
        toKeep=find(data_season{1,j}.ob_end_time.Hour==(i-1));
        data908{i,j}=data_season{1,j}(toKeep,:);
    end
end
data_distr_908=data908;
%% Fit Weibull Distribution
%remove all Nans before applying Weibull fit and count
nan_count908=cell(24,4);
for i=1:24
    for j=1:4
        nan_val=isnan(data908{i,j}.mean_wind_speed);
        nan_count908{i,j}=sum(isnan(data908{i,j}.mean_wind_speed));
        data908{i,j}(nan_val,:)=[];
    end
end
%% Fit Weibull distributions
par908=cell(24,4);
for i=1:24
    for j=1:4
        temp=data908{i,j}.mean_wind_speed;
        mean_wind908(i,j) = nanmean(temp);
        max_wind908(i,j) = nanmax(temp);
```

```
        min_wind908(i,j) = nanmin(temp);
        isvector(temp);%check if vector
        if any(temp<=0)%check there are non zero values
            temp(temp==0)=nan;
        end
        pd=fitdist(temp,'weibull');
        par908{i,j}=pd.ParameterValues;
        c_shape908(i,j)=par908{i,j}(1);
        k_scale908(i,j)=par908{i,j}(2);
    end
end
% Weibull parameters for anemometer height
save('c_imported_908.mat','c_shape908');
save('k_imported_908.mat','k_scale908');
%% Adjust wind speeds for wind turbine height
%based on an Enercon E82 E2 turbine of height h=85 m
clearvars -except data20 data_distr_908
z0=0.03;%30mm roughness surface
zh=85;%hub height
zr=10;%21m anemometer height in previous wrong analysis
data908_long=data20;
data908_long.mean_wind_speed=data908_long.mean_wind_speed*(log(zh/z0)
   )/(log(zr/z0));
data908_ms=data_distr_908;
%remove all Nans before applying Weibull fit
for i=1:24
    for j=1:4
        nan_val=isnan(data908_ms{i,j}.mean_wind_speed);
        data908_ms{i,j}(nan_val,:)=[];
    end
end
for j=1:4
    for i=1:24
        %extrapolate from anemometer to hub height
        data908_ms{i,j}.mean_wind_speed=data908_ms{i,j}.
           mean_wind_speed*(log(zh/z0))/(log(zr/z0));
        data_distr_908{i,j}.mean_wind_speed=data_distr_908{i,j}.
           mean_wind_speed*(log(zh/z0))/(log(zr/z0));
    end
end
%% Fit Weibull distribution for hub height
par908_85=cell(24,4);
```

```
temp=[];
for i=1:24
    for j=1:4
        temp=data908_ms{i,j}.mean_wind_speed;
        mean_wind908_85(i,j) = nanmean(temp);
        max_wind908_85(i,j) = nanmax(temp);
        min_wind908_85(i,j) = nanmin(temp);
        isvector(temp);%check if vector
        if any(temp<=0)%check there are non zero values
            temp(temp==0)=nan;
        end
        pd=fitdist(temp,'weibull');
        par908_85{i,j}=pd.ParameterValues;
        c_shape908_85(i,j)=par908_85{i,j}(1);
        k_scale908_85(i,j)=par908_85{i,j}(2);
    end
end
c_908=c_shape908_85*0.514444;%convert to m/s
save('c_908.mat','c_908');
save('k_908.mat','k_scale908_85');
%% Save data for in long and seasonal format
save('data_seas_908.mat','data_distr_908');
save('data_long_908.mat','data908_long');
```

Listing A.9 Sample code for simulation analysis in Section 5.3.1: Sigmoid fit for wind power output

```
%% Wind power output
% Enercon E82 E2 values
u=[0:28].*1.94384;% in knots
Pw=[0;0;3;25;82;174;321;532;815;1180;1580;1810;1980;2050;..];
P=Pw'/2050;%per unit
%% Sigmoid fit
[x,y]=createFit(u,P);
par=coeffvalues(x);
a=par(1,1);
c=par(1,2);
%% Import and make zero if u>28m/s and apply sigmoid
load data_seas_908;
data908_ms=data_distr_908;
Umax=28*1.94384;
for i=1:24
    for j=1:4
```

```
        temp=data908_ms{i,j}.mean_wind_speed;
        temp(temp>Umax)=0;
        temp=1./(1+exp(-a*(temp-c)));
        newdata=table(data908_ms{i,j}.ob_end_time,temp,'VariableNames
            ',{'ob_end_time' 'power_output'});
        power_data908{i,j}=newdata;
    end
end
save('power_data_908.mat','power_data908')
save('sigmoid_fit908.mat','par')
```

Listing A.10 Sample code for simulation analysis in Section 5.3.1: Beta fit for power output distribution

```
%% Fit Beta distibutions to wind power output data
load power_data_908;
temp=[];
par_beta908=cell(24,4);
for i=1:24
    for j=1:4
        temp=power_data908{i,j}.power_output;
%         figure;
%         histogram(temp)
        isvector(temp);%check if vector
        if any(temp<0)%check there are non negative values
            temp(temp<0)=nan;
        end
        if any(temp==0)%check there are non zero values
            temp(temp==0)=0+10^(-6);
        end
        if any(temp==1)%check any values equal to 1
            temp(temp==1)=1-10^(-6);
        end
        pd=fitdist(temp,'beta');
        par_beta908{i,j}=pd.ParameterValues;
        alpha908(i,j)=par_beta908{i,j}(1);
        beta908(i,j)=par_beta908{i,j}(2);
    end
end
save('alpha_908.mat','alpha908');
save('beta_908.mat','beta908');
```

The analysis is based on the UK National Demand data obtained by the UK's system operator, i.e. National Grid (http://www2.nationalgrid.com/UK/Industry-information/Electricity-transmission-operational-data/Data-Explorer/). The data used for the study span from 2006 to 2015. The observations include national demand data in half-hourly settlement intervals.

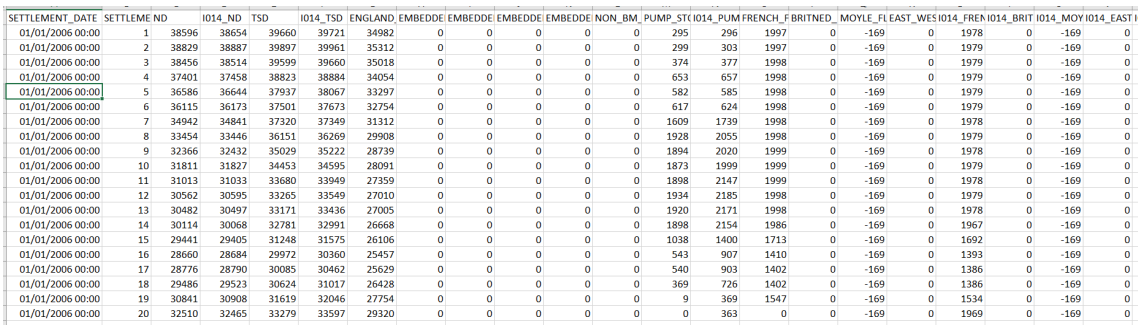

SETTLEMENT_DATE	SETTLEME	ND	I014_ND	TSD	I014_TSD	ENGLAND_	EMBEDDE	EMBEDDE	EMBEDDE	EMBEDDE	NON_BM_	PUMP_ST(	I014_PUM	FRENCH_F	BRITNED_	MOYLE_FL	EAST_WES	I014_FREN	I014_BRIT	I014_MOY	I014_EAST
01/01/2006 00:00	1	38596	38654	39660	39721	34982	0	0	0	0	0	295	296	1997	0	-169	0	1978	0	-169	0
01/01/2006 00:00	2	38829	38887	39897	39961	35312	0	0	0	0	0	299	303	1997	0	-169	0	1979	0	-169	0
01/01/2006 00:00	3	38456	38514	39599	39660	35018	0	0	0	0	0	374	377	1998	0	-169	0	1979	0	-169	0
01/01/2006 00:00	4	37401	37458	38823	38884	34054	0	0	0	0	0	653	657	1998	0	-169	0	1979	0	-169	0
01/01/2006 00:00	5	36586	36644	37937	38067	33297	0	0	0	0	0	582	585	1998	0	-169	0	1979	0	-169	0
01/01/2006 00:00	6	36115	36173	37501	37673	32754	0	0	0	0	0	617	624	1998	0	-169	0	1979	0	-169	0
01/01/2006 00:00	7	34942	34841	37320	37349	31312	0	0	0	0	0	1609	1739	1998	0	-169	0	1978	0	-169	0
01/01/2006 00:00	8	33454	33446	36151	36269	29908	0	0	0	0	0	1928	2055	1998	0	-169	0	1979	0	-169	0
01/01/2006 00:00	9	32366	32432	35029	35222	28739	0	0	0	0	0	1894	2020	1999	0	-169	0	1978	0	-169	0
01/01/2006 00:00	10	31811	31827	34453	34595	28091	0	0	0	0	0	1873	1999	1999	0	-169	0	1979	0	-169	0
01/01/2006 00:00	11	31013	31033	33680	33949	27359	0	0	0	0	0	1898	2147	1999	0	-169	0	1978	0	-169	0
01/01/2006 00:00	12	30562	30595	33265	33549	27010	0	0	0	0	0	1934	2185	1998	0	-169	0	1979	0	-169	0
01/01/2006 00:00	13	30482	30497	33171	33436	27005	0	0	0	0	0	1920	2171	1998	0	-169	0	1978	0	-169	0
01/01/2006 00:00	14	30114	30068	32781	32991	26668	0	0	0	0	0	1898	2154	1986	0	-169	0	1967	0	-169	0
01/01/2006 00:00	15	29441	29405	31248	31575	26106	0	0	0	0	0	1038	1400	1713	0	-169	0	1692	0	-169	0
01/01/2006 00:00	16	28660	28684	29972	30360	25457	0	0	0	0	0	543	907	1410	0	-169	0	1393	0	-169	0
01/01/2006 00:00	17	28776	28790	30085	30462	25629	0	0	0	0	0	540	903	1402	0	-169	0	1386	0	-169	0
01/01/2006 00:00	18	29486	29523	30624	31017	26428	0	0	0	0	0	369	726	1402	0	-169	0	1386	0	-169	0
01/01/2006 00:00	19	30841	30908	31619	32046	27754	0	0	0	0	0	9	369	1547	0	-169	0	1534	0	-169	0
01/01/2006 00:00	20	32510	32465	33279	33597	29320	0	0	0	0	0	0	363	0	0	-169	0	1969	0	-169	0

Fig. A.6 First 20 demand data points provided my the UK national demand database

Listing A.11 Sample code for demand data import in Section 5.3.2: Data imported from UK national demand

```
%% Demand data import and analysis
numfiles=10; %10 years of available data
temp_data = cell(1, numfiles);
demand_data=cell(1,numfiles);%data without NaN
%%  Import files
for k = 1:numfiles
    myfilename = sprintf('demand_data%d.csv', k);
    temp_data{k} = importfile_demand(myfilename, 1, 20000);
end
%% Data analysis
for k=1:numfiles
    %% Assign data to different variable
    T=temp_data{k};
    T(1,:)=[];
    T.FRENCH_FLOW(T.FRENCH_FLOW<0)=0;
    T.BRITNED_FLOW(T.BRITNED_FLOW<0)=0;
    T.MOYLE_FLOW(T.MOYLE_FLOW<0)=0;
    T.EAST_WEST_FLOW(T.EAST_WEST_FLOW<0)=0;
    Imports=T.FRENCH_FLOW+T.BRITNED_FLOW+T.MOYLE_FLOW+T.
        EAST_WEST_FLOW;
    real_demand=T.ND+T.EMBEDDED_WIND_GENERATION+T.
        EMBEDDED_SOLAR_GENERATION+Imports;
    demand_data{1,k}=table(T.SETTLEMENT_DATE,T.SETTLEMENT_PERIOD,
        real_demand,'VariableNames',{'SETTLEMENT_DATE' '
        SETTLEMENT_PERIOD' 'Real_demand'});
```

```
end
save('real_demand.mat','demand_data');
```

Listing A.12 Sample code for demand data analysis in Section 5.3.2: Data analysis and quality check

```
%% Demand data analysis
load real_demand.mat
numfiles=10;
final_demand=cell(1,numfiles);
for k=1:numfiles
    T=demand_data{k};
    x=T.Real_demand;
    length=numel(x)/2;
    x=reshape(x,[2,length]);
    aver=mean(x);
    aver=aver';
    T.SETTLEMENT_PERIOD=round(T.SETTLEMENT_PERIOD/2,0);%hourly mean
    %delete odd rows
    T(2:2:end,:)=[];
    %replace with average
    T.TSD=aver;
    %merge date with hours
    A=datenum(T.SETTLEMENT_DATE);
    for i=1:1:numel(A)
        temp=A(i,1);
        add_hour=T.SETTLEMENT_PERIOD(i,1)-1;
        temp=addtodate(temp, add_hour, 'hour');
        A(i,1)=temp;
    end
    A=datetime(A, 'ConvertFrom', 'datenum');
    A=dateshift(A, 'start', 'second', 'nearest');
    data=table(A,aver,'VariableNames',{'time' 'demand'});
    final_demand{1,k}=data;
end
save('final_demand.mat','final_demand');
%% Put data in one table
data=[];
for k=1:10 %12-31
    data=cat(1,data,final_demand{1,k});%put data in one table
end
%% Hourly-Season distributions
%Hourly data
```

```
data_hr=cell(1,24);
for i=1:24
    toKeep=find(data.time.Hour==(i-1));
    data_hr{1,i}=data(toKeep,:);
end
%Data by season
data_season=cell(1,4);
%Spring
toKeep=[];
toKeep=find((data.time.Month==3)|(data.time.Month==4)|(data.time.
   Month==5));
data_season{1,1}=data(toKeep,:);
%Summer
toKeep=[];
toKeep=find((data.time.Month==6)|(data.time.Month==7)|(data.time.
   Month==8));
data_season{1,2}=data(toKeep,:);
%Autumn
toKeep=[];
toKeep=find((data.time.Month==9)|(data.time.Month==10)|(data.time.
   Month==11));
data_season{1,3}=data(toKeep,:);
%Winter
toKeep=[];
toKeep=find((data.time.Month==12)|(data.time.Month==1)|(data.time.
   Month==2));
data_season{1,4}=data(toKeep,:);
data_all=cell(24,4);
for j=1:4
    for i=1:24
        toKeep=[];
        toKeep=find(data_season{1,j}.time.Hour==(i-1));
        data_all{i,j}=data_season{1,j}(toKeep,:);
    end
end
```

Listing A.13 Sample code for simulation analysis in Section 5.4.2: Effects of local generators' generation cost c_{G_2}

```
%% Stackelberg game analysis for Scenario 2
% Initialisation
line_cap=150;% 150MW is the capacity of the transmission line
load demand;%scaled down from UK national demand
```

```
load power_data_908
load power_data_23417
%% Define search space
dP=0.5;%Granularity of x MW
PnMax=415;%Maximum power in search space
Pn1=0:dP:PnMax;%in MW
Pn2=0:dP:PnMax;
ss1=size(Pn1,2);
ss2=size(Pn2,2);
%% Compute curtailment
all_sum=cell(ss1,ss2);
for k=1:ss1
    PN1=Pn1(1,k);
    for l=1:ss2
        PN2=Pn1(1,l);
        EG1=0;
        EG2=0;
        EC1=0;
        EC2=0;
        EC=0;
        num_elem=0;
        for i=1:24
            for j=1:4
                gen1=PN1*power1{i,j};
                gen2=PN2*power2{i,j};
                ll=length(gen1);
                d=[];
                d(1:ll,:)=demand(i,j);
                dif=gen1+gen2-d;
                indd=find(dif<0);
                dif(indd)=0;
                pc1=gen1.*dif./(gen1+gen2);
                pc2=gen2.*dif./(gen1+gen2);
                num_elem=num_elem+size(gen1,1);
                EG1=EG1+sum(gen1);
                EG2=EG2+sum(gen2);
                EC1=EC1+sum(pc1);
                EC2=EC2+sum(pc2);
                EC=EC+sum(dif);
            end
        end
```

```
        all_sum{k,l}=table(EG1,EG2,EC1,EC2,EC,num_elem,'VariableNames
            ',{'Gen1' 'Gen2' 'Curt1' 'Curt2' 'Curtailment' 'Num_Elem'
            });
    end
end
clearvars -except all_sum Pn1 Pn2 ss1 ss2
pg=73.4;%in pounds/MWh
Ct=230*10^6;%cost of building the line
%% Scenario 2
dx=0.02*pg;
cg1=0.24*pg;
pt=0.3*pg;
cg2=0.06*pg:dx:0.6*pg;
for n=1:size(cg2,2)
    profits=cell(ss1,ss2);
    for k=1:ss1
        for l=1:ss2
            EG1=all_sum{k,l}.Gen1;
            EG2=all_sum{k,l}.Gen2;
            EC1=all_sum{k,l}.Curt1;
            EC2=all_sum{k,l}.Curt2;
            prof_1(k,l)=pg*(EG1-EC1)-cg1*EG1+pt*(EG2-EC2)-Ct;
            prof_2(k,l)=(pg-pt)*(EG2-EC2)-cg2(1,n)*EG2;
        end
    end
    %Find first maxP2 for each row
    [val_2 id_2]=max(prof_2,[],2);
    id_1=sub2ind(size(prof_1),[1:size(prof_2)]',id_2);
    %collect corresponding P1 for each maxP2
    val_1=prof_1(id_1);
    %Find maxP1
    [max_1,loc_k]=max(val_1);
    %The equilibrium is max_1,max_2 at the location specified by
        indeces
    %(loc_k,loc_l)
    loc_l=id_2(loc_k,1);
    max_2=prof_2(loc_k,loc_l);
    %Find corresponding rated capacities built
    Cap1=Pn1(1,loc_k);
    Cap2=Pn2(1,loc_l);
    %Find statistics of equilibrium
    all_sum{loc_k,loc_l};
```

```
85      EG1=all_sum{loc_k,loc_l}.Gen1;
86      EG2=all_sum{loc_k,loc_l}.Gen2;
87      EC1=all_sum{loc_k,loc_l}.Curt1;
88      EC2=all_sum{loc_k,loc_l}.Curt2;
89      EC=all_sum{loc_k,loc_l}.Curtailment;
90      num_elem=all_sum{loc_k,loc_l}.Num_Elem;
91      all_profits{1,n}=table(Cap1,Cap2,max_1,max_2,EG1,EG2,EC1,EC2,EC,
            num_elem,'VariableNames',{'Cap1' 'Cap2' 'max_1' 'max_2' 'Gen1'
             'Gen2' 'Curt1' 'Curt2' 'Curtailment' 'Num_Elem'});
92      clearvars val_1 val_2 id_1 id_2 prof_1 prof_2 max_1 max_2 loc_k
            loc_l Cap1 Cap2 EG1 EG2 EC1 EC2 EC num_elem
93  end
```

Calculated power curve

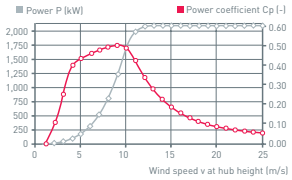

Wind (m/s)	Power P (kW)	Power-coefficient Cp (-)
1	0.0	0.00
2	3.0	0.12
3	25.0	0.29
4	82.0	0.40
5	174.0	0.43
6	321.0	0.46
7	532.0	0.48
8	815.0	0.49
9	1,180.0	0.50
10	1,580.0	0.49
11	1,810.0	0.42
12	1,980.0	0.35
13	2,050.0	0.29
14	2,050.0	0.23
15	2,050.0	0.19
16	2,050.0	0.15
17	2,050.0	0.13
18	2,050.0	0.11
19	2,050.0	0.09
20	2,050.0	0.08
21	2,050.0	0.07
22	2,050.0	0.06
23	2,050.0	0.05
24	2,050.0	0.05
25	2,050.0	0.04

ρ = 1.225 kg/m³

Technical specifications E-82 E2

Rated power:	**2,000 kW**
Rotor diameter:	**82 m**
Hub height in meter:	**78 / 84 / 85 / 98 / 108 / 138**
Wind zone (DIBt):	**WZ III**
Wind class (IEC):	**IEC/EN IIA**
WEC concept:	Gearless, variable speed, single blade adjustment
Rotor	
Type:	Upwind rotor with active pitch control
Rotational direction:	Clockwise
No. of blades:	3
Swept area:	5,281 m²
Blade material:	GRP (epoxy resin); Built-in lightning protection
Rotational speed:	Variable, 6 - 18 rpm
Pitch control:	ENERCON single blade pitch system; one independent pitch system per rotor blade with allocated emergency supply
Drive train with generator	
Main bearing:	Double row tapered/cylindrical roller bearings
Generator:	ENERCON direct-drive annular generator
Grid feed:	ENERCON inverter
Brake systems:	– 3 independent pitch control systems with emergency power supply – Rotor brake – Rotor lock
Yaw system:	Active via yaw gear, load-dependent damping
Cut-out wind speed:	28 - 34 m/s (with ENERCON storm control*)
Remote monitoring:	ENERCON SCADA

* For more information on the ENERCON storm control feature, please see the last page.

E-82
2,000 kW

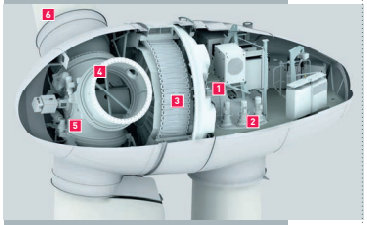

1 Main carrier
2 Yaw drive
3 Annular generator
4 Blade adapter
5 Rotor hub
6 Rotor blade

Fig. A.7 Power curve for Enercon E-82 wind turbine of 2000 kW nominal capacity

A.4 Simulation analysis presented in Chapter 6

Listing A.14 Sample code for simulation analysis in Section 6.2: Estimation of conditional probability distributions

```
%% Gibbs sampling data
x1 % Wind speed at location 1
x2 % Wind speed at location 2
X3D % Demand
ii=48;% number of bins for step=1knot/number of bins is kept equal
   for all variables
line_cap=150;%line capacity
XD3(find(XD3>line_cap))=line_cap;% adjust demand for line capacity
aver=(x1+x2)/2;%average wind speed for cond. distribution
%dstepi computes the step size required to achieve ii bins (=48)
dstep1=(max(max(x1,x2))-min(min(x1,x2)))/(ii-1);
dstep2=(max(max(x1,x2))-min(min(x1,x2)))/(ii-1);
dstep3=(((max(x1)+max(x2)))/2-(min(x1)+min(x2))/2)/(ii-1);
%li computes the bin edges to achieve 48 bins/49 bin edges
%bin edges are [,)-> closed,open
l1=min(min(x1,x2)):dstep1:max(max(x1,x2))+dstep1;
l2=min(min(x1,x2)):dstep2:max(max(x1,x2))+dstep2;
l3=min(min(x1,x2)):dstep3:max(max(x1,x2))+dstep3;
%% Derive conditional distributions
%conditional distribution of x1 given x2
for k=1:1:ii
    ind=find(x2>=l1(1,k) & x2<l1(1,k+1));
    %ind_final=intersect(ind1,ind2);
    X1=x1(ind);
    condx1_x2{k,:}=X1;
end
%conditional distribution of x2 given x1
ind=[];
X2=[];
j=[];
k=[];
for k=1:1:ii
    ind=find(x1>=l2(1,k) & x1<l2(1,k+1));
    X2=x2(ind);
    condx2_x1{k,:}=X2;
end
%conditional distribution of demand given mean(x1+x2)
ind=[];
```

```
X3=[];
j=[];
k=[];
for k=1:1:ii
    ind=find(aver>=l3(1,k) & aver<l3(1,k+1));
    X3=XD3(ind);
    condx3_x1x2{k,:}=X3;
end
%% Merge sparse bins with bin numbers: [39,40]->[39],
   [41,42,43]->[40], [44,45,46,47,48]->[41]
newbin1=[condx1_x2{39,1};condx1_x2{40,1}];
newbin2=[condx1_x2{41,1};condx1_x2{42,1};condx1_x2{43,1}];
newbin3=[condx1_x2{44,1};condx1_x2{45,1};condx1_x2{46,1};condx1_x2
   {47,1};condx1_x2{48,1}];
for i=1:1:38
    newcondx1_x2{i,1}=condx1_x2{i,1};
end
newcondx1_x2{39,1}=newbin1;
newcondx1_x2{40,1}=newbin2;
newcondx1_x2{41,1}=newbin3;
condx1_x2=[];
condx1_x2=newcondx1_x2;

newbin1_a=[condx2_x1{39,1};condx2_x1{40,1}];
newbin2_a=[condx2_x1{41,1};condx2_x1{42,1};condx2_x1{43,1}];
newbin3_a=[condx2_x1{44,1};condx2_x1{45,1};condx2_x1{46,1};condx2_x1
   {47,1};condx2_x1{48,1}];

for i=1:1:38
    newcondx2_x1{i,1}=condx2_x1{i,1};
end
newcondx2_x1{39,1}=newbin1_a;
newcondx2_x1{40,1}=newbin2_a;
newcondx2_x1{41,1}=newbin3_a;
condx2_x1=[];
condx2_x1=newcondx2_x1;

newbin1_b=[condx3_x1x2{39,1};condx3_x1x2{40,1}];
newbin2_b=[condx3_x1x2{41,1};condx3_x1x2{42,1};condx3_x1x2{43,1}];
newbin3_b=[condx3_x1x2{44,1};condx3_x1x2{45,1};condx3_x1x2{46,1};
   condx3_x1x2{47,1};condx3_x1x2{48,1}];
for i=1:1:38
```

```
    newcondx3_x1x2{i,1}=condx3_x1x2{i,1};
end
newcondx3_x1x2{39,1}=newbin1_b;
newcondx3_x1x2{40,1}=newbin2_b;
newcondx3_x1x2{41,1}=newbin3_b;
condx3_x1x2=[];
condx3_x1x2=newcondx3_x1x2;

newl3=l3(1,1:38);
newl3(1,39)=l3(1,40);
newl3(1,40)=l3(1,43);
newl3(1,41)=l3(1,48);

save('newl3','newl3')%saves bin edges
%save finalised conditional probabilities
save('condx1_x2','condx1_x2')
save('condx2_x1','condx2_x1')
save('condx3_x1x2','condx3_x1x2')
```

Listing A.15 Sample code for simulation analysis in Section 6.2: Gibbs sampling process

```
%% Gibbs sampler
% Input required data
x1 % Wind speed at location 1
x2 % Wind speed at location 2
X3D % Demand
%conditional distributions/bin edges for aver
load condx1_x2;
load condx2_x1;
load condx3_x1x2;
load newl3;
%sigmoid fit parameters
load a
load c
load Umax
line_cap=150;% 150MW is the capacity of the transmission line
x1=X(:,1);
x2=X(:,2);
aver=(x1+x2)/2;%average wind speed for 17years
%% Gibbs sampling winds and demand by joint/average wind only
niter=500;% number of iterations N
nsampl=50000;% number of sampling size/how many hours are enough in
   Gibbs sampling
```

```
%preallocation/initialisations
pair=zeros(nsampl,3);
gsamp{niter,1}=[];
l3=newl3;
for run=1:1:niter
    u1_t=datasample(x1,1);
    u2_t=datasample(x2,1);
    k=[];
    for k=1:1:nsampl
        if u2_t<38
            y1=condx1_x2(u2_t+1);
        else
            if or(u2_t==38,u2_t==39)
                y1=condx1_x2(39);
            elseif or(or(u2_t==40,u2_t==41),u2_t==42)
                y1=condx1_x2(40);
            else
                y1=condx1_x2(41);
            end
        end
        u1_tnext=datasample(y1{1,1},1);

        if u1_tnext<38
            y2=condx2_x1(u1_tnext+1);
        else
            if or(u1_tnext==38,u1_tnext==39)
                y2=condx2_x1(39);
            elseif or(or(u1_tnext==40,u1_tnext==41),u1_tnext==42)
                y2=condx2_x1(40);
            else
                y2=condx2_x1(41);
            end
        end
        u2_tnext=datasample(y2{1,1},1);
        aver_U=(u1_tnext+u2_tnext)/2;
        posu3=find(l3>=aver_U,1)-1;
        y3=condx3_x1x2(posu3+1);
        u3_tnext=datasample(y3{1,1},1);
        pair(k,:)=[u1_tnext,u2_tnext,u3_tnext];
        u1_t=u1_tnext;
        u2_t=u2_tnext;
        posu3=[];
```

```
        aver_U=[];
    end
    gsamp{run,1}=pair;
    pair=zeros(nsampl,3);
end
save('gsamp','gsamp')%save sampled data by Gibbs sampler
%% Adjust to wind turbine height and compute power outputs
% Adjust for wind turbine height based on an Enercon E82 E2 turbine
   of height h=85 m
z0=0.03;%30mm roughness surface
zh=85;%hub height
zr=10;%anemometer height
for run=1:1:niter
    ggsamp=gsamp{run,1};
    ggsamp(:,1)=ggsamp(:,1)*0.514444;%make wind speeds m/s
    ggsamp(:,2)=ggsamp(:,2)*0.514444;
    ggsamp(:,1)=ggsamp(:,1)*(log(zh/z0))/(log(zr/z0));
    ggsamp(:,2)=ggsamp(:,2)*(log(zh/z0))/(log(zr/z0));
    %compute power produced
    temp1=ggsamp(:,1);
    temp1=1./(1+exp(-a*(temp1-c)));
    temp1(ggsamp(:,1)>Umax)=0;%adjust for cut out wind speed
    temp2=ggsamp(:,2);
    temp2=1./(1+exp(-a*(temp2-c)));
    temp2(ggsamp(:,2)>Umax)=0;%adjust for cut out wind speed
    ggsamp(:,1)=temp1;
    ggsamp(:,2)=temp2;
    gsamppow{run,1}=ggsamp;
end
save('gsamppow','gsamppow')%save power data (per unit)
```

Listing A.16 Sample code for simulation analysis in Section 6.2: Energy quantities estimation

```
%% Search space for building rated capacities
up_lim=500;%Search space maximum
dP=0.5;%Granularity of rated capacity built set to 0.5MW
Pn1=0:dP:up_lim+dP;%rated capacity for player 1
Pn2=0:dP:up_lim+dP;%rated capacity for player 2
ss1=size(Pn1,2);%size of search space
ss2=size(Pn2,2);%size of search space
load gsamppow
niter=500;% number of iterations N
```

```
nsampl=50000;% number of sampling size/how many hours are enough in
   Gibbs sampling
%% Compute generation/curtailment
for run=1:1:niter
    power1=gsamppow_part1{run,1}(:,1);
    power2=gsamppow_part1{run,1}(:,2);
    %initialise
    G1=zeros(size(power1,1),ss1);
    G2=zeros(size(power2,1),ss1);
    %estimate generation for all Pni
    G1=power1*Pn1;
    G2=power2*Pn1;
    %save total generation for all Pni
    EG1{run,1}=sum(G1);
    EG2{run,1}=sum(G2);
    %curtailment initialise
    ec1=zeros(ss1,ss2);
    ec2=zeros(ss1,ss2);
    %curtailment
    for i=1:ss1
        for j=1:ss2
            dif=G1(:,i)+G2(:,j)-gsamppow_part1{run,1}(:,3);
            dif(dif<0)=0;
            pc1=G1(:,i).*dif./(G1(:,i)+G2(:,j));
            pc2=G2(:,j).*dif./(G1(:,i)+G2(:,j));
            ec1(i,j)=nansum(pc1);
            ec2(i,j)=nansum(pc2);
        end
    end
    EC1{run,1}=ec1;
    EC2{run,1}=ec2;
end
save('EG1.mat','EG1');
save('EG2.mat','EG2');
save('EC1.mat','EC1');
save('EC2.mat','EC2');
```

Listing A.17 Sample code for simulation analysis in Section 6.3.2: Effects of local generators' generation cost c_{G_2}

```
%% Stackelberg game Scenario 2
%%
niter=170;
```

```
nsampl=50000;%number of samples
resiz=145071/nsampl;%for cost adaption to period of analysis
pg=74.3;%in pounds/MWh
%resize cost of line
Ct=230*10^6/resiz;%cost of building the line
dx=0.02*pg;
cg1=0.3*pg;
pt=0.26*pg;
cg2=0.0*pg:dx:0.7*pg;
%% Equilibrium estimation
for run=1:1:niter
    eg1=EG1{run,1};
    ec1=EC1{run,1};
    eg2=EG2{run,1};
    ec2=EC2{run,1};
    for n=1:size(cg2,2)
        for i=1:ss1
            for j=1:ss2
                prof_1(i,j)=pg*(eg1(1,i)-ec1(i,j))-cg1*eg1(1,i)+pt*(
                    eg2(1,j)-ec2(i,j))-Ct;
                prof_2(i,j)=(pg-pt)*(eg2(1,j)-ec2(i,j))-cg2(1,n)*eg2
                    (1,j);
            end
        end
        %Find first maxP2 for each row
        [val_2 id_2]=max(prof_2,[],2);
        id_1=sub2ind(size(prof_1),[1:size(prof_2)]',id_2);
        %collect corresponding P1 for each maxP2
        val_1=prof_1(id_1);
        %Find maxP1
        [max_1,loc_k]=max(val_1);
        %The equilibrium is max_1,max_2 at the location specified by
            indeces
        %(loc_k,loc_l)
        loc_l=id_2(loc_k,1);
        max_2=prof_2(loc_k,loc_l);
        %Find corresponding rated capacities built
        Cap1=Pn1(1,loc_k);
        Cap2=Pn2(1,loc_l);
        %Other variables to save
        Gen1=eg1(1,loc_k);
        Gen2=eg2(1,loc_l);
```

```
        Curt1=ec1(loc_k,loc_l);
        Curt2=ec2(loc_k,loc_l);
        %save profits
        all_profits{run,n}=table(Cap1,Cap2,max_1,max_2,Gen1,Gen2,
           Curt1,Curt2,'VariableNames',{'Cap1' 'Cap2' 'max_1' 'max_2'
            'Gen1' 'Gen2' 'Curt1' 'Curt2'});
        clearvars val_1 val_2 id_1 id_2 prof_1 prof_2 max_1 max_2
           loc_k loc_l Cap1 Cap2 Gen1 Gen2 Curt1 Curt2
    end
end
save 'all_profits_scen1.mat' 'all_profits'
%% For graphs
for run=1:1:niter
    for n=1:size(cg2,2)
        cap1(run,n)=all_profits{run,n}.Cap1;
        cap2(run,n)=all_profits{run,n}.Cap2;
        prof1(run,n)=all_profits{run,n}.max_1;
        prof2(run,n)=all_profits{run,n}.max_2;
        gen1(run,n)=all_profits{run,n}.Gen1;
        gen2(run,n)=all_profits{run,n}.Gen2;
        curt1(run,n)=all_profits{run,n}.Curt1;
        curt2(run,n)=all_profits{run,n}.Curt2;
    end
end
```

A.5 Simulation analysis presented in Chapter 7

Listing A.18 Sample code for simulation analysis in Section 7.4.1: Gibbs sampling process

```
%% Gibbs sampling winds
nsampl %Sampling size
pair=zeros(nsampl,2);
u1_t=datasample(x1,1);
u2_t=datasample(x2,1);
k=[];
for k=1:1:nsampl
    if u2_t<38
        y1=condx1_x2(u2_t+1);
    else
        if or(u2_t==38,u2_t==39)
            y1=condx1_x2(39);
        elseif or(or(u2_t==40,u2_t==41),u2_t==42)
```

```
            y1=condx1_x2(40);
        else
            y1=condx1_x2(41);
        end
    end
    u1_tnext=datasample(y1{1,1},1);

    if u1_tnext<38
        y2=condx2_x1(u1_tnext+1);
    else
        if or(u1_tnext==38,u1_tnext==39)
            y2=condx2_x1(39);
        elseif or(or(u1_tnext==40,u1_tnext==41),u1_tnext==42)
            y2=condx2_x1(40);
        else
            y2=condx2_x1(41);
        end
    end
    u2_tnext=datasample(y2{1,1},1);
    pair(k,:)=[u1_tnext,u2_tnext];
    u1_t=u1_tnext;
    u2_t=u2_tnext;
end
 %% Demand sampling
 %Demand: random samples from hourly-seasonal distributions
t1 = datetime(2000,1,1,0,0,0);% create a vector for 20 years
t2 = datetime(2019,12,31,23,0,0);
time_vect = t1:hours(1):t2;
%find hour indeces
ind_h=cell(24,1);
for i=1:1:24
    ind_h{i,1}=find(time_vect.Hour==i-1);
end
%find indeces that correspond to seasons
ind_s=cell(1,4);
ind_s{1,4}=find(ismember(time_vect.Month,[1,2,12]));
ind_s{1,1}=find(ismember(time_vect.Month,[3,4,5]));
ind_s{1,2}=find(ismember(time_vect.Month,[6,7,8]));
ind_s{1,3}=find(ismember(time_vect.Month,[9,10,11]));
%intersect hour-seasons indeces with real demand data and draw random
    samples
sect=cell(24,4);
```

```
for i=1:1:24
    for j=1:1:4
        sect{i,j}=intersect(ind_h{i,1},ind_s{1,j})';
        sect{i,j}(:,2)=datasample(data_all_norm{i,j}.demand,size(sect
            {i,j},1));
    end
end
%Put data in one table
demand_table=[];
for i=1:1:24
    for j=1:1:4
        demand_table=cat(1,demand_table,sect{i,j});%put data in one
            table
    end
end
% sort table data according to first column that represents time
xD=sortrows(demand_table);
%% Burn-in period of 20%
pair(1:43830,:)=[];
save('pair','pair')
gsamp=pair;
%% Adjust for hub height and calculate power outputs
z0=0.03;%30mm roughness surface
zh=85;%hub height
zr=10;%27m anemometer height
gsamp(:,1)=gsamp(:,1)*0.514444;%make wind speeds m/s
gsamp(:,2)=gsamp(:,2)*0.514444;
gsamp(:,1)=gsamp(:,1)*(log(zh/z0))/(log(zr/z0));
gsamp(:,2)=gsamp(:,2)*(log(zh/z0))/(log(zr/z0));
%compute power produced
temp1=gsamp(:,1);
temp1=1./(1+exp(-a*(temp1-c)));
temp1(gsamp(:,1)>Umax)=0;%adjust for cut out wind speed
temp2=gsamp(:,2);
temp2=1./(1+exp(-a*(temp2-c)));
temp2(gsamp(:,2)>Umax)=0;%adjust for cut out wind speed
gsamp(:,1)=temp1;
gsamp(:,2)=temp2;
%% Save data produced by Gibbs sampler
final_data=gsamp;
final_data(:,3)=xD(:,2);
final_data(:,4)=xD(:,1);
```

```
save('final_data','final_data')
```

Listing A.19 Sample code for simulation analysis in Section 7.3.1: Energy quantities estimation

```
%% Energy calculations (in parallel proccessing cluster 36 workers)
% Initialisations
load final_data
proj_life=8760;
x1=final_data(1:proj_life,1);%per unit loc1
x2=final_data(1:proj_life,2);%per unit loc2
x3=final_data(1:proj_life,3);%per unit demand

% Generation
Pn1max=500;
dP=1
Pn1=0:dP:Pn1max;%in MW rated capacity for player 1
s1=size(Pn1,2);
Pn2max=500;
Pn2=0:dP:Pn2max;%rated capacity for player 2
s2=size(Pn2,2);

% Storage
Smax=300;
dS=1;
S=0:dS:Smax;% storage capacity in MWh
n_rt=0.81;% round trip efficiency
n_ch=(n_rt)^0.5;
n_dch=(n_rt)^0.5;
self_dch=0;%self-discharge rate
Pch_max=10^6;%if no charging/discharging power constraints set to
    high number
Pdch_max=10^6;
s3=size(S,2);
SOCmin=0.2;
S0=S/2;
Smin=S*SOCmin;

% Demand
Dmax=150;%max remote load that can be satified by RES (no line
    considered)
D=x3*Dmax;%remote demand (no line considered)
d=D*0.20;%local demand
```

```
% Line capacity
%T=150;%line capacity in MWs
T=[0,75,100,125,150,175];% Line capacity in MW
s4=size(T,2);

% index i corresponds to combination of strategies (Pn1,T)
TT=repmat(T',s1);
TT(s4+1:end,:)=[];
PPn1=repmat(Pn1,s4);
PPn1(:,s1+1:end)=[];

% Preallocation
X=cell(s2,s3,s1*s4);
LD=zeros(proj_life,s1*s4);
EG1=zeros(proj_life,s1*s4);
for i=1:s1*s4
    ld=D;
    ld(ld>TT(i))=TT(i);
    LD(:,i)=ld;
    clear ld
    EG1(:,i)=x1*PPn1(i);
end
EG2=x2*Pn2; % RES available player 2
iterations=size(X);
parfor ix=1:prod(iterations)
    [j,k,i]=ind2sub(iterations,ix);

    EG1_now=EG1(:,i);
    EG2_now=EG2(:,j);
    LD_now=LD(:,i);
    EG=EG1_now+EG2_now; % RES available
    dif=EG-(LD_now+d);
    E_t=zeros(proj_life+1,1);%added +1 because simul_control seaches
        i+1
    E_t(1,1)=S0(1,k);
    S_now=S(1,k);
    Smin_now=Smin(1,k);

    %call function
    [SEG1,SEG2,SEC1,SEC2,SEd,SEd1,SEd2,SED,SED1,SED2,SEs_in1,SEs_in2,
        SEsd,SESD,SEOthd,SEOthD]=simul_control_final(proj_life,dif,
```

```
    LD_now,EG1_now,EG2_now,EG,d,D,Pch_max,Pdch_max,E_t,n_ch,n_dch,
    self_dch,S_now,Smin_now);
%generation RES
sumEG1(ix)=SEG1;
sumEG2(ix)=SEG2;
sumEC1(ix)=SEC1;
sumEC2(ix)=SEC2;
%local demand RES
sumEd(ix)=SEd;
sumEd1(ix)=SEd1;
sumEd2(ix)=SEd2;
%remote demand RES
sumED(ix)=SED;
sumED1(ix)=SED1;
sumED2(ix)=SED2;
%storage
sumEs_in1(ix)=SEs_in1;
sumEs_in2(ix)=SEs_in2;
sumEsd(ix)=SEsd;
sumESD(ix)=SESD;
%others
sumEOthd(ix)=SEOthd;
sumEOthD(ix)=SEOthD;

%clear variables
E_t=[];
S_now=[];
Smin_now=[];
SEG1=[];
SEG2=[];
SEC1=[];
SEC2=[];
SEd=[];
SEd1=[];
SEd2=[];
SED=[];
SED1=[];
SED2=[];
SEs_in1=[];
SEs_in2=[];
SEsd=[];
SESD=[];
```

```
    SEOthd=[];
    SEOthD=[];
    EG2_now=[];
    EG=[];
    dif=[];
    S_now=[];
    Smin_now=[];
    EG1_now=[];
    EG2_now=[];
    LD_now=[];
end
%%
for ix=1:prod(iterations)
    [j,k,i]=ind2sub(iterations,ix);
    SumED1(j,k,i)=sumED1(ix);
    SumED2(j,k,i)=sumED2(ix);
    SumEd1(j,k,i)=sumEd1(ix);
    SumEd2(j,k,i)=sumEd2(ix);
    SumEsd(j,k,i)=sumEsd(ix);
    SumESD(j,k,i)=sumESD(ix);
    SumEs_in1(j,k,i)=sumEs_in1(ix);
    SumEs_in2(j,k,i)=sumEs_in2(ix);
    SumEG1(j,k,i)=sumEG1(ix);
    SumEG2(j,k,i)=sumEG2(ix);
end
clearvars -except SumED1 SumED2 SumEd1 SumEd2 SumEsd SumESD SumEs_in1
    SumEs_in2 SumEG1 SumEG2
save('c_main.mat')
```

Listing A.20 Sample code for simulation analysis in Section 7.3.1: Control scheme for power flow estimation

```
function [SEG1,SEG2,SEC1,SEC2,SEd,SEd1,SEd2,SED,SED1,SED2,SEs_in1,
   SEs_in2,SEsd,SESD,SEOthd,SEOthD]=simul_control2(Proj_life,diff,LLD
   ,EEG1,EEG2,EEG,dd,DD,PPch_max,PPdch_max,EE_t,nn_ch,nn_dch,
   sself_dch,SS_now,SSmin_now)
for i=1:Proj_life
    if diff(i)>=0 % excess of RES generation
        %compute pro rata RES
        prorata_res=EEG1(i,1)/(EEG1(i,1)+EEG2(i,1));
        %satisfy local demand
        Ed(i,1)=dd(i,1);%local demand at time i
        Ed1(i,1)=prorata_res*Ed(i,1);
```

```
        Ed2(i,1)=Ed(i,1)-Ed1(i,1);
        %satisfy remote demand
        ED(i,1)=LLD(i,1);%remote demand at time i
        ED1(i,1)=prorata_res*ED(i,1);
        ED2(i,1)=ED(i,1)-ED1(i,1);
        %STORE whatever remains if possible
        if diff(i)>PPch_max%check if max charge power is violated
            %if more than permitted
            for_store=EE_t(i,1)*(1-sself_dch)+PPch_max*nn_ch;
            Pch=PPch_max;
        else
            for_store=EE_t(i,1)*(1-sself_dch)+diff(i)*nn_ch;
            Pch=diff(i);
        end
        %check if capacity of battery is exceeded
        if for_store<SS_now %check if capacity is exceeded
            EE_t(i+1,1)=for_store; %if not update storage
            Es_in(i,1)=Pch;%from res to store
            Es_in1(i,1)=prorata_res*Es_in(i,1);
            Es_in2(i,1)=Es_in(i,1)-Es_in1(i,1);
            EC(i,1)=diff(i)-Es_in(i,1);
            EC1(i,1)=prorata_res*EC(i,1);
            EC2(i,1)=EC(i,1)-EC1(i,1);
        else
            EE_t(i+1,1)=SS_now; % storage at max capacity
            Es_in(i,1)=(SS_now-EE_t(i,1)*(1-sself_dch))/nn_ch;%there
                is still some energy in for self-discharge
            Es_in1(i,1)=prorata_res*Es_in(i,1);
            Es_in2(i,1)=Es_in(i,1)-Es_in1(i,1);
            EC(i,1)=diff(i)-Es_in(i,1);
            EC1(i,1)=prorata_res*EC(i,1);
            EC2(i,1)=EC(i,1)-EC1(i,1);
        end
        Esd(i,1)=0;%from storage to local demand
        ESD(i,1)=0;%from storage to remote demand
        EOthd(i,1)=0;
        EOthD(i,1)=0;
        for_store=[];
        prorata_res=[];
        Pch=[];
    else % shortage of RES generation
        %how much can storage offer
```

```
        if -diff(i)>PPdch_max
            from_store=EE_t(i,1)*(1-sself_dch)-PPdch_max/nn_dch;
            Pdch=PPdch_max;
        else
            from_store=EE_t(i,1)*(1-sself_dch)+diff(i)/nn_dch;
            Pdch=-diff(i);
        end
        %check battery min SOC constraint
        if from_store>SSmin_now %SOCmin is not exceeded
            EE_t(i+1,1)=from_store; %if not update storage
        else
            EE_t(i+1,1)=SSmin_now; % storage at min capacity
            Pdch=(EE_t(i,1)*(1-sself_dch)-SSmin_now)*nn_dch;%
                calculate how much storage is offering
        end
        %satisfy local demand
        if (EEG1(i,1)+EEG2(i,1)+Pdch)>=dd(i,1)
            Ed(i,1)=dd(i,1);
            Ed1(i,1)=EEG1(i,1)*Ed(i,1)/(EEG1(i,1)+EEG2(i,1)+Pdch);
            Ed2(i,1)=EEG2(i,1)*Ed(i,1)/(EEG1(i,1)+EEG2(i,1)+Pdch);
            Esd(i,1)=Ed(i,1)-Ed1(i,1)-Ed2(i,1);
        else
            Ed(i,1)=EEG1(i,1)+EEG2(i,1)+Pdch;
            Ed1(i,1)=EEG1(i,1);
            Ed2(i,1)=EEG2(i,1);
            Esd(i,1)=Pdch;
        end
        %satisfy remote demand with whatever remains
        ED1(i,1)=EEG1(i,1)-Ed1(i,1);
        ED2(i,1)=EEG2(i,1)-Ed2(i,1);
        ESD(i,1)=Pdch-Esd(i,1);
        ED(i,1)=EEG1(i,1)+EEG2(i,1)+Pdch-(Ed1(i,1)+Ed2(i,1)+Esd(i,1))
            ;
        %shortage is satisfied by others
        EOthd(i,1)=dd(i,1)-Ed(i,1);
        EOthD(i,1)=LLD(i,1)-ED(i,1);
        Es_in(i,1)=0;
        Es_in1(i,1)=0;
        Es_in2(i,1)=0;
        EC(i,1)=0;
        EC1(i,1)=0;
        EC2(i,1)=0;
```

```
        from_store=[];
        Pdch=[];
    end
end
%outputs
%generation
SEG1=sum(EEG1);
SEG2=sum(EEG2);
SEC1=sum(EC1);
SEC2=sum(EC2);
%local demand RES
SEd=sum(Ed);
SEd1=sum(Ed1);
SEd2=sum(Ed2);
%remote demand RES
SED=sum(ED);
SED1=sum(ED1);
SED2=sum(ED2);
%storage
SEs_in1=sum(Es_in1);
SEs_in2=sum(Es_in2);
SEsd=sum(Esd);
SESD=sum(ESD);
%others
SEOthd=sum(EOthd);
SEOthD=sum(EOthD);
end
```

Listing A.21 Sample code for simulation analysis in Section 6.3.2: Effects of line investor's generation cost c_{G_1}

```
%% Stackelberg–Cournot game Sample Scenario 1
load 'c_main.mat'
%% Initialisations
load final_data
proj_life=8760;
x1=final_data(1:proj_life,1);%per unit loc1
x2=final_data(1:proj_life,2);%per unit loc2
x3=final_data(1:proj_life,3);%per unit demand

% Generation
Pn1max=500;%parallel runs till Pn1
   =50,100,150,200,250,300,350,400,450,500
```

```
dP=1;%5 Granularity of rated capacity built set to 0.5MW
Pn1=0:dP:Pn1max;%in MW rated capacity for player 1
s1=size(Pn1,2);
Pn2max=500;
Pn2=0:dP:Pn2max;%rated capacity for player 2
s2=size(Pn2,2);

% Storage
Smax=300%1300;%Smax=3000;
dS=1%20;
S=0:dS:Smax;% storage capacity in MWh
n_rt=0.81;% round trip efficiency
n_ch=(n_rt)^0.5;
n_dch=(n_rt)^0.5;
self_dch=0;%self-discharge rate=0.00001
Pch_max=10^6;%if no charging/discharging power constraints set to
    high number
Pdch_max=10^6;
s3=size(S,2);
SOCmin=0.2;
S0=S/2;
Smin=S*SOCmin;

% Demand
Dmax=150;%max remote load that can be satified by RES (no line
    considered)
D=x3*Dmax;%remote demand (no line considered)
d=D*0.20;%local demand
% Line capacity
%T=150;%line capacity in MWs
T=[0,75,100,125,150,175];% Line capacity in MW
s4=size(T,2);

% index i corresponds to combination of strategies (Pn1,T)
TT=repmat(T',s1);
TT(s4+1:end,:)=[];
PPn1=repmat(Pn1,s4);
PPn1(:,s1+1:end)=[];
%% Load cost parameters for Scen1-dependence on local generators'
    cost
pg=74.3;%in pounds/MWh
```

```
ct=(230*10^6/150)/20;%cost for building the line in pounds/MW: yearly
    figure
dx=0.02*pg;
pt=0.3*pg;
cg2=0.3*pg;
ps=0.1*pg;
cs=15000;%cost of storage
CG1=0*pg:dx:0.7*pg;
%% Call function
parfor n=1:size(CG1,2)
    cg1=CG1(1,n);
    [Pn1_eq,T_eq,Pn2_eq,Ps_eq,MPr1_eq,MPr2_eq,MPr3_eq,Prof1,Prof2,
       Prof3]=Find_Equil(self_dch,n_dch,n_ch,Pdch_max,Pch_max,x1,x2,D
       ,proj_life,s1,s2,s3,s4,TT,SumED1,SumEd1,SumED2,SumEd2,SumESD,
       SumEsd,SumEs_in1,SumEs_in2,SumEG1,SumEG2,pg,pt,ps,cg1,cg2,ct,
       cs,S,PPn1,Pn2);
    T_EQ(1,n)=T_eq;
    PN1_EQ(1,n)=Pn1_eq;
    PN2_EQ(1,n)=Pn2_eq;
    PS_EQ(1,n)=Ps_eq;

    MP1_EQ(1,n)=MPr1_eq;
    MP2_EQ(1,n)=MPr2_eq;
    MP3_EQ(1,n)=MPr3_eq;

    T_eq=[];
    Pn1_eq=[];
    Pn2_eq=[];
    Ps_eq=[];

    MPr1_eq=[];
    MPr2_eq=[];
    MPr3_eq=[];
end
```

Listing A.22 Sample code for simulation analysis in Section 7.3.1: Stackelberg-Cournot game estimation

```
function [PPn1_eq,TT_eq,PPn2_eq,PPs_eq,MMPr1_eq,MMPr2_eq,MMPr3_eq,
   Prof1,Prof2,Prof3]=Find_Equil(self_dch,n_dch,n_ch,Pdch_max,Pch_max
   ,x1,x2,D,proj_life,s1,s2,s3,s4,TT,SumED1,SumEd1,SumED2,SumEd2,
   SumESD,SumEsd,SumEs_in1,SumEs_in2,SumEG1,SumEG2,pg,pt,ps,cg1,cg2,
   ct,cs,S,PPn1,Pn2)
```

```
%% For every Sum(j,k,i) and cost parameter set compute profit
   equations
%preallocation
Prof1=zeros(s2,s3,s1*s4);
Prof2=zeros(s2,s3,s1*s4);
Prof3=zeros(s2,s3,s1*s4);
%compute profits
for j=1:1:s2%order reversed here to be the same as (j,k,i)
    for k=1:1:s3
        for i=1:1:s1*s4
            Prof1(j,k,i)=(SumED1(j,k,i)+SumEd1(j,k,i))*pg+(SumED2(j,k
               ,i)+SumESD(j,k,i))*pt+SumEs_in1(j,k,i)*ps-cg1*SumEG1(j
               ,k,i)-ct*TT(i);
            Prof2(j,k,i)=(SumED2(j,k,i)+SumEd2(j,k,i))*pg+SumEs_in2(j
               ,k,i)*ps-cg2*SumEG2(j,k,i)-SumED2(j,k,i)*pt;
            Prof3(j,k,i)=(SumEsd(j,k,i)+SumESD(j,k,i))*pg-(SumEs_in1(
               j,k,i)+SumEs_in2(j,k,i))*ps-SumESD(j,k,i)*pt-cs*S(1,k)
               ;
        end
    end
end
%% Cournot equilibrium
%preallocate cournot best responses and where equilibrium is stored
BR2=cell(1,s1*s4);%local generators best response
BR3=cell(1,s1*s4);%storage investor best response
cournot=cell(1,s1*s4);

%find cournot equilibrium for every strategy of line investot (Pn1,T)
   ->i
for i=1:1:s1*s4
    %for every Pn2 find Ps that makes prof3 max - max for every row
    [max_Prof3,opt_idPs]=max(Prof3(:,:,i),[],2);
    BR3{1,i}=S(opt_idPs);
    %for every Ps find Pn2 that makes prof2 max - max for every
       column
    [max_Prof2,opt_idPn2]=max(Prof2(:,:,i),[],1);
    BR2{1,i}=Pn2(opt_idPn2);
    courn_tmp=intersect([BR2{1,i};S]',[Pn2;BR3{1,i}]','rows');%find
       intersection
    cournot{1,i}=courn_tmp;%save intersections
    %potential outcomes after intersection are i)1 solution OK ii)
       multiple solutions iii) no solution
```

```
    if isempty(cournot{1,i})%if no solution
        Prof_cournot{1,i}=[];%Profits that correspond to cournot are
            set empty
    else%if 1 solution or multiple solutions
        for all_eq=1:size(courn_tmp,1)%all_eq is the size of
            solutions =1 if 1 sol etc
            ja=find(Pn2==courn_tmp(all_eq,1));%(all_eq,1) returns Pn2
                , (all_eq,2) returns S
            ka=find(S==courn_tmp(all_eq,2));%ja,ka are the indeces of
                equilibria
            Prof_cournot{1,i}=[Prof1(ja,ka,i),Prof2(ja,ka,i),Prof3(ja
                ,ka,i)];%retrieve profits for equilibria
            %reset ja,ka
            ja=[];
            ka=[];
        end
        all_eq=[];
    end
    courn_tmp=[];
end
%% Cases ii)Multiple intersections and iii) No intersection
count=0;% counts cases when have multiple/no solutions
cournot_new=cournot;
Prof_cournot_new=Prof_cournot;
for i=1:1:s1*s4
    temp=cournot{1,i};
    if (size(temp,1)>1)| (isempty(temp))
        count=count+1;
        if (size(temp,1)>1)%case of multiple equilibria
            cournot_new{1,i}=[];
            Pn2_sol=(temp(1,1)+temp(2,1))/2;
            S_sol=(temp(1,2)+temp(2,2))/2;
            cournot_new{1,i}=[Pn2_sol,S_sol];
            %calculate also Prof1eq,Prof2eq,Prof3eq for (Pn2_sol,
                S_sol)
            %single_energies returns energy values for given input
            [SED1c,SEd1c,SED2c,SEd2c,SEsdc,SESDc,SEs_in1c,SEs_in2c,
                SEG1c,SEG2c]=single_energies(D,TT,i,PPn1,x1,x2,Pn2_sol
                ,S_sol,proj_life,Pch_max,Pdch_max,n_ch,n_dch,self_dch)
                ;
            prof1eq=(SED1c+SEd1c)*pg+(SED2c+SESDc)*pt+SEs_in1c*ps-cg1
                *SEG1c-ct*TT(i);
```

```
66          prof2eq=(SED2c+SEd2c)*pg+SEs_in2c*ps-cg2*SEG2c-SED2c*pt;
67          prof3eq=(SEsdc+SESDc)*pg-(SEs_in1c+SEs_in2c)*ps-SESDc*pt-
                cs*S_sol;
68          Prof_cournot_new{1,i}=[];
69          Prof_cournot_new{1,i}=[prof1eq,prof2eq,prof3eq];
70          %store in Profi_eq
71          Prof1_eq(1,i)=prof1eq;
72          Prof2_eq(1,i)=prof2eq;
73          Prof3_eq(1,i)=prof3eq;
74      end
75      prof1eq=[];
76      prof2eq=[];
77      prof3eq=[];
78      if (isempty(temp))%no intersection
79          %retrieve best responses = lines
80          S_test=S';
81          Pn2_test=Pn2';
82          %find intersection of line segments through
                intersect_solution
83          %call function line intersect
84          sseg1=[BR2{1,i}',S_test];
85          sseg2=[Pn2_test,BR3{1,i}'];
86          [Pn2_sol,S_sol]=intersect_solution(sseg1,sseg2);
87          cournot_new{1,i}=[Pn2_sol,S_sol];%equilibrium solution
88          %calculate also Prof1eq,Prof2eq,Prof3eq for (Pn2_sol,
                S_sol)
89          [SED1c,SEd1c,SED2c,SEd2c,SEsdc,SESDc,SEs_in1c,SEs_in2c,
                SEG1c,SEG2c]=single_energies(D,TT,i,PPn1,x1,x2,Pn2_sol
                ,S_sol,proj_life,Pch_max,Pdch_max,n_ch,n_dch,self_dch)
                ;
90          prof1eq=(SED1c+SEd1c)*pg+(SED2c+SESDc)*pt+SEs_in1c*ps-cg1
                *SEG1c-ct*TT(i);
91          prof2eq=(SED2c+SEd2c)*pg+SEs_in2c*ps-cg2*SEG2c-SED2c*pt;
92          prof3eq=(SEsdc+SESDc)*pg-(SEs_in1c+SEs_in2c)*ps-SESDc*pt-
                cs*S_sol;
93          Prof_cournot_new{1,i}=[];
94          Prof_cournot_new{1,i}=[prof1eq,prof2eq,prof3eq];
95          %store in Profi_eq
96          Prof1_eq(1,i)=prof1eq;
97          Prof2_eq(1,i)=prof2eq;
98          Prof3_eq(1,i)=prof3eq;
99      end
```

```
    else %Case i) single intersection
        Prof1_eq(1,i)=Prof_cournot{1,i}(1);;
        Prof2_eq(1,i)=Prof_cournot{1,i}(2);
        Prof3_eq(1,i)=Prof_cournot{1,i}(3);
    end
end
%% Estimate Stackelberg–Cournot equilibrium
[maxProf1,opt_idPn1]=max(Prof1_eq);
PPn1_eq=PPn1(opt_idPn1);
TT_eq=TT(opt_idPn1);
PPn2_eq=cournot_new{1,opt_idPn1}(1);
PPs_eq=cournot_new{1,opt_idPn1}(2);
MMPr1_eq=Prof_cournot_new{1,opt_idPn1}(1);
MMPr2_eq=Prof_cournot_new{1,opt_idPn1}(2);
MMPr3_eq=Prof_cournot_new{1,opt_idPn1}(3);
end
```

A.6 Summary of assumptions used in simulation analysis

	Chapter 4	Chapter 5	Chapter 6	Chapter 7
Demand	Average demand based on long-term view	Hourly average of real demand	Generated by Gibbs sampler and average of wind speeds	Generated by Gibbs sampler with time-wise component preserved
Wind speed	-	Real wind speed data used	Generated by Gibbs sampler with cross-correlation	Generated by Gibbs sampler with cross-correlation
Wind power output	Average power output based on long-term view	Generated from wind speed data	Generated from wind speed data	Generated from wind speed data

Fig. A.8 Summary of assumptions used in simulation analysis and model evolution across different chapters